

CSNI Report No. 65

COMPARISON REPORT  
ON OECD-CSNI CONTAINMENT STANDARD PROBLEM No. 2:

"Water Line Rupture  
in a Branched Compartment Chain"

by  
D.L. Nguyen  
W. Winkler

Gesellschaft für Reaktorsicherheit (GRS) mbH  
Garching near Munich, F.R. Germany

May 1982

Submission to  
OECD-CSNI Working Group on Reactor Containment Safety

### Acknowledgements

This report is made with the financial support of the Federal Ministry for Research and Technology (BMFT) under Contract No. RS 470. Special thanks are due to Mrs. U. Fahnroth and Mr. Soelarto for their valuable assistance in preparing this report.

June 24, 1982

## CONCLUSIONS AND RECOMMENDATIONS

Arising from the result of discussions during the Workshop on OECD-CSNI Containment Standard Problem (SP) No. 2:

"Waterline Rupture in a Branched Compartment Chain"

the following was agreed upon:

In general, best-estimate "open" calculations of this more complicated test are quite satisfactory.

Reasons for deviations from experimental results are due to

- possible effects of uncertainties of measured input data (e.g. boundary conditions, coating thickness),
- code handling (e.g. choice of options, input parameters, nodalization),
- simplified models including unfavourably defined input parameters.

### Conclusions:

- On the average, calculational bandwidths of "open" results are equal to those of "blind" results for this and the 1st Containment SP and are of the same order of magnitude as experimental margins of uncertainty. Nevertheless a few systematic deviations between experimental and the average of calculated data can be observed.
- Relations between choice of input parameter values and quality of calculated results are difficult to be detected (hardly separable and partly compensating effects).
- Two Containment SP performed on basis of the same facility do not yet allow to draw quantitative conclusions with respect to the application of codes on full size plants. Future use of these experiments should take note of a leakage of the facility of unknown magnitude.

## Recommendations

- Improvement of measuring technique (e.g. for break mass- and enthalpy-flow, water transport, heat transfer mechanism) to reduce future margins of interpretation of experimental results.
- Extended quantification of the sensitivity of codes to uncertainties of measured input data.
- A finer nodalization of the system for long term calculations is necessary to predict temperature stratification (e.g. in dome compartment).
- Improvement of some physical models as for heat transfer, two-phase flow, water transport and thermal non-equilibrium between phases is desirable. Some basic laboratory experiments may be required to accomplish this.
- Further, a "blind" Containment SP based on a water-blowdown test, preferably in a large-scaled facility is recommended to perform an important step for extrapolation of findings towards full size facilities.
- The results of the numerical Benchmark activity on heat soakage problems is addressed in specific to improve treatment of these processes within containment codes.



## CONTENTS

1	Introduction	1
2	Short description of the problem	5
2.1	Test facility	5
2.2	Initial conditions	10
2.3	Boundary conditions	11
2.4	Instrumentation	13
2.5	Consideration of errors	23
2.5.1	Special events in the experiment	23
2.5.2	Measuring errors and geometric deviations	26
2.5.3	Effects of deviations from nominal values	32
2.5.3.1	Time interval 0 to 2.5 s	32
2.5.3.2	Time interval 0 to 50 s	39
2.6	Variables to be calculated	43
3	Presentation of results	44
3.1	Comments on the experimental results and deductions for the comparison	44
3.2	Selection of important variables	46
3.3	Listing of important features and input parameters of the codes used	47
3.4	Supplementary information of individual participants	53
3.5	Comparison of selected variables	61
3.5.1	Listing of important characteristic quantities	61
3.5.2	Time interval 0 to 2.5 s	65
3.5.3	Time interval 0 to 50 s	110
3.5.4	Time interval 0 to 1000 s	124
3.6	Comparison of remaining specified variables	132
3.7	Measured results of non-specified variables	133
3.8	Comparison with the results of OECD-CSNI Containment Standard Problem No. 1	135
3.8.1	Compartment scheme and flow paths	135
3.8.2	Boundary conditions	138
3.8.3	Comparison of important characteristic variables	150
4	Abstract and Conclusions	164
	References	167
	Appendix 1 (Results of "Blind" Predictions)	
	Appendix 2 (Additional Information of Participants)	

## FIGURES

Fig. 1:	Model containment in experiment D16/CASP2	6
Fig. 2:	Scheme of the containment and flow paths	7
Fig. 3:	Positions of measuring points, compartment R4	17
Fig. 4:	Positions of measuring points, compartment R5	18
Fig. 5:	Positions of measuring points, compartment R7	19
Fig. 6:	Positions of measuring points, compartment R8	20
Fig. 7:	Positions of measuring points, compartment R9	21
Fig. 8:	Positions of measuring points, compartment R6	22
Fig. 9:	Gap between compartments R4 and R9 after partial failure of a sealing	24
Fig. 10:	Break mass flow $\dot{m}$ with error band (experiment D16/CASP2)	28
Fig. 11:	Break mass flow $\dot{m}$ with error band (experiment D16/CASP2)	29
Fig. 12:	Specific enthalpy $h$ of the escaping fluid with error band (experiment D16/CASP2)	30
Fig. 13:	Specific enthalpy $h$ of the escaping fluid with error band (experiment D16/CASP2)	31
Fig. 14:	Model calculations on the influence of gap R4/R9 on pressure built-up	33
Fig. 15:	Pressure history in compartment R4	36
Fig. 16:	History of pressure difference R4-R9	37
Fig. 17:	Pressure history in compartment R9	38
Fig. 18:	Pressure history in compartment R9	42
Fig. 19:	Pressure history in compartments R4, R5, R7, R9	45
Fig. 20:	The heat transfer coefficients in different compartments (CASP2, "open" problem), Finland	56
Fig. 21:	Energy flow and heat transfer coefficients, Italy (CNEN/Pisa)	58

### Time interval 0 to 2.5 s

Fig. 22A:	Pressure history in compartment R4	70
Fig. 22B:	Pressure history in compartment R4	71
Fig. 23A:	Pressure history in compartment R5	72
Fig. 23B:	Pressure history in compartment R5	73
Fig. 24A:	Pressure history in compartment R9	74
Fig. 24B:	Pressure history in compartment R9	75

Fig. 25A:	History of pressure difference R4-R9	78
Fig. 25B:	History of pressure difference R4-R9	79
Fig. 26A:	History of pressure difference R4-R5	80
Fig. 26B:	History of pressure difference R4-R5	81
Fig. 27A:	History of pressure difference R5-R7	82
Fig. 27B:	History of pressure difference R5-R7	83
Fig. 28A:	History of pressure difference R5-R9	84
Fig. 28B:	History of pressure difference R5-R9	85
Fig. 29A:	History of pressure difference R7-R8	86
Fig. 29B:	History of pressure difference R7-R8	87
Fig. 30A:	Temperature history in compartment R4	90
Fig. 30B:	Temperature history in compartment R4	91
Fig. 31A:	Temperature history in compartment R4	92
Fig. 31B:	Temperature history in compartment R4	93
Fig. 32A:	Temperature history in compartment R5	94
Fig. 32B:	Temperature history in compartment R5	95
Fig. 33A:	Temperature history in compartment R5	96
Fig. 33B:	Temperature history in compartment R5	97
Fig. 34A:	Temperature history in compartment R7	98
Fig. 34B:	Temperature history in compartment R7	99
Fig. 35A:	Temperature history in compartment R7	100
Fig. 35B:	Temperature history in compartment R7	101
Fig. 36A:	Temperature history in compartment R8	102
Fig. 36B:	Temperature history in compartment R8	103
Fig. 37A:	Temperature history in compartment R8	104
Fig. 37B:	Temperature history in compartment R8	105
Fig. 38A:	Temperature history in compartment R9	106
Fig. 38B:	Temperature history in compartment R9	107
Fig. 39A:	Temperature history in compartment R6	108
Fig. 39B:	Temperature history in compartment R6	109

Time interval 0 to 50 s

Fig. 40A:	Pressure history in compartment R4	112
Fig. 40B:	Pressure history in compartment R4	113
Fig. 41A:	Pressure history in compartment R9	114
Fig. 41B:	Pressure history in compartment R9	115
Fig. 42A:	Temperature history in compartment R4	116
Fig. 42B:	Temperature history in compartment R4	117

Fig. 43A:	Temperature history in compartment R8	118
Fig. 43B:	Temperature history in compartment R8	119
Fig. 44A:	Temperature history in compartment R9	120
Fig. 44B:	Temperature history in compartment R9	121
Fig. 45A:	Temperature history in compartment R6	122
Fig. 45B:	Temperature history in compartment R6	123

Time interval 0 to 1000 s

Fig. 46A:	Pressure history in containment	126
Fig. 46B:	Pressure history in containment	127
Fig. 47A:	Temperature history in containment	128
Fig. 47B:	Temperature history in containment	129
Fig. 48A:	History of water mass in containment	130
Fig. 48B:	History of water mass in containment	131
Fig. 49A:	Scheme of the compartment chain and associated flow paths (D15)	136
Fig. 49B:	Scheme of the containment and flow paths (CASP2)	137
Fig. 50A:	Break mass flow $\dot{m}$ with error band (D15/0-2.5s)	140
Fig. 50B:	Break mass flow $\dot{m}$ with error band (CASP2/0-2s)	141
Fig. 51A:	Break mass flow $\dot{m}$ with error band (D15/0-70s)	142
Fig. 51B:	Break mass flow $\dot{m}$ with error band (CASP2/0-50s)	143
Fig. 52A:	Specific enthalpy $h$ of the escaping fluid with error band (D15/0-2.5s)	144
Fig. 52B:	Specific enthalpy $h$ of the escaping fluid with error band (CASP2/0-2s)	145
Fig. 53A:	Specific enthalpy $h$ of the escaping fluid with error band (D15/0-70s)	146
Fig. 53B:	Specific enthalpy $h$ of the escaping fluid with error band (CASP2/0-50s)	147
Fig. 54:	Total enthalpy flown in (0 to 2.5 s)	148
Fig. 55:	Total enthalpy flown in (0 to 70 s)	149
Fig. 56A:	Pressure history in compartment R6	152
Fig. 56B:	Pressure history in compartment R4	153
Fig. 57A:	Pressure history in compartment R9	154
Fig. 57B:	Pressure history in compartment R9	155

Fig. 58A:	History of pressure difference R6-R9	156
Fig. 58B:	History of pressure difference R4-R9	157
Fig. 59A:	History of pressure difference R6-R8	158
Fig. 59B:	History of pressure difference R4-R5	159
Fig. 60A:	Pressure history in compartment R9	162
Fig. 60B:	Pressure history in compartment R9	163

## TABLES

Table 1:	Participants and codes	3
Table 2:	Dimensions of containment compartments and vents in experiment CASP2	8
Table 3:	Coating of the containment concrete walls	9
Table 4:	Break mass flow and specific enthalpy	12
Table 5:	Designation of measuring points	14
Table 6:	Measuring errors at the test CASP2	26
Table 7:	Important features and input parameters of codes	48
Table 8:	Important characteristic variables	62
Table 9:	Mean values, bandwidths and deviations of important characteristic variables	63

## NOMENCLATURE

abs.	absolute
acc.	according
add.	additional
atm	atmosphere
A	surface area
$A_{\text{cond}}$	condensation area
$A_{\text{ij}}$	vent area
AAEC	Australian Atomic Energy Commission
AECL-EC	Atomic Energy of Canada Limited-Engineering Company
AEW	Atomic Energy Establishment Winfrith
AW	wall area
BMFT	Federal Ministry for Research and Technology
BWR	Boiling Water Reactor
c	spec. heat
$c_{\text{WA}}$	water separation factor
calc.	calculation
$C_{\text{wc}}$	water carry-over fraction = $= \frac{\text{water flow quality}}{\text{homogeneous upstream node quality}}$
$C_{\text{D}}$	discharge coefficient
CEA/EDF	Commissariat à l'Energie Atomique/Electricité de France
CNEN	Comitato Nazionale per l'Energia Nucleare
CSNI	Committee on the Safety of Nuclear Installations
decr.	decreasing
D	diameter
DG	density
DMS	strain gauge transducer
E	energy content
$E_{\text{K}}$	kinetic energy
ECN	Energieonderzoek Centrum Nederland
EXP.	experiment(al)
$f_{\text{r}}$	relative atmospheric humidity
$F_{\text{w}}$	$\frac{\text{water mass flow}}{\text{total mass flow}}$
FD	force on drag body
FRG	Federal Republic of Germany

GRS	Gesellschaft für Reaktorsicherheit
h	spec. enthalpy; htc
$h_{\max}$	maximum htc
$h_{T, \text{concrete}}$	htc for concrete acc. to Tagami
$h_{T, \text{steel}}$	htc for steel acc. to Tagami
$h_U$	htc. acc. to Uchida
hom.	homogeneous
htc	heat transfer coefficient
H	total enthalpy; htc
HDR	Heißdampfreaktor
incr.	increasing
JAERI	Japan Atomic Energy Research Institute
lin.	linear(ly)
liq.	liquid
L	length
m	mass
$\dot{m}$	mass flow rate
$m_A$	air mass
$m_V$	vapour mass
max.	maximum
min.	minimum
M	distribution box for transducer cables
MOD.	modified
n	number of orifices
NEA	Nuclear Energy Agency
NIRA	Nucléare Italiana Reattori Avanzati
NW	nominal width
o.d.	outer diameter
OECD	Organization for Economic Cooperation and Development
$P_n$	pressure, with index
PD	pressure difference
PL	static pressure (slow)
PP	dynamic pressure
PS	static pressure (fast)
PWR	Pressurized Water Reactor



R	radius
Rn	compartment, with no.
s	coating thickness
spec.	specific
SP	Standard Problem
t	time
$t_p$	time up to end of blowdown
$T_n$	temperature, with index
TL	temperature (slow)
TS	temperature (fast)
TW	temperature (slow)
$\dot{U}_n$	vent, with no.
UKAEA	United Kingdom Atomic Energy Authority
v	specific volume
V	volume
VTT	Valtion Teknillinen Tutkimuskeskus
$W_{M_n}$	water mass, with index
WS	water level
x	$\frac{\text{total vapour mass}}{\text{total air mass}}$
$\alpha$	htc
$\alpha_w$	wall htc
$\delta$	coating thickness
$\Delta P$	pressure difference
$\Delta T$	temperature difference
$\eta_w$	water in mixture flow
$\xi$	pressure loss coefficient
$\lambda$	thermal conductivity
$\xi_{sw}$	water carry-over factor = $\frac{\text{transportable}}{\text{total}}$ mass of water in node
$\rho$	density

## 1 INTRODUCTION

In September 1979, at the workshop on the results of OECD-CSNI\* Containment Standard Problem (SP) No. 1 the Federal Republic of Germany (F.R. Germany) offered experiment CASP2 to be the basis for OECD-CSNI Containment SP No. 2. Specifications /1, 2/ taken from "blind" German SP No. 3 (2nd Containment SP), based on the same experiment, were distributed. The workshop participants agreed to propose to CSNI this SP, but as an "open" calculation. On its November 1979 full meeting CSNI approved this proposal and Gesellschaft für Reaktorsicherheit (GRS) agreed to act as the lead organization.

As well as experiment D15 (basis for OECD-CSNI Containment SP No. 1) experiment CASP2 was performed (September 21, 1979) in the model containment of Battelle-Institut, Frankfurt, FRG, and sponsored by the Federal Ministry for Research and Technology (BMFT) within the frame of the German Reactor Safety Research Program (RS 50: Pressure Distribution in Containment). With letter of December 19, 1979 /3/ the measured initial and boundary conditions /4/, mid of April 1980 after deadline of the "blind" problem the experimental results /5, 6/ and mid of July 1980 some additional information /7, 8/ were communicated to 16 organizations from 13 countries who originally wished to participate.

In contrast to the 1st Containment SP (steam-blowdown, simple chain of compartments) the 2nd Containment SP is based on a pressurized water-blowdown experiment to further go to accident conditions more closely approximating those to be assumed for design of full-pressure containments. In addition, locating the rupture within a relatively small compartment and arranging the compartments in a branched chain with asymmetrical flow paths means that water transport will more heavily influence the results.

The technical purpose of the problem is to compare experimental results of history of pressure, pressure difference, temperature, and water mass with the corresponding results of best-estimate posttest-calculations from computer codes for three different time intervals.

---

\*Organization for Economic Cooperation and Development - Committee on the Safety of Nuclear Installations

At the first meeting of the CSNI Working Group on Water Reactor Containment Safety (May 1980) the original deadline for submitting calculated results of August 1980 was shifted to November 1, 1980. Finally, in the comparison took part 12 organizations representing 11 countries and using 12 different computer codes and, partly, several versions (see table 1). Except one (June/August 1980) "open" contributions arrived at GRS mainly between October 30 and November 14, 1980, further two and one revised in mid of December 1980.

6 international organizations felt it beneficial to "blind" participate in this SP. These results /9/ were discussed at an informal meeting held at GRS, Garching, in January 1981 after the workshop on the results of German SP No. 3 and are included here in Appendix 1. A short note /39/ summarizes these discussions.

The workshop on the results of the Standard Problem was held at GRS, Garching, FRG on May 25/26, 1981. Comparison results and the results of the individual participants were presented and discussed in detail (see /41, 42/).

Supplementary information to and comments on the draft comparison report /40/ came from Belgium, Canada, France, Italy (CNEN/Pisa), Italy (NIRA) and Sweden and are far extendingly considered in the present final report.

Special supplementary information on submitted results - as requested at the workshop - and results of parametric studies (Belgium, France, Italy (CNEN/Pisa), Sweden) are content of Appendix 2.

The scales used in the comparative plots of this report equal with minor inevitable exceptions those used in the comparison report on OECD-CSNI Containment SP No. 1 /10/. By this a direct comparison of experimental and calculational results and bandwidths between both SP is possible.

Country (Organization)	Contributor	Computer Code	Time Interval
Australia (AAEC)	P.G. Holland J. Marshall	ZOCO V	0.0 - 2.5
			0.0 - 50
			0.0 - 1000
Belgium (Tractionel)	E.J. Stubbe	TRAP-SCO	0.0 - 2.5
		TRAP-CON	0.0 - 50
			0.0 - 1000
Canada (AECL-EC)	W.M. Collins	PRESCON-2	0.0 - 2.5
			0.0 - 50
			0.0 - 1000
Finland (VTT)	E. Pekkarinen	RELAP4/MOD6	0.0 - 2.5
		CONTEMPT-LT/026**	0.0 - 1000
France (CEA/EDF)	A. Sonnet A. Mattei/ F. Herber	GRUYER	0.0 - 2.5
			0.0 - 50 *
			0.0 - 1000*
F.R. Germany (GRS)	W. Erdmann M. Tiltmann	COFLOW	0.0 - 2.5*
		CONDUR	0.0 - 50
			0.0 - 1000
Italy (CNEN/Pisa Univ.)	R. Romanacci/ F. Cassano A.M. Gorlandi M. Marchi M. Mazzini F. Oriolo	ARIANNA-0	0.0 - 2.5
		CONTEMPT-LT-26	0.0 - 50
			0.0 - 1000
Italy (NIRA)	B. Chiantore R. Monti A. Pennese	PACO	0.0 - 2.5
			0.0 - 50
			0.0 - 1000
Japan (JAERI)	K. Namatame I. Takeshita Y. Kukita	RELAP4/MOD5	0.0 - 2.5
			0.0 - 50
			0.0 - 1000
Netherlands (ECN)	J.P.A. van den Bogaard A. Woudstra	ZOCO-V/MOD.	0.0 - 2.5 *
			0.0 - 50 *
			0.0 - 1000 *
Sweden (Studsvik)	J.E. Marklund	COPTA-6	0.0 - 2.5
			0.0 - 50
			0.0 - 1000
United Kingdom (UKAEA, AEEW)	W.H.L. Porter	CLAPTRAP II	0.0 - 2.5
		CLAPTRAP I	0.0 - 50
			0.0 - 1000

\* "blind" calculation      \*\* (VTT version)

Table 1: Participants and Codes



## 2 SHORT DESCRIPTION OF THE PROBLEM

More details can be found, among others, in the specification /1, 2/, the report on the initial and boundary conditions /4/ and on the experimental results /5, 6/.

### 2.1 Test Facility

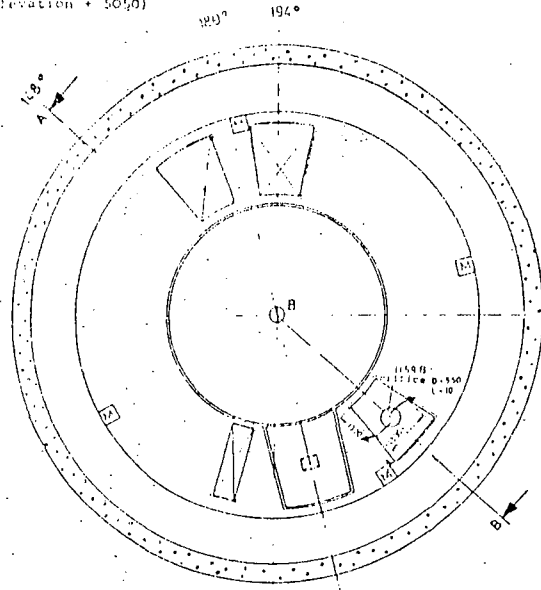
The test facility essentially consists of a high pressure system, and a model containment. The high pressure system is installed mainly outside the containment and consists of a pressure vessel, a pipeline with a length of approx. 26 m, and a recirculation system. The pipeline is connected to the pressure vessel and leads through the containment to the break compartment.

Before rupture, the heated water in the pressure vessel and in the piping is kept at an approximately homogeneous temperature by the recirculation system. The model containment consists of 6 compartments arranged according to figs. 1 and 2. The location of the rupture (baffle plate at a distance of 5 D) is approximately in the middle of the smallest compartment R4. The fluid branches at the upper part of compartment R4. One portion flows into compartment R5 via vent Ü45 (orifice) and from there, over a short flow path, through the ceiling of the compartment (vent Ü59B, orifice) into the dome of the big compartment R9. The other portion flows through vent Ü47 (orifice) into compartment R7 and from there, after flowing longitudinally through R7, via vent Ü78B (orifice) at the floor into compartment R8. Compartment R8 as well as compartment R6, which is symmetrical to it, are open to compartment R9 by several holes in the walls. During the experiment a small additional gap formed between rupture compartment R4 and dome compartment R9.

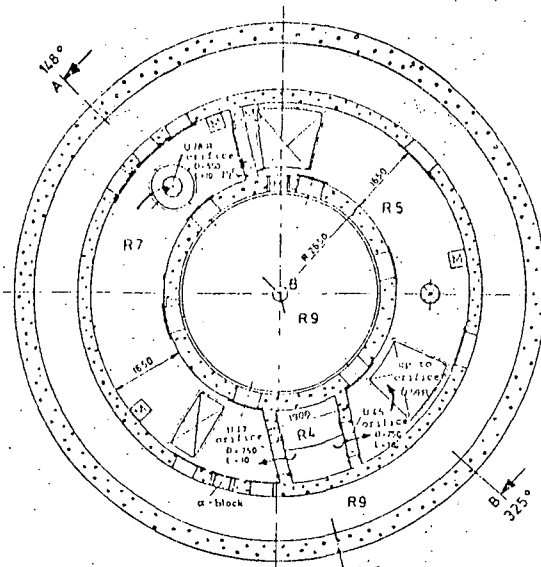
The most important containment dimensions are given in table 2.

The steel surfaces are not coated; the concrete surfaces are provided with coating (see table 3).

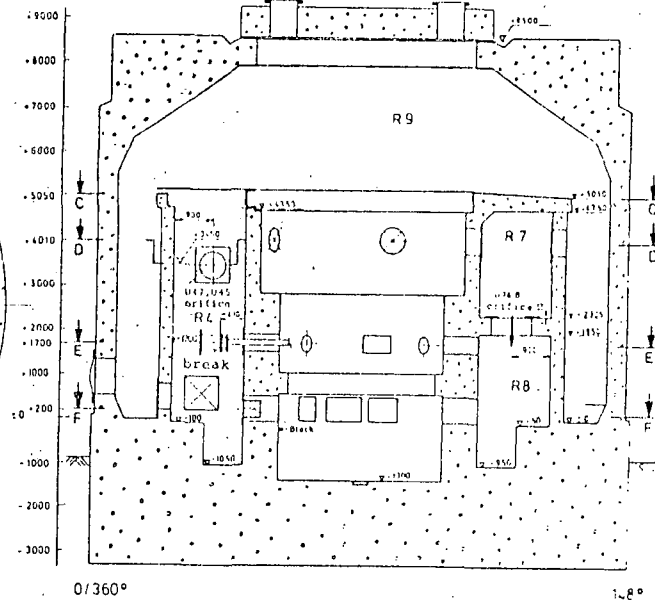
cross section C-C  
(elevation + 3050)



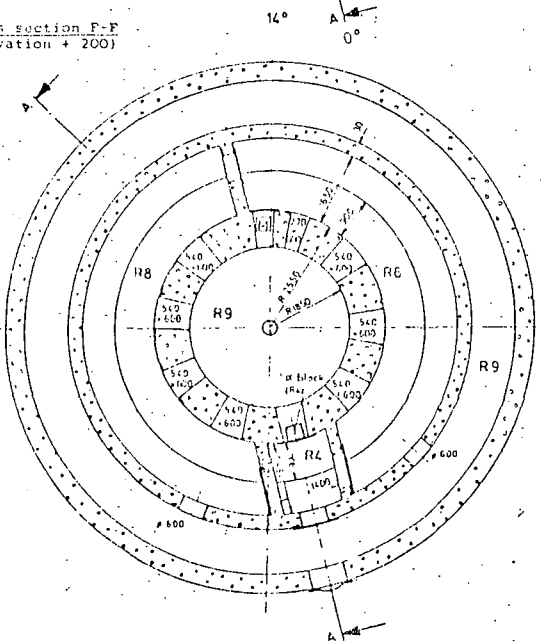
cross section D-D  
(elevation + 4010)



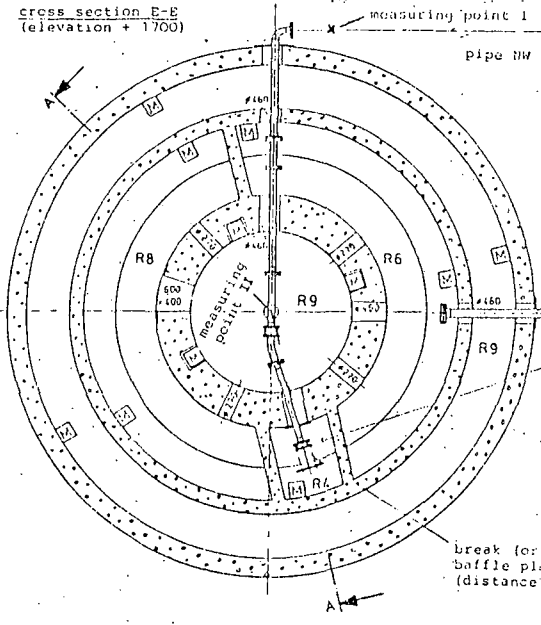
cross section A-A



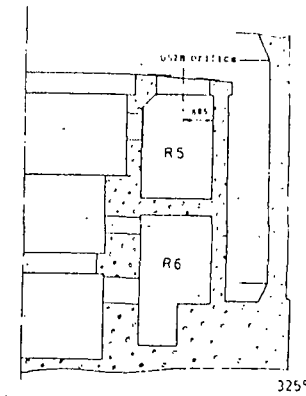
cross section F-F  
(elevation + 200)



cross section E-E  
(elevation + 1700)



cross section B-B



pressure vessel I  
(5,3m<sup>3</sup>)

pipe NW200  
not operational

rupture compartment

Ⓜ distribution box for  
transducer cables

U vent, with no.

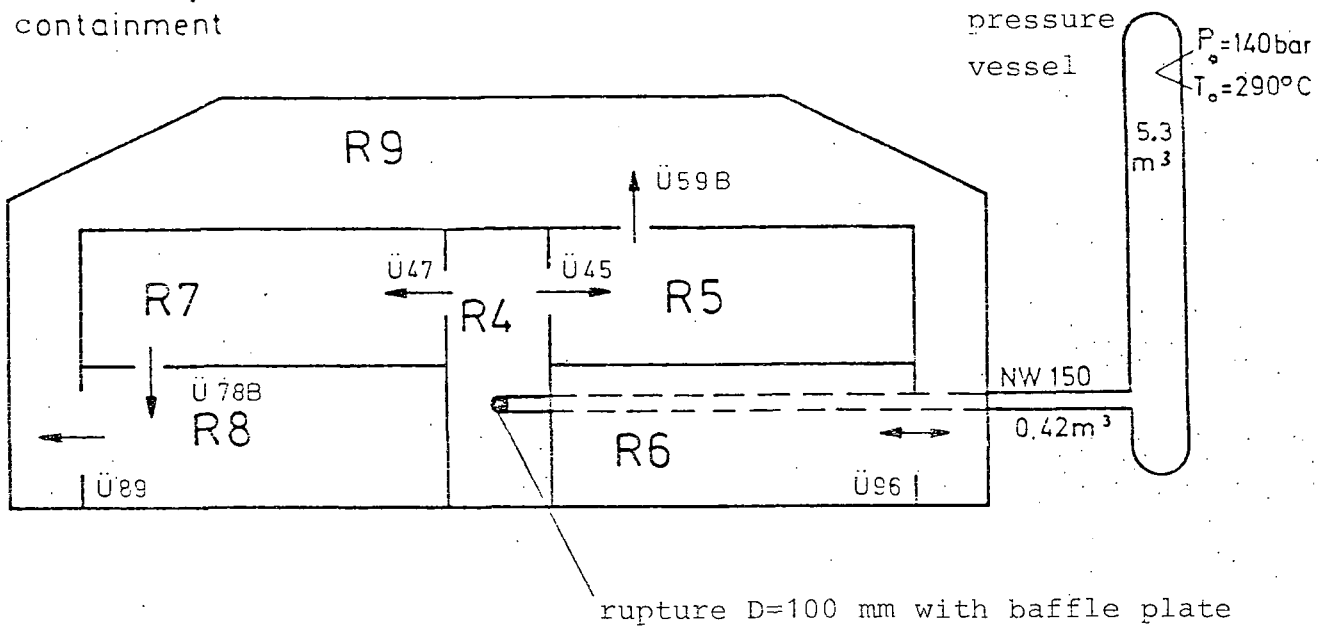
→ main flow direction

⊗ closed vent

break (orifice Ø 100) with  
baffle plate Ø 600  
(distance 500)

measures in mm

Fig. 1 : Model Containment in Experiment D16/CASP2



rupture compartment : R4

vents : : Ü45, Ü47, Ü59B, Ü78B sharp-edged orifices  
Ü89, Ü96 wall holes

flow paths :

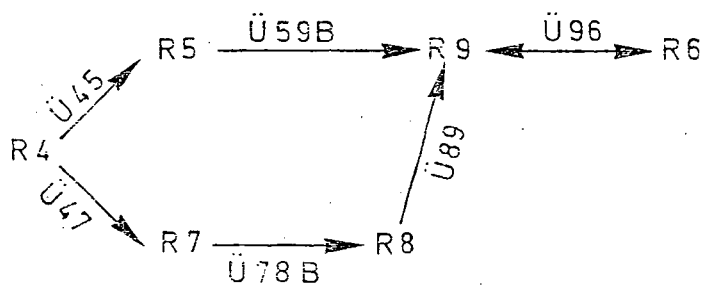


Fig. 2 : Scheme of the Containment and Flow Paths



Table 2 Dimensions of containment compartments and vents in experiment CASP2

Compartment No.	Volume (m <sup>3</sup> )	Surface area	
		Concrete (m <sup>2</sup> )	Metal (m <sup>2</sup> )
R4 (rupture)	13.66	38.63	8.83
R5	41.05	76.08	17.23
R6	41.26	90.12	9.58
R7	40.40	76.63	15.41
R8	40.53	92.00	6.17
R9	465.00	645.82	57.30
Sum of all compartments	641.90	1019.28	114.52

Vent No.	Compartments connected	Vent shape	Vent diameter (mm)	Vent area (geometrical) (m <sup>2</sup> )
Ü 45	R4/R5	sharp-edged orifice	750	0.442
Ü 47	R4/R7	sharp-edged orifice	750	0.442
Ü 59B	R5/R9	sharp-edged orifice	550	0.238
Ü 78B	R7/R8	sharp-edged orifice	550	0.238
	R8/R9	} several holes in the walls	-	1.933
	R9/R6		-	2.109
	R4/R9	gap*	-	max. 0.0292

\* see fig. 9

Table 3 : Coating of the containment concrete walls

To prevent water exchange between the containment atmosphere and the concrete walls, the concrete surfaces of the RS 50 model containment are covered with a coating which consists of the following layers:

Layer (material)	Thickness <sup>*)</sup> (mm)	Density $\rho$ (kg/m <sup>3</sup> )	Spec. heat c (kJ/kgK)	Thermal conductivity $\lambda$ (W/mK)
Sealer (EP-Tiefensiegel)	$\approx 0$	-	-	-
Filler for porous spots (EP-Betonspachtel)	variable	1,900	1.4	0.3
Flat coat (filler) (EP-Betonspachtel)	0.5-1	1,900	1.4	0.3
Bonding agent (2K-Haftvermittler)	$\approx 0$	-	-	-
Main coat (faserverstärkter PC- Anstrich)	$\approx 0.1$	1,100	0.95	0.2
Top coat (2x) (PC-Anstrich)	$\approx 2x 0.05$	1,100	0.72	0.2

\*) The thickness of the individual layers varies. Systematic measurements of the thickness has not been possible, because a suitable non-destructive measuring method is not available. The thickness values indicated have been estimated on the basis of samples taken at various sites.

2.2 Initial Conditions

Initial Conditions Prior to Blowdown

Pressure Vessel and Piping:

$P_0$	=	141.0 bar	
$T_1$	=	288.3°C (level A)	} pressure vessel (mean temperature: $T_m = 289.3°C$ )
$T_2$	=	288.5°C (level B)	
$T_3$	=	293.1°C (level C)	
$T_4$	=	295.3°C (level D)	
$T_5$	=	292.5°C (level E)	
$T_6$	=	286.1°C (level F)	
$T_8$	=	288.1°C (circulating pump)	} pipe, dia. 150 mm <sup>*</sup> )
$T_9$	=	290.8°C (rupture site)	
$T_{10}$	=	286.6°C (near gate valve)	
$m_{B0}$	=	3995 kg (pressure vessel)	} initial fluid mass
$m_{R0}$	=	315 kg (pipe)	

Containment:

$P_{Co}$	=	1.0 bar	
$T_{R4}$	=	23.5°C	} mean values of compartments R4 to R9, volumetric average for whole containment: $T_{Co} = 27.6°C$
$T_{R5}$	=	23.0°C	
$T_{R6}$	=	26.0°C	
$T_{R7}$	=	24.0°C	
$T_{R8}$	=	24.5°C	
$T_{R9}$	=	30.5°C (centre and dome)	
$T_{R9a}$	=	25.0°C (annulus)	
$f_r$	=	100.% (relative atmospheric humidity)	

\*) These values were obtained with two gauges of the plant instrumentation located at the two pipe ends. Values measured with the standard experimental instrumentation, however, indicate an inhomogeneous temperature distribution in the pipe within the temperature range from 255 to 290°C.

### 2.3 Boundary Conditions

The boundary conditions for the containment are the measured mass flow rates at the measuring point II (at a distance of about 2.7 m from the rupture) with the associated specific enthalpy as a function of time (table 4).

These mass flow values are determined from the signals of a gamma-densitometer and from the mean value of the measured curves of two drag bodies.

The mass flow values measured for the short-term period up to 1.2 s have been taken without any correction. The measured mass flow values for the long-term period after 4 s have been corrected by a factor of about 1.2, so that the time integral for mass flow rate up to 50 s is equal to the discharged mass predicted from an integral mass balance. For the intermediate period from 1.2 to 4 s an interpolation is done.

The specific enthalpy of the fluid is determined by the measurement for density and temperature (for single-phase flow) respectively pressure (for two-phase flow).

Table 4 : Break mass flow and specific enthalpy

D16/CASP2

Time (s)	Mass flow (kg/s)	Temperature (°C)	Density (kg/m <sup>3</sup> )	Spec. enthalpy (kJ/kg)
0	0	260	795	1134
0.004	52	260	784	1135
0.005	145	260	784	1135
0.028	200	260	784	1135
0.056	200	260	784	1135
0.067	340	260	784	1135
0.086	335	260	784	1135
0.105	405	260	784	1135
0.200	368	260	784	1135
0.350	270	283	715	1255
0.400	210	282	640	1260
0.500	205	281	600	1260
0.750	300	272	764	1195
0.850	324	272	764	1195
0.920	374	273	763	1201
1.20	230	281	580	1263
2.00	200	280	530	1267
2.50	180	279	500	1267
4.00	165	275	430	1261
10.00	145	268.5	310	1266
16.33	130	261	300	1225
23.50	115	252.5	255	1195
24.30	78	250	125	1323
30.00	25	207	20	1737
40.00	3	156	3	2752
50.00	0	152	2.7	2748

integral mass outflow : 4075 kg ± 55 kg

## 2.4 Instrumentation

Table 5 shows the designation scheme for the measuring points which also gives information on object of measurement, measured variable and type of sensor, positions of the measuring points, and the kind of installation.

Figs. 3 to 8 show the, partly redundant, measuring point positions in each compartment of the containment.

The individual values are measured in the following way:

PS static pressure by piezoelectric transducer directly installed at the measuring point (fast).

PL static pressure by strain gauge transducer installed outside the containment (measuring point connected to transducer by pressure lines) or piezoresistive transducer installed inside some containment compartments (measuring channels 113, 128 and 130) (slow).

PD pressure difference by piezoresistive transducer or DMS-basis directly installed at the measuring point position.

TS temperature by Ni/CrNi sheathed thermocouple (0.25 mm o.d., fast, response time in water 15 to 20 ms).

TL temperature by Ni/CrNi sheathed thermocouple (1.5 mm o.d., slow).

TW temperature by miniature resistance thermometer (slow).

WS water level by capacitive transducer installed outside.

Out of a total of 117 measuring points in the containment about 10 failed totally and 3 partly.

Table 5 : Designation of measuring points

for instance	9	P	S	3	1	8	A	Ø	5	M
or	B	T	S	1	Ø	Ø	2	G	2	
	1	2	3	4	5	6	7	8	9	10
	-----			-----						-----
	1	2+3		4-9						10
	Object of measurement	Measured value and type of sensor		Positions of measuring points						Special type of installation

Digit 1: Object of measurement

- 4 to 9      Containment compartment number R4 to R9
- B            Pressure vessel
- R            High-pressure pipeline

Digits 2 to 3: Measured value and type of sensor

- DG            Density (gamma-ray absorption system)
- FD            Force on drag body (strain gauges)
- PD            Pressure differential (piezoresistive transducer )
- PL            Static pressure, slow (strain gauge transducer or piezoresistive transducer)
- PP            Dynamic pressure (piezoresistive transducer)

Table 5 (continued)

PS	Static pressure, fast (piezoelectric transducer)
TL	Temperature, slow (thermocouple 1 or 1.5 mm O.D.)
TS	Temperature, fast (thermocouple 0.25 mm O.D.)
TW	Temperature (ohmic thermometer)
WS	Water level (capacitive transducer)

Digits 4 to 9: Positions of measuring points

I. Designations for pressure vessels (digit 1: "B"):

Digits 4 to 7: Height in cm, measured from the vessel floor

Digits 8 + 9: A1 to A4

·           ·  
·           ·  
G1. to G2

} Horizontal nozzles

H-           Upper vertical nozzle

U-           Lower vertical nozzle

--           Other

II. Designations for containment and pipeline

(digit 1: "4" to "9" or "R")

Digits 4 to 6:  $\emptyset\emptyset\emptyset$  to  $36\emptyset$  polar angle, in angular degrees, from manhole (=  $0^\circ$ ) in clockwise direction

Digit 7: 4 to 9 In wall to compartment R4 to R9

A           On/in outer wall

F           In intermediate flange

I           On/in inner wall

U           On/in overflow opening

W           In heat transfer measuring block or disc



Table 5 (continued)

Digits 8 + 9: Height in dm above bottom of the containment compartment in question (in compartments R4, R6 and R8 above sump floor, and in the case of pipelines above the sump floor of compartment R6)

Digit 10: Special type of installation

M In spray protection tube

L At end of pressure measurement line

T In dead-water area

W In wall

- Other

Fig. 3 Positions of measuring points

		Compartment 4	
		Designation of measuring points	channel
	4 PS 000 A 50 M	104	
	4 TS 000 M 55	166	
	4 TS 000 A 23	165	
	4 TS 006 A 13	164	
	4 TS 000 I 13	163	
	4 TS 011 I 02	162	
	4 TL 011 I 00	161	
	Alpha-Block:		
	4 TL 000 W 13	21	
	4 TL 001 W 13	22	
	4 TL 002 W 13	23	
	4 TL 004 W 13	25	
	4 TL 005 W 13	26	
	4 TL 006 W 13	27	
	4 TL 007 W 13	28	
	4 TL 008 W 13	29	
	4 PS 006 A 13 M	105	
	Alpha-Disk		
	4 TS 356 W 27	167	
	4 TS 357 W 27	168	
4 PL 354 A 46 L	116		
4 PL 008 A 25 L	114		
4 PD 000 9 21 W	149		
7 PD 010 4 16 W	148		
5 PD 350 4 16 W	147		
4 PL 000 A 27	113		
4 PD 354 9 46 W	150		
4 WS	203		

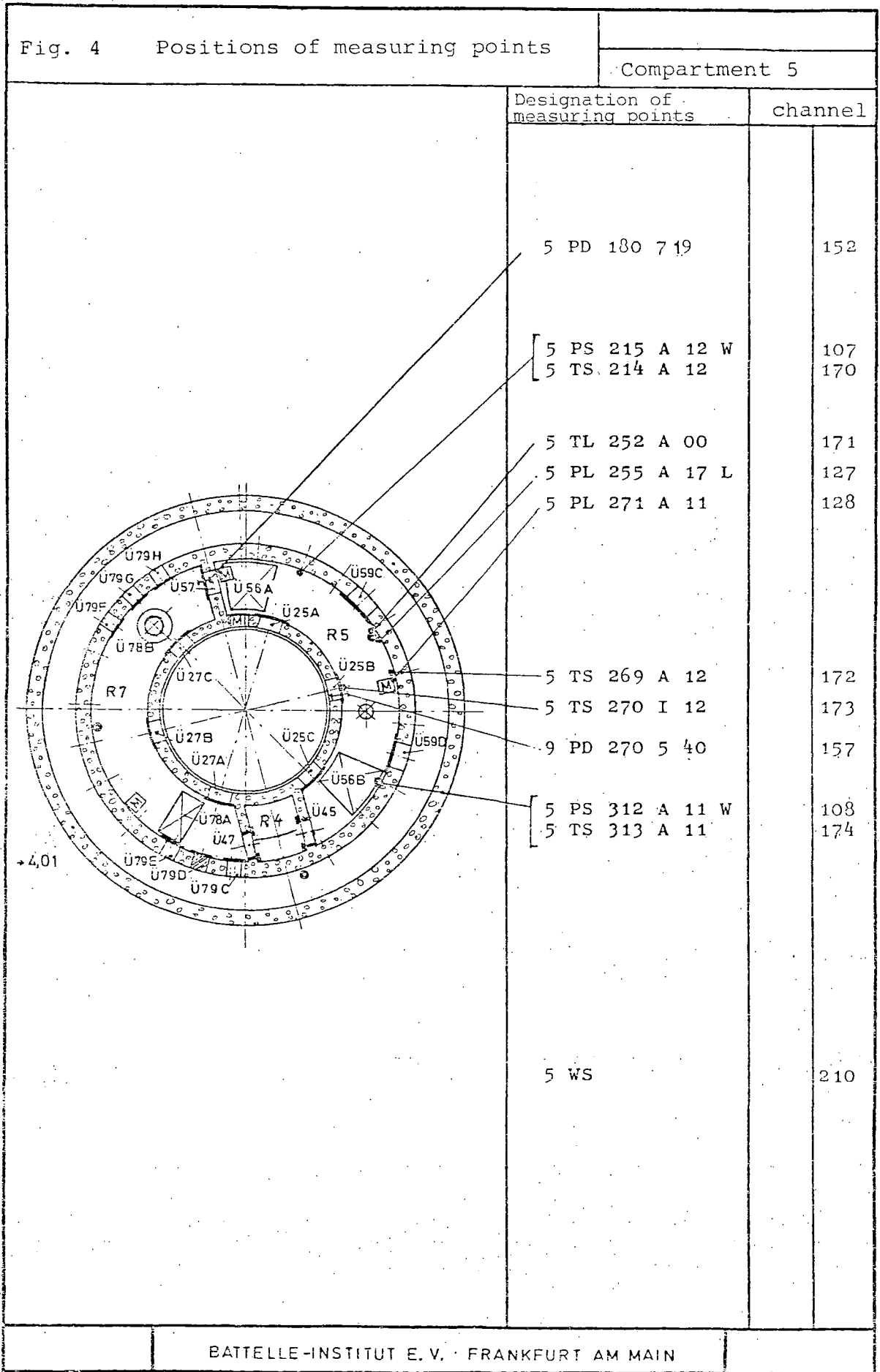


Fig. 5 Positions of measuring points

Compartment 7

Designation of measuring points	channel	
[ 7 PS 143 A 12 W 7 TS 144 A 12	111	180
[ Alpha-Disk 7 TS 150 W 12 7 TS 151 W 12 7 TS 150 I 12	181	182 183
7 TL 095 A 00	179	
7 TS 090 A 12	177	
7 TS 089 I 12	176	
9 PD 090 7 40	158	
7 PL 090 A 11	130	
7 PL 047 A 16 L	129	
[ 7 PS 38 A 11 W 7 TS 38 A 12	110	175
7 WS	212	

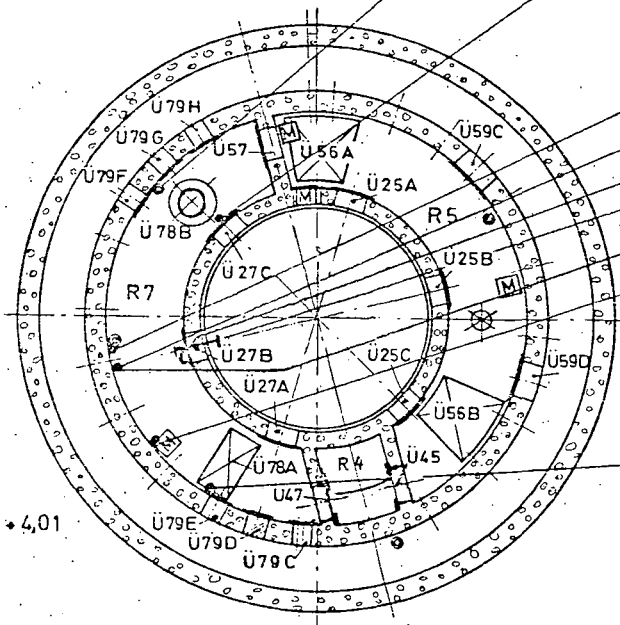


Fig. 6 Positions of measuring points

Compartment 8

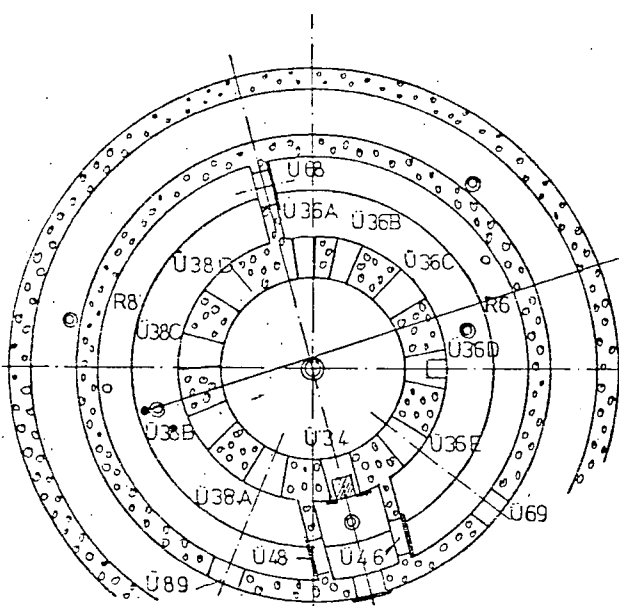
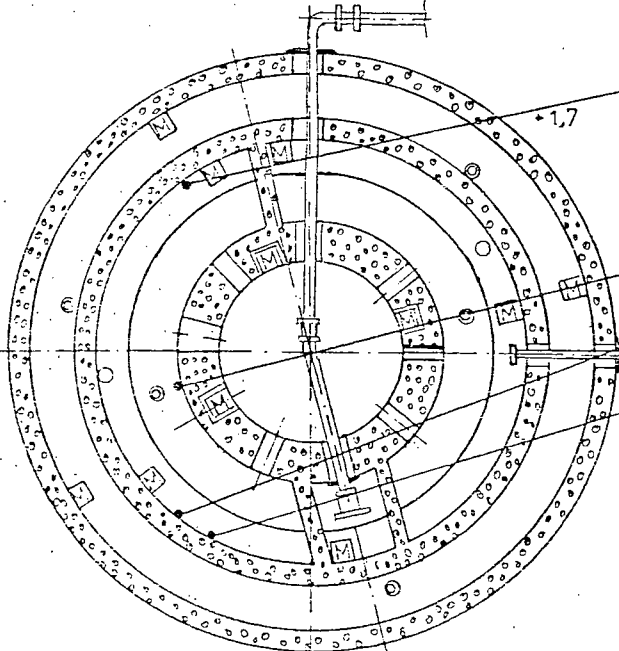
Designation of measuring points	channel	
	8 TL 090 M 00	189
	[ 8 PS 153 A 21 W 8 TS 158 A 21	112 190
	8 TS 090 I 21	188
	8 PL 053 A 25 L	131
	8 TS 042 A 21	186
	8 WS	213
BATELLE INSTITUT E. V. FRANKFURT AM MAIN		

Fig. 7 Positions of measuring points

Compartment 9

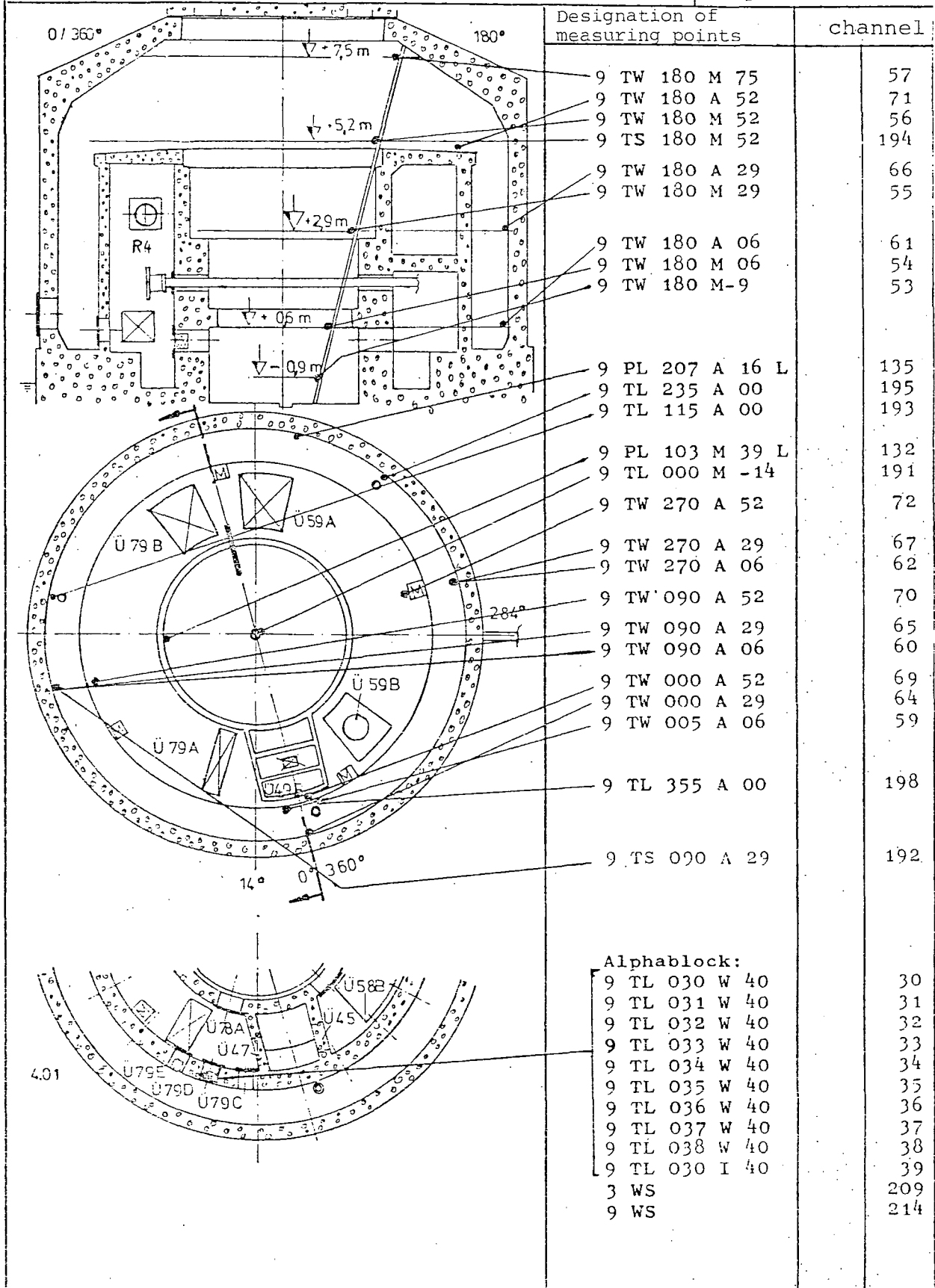
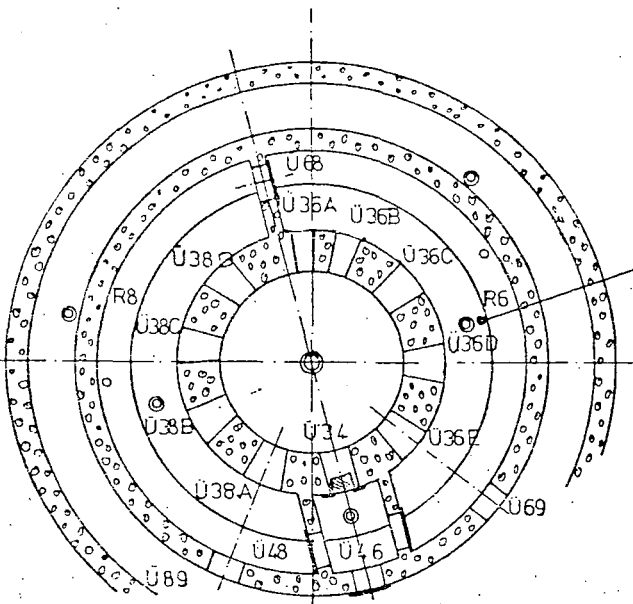
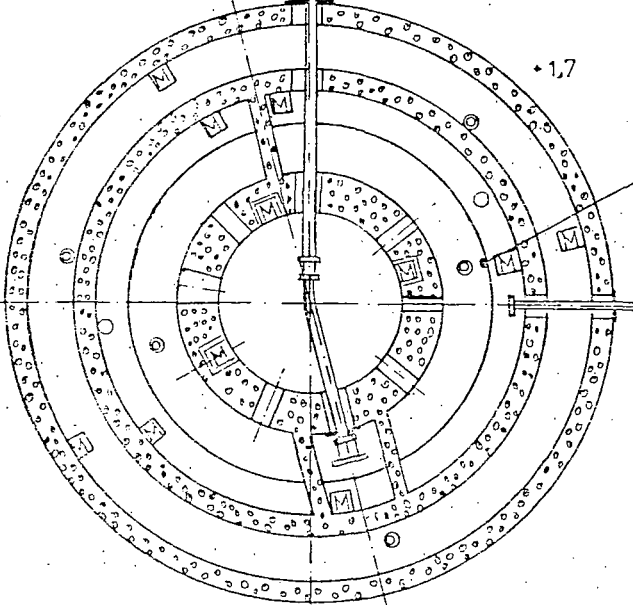


Fig. 8 Positions of measuring points		Compartment 6	
		Designation of measuring points	channel
		<p>6 TL 270 M 00</p>	<p>184</p>
		<p>6 TS 270 M 21 6 PS 270 M 21 M</p>	<p>185. 109</p>
		<p>6 WS</p>	<p>211</p>

Datum:

BATTELLE INSTITUT E. V. FRANKFURT AM MAIN

## 2.5 Consideration of Errors

### 2.5.1 Special events in the experiment

#### - Gap:

As explained in /4/, during the test a relatively small additional vent (cross section area = 236 cm<sup>2</sup> = blown out sealing + lasting, plastical deformation of the plate  $\cong$  2.7 % of the cross section areas of both specified orifices in compartment R4) has formed between compartment R4 and the dome compartment R9, caused by the overpressure in rupture compartment R4 at the upper cover (steel plate).

Originally, this gap should not be considered for the calculations (see arguments in /3/).

In May 1980 at the first meeting of the OECD-CSNI Working Group on Water Reactor Containment Safety the influence of gap on the results of SP-calculations was discussed with the help of some preliminary comparison plots with the results of "blind" predictions from international participants. The participants of the working group agreed that for the "open" calculations this additional gap (see fig. 9) should be accounted for. Therefore the experimentator suggested after examining the measured results, as a rough approximation a time function of the gap size as follows /7/:

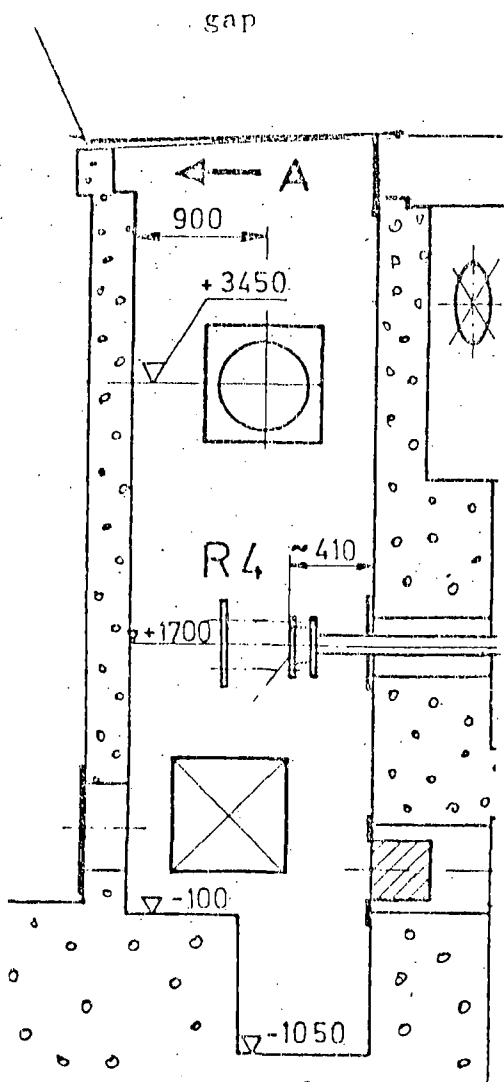
0 to 0.15 s : linear increase of gap size from 0 to 292 cm<sup>2</sup>  
0.15 to 1.5 s : constant gap size of 292 cm<sup>2</sup>  
1.5 to 5 s : linear decrease of gap size from 292 cm<sup>2</sup> to 236 cm<sup>2</sup>  
over 5 s : constant gap size of 236 cm<sup>2</sup>.

However, it results from a relation taken from Hütte I /11/ (vaulting of a rectangular plate under surface load: plate clamped at the back, supported at the sides, unfixed at the front) that a plate's maximum vault of 12 mm can be already caused by a differential pressure of 0.04 bar between R4 and R9. The experimental history of the differential pressure indicates that the maximum gap size of 292 cm<sup>2</sup> (immediately blown out sealing + maximum vault of the plate) might be already reached at 0.01 s and sustained until approximately 16 s.



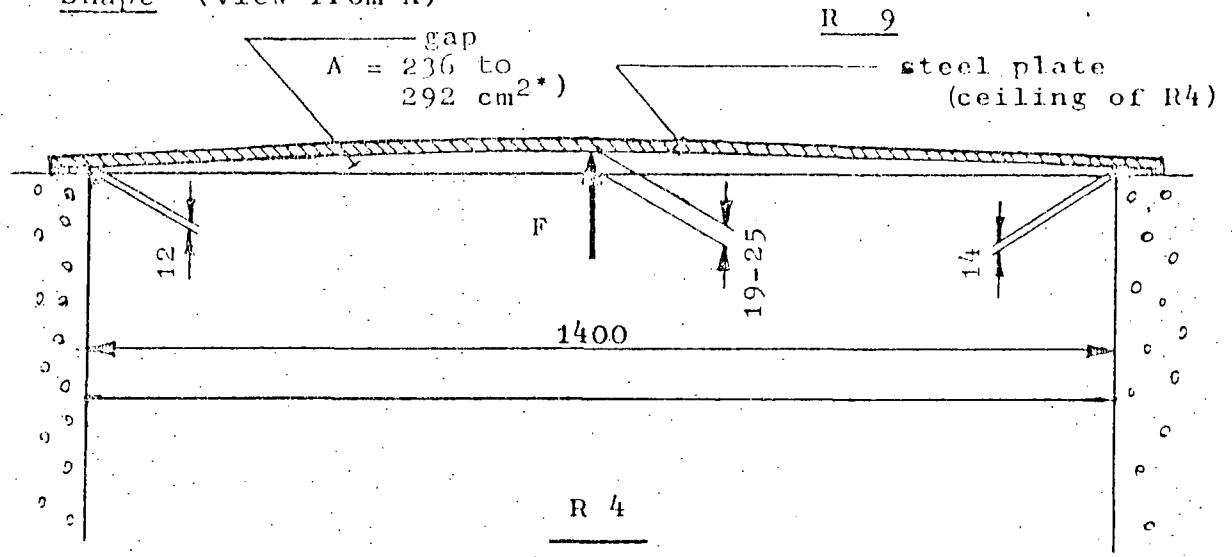
BETHLEEM-INGENIEURBÜRO FRANKFURT AM MAIN

Position



scale 1 : 50

Shape (view from A)



scale 1 : 10

- \*) 19 mm (236 cm<sup>2</sup>) without load acting on ceiling of R4
- 25 mm (292 cm<sup>2</sup>) maximum gap (load 30 ≥ kN)

Fig. 9 : Gap between compartments R4 and R9 after partial failure of a sealing (measures in mm)

- Non-insulation of high-pressure pipe:

Especially the part of the piping inside the containment (appr. 9.5 m; NW 150) leading to the rupture was not insulated during the test CASP2. This caused an increase of the containment initial temperatures. The lowest/highest measured results in the individual compartments amounted to:

$$\begin{aligned}T_{R4} &= 18.6 / 26.2 \text{ } ^\circ\text{C} \\T_{R5} &= 21.6 / 27.8 \text{ } ^\circ\text{C} \\T_{R7} &= 21.6 / 24.2 \text{ } ^\circ\text{C} \\T_{R8} &= 22.0 \text{ } ^\circ\text{C} \\T_{R9} &= 25.2 / 32.9 \text{ } ^\circ\text{C} \\T_{R9a} &= 18.2 / 29.7 \text{ } ^\circ\text{C} \\T_{R6} &= 26.6 \text{ } ^\circ\text{C}\end{aligned}$$

Compared to the mean values given in Chapter 2.2 the temperature in the individual compartments can deviate up to appr.  $\pm 5$  K. The question remains open of how much the structures were heated by it.

- Leakage in the high-pressure system:

Probably (over a longer period of time before the experiment) a small leak occurred in the high-pressure system inside the containment (centre of R9). This caused an increase in the relative humidity of the containment atmosphere to 100 % and probably also a slight condensation at the containment walls. In combination with the heat release from the high-pressure pipe the leak may also have contributed to the above-mentioned increase in initial temperatures of the compartments, and eventually of the walls.

- Reduced circulation:

It is to be assumed that shortly before the blowdown the circulation in the high-pressure pipe has been reduced considerably. In combination with the non-insulation this led to a relatively inhomogeneous distribution of initial temperature along the pipe (differences up to 35K) and probably to a vertical stratification of temperature, too (at measuring point I  $\Delta T \cong 30\text{K}$ ). Therein is certainly caused the appearance of a distinct 2nd maximum in the history of mass flow at 0.92 s, which was indicated in relatively good agreement between both drag bodies at measuring point II. Up to approximately 1 s the mass flow history depends very sensitively on the distribution of initial temperature along the pipe.

### 2.5.2 Measuring errors and geometric deviations

Table 6 shows the error bands of the initial conditions in the containment and the measured values in it, as well as the geometric deviations /6/, which were essentially estimated by Battelle-Institut.

Table 6: Measuring errors at the test CASP2

Measurand (range)	absolute error	relative error of measured value
$P_{Co}$	$\pm 0.005$ bar	$\pm 0.5$ %
$T_{oR4} - T_{oR9a}$	s. chap. 2.5.1	
PL ( $1 \div 4$ bar)	$\pm 0.025$ bar	
PD (0.5 bar)	$\pm 0.018$ bar	
PD (1 bar)	$\pm 0.02$ bar	
TS	$-2.5 \div +1.4$ K	
TW	$\pm 1.2$ K	
WS ( $7 \div 20$ cm)	$\pm 0.5$ cm	
$\Sigma WM_{\text{sump}}$	$\pm 345$ kg	
$WM_{\text{integral}}$	$\pm 57$ kg	$\pm 1.4$ %
V		$\pm 1.5$ %
$A_{\text{cond.}}$		$\pm 5$ %
$A_{\text{Ü}}$		$\pm 0.5$ %

In addition to the errors given in table 6 and the uncertainty concerning the thickness of the coating of the concrete walls (see table 3) there are other parameters to the containment calculations which are still uncertain:

- thickness of the heat absorbing or heat releasing metal structures,
- density, thermal conductivity, and specific heat capacity of the con-

crete coating (acc. to manufacturer:  $\pm 10 \%$ ),

- density, thermal conductivity, and specific heat capacity of the concrete (taken from the literature for pure, dry gravelly concrete:  $\rho = 2200 \text{ kg/m}^3$ ,  $\lambda = 1.28 \text{ W/(mK)}$ ,  $c = 879 \text{ J/(kgK)}$ ; because of steel reinforcement described in /1, 2/:  $\rho = 2200 \text{ kg/m}^3$ ,  $\lambda = 1.73 \text{ W/(mK)}$ ,  $c = 960 \text{ J/(kgK)}$ ; steel reinforcement beginning 20 to 30 mm off the surface),
- density, thermal conductivity, and specific heat capacity of the metal structures,
- temperature and other dependencies of transport properties.

In general, errors of variables measured in containment are small and most of the time within the oscillatory margins of the measured variables. Therefore, in the comparative plots they are not shown as errorbands but only as bars according to scale to improve comparability of experimental errors with the calculational bandwidths.

For pure containment problems the uncertainty in calculating mass flow rate and specific enthalpy at the break in the primary system with blow-down codes is atypical. To reduce this, both variables are determined from measurements. For reasons of uniformity in the boundary conditions, it was suggested /3/ basing the SP-calculations on their nominal values. As far as the participants communicated on this, these values were used.

In figs. 10, 11, 12 and 13 these values are depicted along with their error bandwidths estimated by Battelle-Institut. The errors are lower than the ones of the test D15 on which the first Containment-SP was based. However, within certain time intervals they are to be described as relatively high, especially in regards to SP.

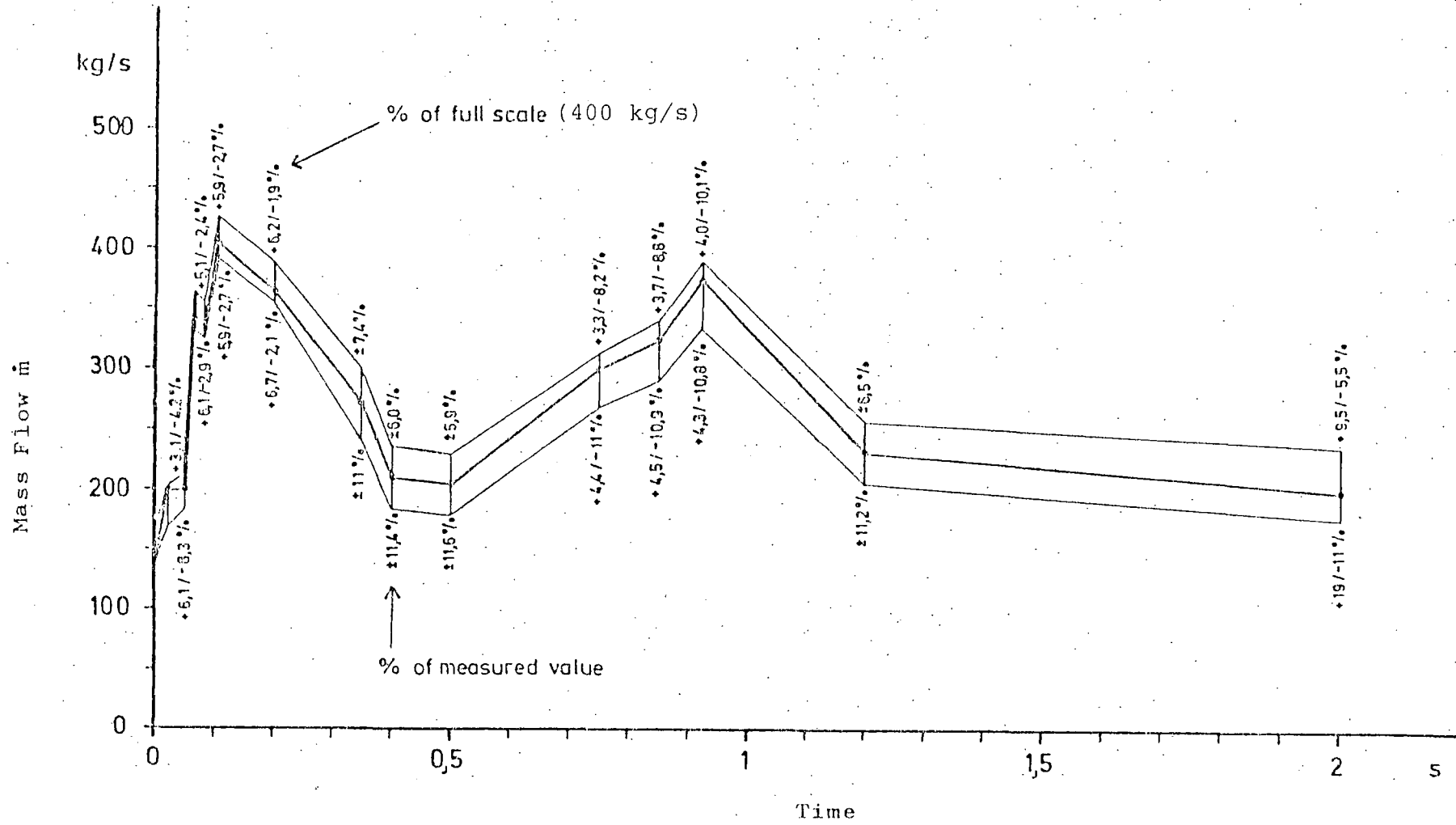


Fig. 10 : Break mass flow  $\dot{m}$  with error band (experiment D16/CASP2)

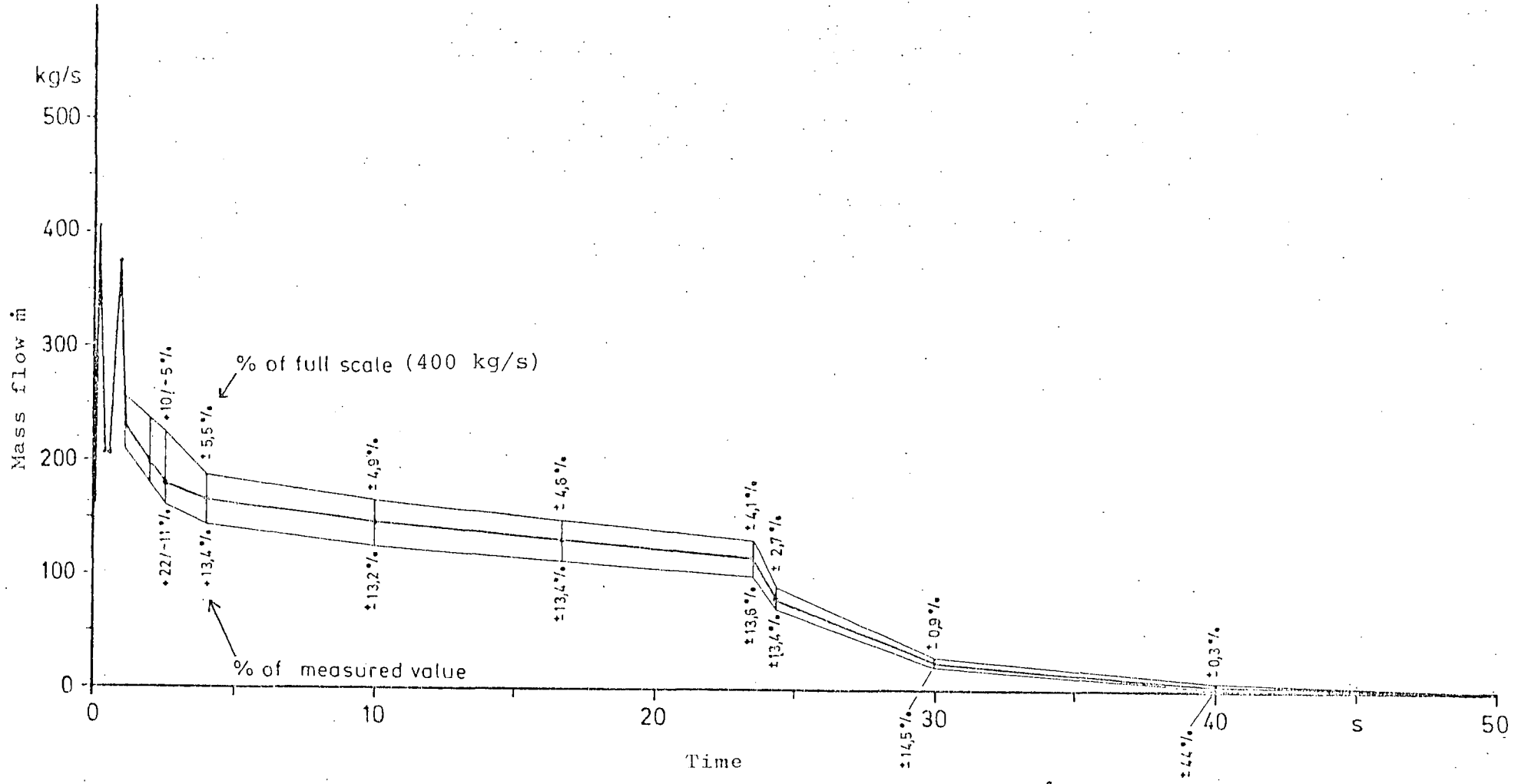


Fig. 11 : Break mass flow  $\dot{m}$  with error band (experiment D16/CASP2)

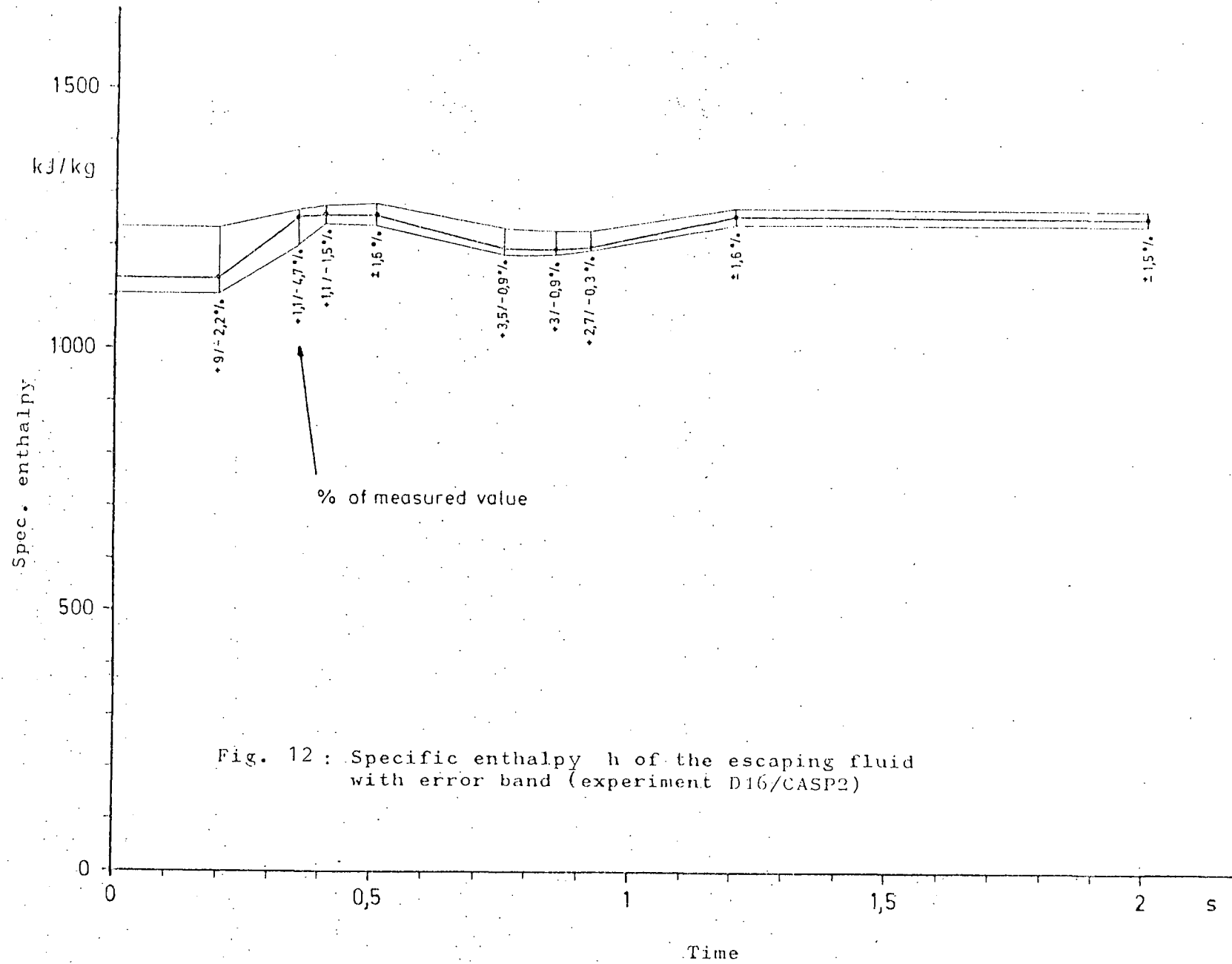


Fig. 12 : Specific enthalpy  $h$  of the escaping fluid with error band (experiment D16/CASP2)

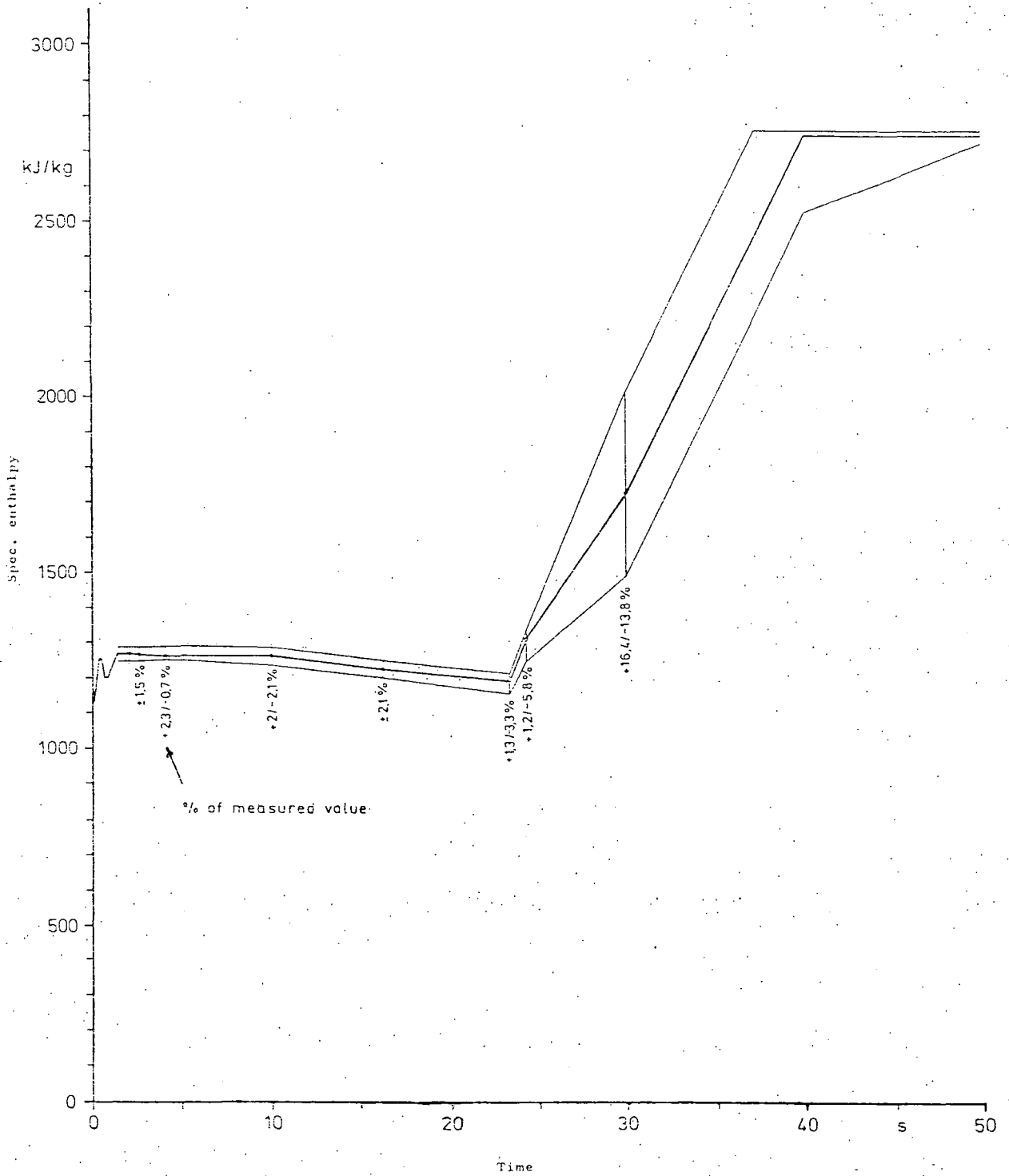


Fig.13: Specific enthalpy  $h$  of the escaping fluid with error band (experiment D16/CASP2).



### 2.5.3 Effects of deviations from nominal values

With few exceptions the SP participants based the calculations on the nominal values listed in chapters 2.1 to 2.3. In this chapter the effects of the deviations described in chapters 2.5.1 and 2.5.2 on the calculational results shall be considered somewhat more closely. Results concerning these effects are mainly supported by estimates and parameter studies as far as given by the experimentator (see /6/) and participants of the SP (Australia, Belgium, F.R. Germany, Sweden, United Kingdom).

These are supposed to better safeguard and interpret the results. Regarding the most important deviations, mostly quantitative statements could be found. However, the investigations carried out here are to be more understood as a starting point, in respect to a more systematic analysis of other important values.

#### 2.5.3.1 Time interval 0 to 2.5 s

For the time interval 0 to 2.5 s parameter studies are available:

- on the influence of the gap (see also chapt. 2.5.1):

With the aid of code ZOCO VI, Battelle-Institut determined (see fig. 14 from /6/) that for a gap size of  $236 \text{ cm}^2 = \text{const (t)}$  the calculational results without gap for the following variables are higher in percentage than the calculational results with gap (related to pressure built-up, respectively pressure difference of calculational results with gap):

calculated variable	1st maximum	2nd maximum
$P_{R4}$	3.4 %	6.8 %
$P_{R5, R7}$	2.2 %	6 %
$\Delta P_{R4-R9}$	3.9 %	8.3 %
$\Delta P_{R4-R5, R4-R7}$	0	3.8 %
$\Delta P_{R5-R9, R7-R8}$	2.7 %	8.8 %

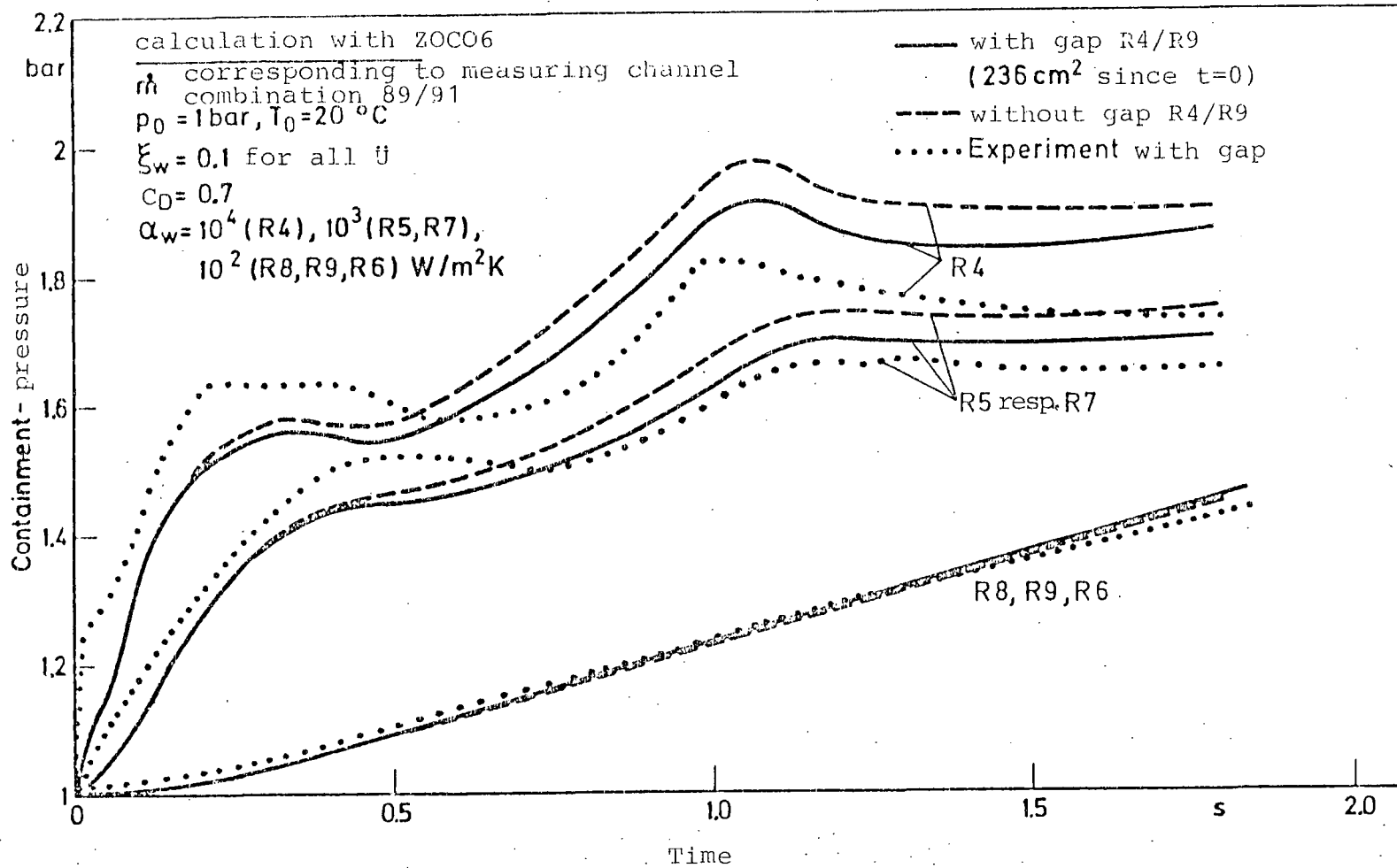


Fig. 14: Model calculations on the influence of gap R4/R9 on pressure build-up

The maximum pressure differences calculated by the computer program COPTA (Sweden) /34/, neglecting the gap formed between R4 and R9, increased with 0.01 to 0.05 bar and the pressure in compartment R4 at 2.5 s with approximately 0.02 bar.

The calculational results of the SP participants not considering the gap (F.R. Germany, Netherlands) would have to be systematically decreased. Different computer codes (differing simplifications) and similar computer codes (differing input assumptions) would very likely result in differing outcomes. In comparison to the influence of other errors (for example the boundary conditions, see below) this systematic influence, approximately determined in size, is nonetheless to be described as of minor importance.

- on the influence of the error bandwidths of the boundary conditions: On the basis of the information in figs. 10 and 12 the experimentator also computed the influence of the boundary conditions' error bandwidths for the lower limit of errors /6/. Hereby receiving the following deviations in percentage (related to pressure built-up or pressure difference of the calculation without gap and nominal values according to table 4):

calculated variable	1st maximum	2nd maximum
$P_{R4}$	-9.5 %	-12.6 %
$\Delta P_{R4-R9}$	-8.9 %	-14.1 %

The results of a calculation with code COFLOW (see /12/) (also for the lower limit of errors without consideration of gap) for the 2nd maximum concur favourably with the experimentator's results. For the 1st maximum the results are somewhat higher than the ones in the computation of Battelle-Institut:

calculated variable	1st maximum	2nd maximum
$P_{R4}$	-12.3 %	-14.4 %
$\Delta P_{R4-R9}$	-12.6 %	-16.0 %
$P_{R9}(2.5 \text{ s})$	-12.2 %	

A corresponding COFLOW-calculation for the upper limit of error indicates for the 1st maximum higher deviations than for the lower limit of error, caused by the higher upper limits of error of the spec. enthalpy and of the mass flow at the rupture site between 0 and 0.2 s. For the 2nd maximum the values are in approximate agreement:

calculated variable	1st maximum	2nd maximum
$P_{R4}$	+23.0 %	+15.0 %
$\Delta P_{R4-R9}$	+23.6 %	+15.3 %
$P_{R9}(2.5 \text{ s})$	+15.7 %	

In figs. 15, 16 and 17 taken from /12/ the influence of the boundary conditions' upper and lower limits of error, as it was computed by COFLOW, is shown for the history of selected quantities.

Under the assumption that the measured curves correspond to the nominal values of the boundary conditions and that the effects of deviations from nominal values on the experiment (with gap) are identical percentagewise with those of an assumed COFLOW-calculation (with gap), in addition arrows related to experiment are drawn to scale. They indicate in the order of magnitude at selected points in time, how much higher/ lower the experimental results could have been, if not the nominal energy but the upper or lower limits of it had flown in the containment.

# 2<sup>ND</sup> CONTAINMENT STANDARD PROBLEM (CASP 2)

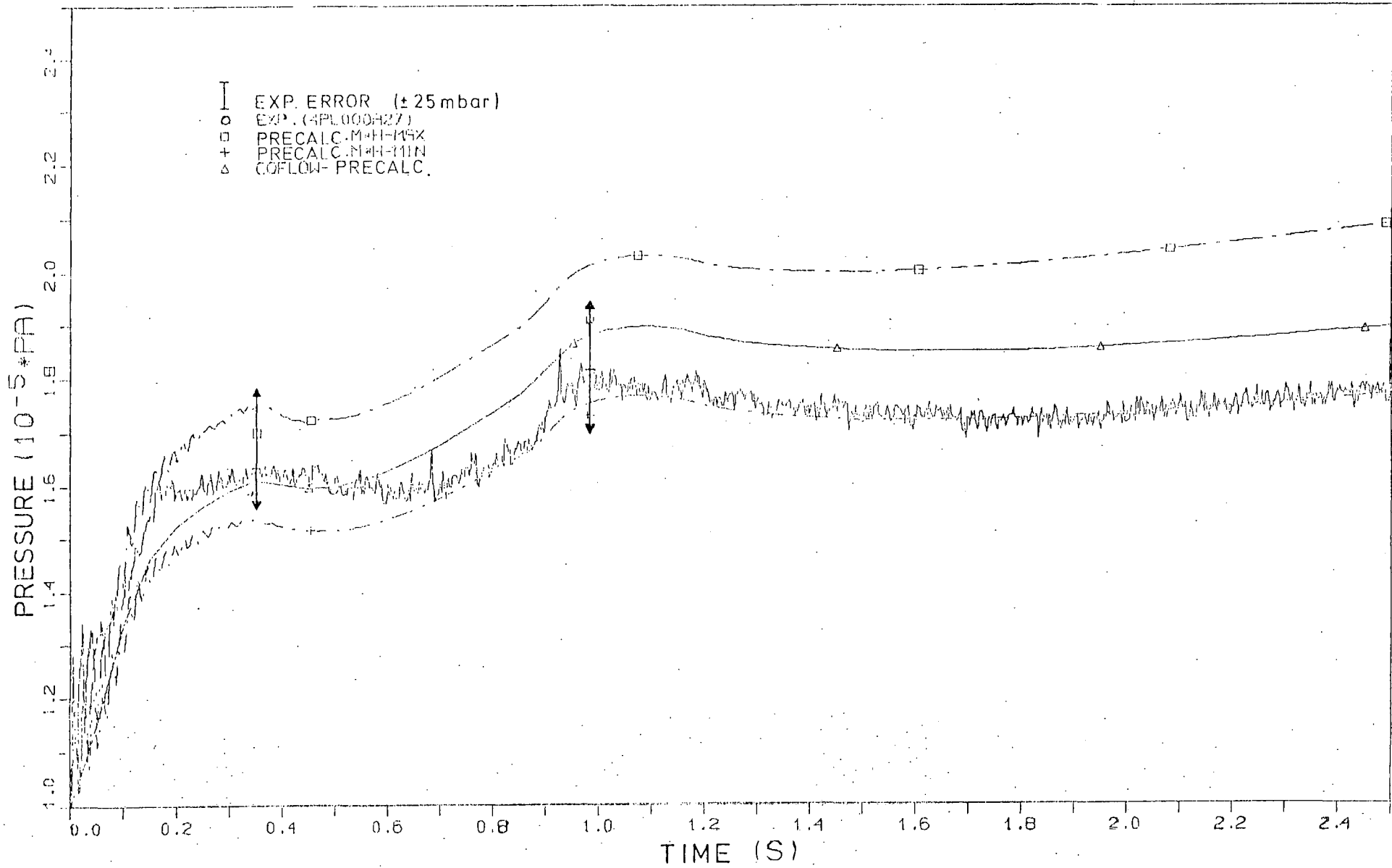


FIG. 15: PRESSURE HISTOR IN COMPARTMENT R4

# 2<sup>ND</sup> CONTAINMENT STANDARD PROBLEM (CASP 2)

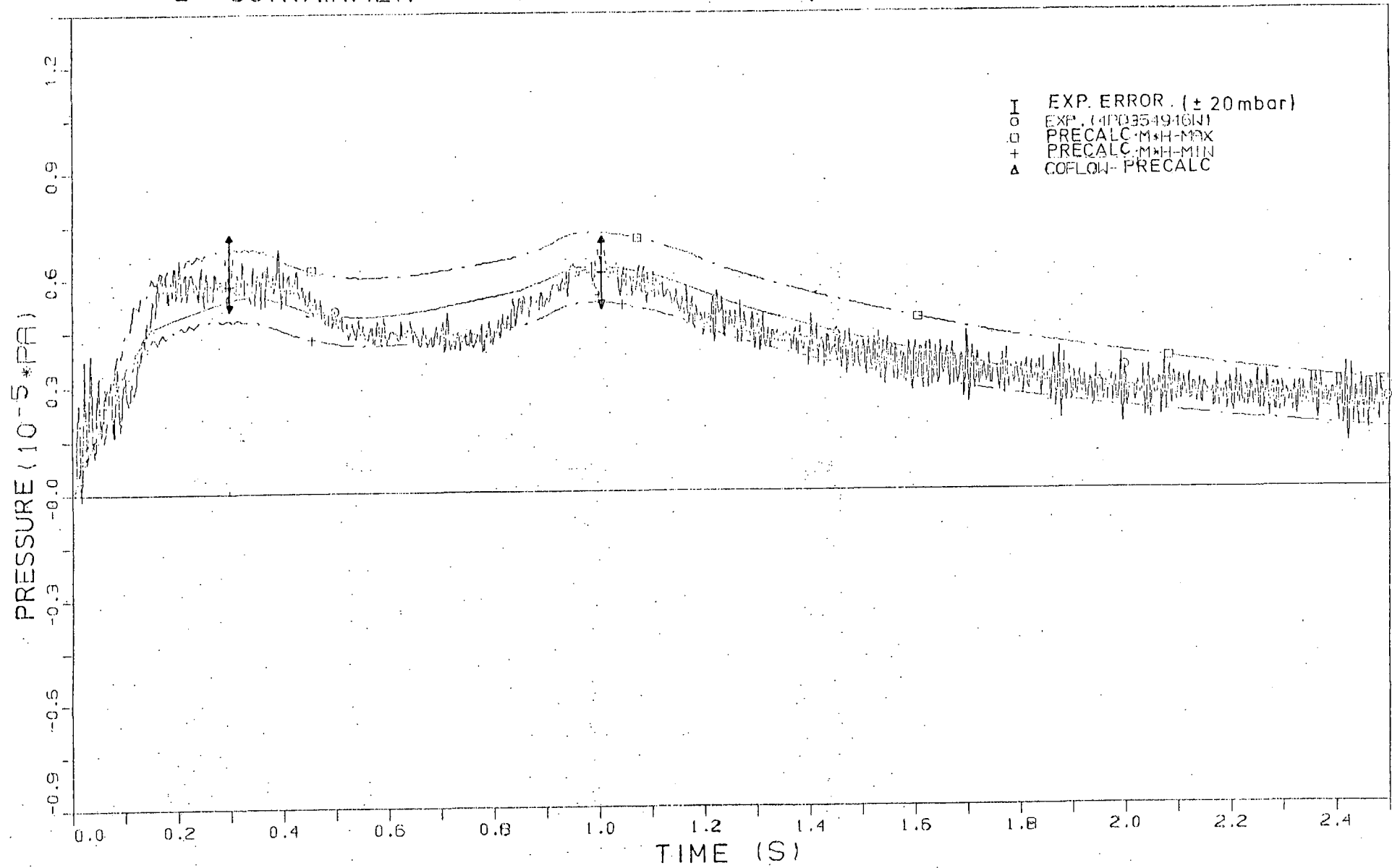


FIG. 16: HISTORY OF PRESSURE DIFFERENCE R4 - R9

# 2<sup>ND</sup> CONTAINMENT STANDARD PROBLEM (CASP 2)

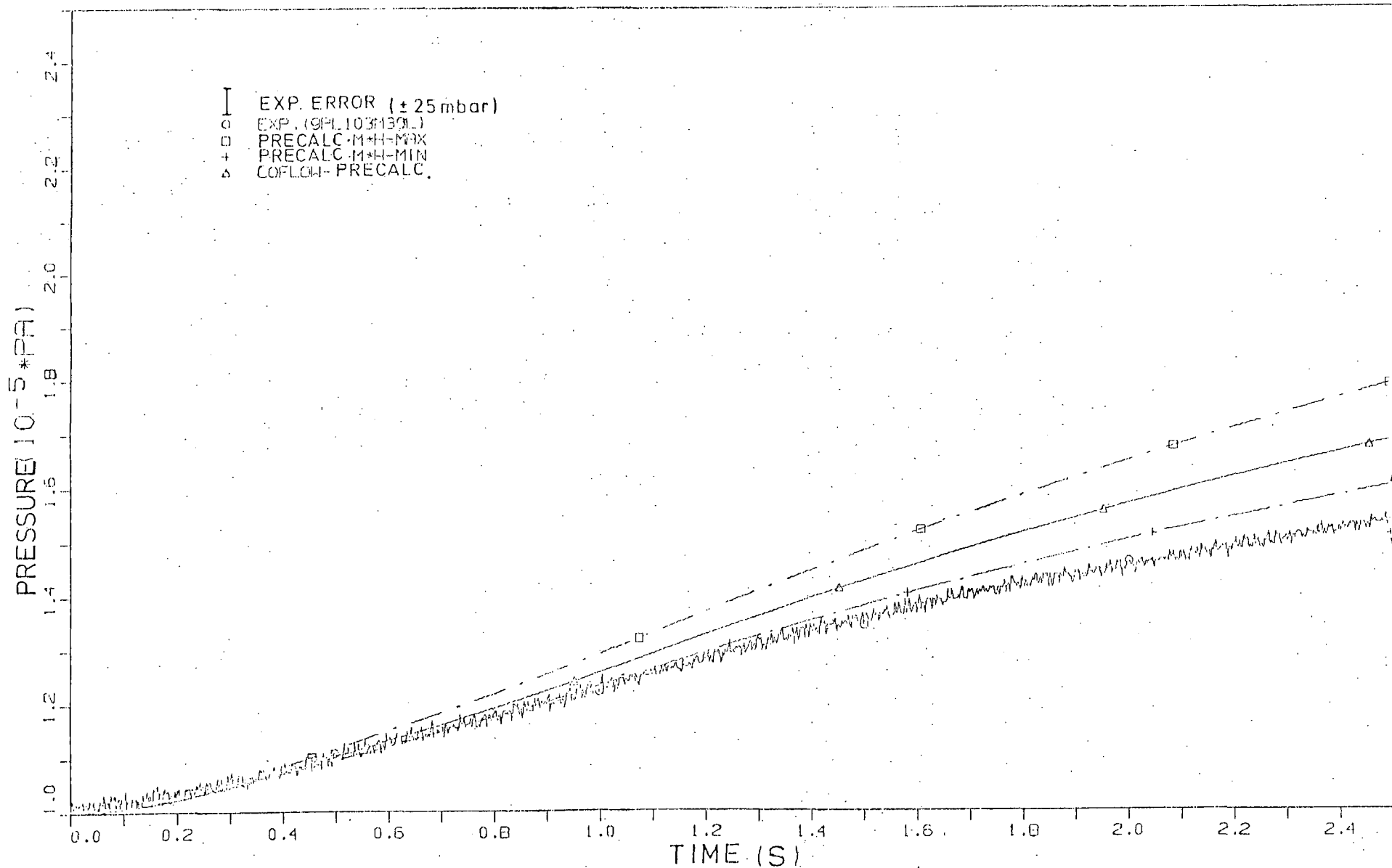


FIG. 17: PRESSURE HISTORY IN COMPARTMENT R9

Nonetheless one has to add that by the approach applied above systematic errors are treated like accidental errors. The share of systematic errors more or less eludes analysis. Therefore, the most certainly, smaller effects on the calculations resulting from accidental errors cannot be quantitatively considered.

- on the influence of geometric deviations and of uncertainty concerning initial temperature of walls:

In a further computation with the boundary conditions' upper limit of error additional changes were made in light of a high pressure built-up in R4 respectively, a high pressure difference between R4 and R9: the volumes (-1.5 % in R4, +1.5 % in R9), the structural surfaces (-1 % in R4, +1 % in R9), orifice cross-sections (-0.5 % in Ü45, Ü47 and Ü59B, Ü78B), and the initial temperatures of walls (+3K in R4, -3K in R9).

The effects of the additional changes on the parameters shown in figs. 15, 16 and 17 differ hardly from those resulting from the calculation with the upper limits of error of boundary conditions (see /12/).

The influence of the uncertainty in the concrete coating's thickness is to be regarded as minor in this time interval (see chapter 2.5.3.2, fig. 18 at 4 s). On the somewhat uncertain parameters given in chapter 2.5.2 the following might have a not at all negligible influence on containment variables in this time interval, namely the thickness of metal structures, the transport properties of the concrete coating, and a higher error in condensation surface areas.

### 2.5.3.2 Time interval 0 to 50 s

For the time interval 0 to 50 s parameter studies are available:

- on the influence of the boundary conditions' error bandwidths, including geometric deviations and uncertainty in the structures' initial temperature:

The history of containment pressure (after appr. 16 s pressure compensation in the whole containment) mainly depends on the total enthalpy flown in and the heat transfer to the structures (high surface



area/ volume ratio of  $\cong 1.8$  in model containment,  $\cong 0.4$  in an operating reactor). Compared to a postcalculation with nominal values and a mean coating thickness of concrete of  $s = 0.95$  mm (= reference calculation), another postcalculation was realized with increasing the break mass flow of +1.4 %, with an associated specific enthalpy according to the upper limit (on the average  $\cong +4.5$  %), and the initial temperature of the structures of +3K. Similarly the structural surfaces were decreased -1 % as well as the containment volumes -1.5 %. These systematic changes were to be expected to cause a high containment pressure. The result can be seen in fig. 18 from /12/. Maximum containment pressure is appr. 0.39 bar or related to the pressure built-up of the reference calculation appr. 12.2 % higher.

- on the influence of a deviation in the initial temperature of the structures:

In /12a/ among others two postcalculations can be found only differing in initial temperatures (23 °C and 12 °C). Maximum containment pressure is appr. 0.1 bar higher in the calculation with higher temperature. This result is in accordance with a parameter study on steam-blowdown experiments D10 and D15 /13/ ( $\Delta T \cong 11K \rightarrow \Delta P_{\max} \cong 0.1$  bar). With a possible deviation of  $\pm 5K$  at the maximum, resp. of  $\pm 4K$  on the average during experiment CASP2 (see chapter 2.5.1) one can anticipate that only from this the maximum containment pressure can deviate by appr.  $\pm 0.05$  bar resp. appr.  $\pm 0.04$  bar. Since the heat penetration of the structures is probably less than maximum, the deviation will more likely be close to the lower limit.

- on the influence of uncertainty in the thickness of coating:

Fig. 18 also shows the results of COFLOW-postcalculations considering the uncertainty in the thickness of concrete coating (see table 3). The application of the lower resp. upper limit ( $s = 0.7$  mm resp.  $s = 1.2$  mm) as supplied by Battelle-institut results in well perceptible deviations from the reference calculation in the amount of -0.15 bar, resp. +0.08 bar (concerning the maximum pressure) or related to the pressure built-up in the reference calculation -4.7 %, resp. +2.4 %.

In fig. 18 the above-mentioned influences on the maximum pressure in the containment (with the exception of initial temperature) are drawn as ar-

rows to scale under the assumption that the computed deviations are valid percentagewise for the experimental results. Parameter studies concerning the influence of coating thickness have also been conducted by Australia; by reducing the coating thickness of 1.2 mm by 25 % the maximum pressure of the dome compartment R9 was reduced by 1.3 %. The gap certainly does not play an important role in the overall pressure built-up. Additional cases worth examining in this time interval may be:

- corresponding maximum lower limit for containment pressure,
- a higher deviation in structural surfaces,
- separate consideration of the boundary conditions' error bandwidths and geometric deviations,
- deviations in the transport properties of the concrete coating,
- deviations in the transport properties of concrete,
- deviations in the thickness of metal structures.

Concerning the manner of maximum error consideration the statements for time interval 0 to 2.5 s should also be pointed to in this time interval (0 to 50 s).

## 2<sup>ND</sup> CONTAINMENT STANDARD PROBLEM (CASP 2)

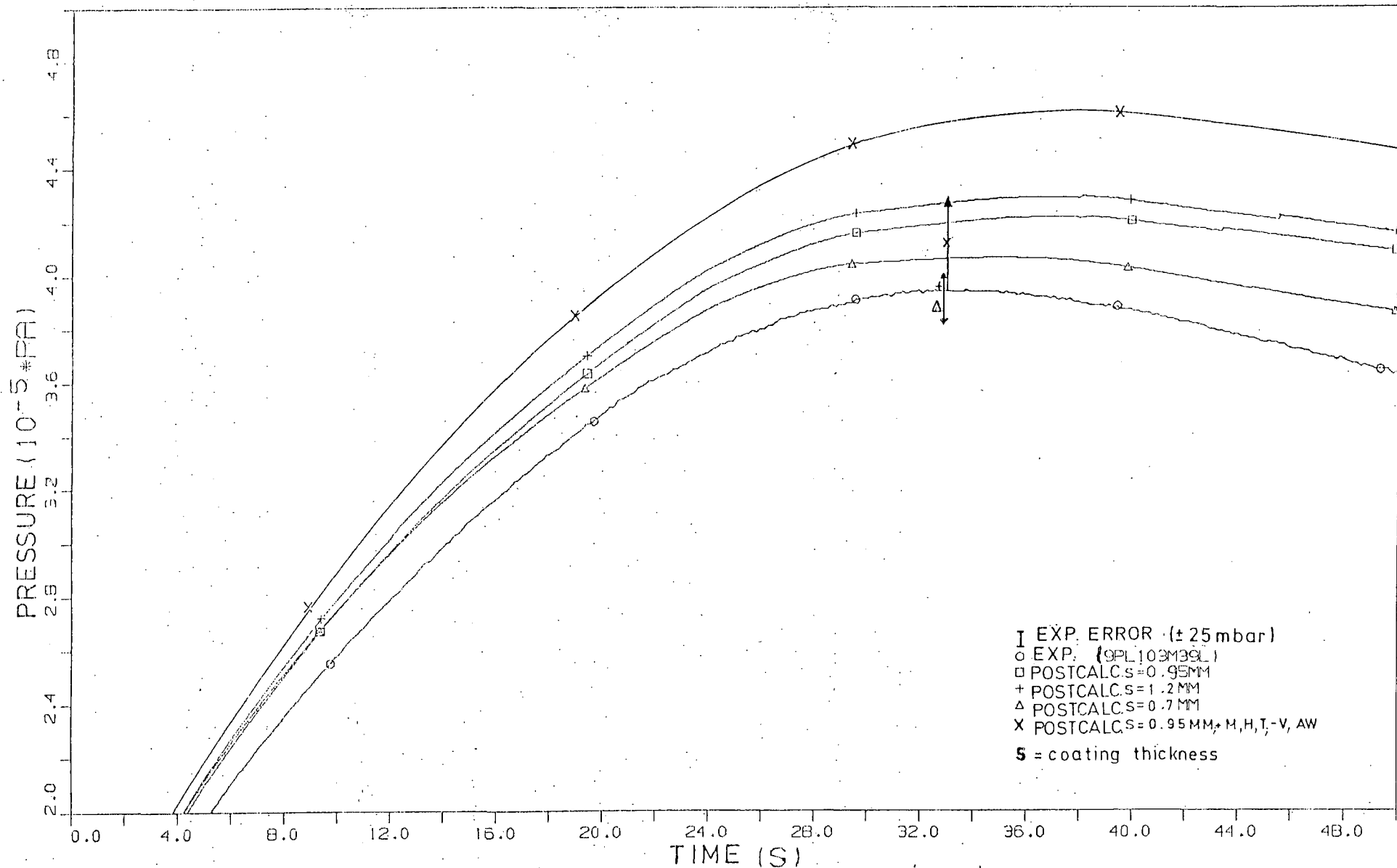


FIG. 18: PRESSURE HISTORY IN COMPARTMENT R9

## 2.6 Variables to be Calculated

As stated in /2/, corresponding to distinct measuring point positions, each SP participant should best-estimate post-calculate the following variables as function of time;

for time interval 0 to 2.5 s:

- 1 pressure in each compartment
- 7 pressure differences between different compartments
- 3 temperatures each in compartments R4, R5, R7
- 2 temperatures each in compartments R8, R9
- 1 temperature in compartment R6

for time interval 0 to 50 s:

- 1 pressure each in compartments R4, R5, R7, R9
- 1 temperature each in compartments R4, R5, R7, R8, R6
- 2 temperatures in compartment R9

for time interval 0 to 1000 s:

- pressure in compartment R9
- 2 temperatures in compartment R9
- water mass in the whole containment.

### 3 PRESENTATION OF RESULTS

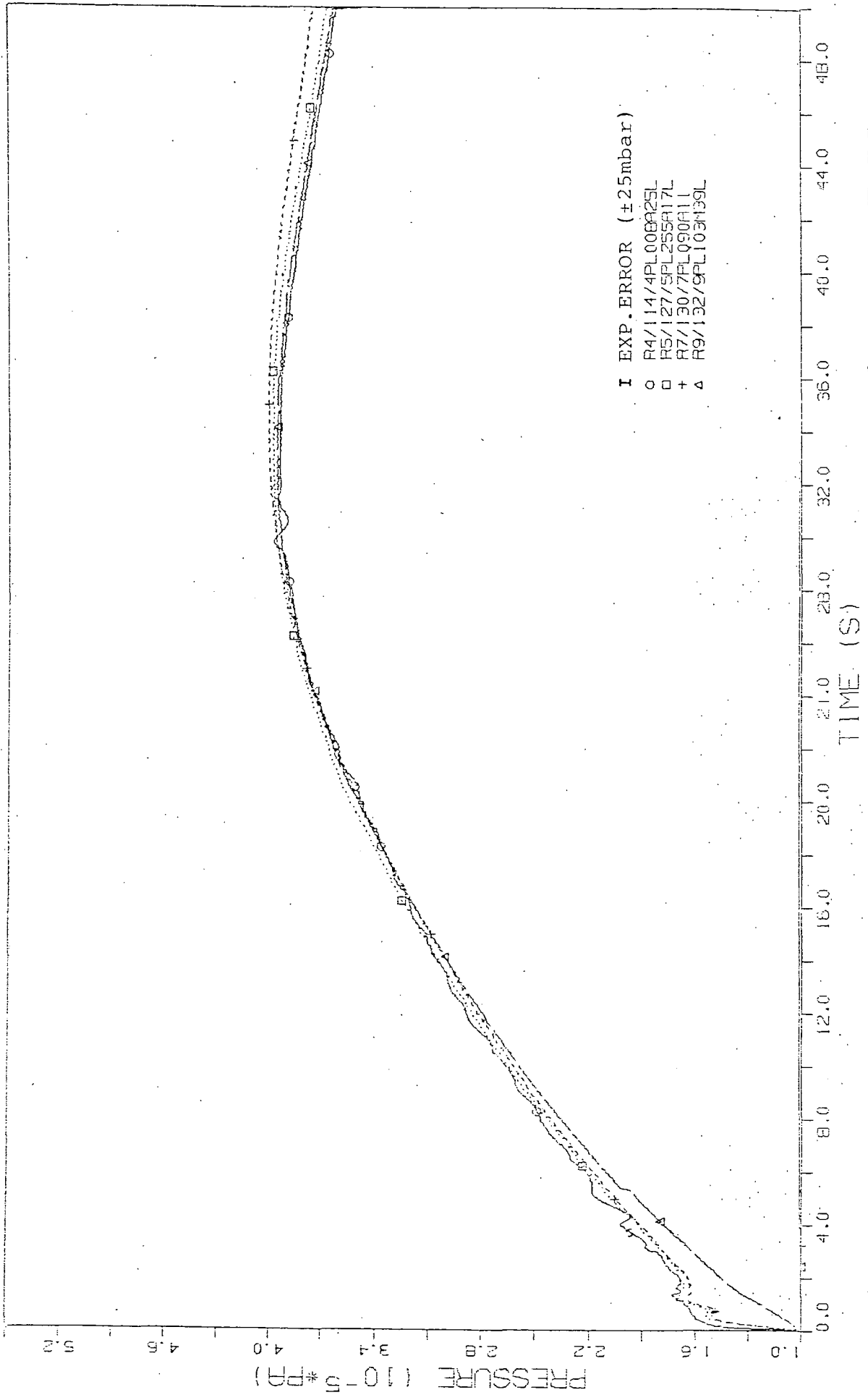
#### 3.1 Comments on the Experimental Results and Deductions for the Comparison

---

In /8/ some explanations are given with regard to minor changes with some specified measuring points and to measuring errors for a few specified parameters. Also the measured results are - as far as possible - depicted in the scales used here and in the comparison report to the first Containment-SP. Thereby a direct comparison between both Containment-SP is possible on what concerns error bandwidths of measurements and, especially, bandwidths of calculations. In chapter 3.8 this will be treated in somewhat more detail.

The pressures measured in all compartments for time interval 0 to 50 s are jointly shown in fig. 19 for the purpose of visualizing extensive pressure equalization in the containment after about 5 s. The diagram also demonstrates that in view of total pressure built-up in the containment identical scales for both Containment SP can be used without any loss of information even if the pressure range 1.0 to 2.0 bar (corresponding to 0 to about 5 s) is omitted.

OECD-CSNI CONTAINMENT STANDARD PROBLEM NO.2 (TEST CASP2)



I EXP.ERROR ( $\pm 25$ mbar)  
o R4/1114/4PL00BA25L  
□ R5/127/5PL255A17L  
+ R7/130/7PL090A11  
△ R9/132/9PL103M39L

FIG. 19. PRESSURE HISTORY IN COMPARTMENTS R4, R5, R7, R9

### 3.2 Selection of Important Variables

As stated in the specification a number of variables was to be calculated. For assessment of the results it seems necessary only to consider important variables. All variables additionally wanted become important, especially when deviations are to be analysed more exactly and more individually. In the following a brief argumentation for selection made (mostly in parentheses) is given. Fluid temperatures instead of wall temperatures not measured in this test, give an approximate indication on the temperature loads the walls are exposed to.

Time interval 0 to 2.5 s:

Pressure: 1 pressure each (pressure differences within a compartment are negligibly small)

- in rupture compartment R4 (compartment with the highest pressure built-up)
- in first follow-up compartment R5 (highest but one pressure built-up, after flowing from R4 through orifice U45)
- in dome compartment R9 (energy sink with slowest and time-delayed pressure built-up)

Pressure difference:

- between R4 and R9 (highest pressure difference)
- between R4 and R5 (outflow from rupture compartment R4)
- between R5 and R7 (information about influence of different heat transfer and different water carry-over on pressure built-up at different outflow conditions)
- between R5 and R9 (outflow upwards after short flow path)
- between R7 and R8 (outflow downwards after long flow path)

Temperature: Because of differences expected inside the compartments

- 2 temperatures in rupture compartment R4 (highest temperature load)
- 2 temperatures in compartment R5 (highest but one temperature, long dead end)
- 2 temperatures in compartment R7 (short dead end)

- 2 temperatures in compartment R8 (half a dead end)
- 1 temperature each in compartments R6 and R9 (slowest, approx. the same temperature built-up)

Time interval 0 to 50 s:

Pressure: Within this interval the maximum pressure in the whole containment and pressure equalization between all compartments occur. The following pressures are selected as the most important variables:

- in rupture compartment R4 and
- in dome compartment R9.

Temperature: Within this interval the maximum temperatures and extensive temperature equalization occur in each compartment except in R9. The following temperatures are selected as the most important variables:

- in rupture compartment R4 (similar in R5, R7)
- in compartment R8
- in dead end compartment R6
- 2 temperatures in dome compartment R9 (beginning of the temperature stratification)

Time interval 0 to 1000 s:

According to specification pressure-, temperature- (represented by R9), and water mass history in the whole containment during the cooling-down phase.

### 3.3 Listing of Important Features and Input Parameters of the Codes Used

Table 7 combines for various time intervals important features and assumptions of computer programs used by individual participants. This was possible as far as they could be taken from short reports and letters (12 participants) and supplementary information after the workshop.

Calculation results for all 3 specified time intervals were submitted by all participants except Finland (not for 0 - 50 s).



Table 7: Important features and input parameters of codes

$A$  = surface area       $m_A$  = air mass       $V$  = volume       $\Delta T$  = temperature difference       $C_{wc}$  = water flow quality homogeneous upstream node quality  
 $C_D$  = discharge coefficient       $m_V$  = vapour mass       $\Delta P$  = pressure difference       $C_{WA}$  = water separation factor  
 $E_k$  = kinetic energy       $n$  = number of orifices       $\zeta$  = pressure loss coefficient       $T_o$  = initial temperature  
 $H$  = total enthalpy       $R$  = compartment       $\epsilon_w$  = water carry-over factor = transportable mass of water in node  
 $htc$  = heat transfer coefficient       $t$  = time       $F_w$  = water mass flow total mass flow  
 $\eta_w$  = water in mixture flow

Country	Computer Code	Time Interval (s)	Number of Nodes	Water Transport	Orifice Flow		Heat Transfer to Structures correlation acc. to.....		Computer	Computer Time (s)	Other Remarks
					Concept	Coefficients	[ $htc:W/(m^2K)$ ]	coating thickness			
Australia	ZOCO V	0-2.5	6	$\epsilon_w = 0$	compressible flow	$C_D = 1$	Henderson and Marchello	concr. filler = 1 mm surface coating = 0.2 mm	IBM 370/3031	70.2	gapsize=264 cm <sup>2</sup>
		0-50								1306	
		0-1000								15109	
Belgium	TRAP-SCO	0-2.5	6	$C_{WC}$ depends on time (see chapt 3.5)	Fauske subcrit. flow model (i.e.: isentr. expansion f. the vapour phase, incompr. flow f. the liq. phase)	$C_{D4-5,4-7} = 1.5$ $= 1.0$ $C_{D5-9,7-8,8-9,6-9,4-9}$	no (spec. enthalpy input reduced by 0 to 7.5%)	IBM 370/3031	34.5	gapsize = 292 cm <sup>2</sup>	
	TRAP-CON	0-50 0-1000	1	break flow flashing	---	---	Tagami-Uchida	0.2 mm	25.5	condensation film thickness $\leq$ 1mm	
Canada	PRESCON-2	0-2.5	6	$\epsilon_w = 0.5$ $\epsilon_w = 1$	one dimensional momentum equation, hom. flow	$\zeta = 2.85$	1300	0.2 mm	CDC CYBER 170 model 175	12	gapsize = 292 cm <sup>2</sup>
		0-50								20	
		0-1000								1.7	
Finland	RELAP4/MOD5	0-2.5	9(R4,R5,R7:2; R6,R8,R9:1)	$\epsilon_w = 0$	compres. single stream flow with momentum flux	$\epsilon_{4-7,4-5,7-8,5-9}$ $\epsilon_{8-9} = 2.77$ $\epsilon_{9-6} = 2.81$	40 x Dittus-Bölder (liquid forced convection) see fig. 20	CDC CYBER 170	90	gapsize = F(t) (see $E_k \neq 0$ chapt. 3.5) complete separation of phases in each control volume (both phases have same temperatures)	
	CONTEMPT-LT/026 (MOD.)	0-1000	1	---	---	---	all structures; 0-2.5s: lin. incr. from 45.4+10000 2.5-50s: 10000 50-1000s: Uchida	IBM 370/168	264	pool region and gaseous region may have different temperatures	
France	GRUYER	0-2.5	5(R4,R5,R7,R8:1; R6+R9:1)	$\epsilon_w = 1$	steady state adiabatic flow; isentropic expansion; no friction hom. frozen model	$C_D = f(\text{mass gas quality}) > 1$	ECOTRA (see App.2)	0.7 mm	IBM 168	80	gapsize = F(t) $E_k = 0$
		0-37	4(R4,R5,R7:1; R6+R8+R9:1)	$\epsilon_w = 0.5$ $\epsilon_w = 0.25$ $\epsilon_w = 0.75$	$C_{D4-5} C_{D4-7} = 1.2$ $C_{D5-9} C_{D4-9} = 1.1$	$E_k = 0$ "blind" calculation					
		0-1000	1	---	---	$t < 50s: 1300$ $t > 50s: htc = 1.5(\Delta T)^{0.5}$ f. warmer walls; 11.3+454 ( $\frac{m_V}{m_A}$ ) and Uchida f. colder walls				IBM30-33	11

Table 2 (continued)

Germany	COFLOH	0-2.5	3(R4,R5,R7:1; R8 :2; R6,R9 :1)	$\epsilon_w = 0$	between rooms; quasi-stationary compr. orifice flow (hom. without slip) within room: one-dimensional, instat. in-compr. flow with friction	$C_D = C_D \times f \left( \frac{P_2}{P_1} \right)$ (Jobson)	R4(1500), R5(1500, 2X100), R7(1500, 2X100), f. rest (100); f. steel and concrete = const(t); f. atm(10)	0.95 mm	AMDAHL 470V/5	140	without gap "blind" calcul. f. German SP 3 $E_K = 0, T_0 = 20^\circ C$
		0-50	5(R4,R5,R7:1; R6+R8+R9:1; ATM.:1)	$\epsilon_w = 0$			$C_{Dinc} = 0.65$ (incr=incompressible)			Tagami-Uchida (htcconcrete = htcsteel) htc_max = 1200	630
	CONDRO	0-1000	1	---	---	---	0-34s : Tagami X 6 34s - 1000s : Uchida htc_max = 8000 (steel) htc_max = 3200 (concrete)	0.70 mm	---	260	$T_0 = 20^\circ C$ (solid) $25^\circ C$ (air); 0-34 s: thermodyn. nonequilibrium 34-1000 s: thermodyn. equilibrium
Italy (CIEN/Pisa)	ARIANNA-0	0-2.5	4(R4,R5,R7:1; R6+R8+R9:1)	$\epsilon_w = 0$	Moody-Model	$C_D = 0.6$	see fig. 21	0.25mm ( $\lambda = 0.32$ W/mK)	IBM 370/158	204	gapsize = F(t)
		0-50	---	---						---	
	CONEMPT-LT/026	0-1000	2(R4+R5+R7:1; R6+R8+R9:1)	$\epsilon_w = 0$	ideal gas orifice flow model	---	as above up to 40 s then lin. decr. to 20 at t=1000s	---	---	2460	---
Italy (NIRA)	PACO	0-2.5	6	$\epsilon_w = 0.7$ $\epsilon_w = 0.2$	isentropic flow	$C_D = 1.0$	lin. incr. to 10000 f. R4, R5, R7, R8	1.2mm ( $\lambda = \lambda$ )	IBM 370/168	170	gapsize = 292 cm <sup>2</sup>
		0-50	6	$\epsilon_w = 1$ $\epsilon_w = 1$			Uchida f. R6, R9			750	
		0-1000	1	---			2510 up to 50s then Uchida			54	
Japan	RELAP4/MOD5	0-2.5	6	---	one dimensional steady state incompressible flow	$\zeta = 2.85$ $C_D = 1.0$	2000	---	FACOM M-200	16.89	gapsize = 240 cm <sup>2</sup> complete phase separation is assumed
		0-50	2(R4+R5+R7:1; R6+R8+R9:1)	---			1700			70.50	
		0-1000	---	---			---			205.29	
Netherlands	ZOCO V(MOD.)	0-2.5	11(R4 :3; R5,R7,R8:2; R6,R9 :1)	$\epsilon_w(R4A) = 0.01$ f. rest: $\epsilon_w = 0.5$	one dimensional steady state incompressible flow	$C_D = 1$	Henderson and Marchello	1.2 mm	CYBER-175	292	without gap "blind" calculation $E_K = 0$
		0-50	---	---						---	
		0-1000	1	---						---	---
Sweden	COPTA-6	0-2.5	6	$\epsilon_w = 0.7$ $\epsilon_w = 0.2$	steady state compr. orifice flow	$C_D = 0.88$	f. R4, R5, R7, R8: 0-50s: 10000 50-70 s: lin. decr. to 1590 t > 70 s: Uchida; f. R6, R9: 0 - 50s : 3 x Uchida 50 - 1000 s : Uchida	0.95 mm	CYBER 172 CDC	124	gapsize = F(t) flash coeff. $F_{esh} = 2$ $T_0 = 27^\circ C$
		0-50	4(R4,R5,R7:1; R6+R8+R9:1)	$\epsilon_w = 1$			---			725	
		0-1000	1	---			---			---	136
United Kingdom	CLAPTRAP II	0-2.5	6	$\epsilon_w = 0.03$	homogeneous, slip, adiabatic flow	$C_D = 0.8 - 0.2 F_w^{0.25}$	htc = $\frac{128}{n} \sum \frac{\Delta P_i A_i}{\sqrt{2g}}$ 0.4 but $\geq 500$ ; add. component f. R4 htc = $5.48 \times 10^{-7} \left( \frac{1}{\sqrt{2g}} \right)^{1.62}$	0.8 mm	4-70	---	gapsize = 236 cm <sup>2</sup> $E_K \neq 0$
		0-50	6				---			---	
	CLAPTRAP I	0-1000	1	---	---	---	100 - 500	---	---	---	---

The participants nodalized in many different ways:

- In time interval 0 to 2.5 s the containment was simulated by 4 to 13 zones. In relation to measured pressure in the compartments and pressure differences between the compartments a subdivision of the containment into 5 to 6 zones (8 participants) seems to be sufficient. A more detailed subdivision into 9 to 13 zones appears to be more suitable for better describing energetic conditions, processes of water transport and also their influence on pressure distribution: 14 temperatures with widely differing measuring results have to be calculated, longitudinal and short flow paths, dead ends, outflows upwards, downwards and sideways (Germany: 13 nodes, Netherlands: 11 nodes, Finland: 9 nodes).
- In time interval 0 to 50 s the model containment was subdivided into 1 to 11 zones.

One participant (Belgium) simulated the whole containment by one zone. This procedure appears to be acceptable in view of the pressure built-up after about 5 s when an almost complete pressure equalization has taken place. However, the zone temperature should strictly simulate the average temperature in the dome compartment R9 and the results from other participants and the experimental results demonstrate even in this relatively long time interval, that the temperature histories vary strongly in the different compartments, so that a different influence of individual compartments on total pressure built-up is to be expected. Therefore a more detailed subdivision of the containment also in this time interval is recommendable (4 to 6 zones: 8 participants, 11 zones: 1 participant). In this respect it appears suitable on the one hand to simulate compartment R9 with 3 zones (because of the developing temperature stratification), but on the other hand it is also possible to partly lump together compartments near the rupture site (because of their extensive temperature equalization).

- In time interval 0 to 1000 s most of the participants modelled the containment as a single node, except Australia (4 nodes), Italy/CNEN-Pisa and Japan (2 nodes).

Especially, in view of the temperature stratification measured in dome compartment R9 it is to question, whether the cooling process in the containment - so essential for this time interval - could be better des-

cribed in the calculations. This could be done by a subdivision into several zones (e.g.: compartments near rupture-site, dome of compartment R9, centre and annulus of R9 + compartment R6 vertically), though thus certainly the costs of computation would increase.

Processes of water transport have a decisive influence on conditions in the short-term interval. They are generally described in an very simplified way, i.e. water carry-over factor  $\xi_w$  is input under the assumption of a slip free flow. This parameter, mostly constant in time, often valid for all rooms, is between 0 and 1.

According to definition (see nomenclature) for example  $\xi_w = 0.5 = \text{const}(t)$  in conjunction with the homogeneous model means that with increasing time and a correspondingly rising portion of water in the rupture compartment a steadily increasing amount of water is transported off the rupture compartment. However, this amount will increase as well as decrease on the basis of existent flow conditions according to the course of the pressure differences to the neighbouring compartments (two maxima). The inclusion of a time-function for water carry-over factor into the calculations, which would be necessary as a matter of principle, can certainly be regarded as a solution. It is very well possible to obtain such a time-function from post-calculations for one facility under the particular flow conditions of one test. However, it seems to be very difficult to find a function in so general terms of physics that it could be transferred to conditions at another facility or the reactor. A first step towards an improvement certainly is a definition of the portion of water  $\eta_w$  in the mixture flow, and of a water separation factor  $c_{wA}$  (see nomenclature). These parameters could have a chance of being described in more general terms, if experiments with a suitable measuring technique have been performed (density measurement at orifice vents). Supposedly, and as it has to some extent been used in a calculation with a time-function for  $\xi_w$  (see chapter 6.3.4 in /5/),  $\eta_w$  will be substantially more independent on time than  $\xi_w$ . In a further step it will not be possible to avoid the inclusion of slip into the considerations. Hopefully, these complicated processes will then still be described in a simplified but essentially physical manner. A certain indication for water transport conditions during this experiment are the sump temperatures and sump water masses measured in the individual compartments (see chapter 3.7).

Orifice flow is mostly described in a simplified manner. E.g. most of the participants apply one-dimensional, quasi-steady, compressible flow without slip and discharge coefficients between 0.6 and 1.2. As far as can be drawn from the participants' information the high portion of two-phase acceleration losses(= momentum losses) within pressure differences is not accounted for or very indirectly (correction for mass flow).

Heat transfer to structures is treated very differently: with various differing relations respectively with input data, constant or some function of time:

- time interval 0 to 2.5 s:

The heat transfer coefficients of the participants are within 1300 and 15000 W/(m<sup>2</sup>K) for the rupture compartment, in part reduced for near break, flown through compartments [within 1300 and 14000 W/(m<sup>2</sup>K)] and dead ends as well as off break compartments [partly about 100 W/(m<sup>2</sup>K)]. Assuming an isenthalpic expansion of the fluid discharging at the rupture-site, e.g. near zero time, vapour quality is between 0.3 and 0.4, which is equivalent to a void fraction of larger than 0.99 under existing pressure conditions. Therefore, it can be supposed that for the short time interval heat transfer conditions near the rupture-site are existent in a water-blowdown test, as in a steam-blowdown. From this high heat transfer coefficients in an order of 10<sup>4</sup> W/(m<sup>2</sup>K) for more or less droplet condensation seem to be closer to reality. On a reduced level these considerations are also valid for compartment parts near the rupture and flown through by the fluid, while in the rest of compartments and dead ends with a high portion of inert gas (air), heat transfer is substantially lower.

- In time intervals 0 to 50 s and 0 to 1000 s the highly empirical Tagami/Uchida correlation, well-known from licensing, is applied most frequently, partly with multipliers between 3 and 6. As far as found the maximum htc values in these time intervals are within (500) 1200 and 10000 (22000) W/(m<sup>2</sup>K).

With three exceptions [Belgium, Canada: 0.2 mm, Italy (CNEN/Pisa): 0.25 mm] values for the thickness of concrete coating are used which are within the possible limits of 0.7 mm and 1.2 mm from table 3. Quantitative information on different assumptions can be found in chapters 2.5.3.1 and 2.5.3.2.

In general, computation times are short. Kinetic energy is considered by two participants.

### 3.4 Supplementary Information of Individual Participants

In this chapter information beyond the scope of table 7 is given from the brief reports of the participants. In particular, reference to the pertinent literature on the programs used and essential characteristics of modifications are to be briefly described.

Australia /15/: Code ZOCO V /16/ was used for all three time intervals. In addition, a calculation with code ZOCO VI /17/ for time interval 0 to 1000 s was submitted. The results agree less closely with the measurements. But this code has the merit of operating considerably faster than ZOCO V.

Mass flow between compartments is calculated in codes ZOCO V and ZOCO VI by an analytical/empirical method involving the expression

$$\sqrt{P_i/v_i}$$

where  $P_i$  is the pressure in the source compartment  $i$  and  $v_i$  is the mean fluid specific volume for compartment  $i$ .

The effect of the water carry-over factor on the calculated pressures is studied by taking a constant value of 0.65 for all compartments. The maximum pressure in dome compartment increases with ZOCO V by 3.7 %, compared to the reference calculation ( $\xi_w = 0$ ).

Belgium /18/: The essentials of the computer codes TRAP-SCO and TRAP-CON can be found in /19/.

- Vent path simulation:

For the flow paths close to the rupture compartment additional friction and inertia have been introduced; for the other vent paths, a discharge coefficient of unity was used (see table 7).

- The water carry-over fraction is defined as:

$$C_{wc} = \frac{\text{water flow quality}}{\text{homogeneous upstream node quality}}$$

With help of a common multiplier the water carry-over fraction can vary as a function of time:

$$0 \text{ to } 0.3 \text{ s: } C_{wc_{4-5, 4-7, 4-9}} = 1; C_{wc_{5-9, 7-8, 8-9, 6-9}} = 0.5$$

$$0.3 \text{ to } 1.2 \text{ s: } C_{wc_{4-5, 4-7, 4-9}} \text{ linear decrease from } 1 \text{ to } 0.5$$

$$C_{wc_{5-9, 7-8, 8-9, 6-9}} \text{ linear decrease from } 0.5 \text{ to } 0.25$$

$$1.2 \text{ to } 2.5 \text{ s: } C_{wc_{4-5, 4-7, 4-9}} = 0.5$$

$$C_{wc_{5-9, 7-8, 8-9, 6-9}} = 0.25$$

- Heat transfer coefficient:

The Tagami-Uchida correlation was used:

$$\text{Tagami correlation: } h_{T, \text{steel}} = h_{\text{max}} (t/t_p)^{0.5} \text{ [W/m}^2\text{°C]}$$

$$h_{\text{max}} = 0.77 (E/V \cdot t_p)^{0.6}$$

$$h_{T, \text{concrete}} = 0.4 h_{T, \text{steel}}$$

wherein:  $V = 642 \text{ m}^3$ : total containment volume

$t_p = 23.5 \text{ s}$ : end of water blowdown

$E = 10 \text{ GJ}$ : about twice energy content liberated in the containment

$$\text{Uchida correlation: } h_U = 5.678 (2+50x) \text{ [W/m}^2\text{°C]}$$

$$x = \frac{\text{total vapour mass}}{\text{total air mass}}$$

- Coating:

The filler for porous spots and the flat coat (filler) have been ignored and only the main coat and the top coat have been accounted for and simulated by a single coat layer with the thickness 0.2 mm.

- Sensitivity studies:

For the short term, parametric studies were performed to test the sensibility of such parameters as:

1. Water entrainment: This influenced the pressure difference from compartments R4 and R7 to the other compartments. The sign of the pressure difference R7-R5 is influenced by the options chosen.
2. Energy reduction of break flow: This lowers the absolute pressure profiles of all compartments after 0.5 s but does not influence so much the differential pressures.

For the long term, the influence of other parameters is illustrated as follows by varying only one parameter from the reference case:

Reference calculation:	$P_{\max} = 4.032 \text{ bar (+2.8 \%)}$
Total paint thickness: ( $\delta = 1 \text{ mm}$ , $\lambda = 0.2727 \text{ W/m, } ^\circ\text{C}$ )	$P_{\max} = 4.245 \text{ bar (+10 \%)}$
Evaluation models for integrity: ( $E=5 \text{ GJ}$ , $\delta = 1 \text{ mm}$ )	$P_{\max} = 4.325 \text{ bar (+12.7 \%)}$

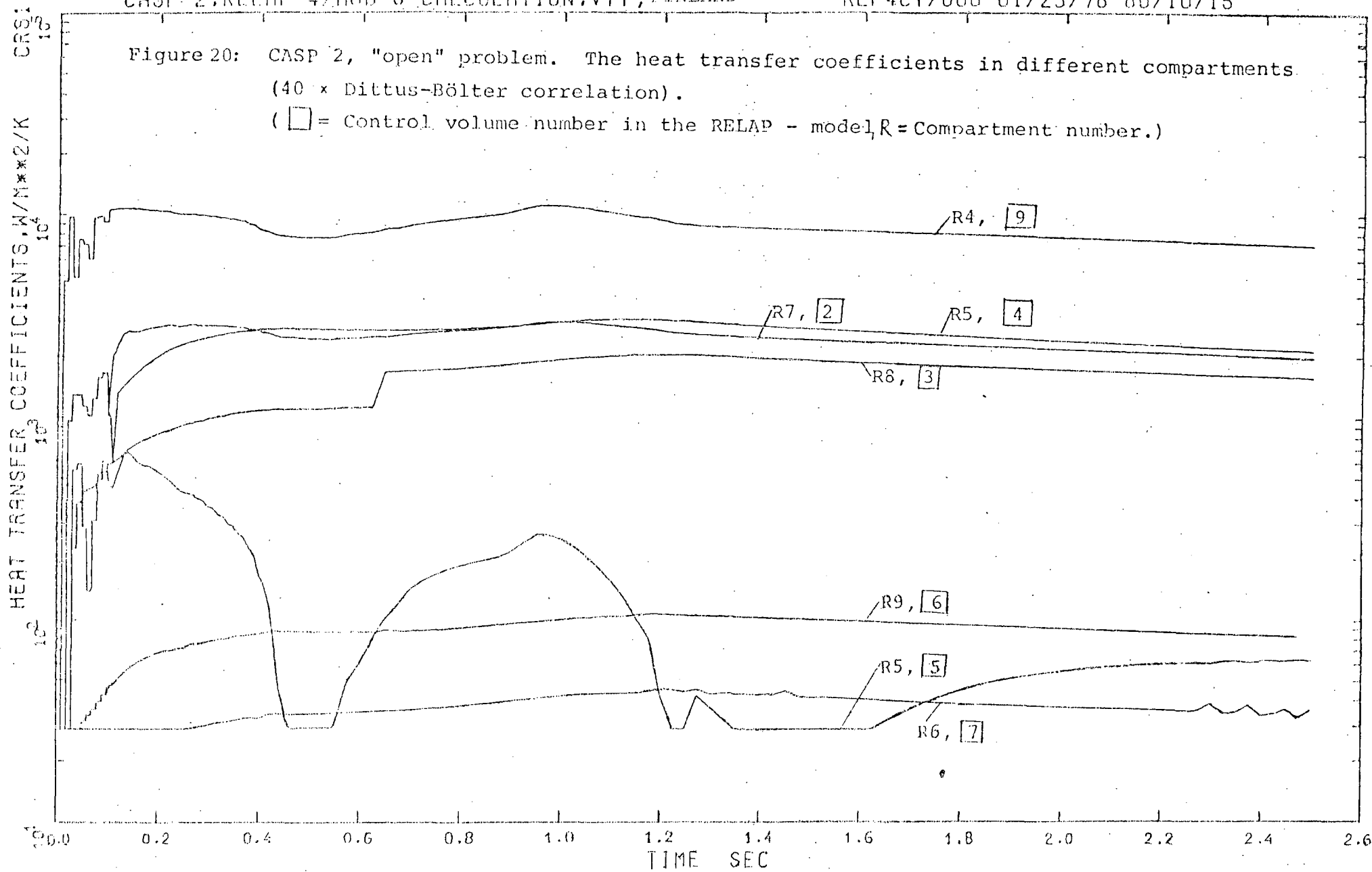
Canada /20/: The used program PRESCON-2 /20/ is based on the assumption of a thermodynamic equilibrium mixture of air and two phase water (i.e. common temperature). The mixture is homogeneously distributed throughout the node. The equilibrium temperature is equal to the saturation temperature corresponding to the partial pressure of the steam.

Finland /21/: Codes RELAP4/MOD6 for time interval 0 to 2.5 s and CONTEMPT-LT/026 (VTT version) for time interval 0 to 1000 s are applied. The heat transfer coefficients in different compartments are given in fig. 20 (from 40 x Dittus-Bölder correlation).

The approximation of the time function of the gap size is as follows:

- 0 to 0.15 s: linear increase in gap size from 0 to 292 cm<sup>2</sup>
- 0.15 to 1.5 s: constant gap size of 292 cm<sup>2</sup>
- 1.5 to 5 s: linear decrease in gap size from 292 cm<sup>2</sup> to 236 cm<sup>2</sup>.





France /22, 22a (for "blind" results 0 to 50 s and 0 to 1000 s)/:

The homogeneous frozen model in code GRUYER /22/ is chosen. The assumptions specific to this model are as follows:

- No transfer of mass from one phase to another.
- No heat transfer between the liquid and the gaseous phase.
- Average velocity of the different phases is the same.
- The air and the steam are at the same temperature and are an ideal mixture of perfect gases undergoing an isentropic expansion.
- The kinetic energy of the emulsion comes entirely from the expansion of the gaseous phase.

The gap between compartments R4 and R9 is considered and the time-function of the gap size is as follows:

- 0 to 0.15 s:  $0.0292 \times t/0.15 \text{ (m}^2\text{)}$
- 0.15 to 1.5 s:  $0.0292 \text{ (m}^2\text{)}$
- 1.5 to 2.5 s:  $0.0292 - (0.0056 (t-1.5))/3.5 \text{ (m}^2\text{)}$

Germany /23/: The COFLOW program /24/ enables the user to compute short time as well as long time relations with the regard to stream rates as well as the heat transfer to solid structures and the heat conduction within them. The main features of the computer model are given below in key-words:

- The thermodynamic conditions within each node are either the state of saturation or superheated steam.
- The energy and continuity equation include the components air, steam and depending on the thermodynamic conditions, also water.
- Velocity terms in the momentum equation can be considered.
- The water transport between the nodes can be taken into account.
- The heat transfer to solid structures can be considered as well as the heat conduction within them.

The CONDRU code /23/ is used for calculating long term pressure and temperature histories in full pressure containments (2-zones-model). Either thermodynamic equilibrium or nonequilibrium can be assumed.

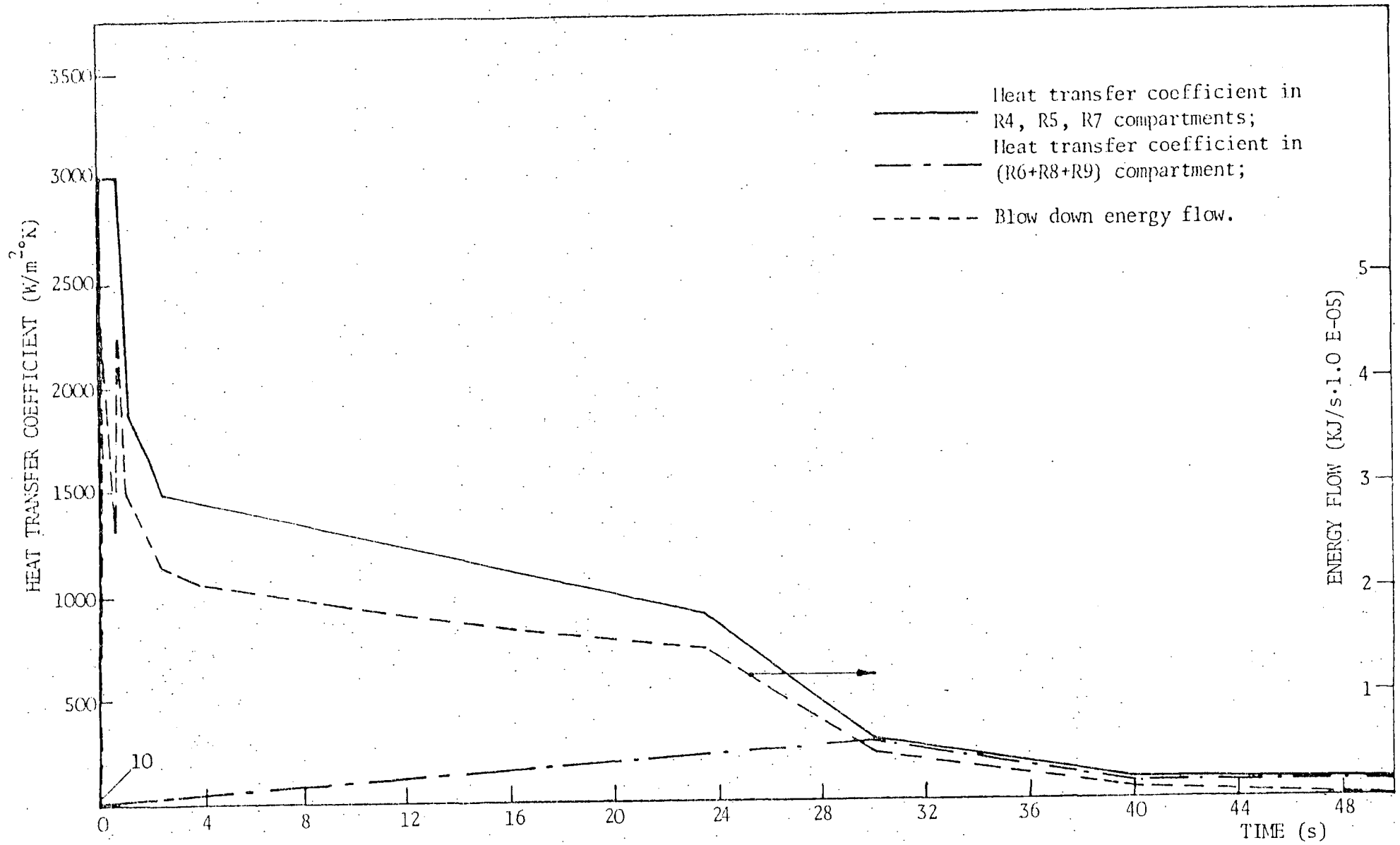


Fig. 21 : Energy flow and heat transfer coefficients (brief and medium term calculations).  
 ITALY (CNEN/Pi )

Italy (CNEN/Pisa) /25/: For the short and the medium term calculation codes ARIANNA-0 /26/ is used which is based on COMPARE code. Thermodynamic equilibrium and a stagnant homogeneous mixture of steam, air and water are assumed in each node. The heat transfer coefficients in different compartments are given in fig. 21 (for details see App. 2).

For the long term calculation code CONTEMPT-LT 25 /27/ is applied.

Italy (NIRA) /28/: Code PACO /29/ is used. For the short and medium term calculations the liquid water is assumed at equilibrium conditions in all compartments. In the long term calculation the liquid water is assumed at equilibrium until the end of blowdown; then separation from the air steam mixture is assumed.

A medium term calculation has been performed using constant htc (10 kW/m<sup>2</sup>°C) in all compartments until the end of blowdown:

Reference calculation	$P_{\max} = 4.4 \text{ bar}$
Constant htc = 10 kW/m <sup>2</sup> °C	$P_{\max} = 4.04 \text{ bar.}$

Two long term calculations have also been performed using constant htc (10 kW/m<sup>2</sup>°C) and assuming:

- a) all the liquid water at equilibrium conditions throughout the transient
- b) no equilibrium of the liquid water throughout the transient.

The results are as follows:

Reference calculation :	$P_{\max} = 4.28 \text{ bar}$
Constant h = 10 kW/m <sup>2</sup> °C	
a)	$P_{\max} = 4.03 \text{ bar}$
b)	$P_{\max} = 4.36 \text{ bar.}$

Japan /30/: The analysis is performed by the use of RELAP4/MOD5 /31/. Code modification is not made except the constant value of fluid/structure heat transfer coefficient is given to the code instead of selecting the built-in heat transfer correlations.

Netherlands /32/: Modified ZOCO-V code /33/ is used. It is assumed that water, steam and air are in homogeneous thermal hydraulic equilibrium with each other.

Sweden /34/: COPTA-6 code /35/ allows choice between seven different models. In the most elaborate models each room is assumed to consist of a liquid phase and a gas phase (or atmosphere). The liquid phase, which may contain bubbles of air and steam, resides on the compartment floor (sump). The atmosphere consists of a homogeneous mixture of air and steam and possibly also water droplets. The liquid phase and the atmosphere may have different temperatures.

The liquid phase and the atmosphere interact in two ways:

- mass exchange by water drops falling down, steam boiling off and air rising (normally only BWR-pool).
- heat exchange through surface heat transfer.

In the simpler models thermodynamic equilibrium is assumed throughout the room.

In the CASP2 runs, for the blowdown period (0-50 s),  $10^4$  W/m<sup>2</sup>·K has been used for the heat transfer coefficient  $\alpha$  in the high-flow compartments (R4, R5, R7 and R8). This value corresponds to the order of magnitude used by most participants in CASP1. For the low-flow compartments (R6 and R9) a parameter study was conducted, using Uchida values times some factor. For the medium-time case computer runs with  $\alpha$  equal to Uchida values times 1, 2, and 3 were made. Using factor 2 gave a significantly better fit to the experimental data while the increased improvement for factor 3 was fairly small. Therefore it was considered not worthwhile to step up further with the factor. The value  $\alpha=3 \cdot \text{Uchida}$  was then chosen for the low-flow compartments (R6 and R9) in the short- and medium-time cases. The results are as follows:

Reference calculations:	$P_{\max} = 4.26$ bar
htc = 2 x Uchida:	$P_{\max} = 4.34$ bar
htc = Uchida:	$P_{\max} = 4.51$ bar.

United Kingdom /36/: The calculations are done with CLAPTRAP I /37/ for time interval 0 to 1000 s and CLAPTRAP II /38/ for time intervals 0 to 2.5 s and 0 to 50 s.

### 3.5 Comparison of Selected Variables

The calculated data used for comparison in chapters 3.5 and 3.6 were taken from the tapes (9 participants) and punched cards (3 participants) submitted. They are identical to the participants' plot data. Most of the participants used the recommended formats, scales and dimensions for plots, tapes (cards) and lists, which facilitated the preparation and checking of comparative plots.

Differences are certainly to be noted comparing the results of the participants. These differences may arise from handling the programs or from the quality of the models used in the programs. However, in the following no evaluation as to a ranking shall be made. The following sections comprise a selection of important quantities characteristic of the processes taking place in the containment.

#### 3.5.1 Listing of important characteristic quantities

In this and the following sections some observations made in the course of this evaluation shall be pointed out during discussion of the individual variables. Prior to consideration of the individual comparative plots, a short outline on the results of the Standard Problem is given by numerically comparing some important characteristic quantities from the experiment and the participants' calculations in table 8. The following symbols mean:

- $P_{R4}$  - pressure in rupture compartment R4
- $P_{R9}$  - pressure in dome compartment R9
- $\Delta P_{R4-R9}$  - pressure difference between R4 and R9
- $\Delta P_{R4-R5}$  - pressure difference between R4 and R5
- $P_{max}$  - maximum pressure in containment.

Country	Computer Code	Time Interval 0 - 2.5 s												Time Interval 0 - 50 s		
		$P_{R4}$				$P_{R9}$	$\Delta P_{R4-R9}$				$\Delta P_{R4-R5}$				$P_{max}$	
		1st Max.		2nd Max.		t=2.5s	1st Max.		2nd Max.		1st Max.		2nd Max.		P(bar)-t(s)	
P(bar)-t(s)		P(bar)-t(s)		P(bar)	P(bar)-t(s)		P(bar)-t(s)		P(bar)-t(s)		P(bar)-t(s)		P(bar)-t(s)			
Australia	ZOCO V	1.46	0.35	1.64	1.10	1.63	0.39	0.30	0.35	1.00	0.12	0.15	0.11	0.95	4.16	37.5
Belgium	TRAP-SCO	1.67	0.35	1.81	0.95	1.68	0.61	0.30	0.53	0.95	0.33	0.15	0.23	0.95	-	-
	TRAP-CON	-	-	-	-	-	-	-	-	-	-	-	-	-	4.03	33.2
Canada	PRESCON-2	1.57	0.35	1.80	1.05	1.64	0.49	0.30	0.51	1.00	0.20	0.15	0.18	0.95	4.04	37.0
Finland	RELAP4/MOD6	1.56	0.35	1.80	1.05	1.61	0.49	0.35	0.55	1.00	0.22	0.15	0.18	0.95	-	-
	CONTEMPT-LT/026 (VTT)	-	-	-	-	-	-	-	-	-	-	-	-	-	(4.29)	(40.0)
France	GRUYER	1.58	0.35	1.83	1.05	1.66	0.50	0.30	0.55	1.00	0.22	0.15	0.19	0.95	3.81*	33.5*
Germany	COFLOW	1.61*	0.35	1.90*	1.10*	1.69*	0.55*	0.35*	0.63*	1.00*	0.25*	0.15*	0.19*	0.95*	4.02	35.5
Italy (CNEN/Pisa)	ARIANNA-0	1.59	0.35	1.84	1.00	1.66	0.52	0.35	0.58	0.95	0.24	0.15	0.19	0.95	3.95	35.0
Italy (NIRA)	PACO	1.63	0.35	1.91	1.00	1.68	0.56	0.30	0.63	1.00	0.24	0.15	0.28	0.95	4.46	38.5
Japan	RELAP4/MOD5	1.50	0.35	1.76	1.15	1.61	0.44	0.35	0.49	1.05	0.16	0.10	0.02	0.90	4.00	36.5
Netherlands*	ZOCO V (MOD.)	1.52	0.35	1.74	1.10	1.63	0.41	0.35	0.40	1.00	0.14	0.10	0.14	0.95	4.14	36.0
Sweden	COPTA-6	1.69	0.35	1.99	1.00	1.61	0.65	0.30	0.76	1.00	0.32	0.20	0.31	0.95	4.29	35.5
United Kingdom	CLAPTRAP II	1.53	0.35	1.83	1.05	1.56	0.47	0.35	0.58	1.00	0.21	0.15	0.17	0.95	4.00	34.0
Experiment. D16/CASP2		1.63	0.35	1.81	0.97	1.55	0.59	0.30	0.62	1.0	0.33	0.17	0.23	1.02	3.95	33.0
± Error		±0.025		±0.025		±0.025	±0.02		±0.02		±0.018		±0.018		±0.025	
Influence of Gap*		-0.03		-0.061		+0.01	-0.02		-0.036		-0.0		-0.007		-	

Table 8: Important characteristic variables

Extreme  
\* "blind" calculation

Variables	Time Interval 0 - 2.5 s							Time Interval 0 - 50 s $P_{max}$
	$P_{R4}$		$P_{R9}$	$\Delta P_{R4-R9}$		$\Delta P_{R4-R5}$		
	1st Max.	2nd Max.	t=2.5s	1st Max.	2nd Max.	1st Max.	2nd Max.	
Mean value (all participants) in bar	1.58	1.82	1.64	0.51	0.55	0.22	0.18	4.10
Spread bandwidth round mean value (all participants) } in bar related to mean value	+ 0.11	+ 0.17	+ 0.05	+ 0.14	+ 0.21	+ 0.11	+ 0.13	+ 0.36
	- 0.12	- 0.18	- 0.08	- 0.12	- 0.20	- 0.10	- 0.16	- 0.29
	+ 19%	+ 21%	+ 3%	+ 27%	+ 38%	+ 50%	+ 72%	+ 12%
	- 21%	- 22%	- 13%	- 24%	- 36%	- 45%	- 89%	- 9%
Mean value (all participants } without extreme) } in bar	1.58	1.82	1.64	0.50	0.55	0.22	0.19	4.09
Spread bandwidth round mean value (all participants } without extreme) } in bar related to mean value	+ 0.09	+ 0.09	+ 0.04	+ 0.11	+ 0.08	+ 0.10	+ 0.09	+ 0.20
	- 0.08	- 0.08	- 0.03	- 0.09	- 0.15	- 0.08	- 0.08	- 0.14
	+ 16%	+ 11%	+ 6%	+ 22%	+ 15%	+ 45%	+ 47%	+ 6%
	- 14%	- 10%	- 5%	- 18%	- 27%	- 36%	- 42%	- 5%
Experiment in bar	1.63	1.81	1.55	0.59	0.62	0.33	0.23	3.95
Exp. error bandwidth } in bar related to experim.	$\pm$ 0.03	$\pm$ 0.03	$\pm$ 0.03	$\pm$ 0.02	$\pm$ 0.02	$\pm$ 0.02	$\pm$ 0.02	$\pm$ 0.03
	$\pm$ 5%	$\pm$ 4%	$\pm$ 5%	$\pm$ 3%	$\pm$ 3%	$\pm$ 6%	$\pm$ 9%	$\pm$ 1%
Deviation mean value f. calculation result (all } participants) to exp. } in bar related to exp.	- 0.05	+ 0.01	+ 0.09	- 0.09	- 0.07	- 0.11	- 0.05	+ 0.15
	- 8%	+ 1%	+ 16%	- 15%	- 11%	- 33%	- 22%	+ 5%
Max. abs. deviation f. calculation result (all } participants) to exp. } in bar related to exp.- exp. error	0.20	0.21	0.17	0.22	0.29	0.23	0.23	0.54
	33%	27%	33%	39%	48%	74%	110%	18%

Table 9: Mean values, bandwidths and deviations of important characteristic variables



Reference values are the pressure built-up values since 0 s (1.0 bar) for pressures and the values of differential pressures themselves. The results of the "blind" calculations of Germany (COFLOW) and the Netherlands, not considering the gap, might be reduced/increased by the influence of gap. In table 8 the approximate small amount of it (see chapter 2.5.3.1) is added but not considered in table 9.

In time interval 0 to 2.5 s, for example, not only the initial maxima of pressure in the rupture compartment R4 but also the differences in pressure between the compartments occur, which are important for safety-related design of thickness of inner walls. The calculation results obtained by Australia with the computer code ZOCO V more frequently are the lower bound, while the results computed by COPTA-6 (Sweden) more frequently are the upper bound of the field of calculations and with a certain distance off the results of the other participants. The participants predicted the time for the first and second maximum, with any exception, closely to the experimental data.

In time interval 0 to 50 s, the maximum pressure occurs, which is important for the structural design of the shell of a containment. The results calculated with computer program PACO (Italy, NIRA) and to a somewhat minor degree the results of COPTA-6 (Sweden) and CONTEMPT-LT/ 026 (Finland; however, taken from a run submitted for the time interval 0 to 1000 s) are to a higher amount distant from the experimental result and the results of the other participants. Disregarding these exceptions the maximum pressure in containment [3.81 to 4.16 bar; exp. result:  $(3.95 \pm 0.03)$  bar] and also the moment of its occurrence (33.2 to 37.5 s; exp. result: 33 s) are quite well post-calculated.

In table 9 some mean values and spread bandwidths of the calculational results are compared to the experimental results and their error bandwidths as well as deviations between calculational and experimental results.

- Mean values of results of all participants and those of all participants without extremes hardly differ.
- Spread bandwidths of calculational results diminish considerably when the extremes are not included.

- Compared to experimental values, the mean values of the computation results are systematically below (by -0.05 to -0.11 bar or by -8 to -33 %) in the case of the 1st maximum more than in the case of the 2nd maximum.
- The systematic over-calculation of pressure in compartment R9 at 2.5 s (+16 %) is to be rated higher than deviations in other compartments, since R9 is the largest compartment of the containment (465 m<sup>3</sup> of altogether 640 m<sup>3</sup> in volume, resp. 700 m<sup>2</sup> of altogether 1130 m<sup>2</sup> in structural surface area).
- Mean values for the computed maximum pressure in the containment are about 0.09 resp. 0.15 bar higher than the experimental result (exp. error: ±0.03 bar) which indicates that the participants have tried to "conservatively" approach the experimental result.
- Maximum absolute deviations of computation results (all participants) for maximum pressure (0.54 bar, resp. 18 %) and especially for selected parameters in the interval 0 to 2.5 s (0.17 to 0.29 bar, resp. 27 to 110 %) are relatively high.
- With these considerations, however, it has to be noted in accordance with chapter 2.5.3, that deviations from nominal values can considerably influence computation results.

### 3.5.2 Time interval 0 to 2.5 s

Because of the high number of SP participants, for each variable two comparative plots (A and B) have been made. Throughout, in each of the two plots, the results of the individual participants and the experiment are shown with the same symbol and the same type of line to facilitate their finding out in the different variables' plots. In the case of a lower nodalisation than that corresponding, e.g. to the number of temperature measuring points to be calculated, those values were taken which the participants wished to see assigned to the measuring point. This way mean values are in part compared to local measurements.

Not only individual characteristic quantities at specified times are important for evaluating the results but also the history of these and other variables. Therefore, in this and the following two sections the selected variables and their behaviour within the different time intervals, are to be investigated in somewhat more detail.

In view of the problem being more realistic compared to the first Containment-SP one may very well call the participants' predictions for this SP as quite well in comparison to the experiment. As has been analysed for some quantities in table 8 also histories of the results of Australia (computer code ZOCO V) and of Sweden (computer code COPTA-6) show somewhat higher deviations for some values during certain time periods, compared to those of most of the participants. With the same program ZOCO V but modified ECN (Netherlands) computed in the mean smaller deviations from the experiment. But on the whole, it seems justified to look upon the results of all participants as lying within a statistical scatter field.

Now a few remarks shall be made on the different variables in the order of their selection.

- Pressure in rupture compartment R4 (figs. 22A, 22B):

The experimental history is basically similar to that of the break mass flow and both its maxima. It shows the expected rapid pressure rise in the small compartment and a type of plateau after the second maximum because of the increasing influence of previous events and the small decrease of the break mass flow.

In the comparison it is to be noted that only Belgium (with a water carry-over factor dependent on time) predicted the first and second maximum quite well while the difference between the first and second maximum in the results of all other participants except Australia is higher than in the experiment (calculational results: from 0.22 to 0.3 bar with a mean value of 0.25 bar; experimental result: 0.18 bar). This difference is mainly caused by using a constant independent on time for the water carry-over factor in the calculations (see chapter 3.3).

For illustration the following table is given:

Country	Computer Code	Water Transport	Difference in Short Term Pressure Maxima (bar)
Australia	ZOCO V	$\xi_w = \begin{cases} 0 \\ 0 \\ 0 \\ 0 \\ ? \\ 0.01 \\ 0.03 \end{cases}$	0.18
Finland	RELAP4/MOD6		0.24
F.R. Germany	COFLOW		0.29
Italy (CNEN/ Pisa)	ARIANNA-O		0.25
Japan	RELAP/MOD5		0.26
Netherlands	ZOCO V (MOD.)		0.22
United Kingdom	CLAPTRAP II		0.30
Canada	PRESCON-2		$\xi_w = 0.5$
Italy (NIRA)	PACO	$\xi_w = 0.7$	0.28
France	GRUYER	$\xi_w = \begin{cases} 1.0 \\ 1.0 \end{cases}$	0.25
Sweden	COPTA-6		0.30
Belgium	TRAP-SCO	$C_{wc} = 1.0$ (0 ÷ 0.3 s) $C_{wc} = 1/0.5$ (0.3/1.2s)	0.14
Experiment D16/CASP2		?	0.18

It is recognizable that there is no indication of a distinct value for the water carry-over factor  $\xi_w = \text{const.}$  between 0 and 1.0 which results in better an agreement of calculational with experimental values.

A further reason for the difference between analytical and experimental maxima difference is that the nominal values given for mass flow and specific enthalpy at the break within 0.1 s, i.e. that the decisive energy input within this period of time, might be too low (see the sharp pressure rise with a crack at approx. 0.03 s, followed by an approximation to the calculational results, which are relatively close together for 0.1 s). A higher enthalpy supply (corresponding to about the area of the triangle between the experimental and the calculational course) has more influence on the first maximum than on the second one and thereafter: the initial excess of pressure is increasingly equalized by an increased flow from compartment R4, i.e. it is more and more distributed throughout the other compartments of the containment. It is to be assumed (see chapter 2.5.1) that the temperature of a short portion of the pipe behind the rupture site was initially above 260 °C (used for determining the specific enthalpy; see also fig. 6.1 in /6/). Furthermore, the mass flow at the break cannot be exactly measured at measuring point III - which is located at a distance of 2.6 m off the break - within approx. the first 0.17 s. An additional indication of the above is provided by the difference between measuring points II and I within this time period. There is a further uncertainty due to the fact that one thermocouple of measuring point II was not working and the measurements of the other can be relatively inaccurate (short installation from design reasons, insulation towards pipe wall?, measurement at the non-insulated bottom part of the pipe). Another reason for the differences between calculations and measured results could be the oblique flow towards vents Ü45 and Ü47. In the experiment falsified measurements from the bent Pitot-tubes in the orifices were noted, since the maximum permissible flow angle of 15° was obviously exceeded (see page 112 in /5/). This means not only a reduction in cross section but also a decrease of e.g. the discharge coefficient by increased contraction.

By this the systematic underestimation around the first pressure maximum (except two participants) may also be explained.

The predicted pressure obtained by Australia, is lower than the measured data up to about 2 s (caused e.g. by neglecting water transport); but the pressure history approaches experimental results more and more. After about 1 s the results of Germany, Sweden and also Italy (NIRA) are relatively higher than the experimental results.

No definite connection is ascertainable between values for input parameters and the quality of the results; this is due to the fact that the relevant input parameters cannot be separated and may have a compensating effect on the results (for example, for low pressure in the rupture compartment  $\xi_w \downarrow$ ,  $\alpha_w \uparrow$ ,  $C_D \uparrow$ ). A more detailed investigation is left to the SP participants in which certainly also differential pressures and temperatures should be taken into account.

- Pressure in first follow-up compartment R5 (figs. 23A; 23B):

The experimental pressure history is in good agreement with the one of R7 in the other sequence of compartments. In comparison to the pressure history in R4 this one is somewhat leveled and delayed in time, due to flowing to and away from the orifices.

What has already been said concerning the maxima for compartment R4 is also true. The considerations for the initial phase in R4 are not valid here. The results of most participants concur favourably with the experiment and the spread range of the computation results is almost identical with the one in compartment R4.

- Pressure in dome compartment R9 (figs. 24A, 24B):

In the largest compartment of the containment, pressure rises slowly and time-delayed similar to compartments R6 and R8.

Nearly over the whole time interval all participants except United Kingdom tend to overestimate the pressure built-up. On the one hand this could be due to the fact that the energy input into the compartment is too high (discharge coefficients may be too high) or that heat release from the compartment is too low (low heat transfer coefficients).

OECD-CSNI CONTAINMENT STANDARD PROBLEM NO.2 (TEST CASP2)

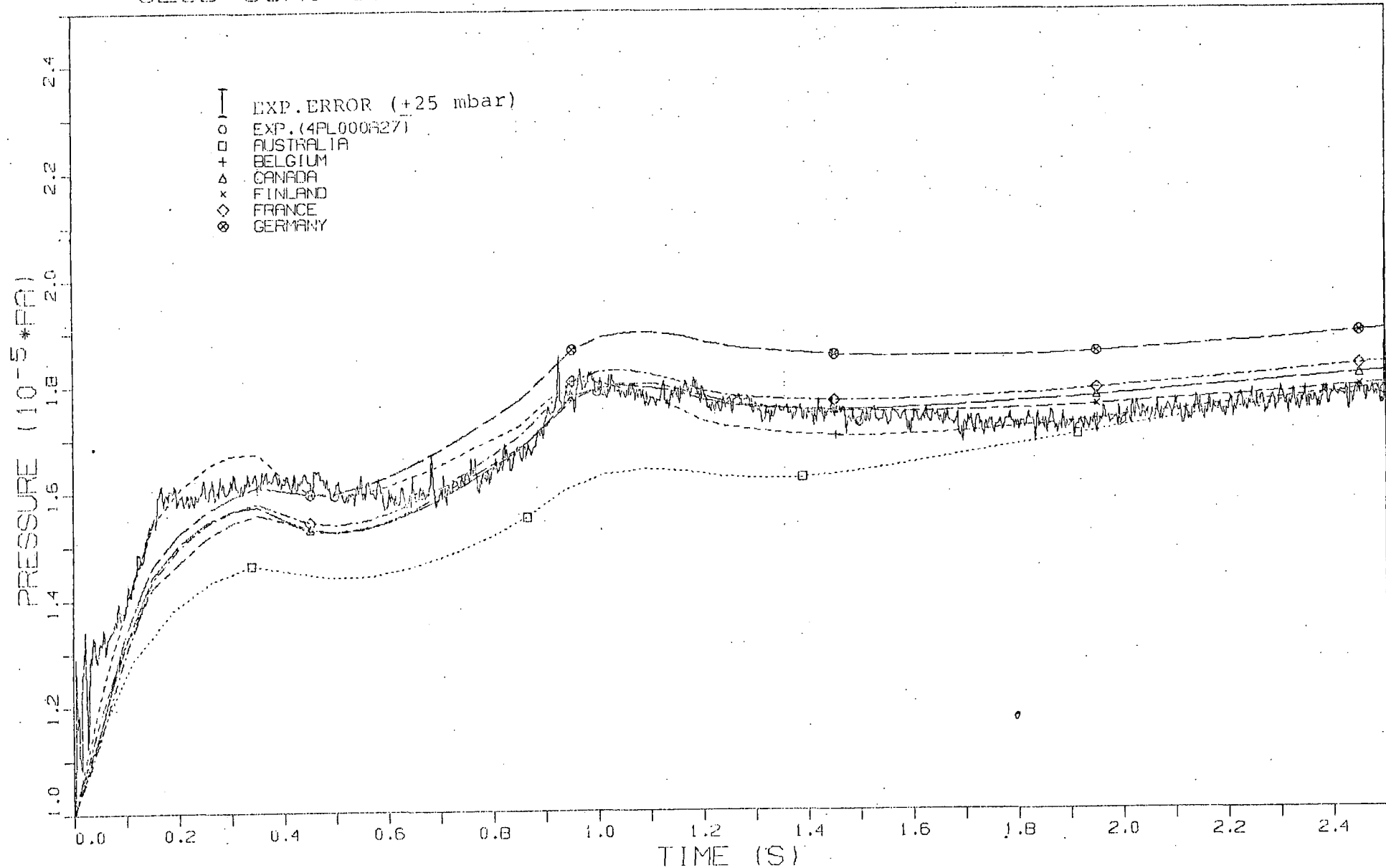


FIG: 22A PRESSURE HISTORY IN COMPARTMENT R4

OECD-CSNI CONTAINMENT STANDARD PROBLEM NO.2 (TEST CASP2)

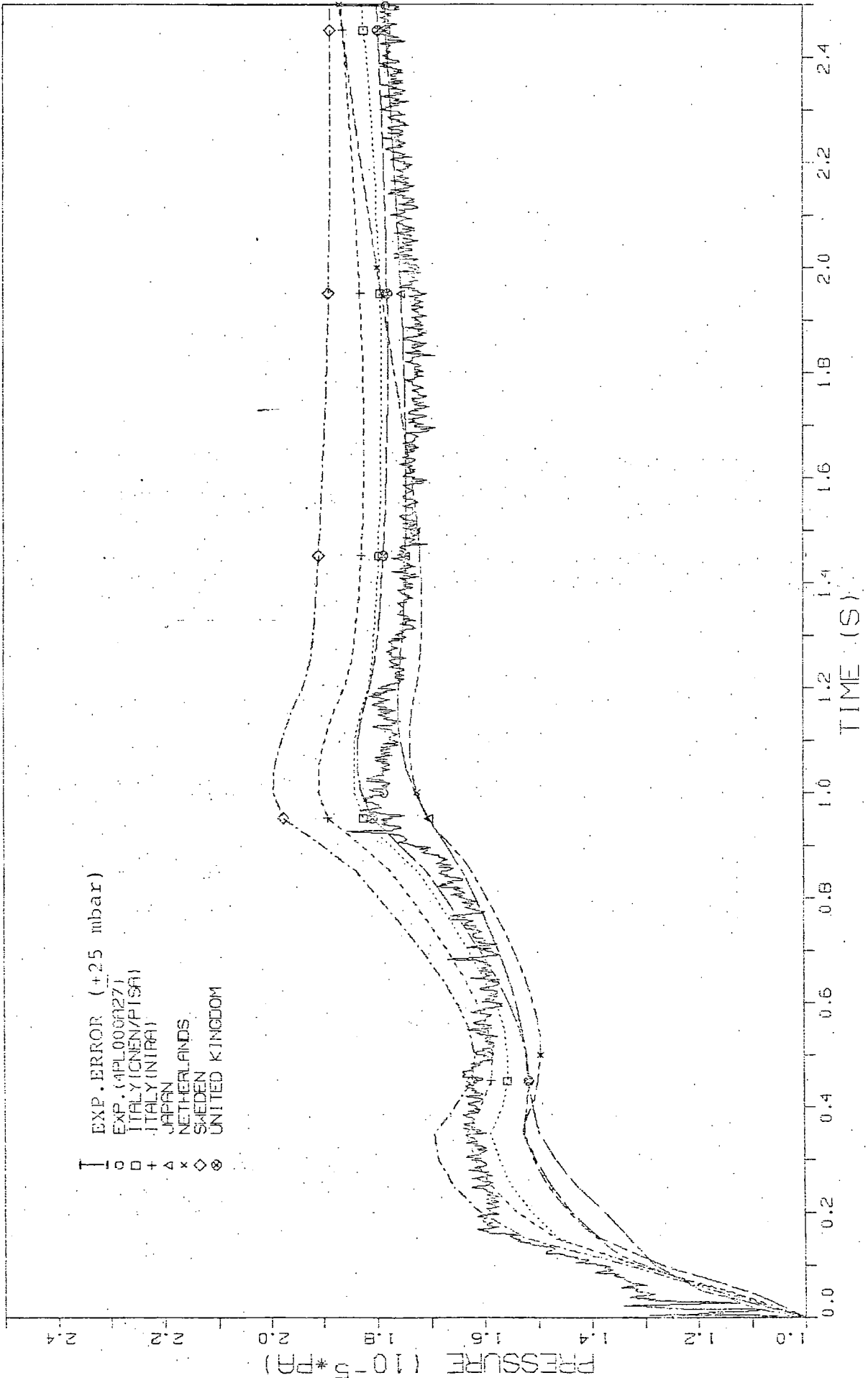


FIG. 22B PRESSURE HISTORY IN COMPARTMENT R4



OECD-CSNI CONTAINMENT STANDARD PROBLEM NO.2 (TEST CASP2)

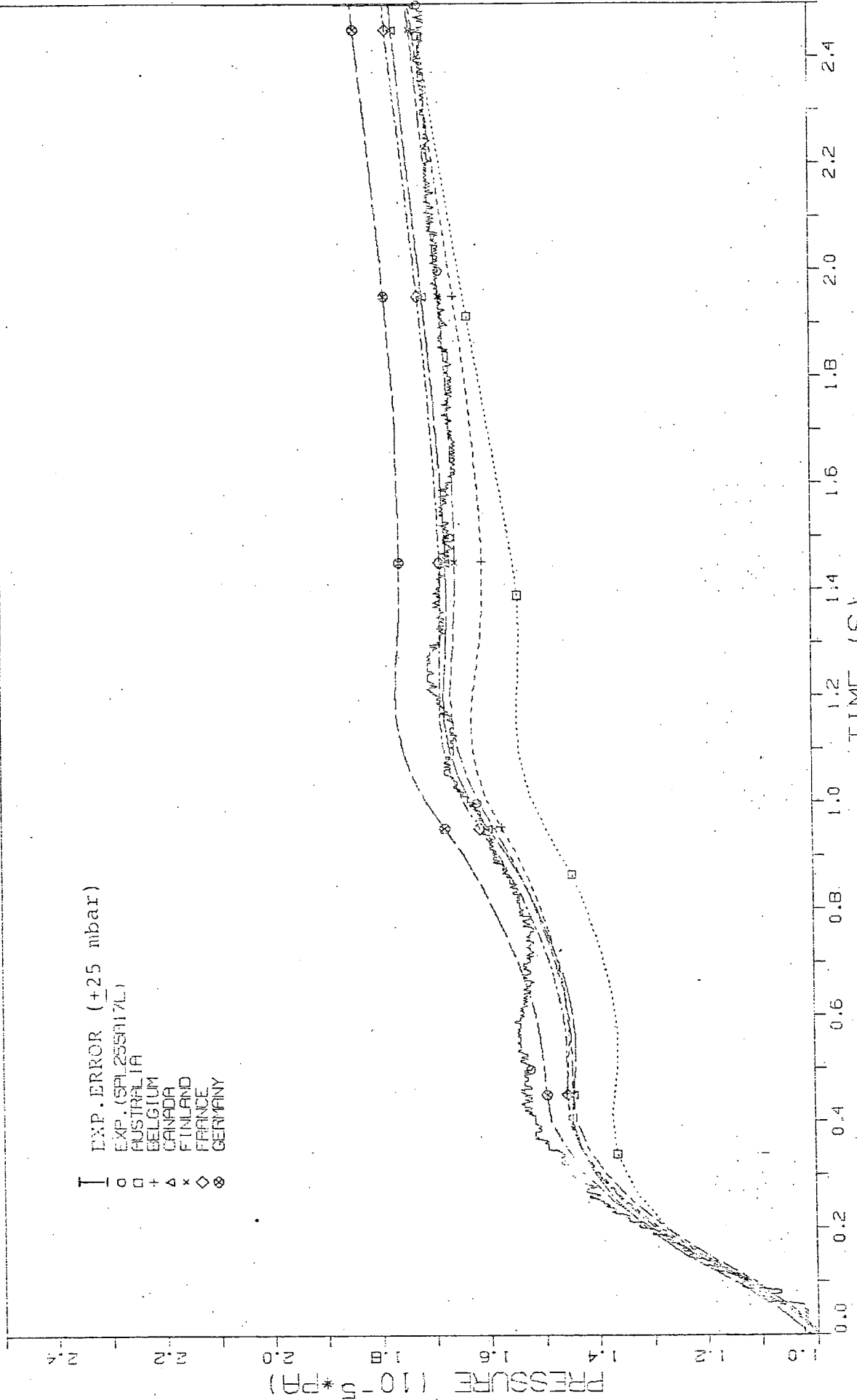


FIG. 23A PRESSURE HISTORY IN COMPARTMENT R5

OECD-CSNI CONTAINMENT STANDARD PROBLEM NO.2 (TEST CASP2)

- I EXP. ERROR (±25 mbar)
- EXP. (SALZSAI 7L)
- ITALY (ONEN/PISA)
- + ITALY (INTRA)
- △ JAPAN
- x NETHERLANDS
- ◇ SWEDEN
- ⊗ UNITED KINGDOM

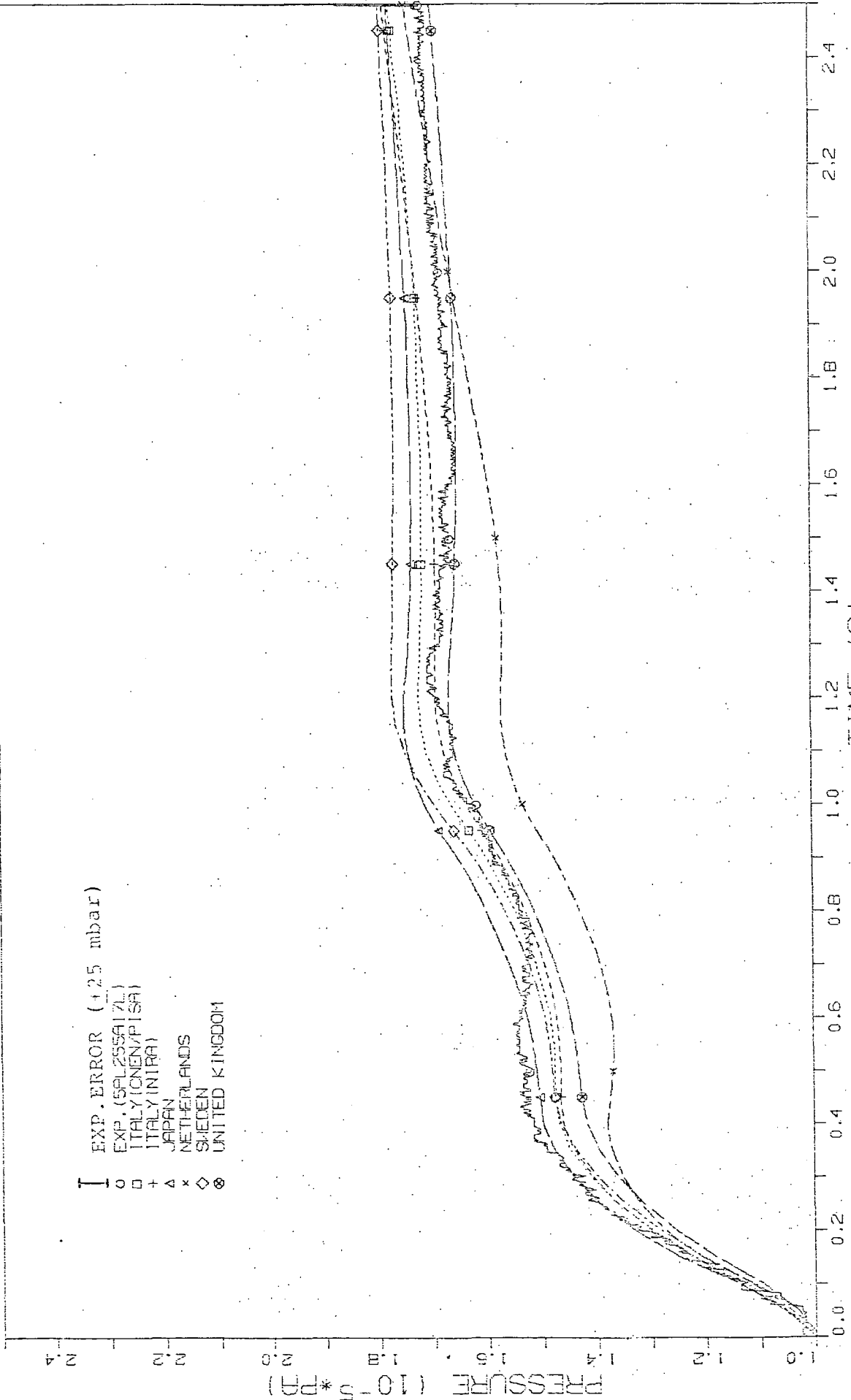


FIG. 23B PRESSURE HISTORY IN COMPARTMENT R5

OECD-CSNI CONTAINMENT STANDARD PROBLEM NO.2 (TEST CASP2)

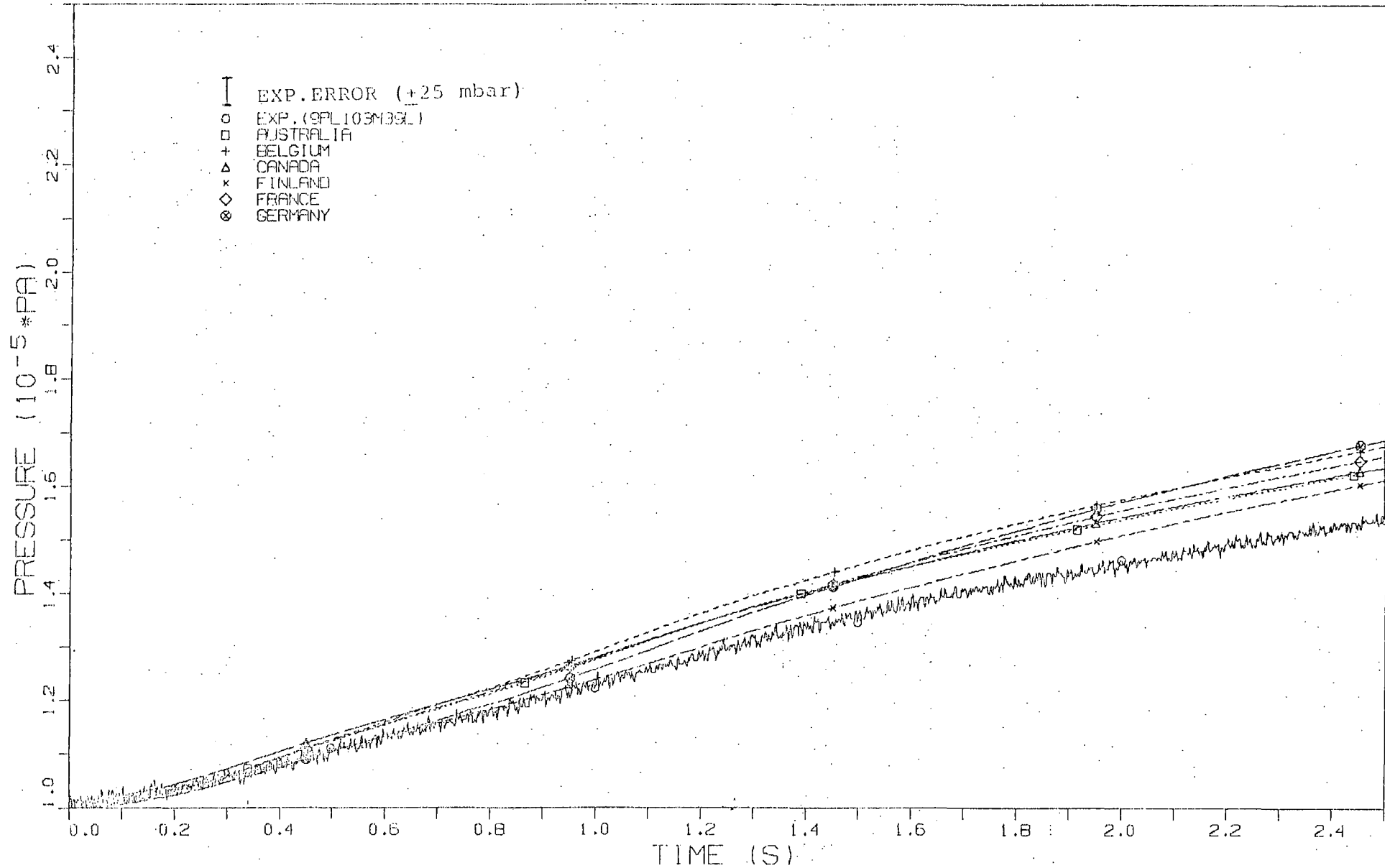


FIG. 24A. PRESSURE HISTORY IN COMPARTMENT R9

OECD-CSNI CONTAINMENT STANDARD PROBLEM NO.2 (TEST CASP2)

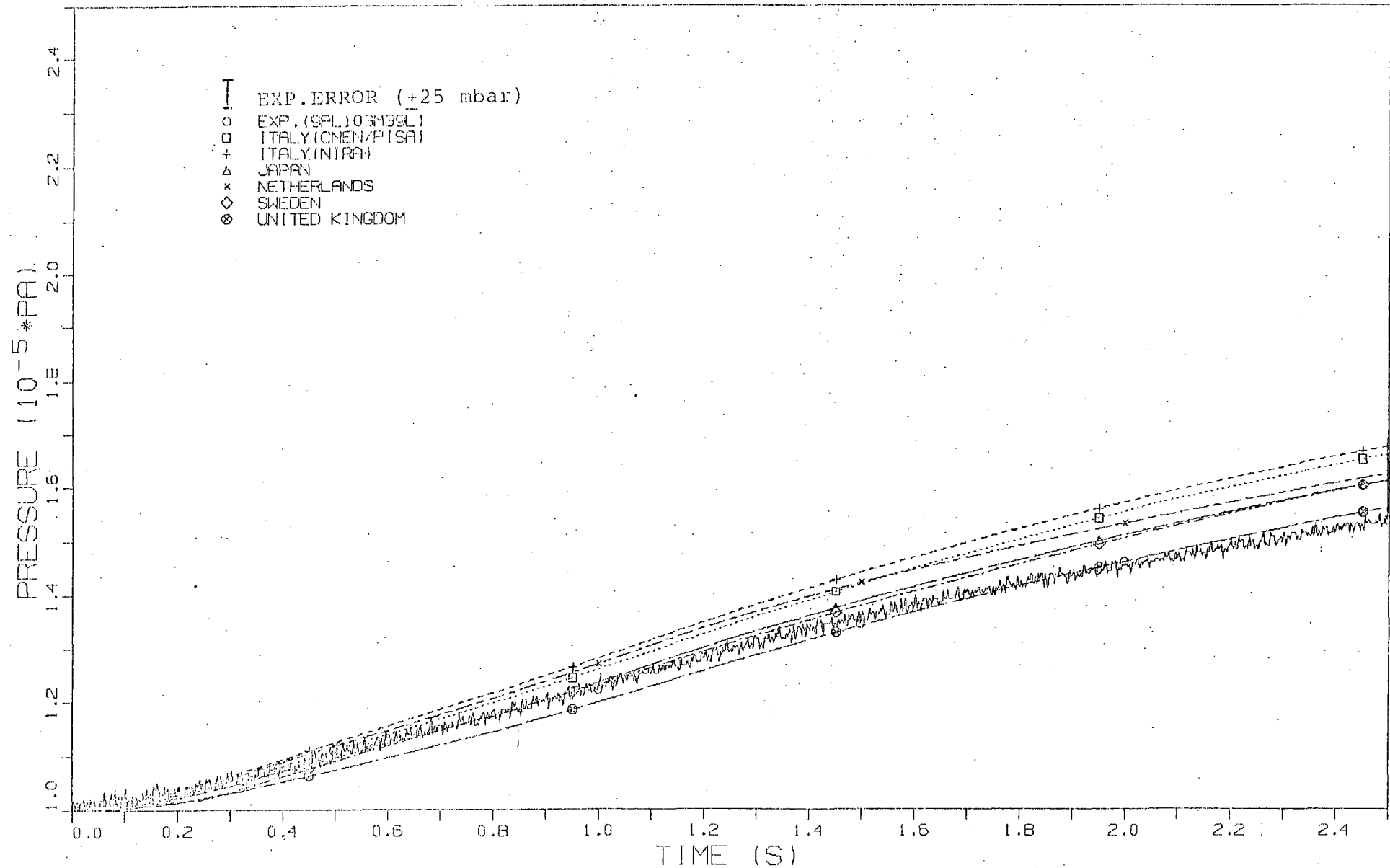


FIG.24B PRESSURE HISTORY IN COMPARTMENT R9

- Pressure difference between compartments R4 and R9 (figs. 25A, 25B):  
What is said for the pressure history in R4 applies correspondingly to this experimental course. The effect of mass flow maxima can be more clearly seen in comparison. The maximum pressure difference within the containment is 0.62 bar. Australia and Netherlands underpredicted, while Sweden overpredicted this variable. The other participants' results are much closer to the measured data and are - except around the first maximum - within in a narrow band partly within the measured error range. Italy (NIRA); Italy (CNEN/Pisa) and Germany calculated the whole course best (although they overpredicted the pressure in compartments R4 and R9), Belgium up to the 2nd maximum.

- Pressure difference between compartments R4 and R5 (figs. 26A, 26B):  
The experimental behaviour of the pressure difference over the vent of compartment R4 is the same as for the pressure difference R4-R9, but somewhat less pronounced.

The scatter range of the results obtained by the participants is relatively small, except around the 1st maximum. The results of Japan deviate from the experiment considerably, i.e. they are surprisingly low.

- Pressure difference between compartments R5 and R7 (figs. 27A, 27B):  
This pressure difference between both the first follow-up compartments expresses differences in flow conditions (R5/R7):
  - short/long flow path
  - upward/downward outflow
  - long/short dead end space.

The experimental results are nearly 0 up to appr. 1 s, then they are somewhat positive. Obviously the effects due to different heat release (in R7 > in R5 by earlier air-washing) and different water transport (from R7 > from R5) compensated for each other. The small difference from 1 s on could be explained by overflow of the sump water from R7 to R8.

Most of the computer codes predict slightly higher pressures in compartment R7 than in R5, while the experimental results show an opposite trend. However, the agreement between the calculations and the

measured data may be regarded as quite good (see also exp. error). Also considerably differing heat transfer coefficients (see e.g. Finland and Germany in table 7) and orifice flow coefficients have only a minor effect on the results.

- Pressure difference between compartments R5 and R9 respectively compartments R7 and R8 (figs. 28A, 28B and 29A, 29B):

In spite of different conditions of outflow - upwards and downwards - visible differences only occur after 1 s, the pressure difference between R5 and R9 being somewhat higher than between R7 and R8.

In both cases the results obtained by the participants show a similar spread range around the experimental results.

OECD-CSNI CONTAINMENT STANDARD PROBLEM NO.2 (TEST CASP2)

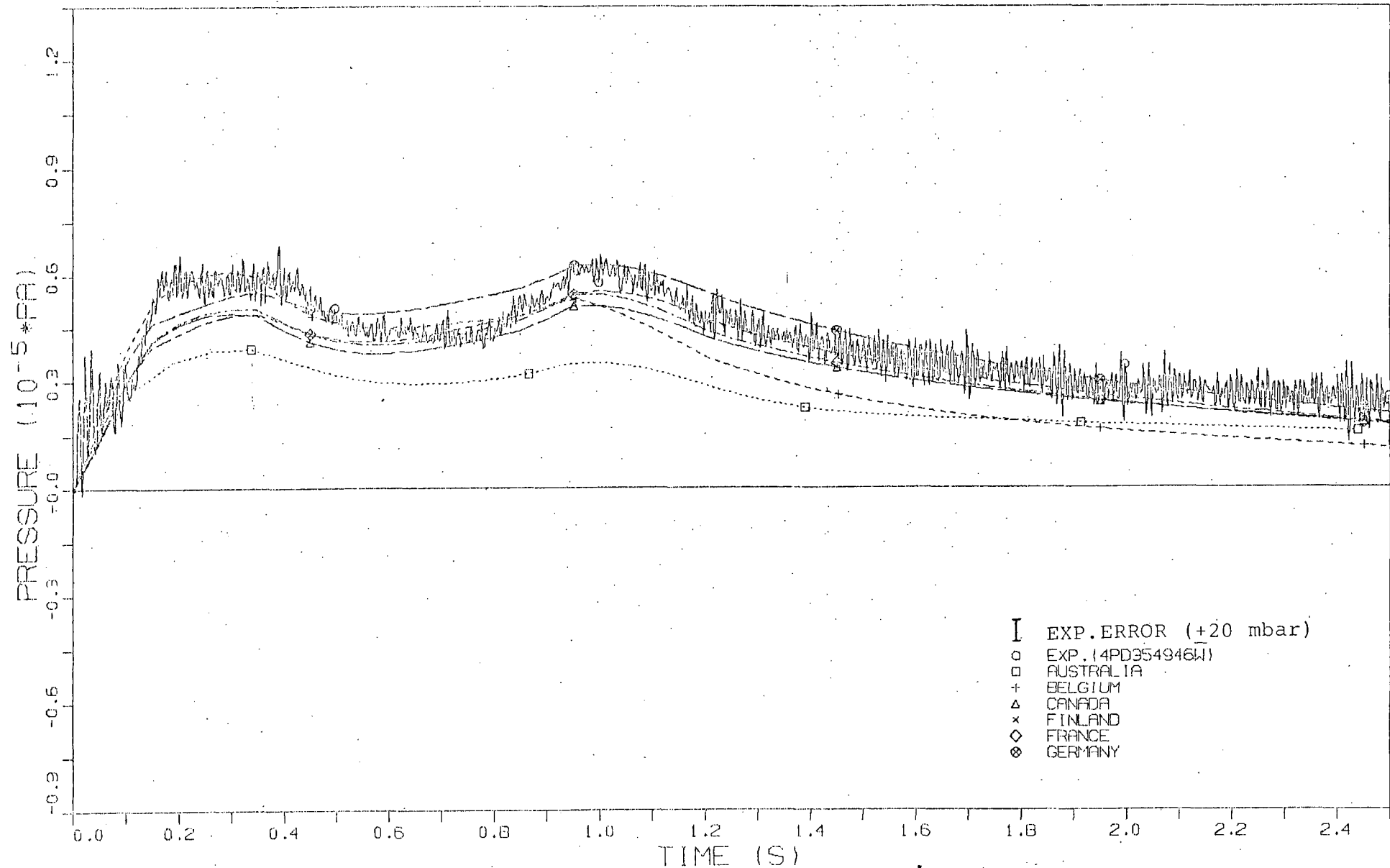


FIG. 25A HISTORY OF PRESSURE DIFFERENCE R4-R9

OECD-CSNI CONTAINMENT STANDARD PROBLEM NO.2 (TEST CASP2)

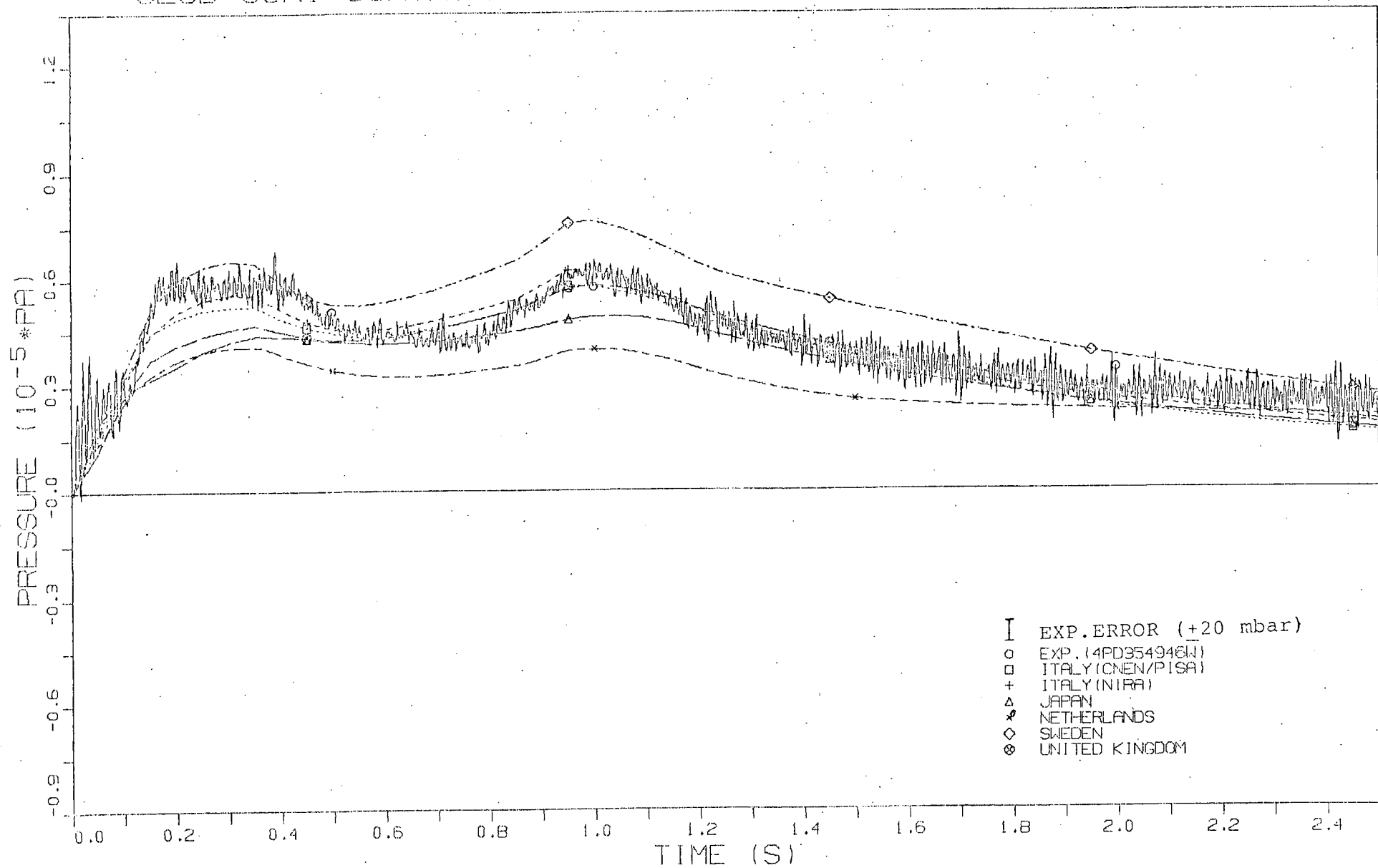


FIG. 25B HISTORY OF PRESSURE DIFFERENCE R4-R9



OECD-CSNI CONTAINMENT STANDARD PROBLEM NO.2 (TEST CASP2)

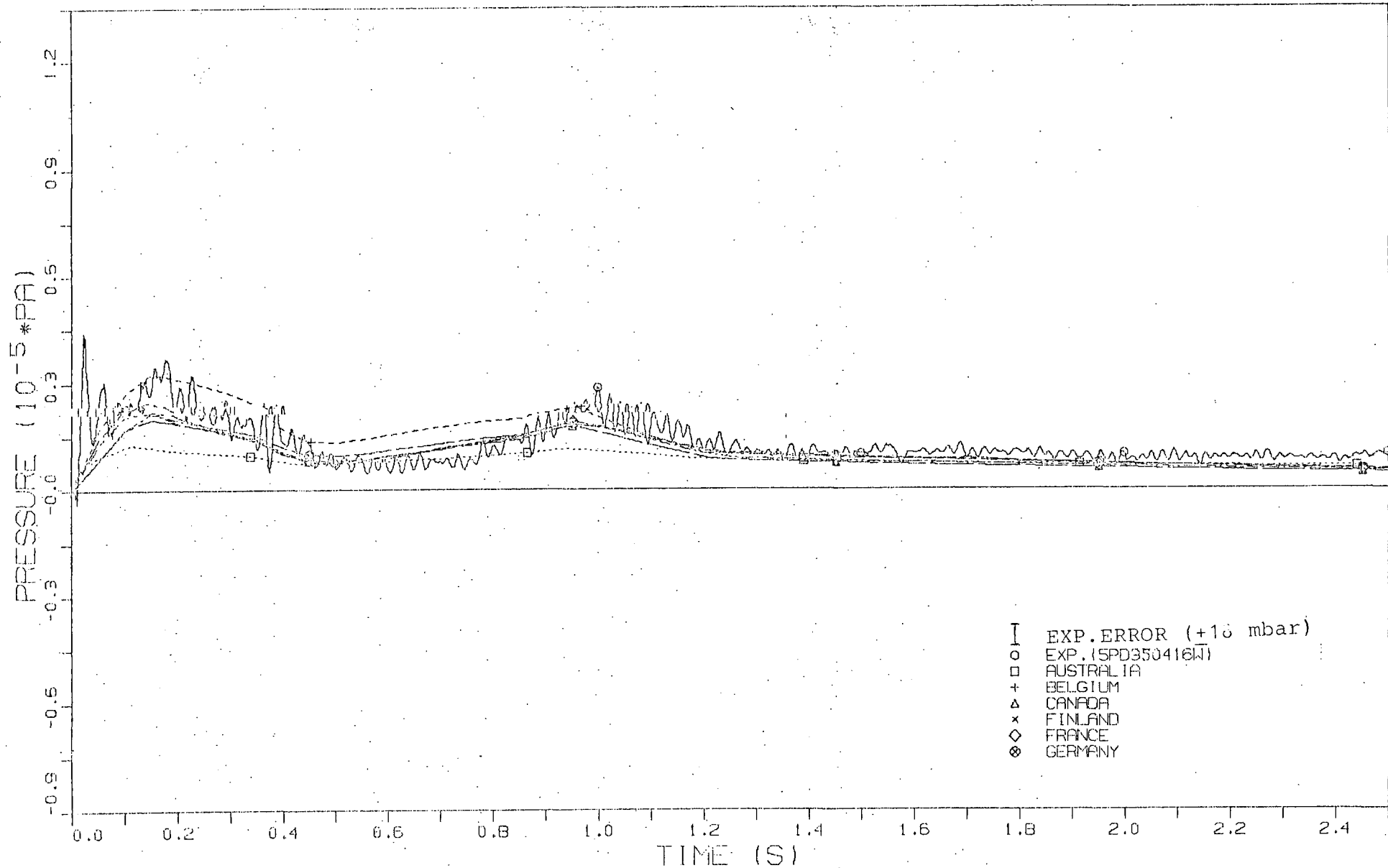


FIG. 26A HISTORY OF PRESSURE DIFFERENCE R4-R5

OECD-CSNI CONTAINMENT STANDARD PROBLEM NO.2 (TEST CASP2)

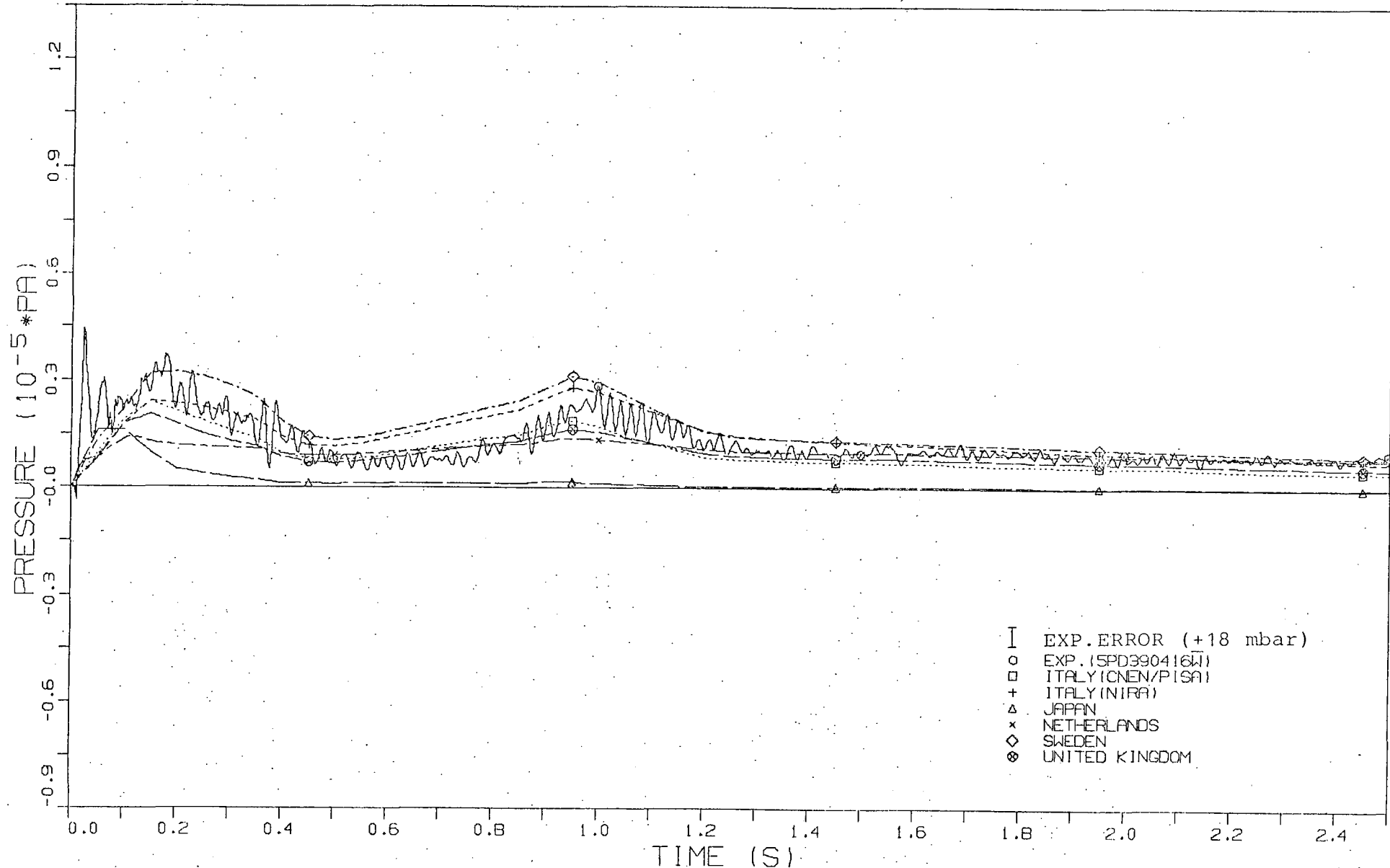


FIG. 26 B HISTORY OF PRESSURE DIFFERENCE R4-R5

OECD-CSNI CONTAINMENT STANDARD PROBLEM NO.2 (TEST CASP2)

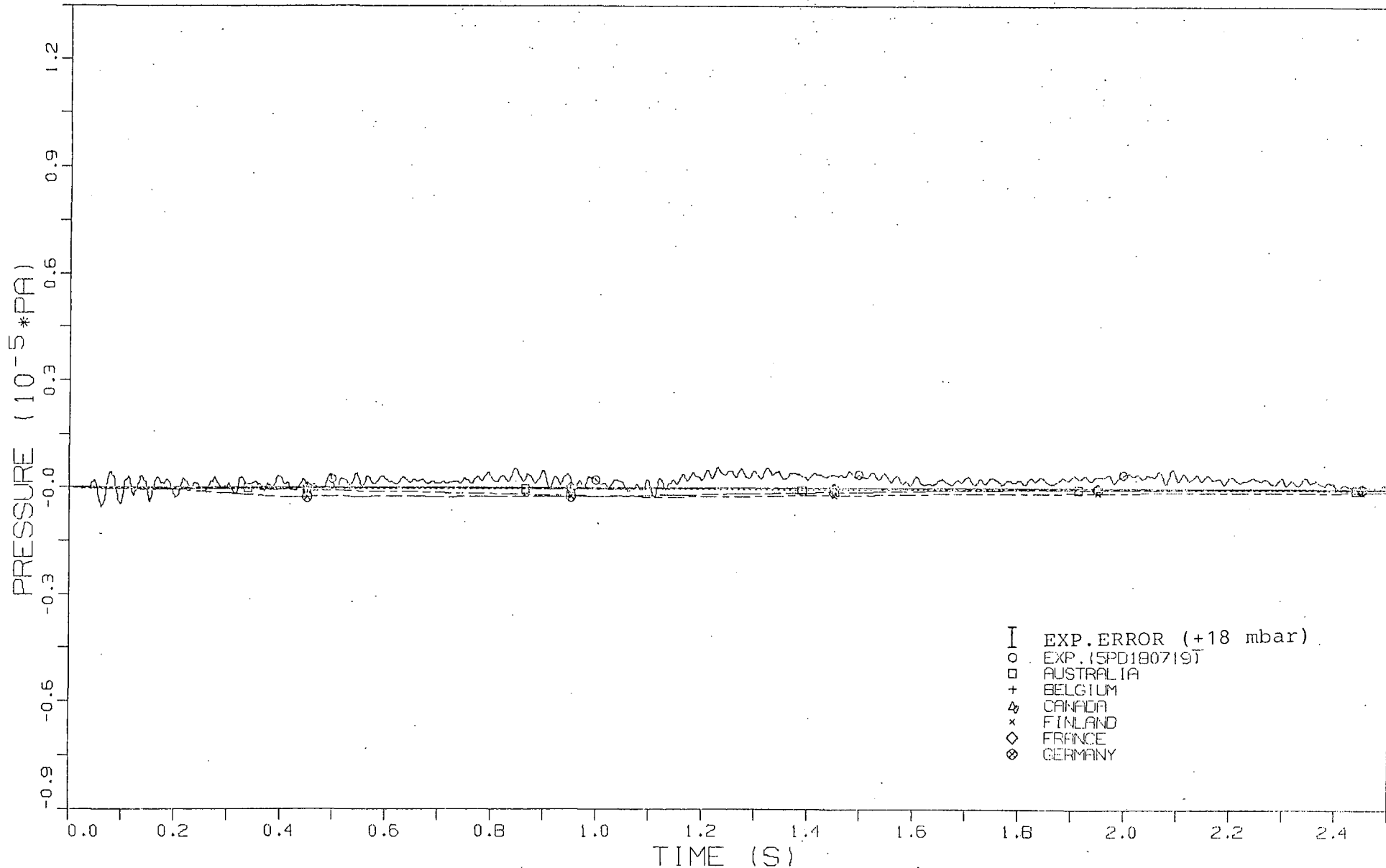


FIG. 27A HISTORY OF PRESSURE DIFFERENCE R5-R7

OECD-CSNI CONTAINMENT STANDARD PROBLEM NO.2 (TEST CASP2)

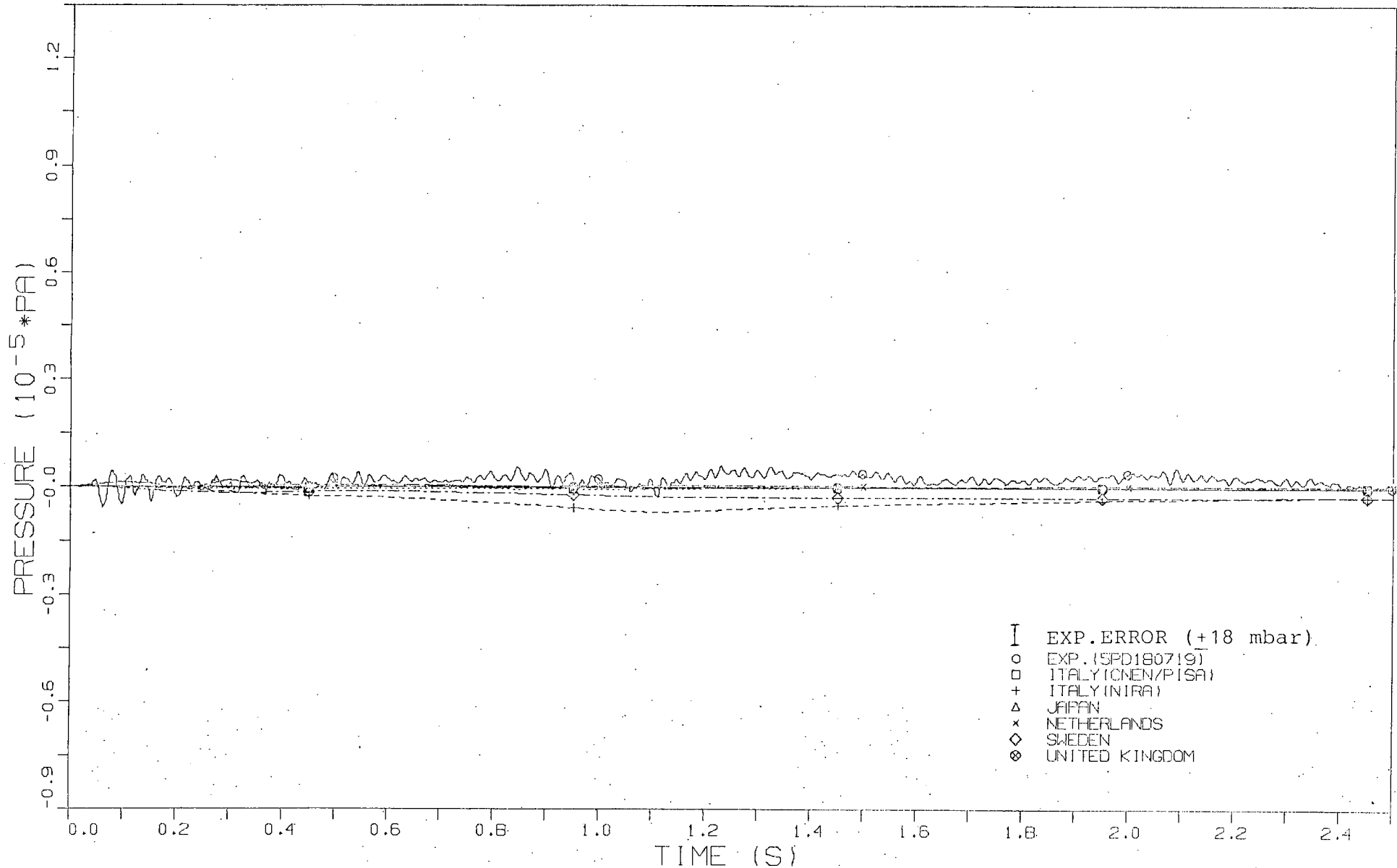


FIG. 27 B HISTORY OF PRESSURE DIFFERENCE R5-R7

OECD-CSNI CONTAINMENT STANDARD PROBLEM NO.2 (TEST CASP2)

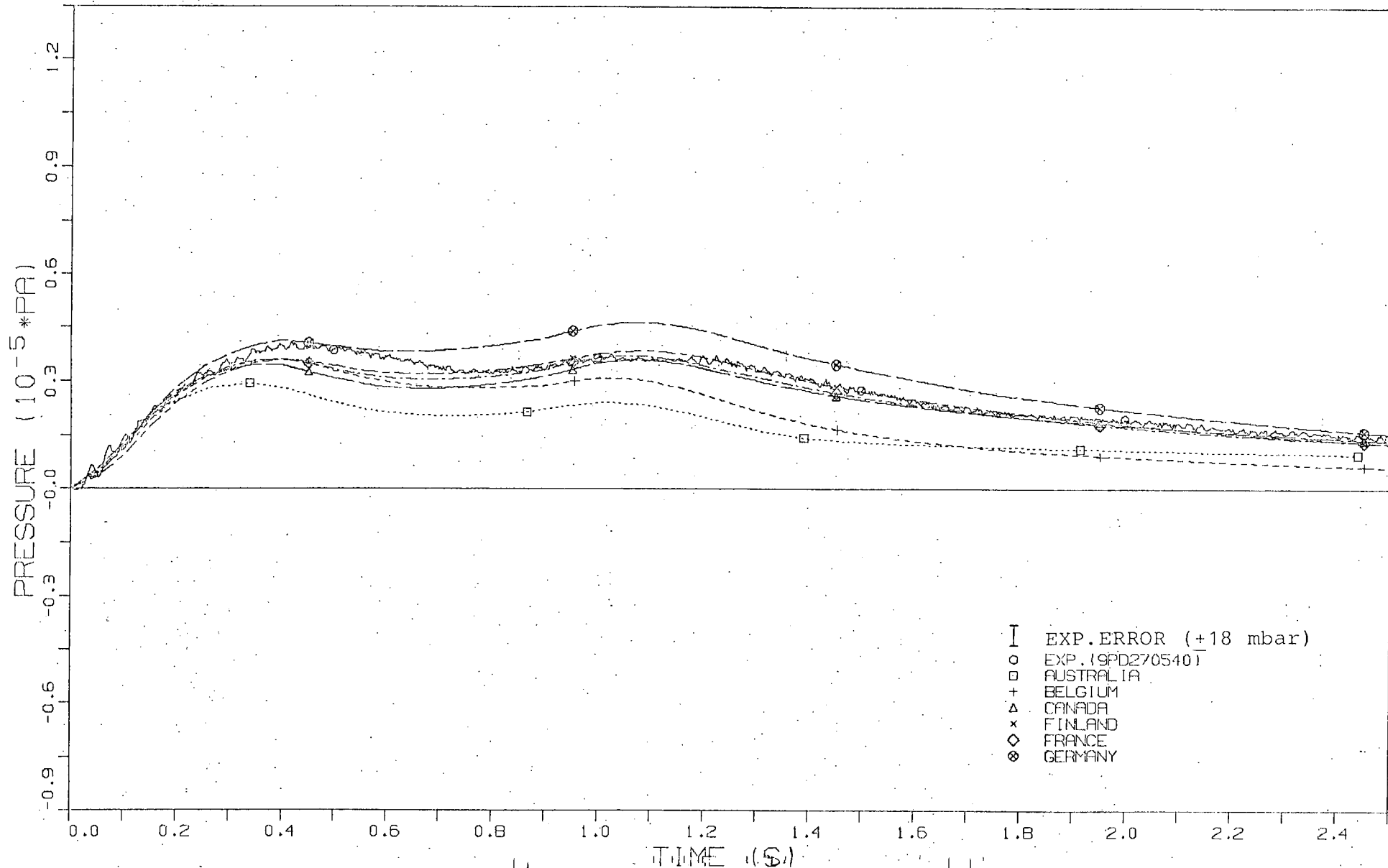


FIG. 28 A HISTORY OF PRESSURE DIFFERENCE R5 R9

OECD-CSNI CONTAINMENT STANDARD PROBLEM NO.2 (TEST CASP2)

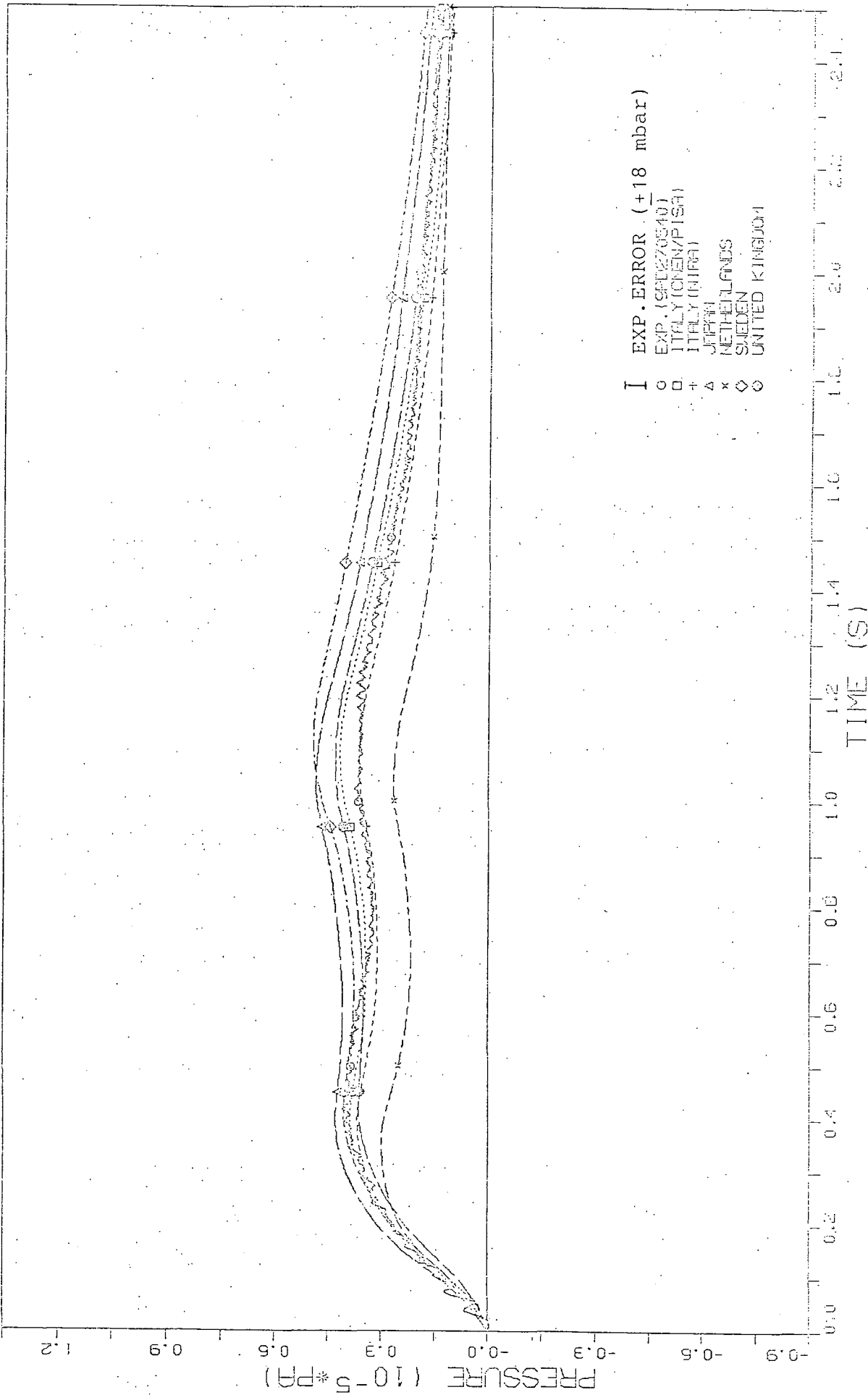


FIG. 28R HISTORY OF PRESSURE DIFFERENCE PE-EE

OECD-CSNI CONTAINMENT STANDARD PROBLEM NO.2 (TEST CASP2)

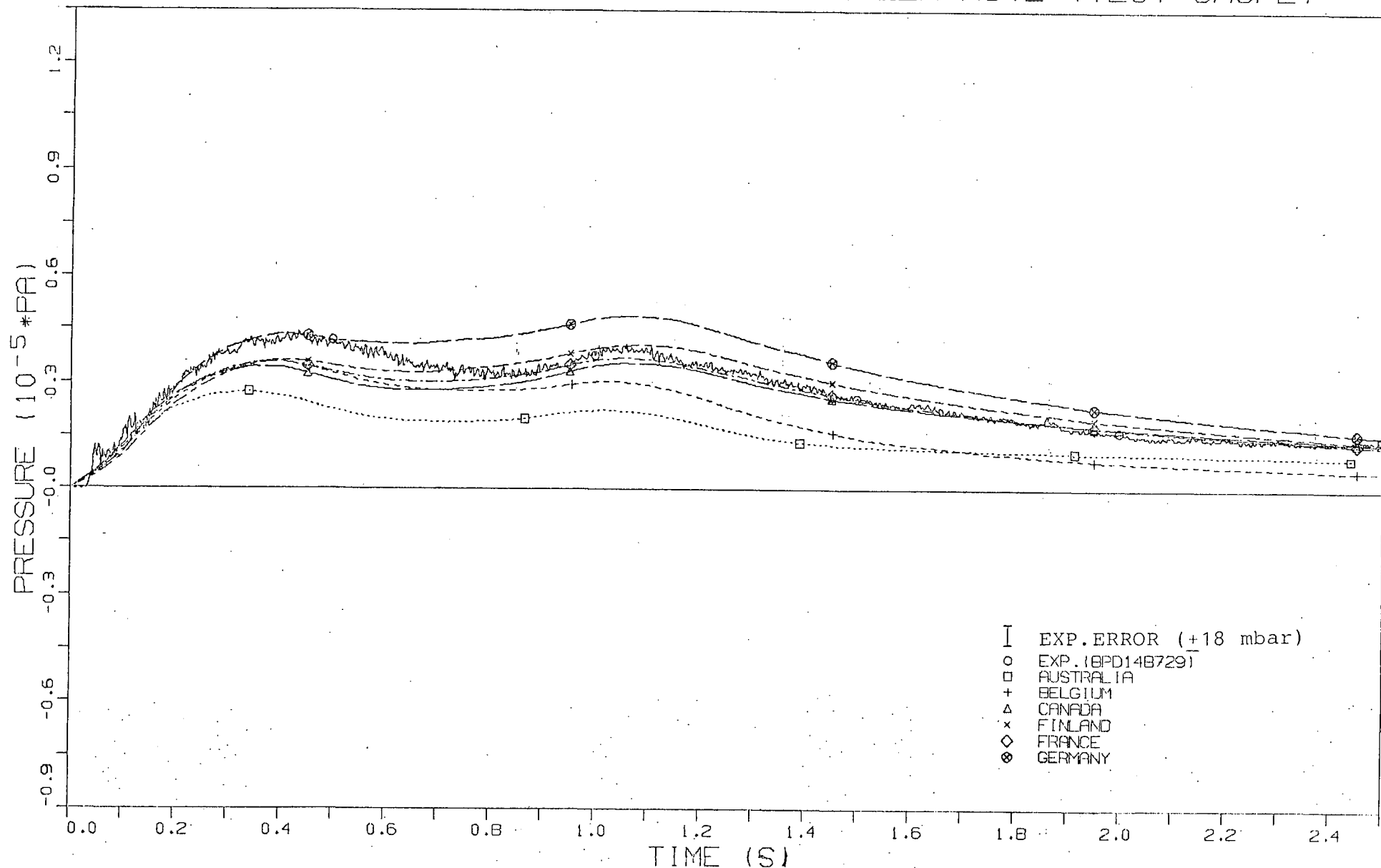


FIG. 29A HISTORY OF PRESSURE DIFFERENCE R7-R8

OECD-CSNI CONTAINMENT STANDARD PROBLEM NO.2 (TEST CASP2)

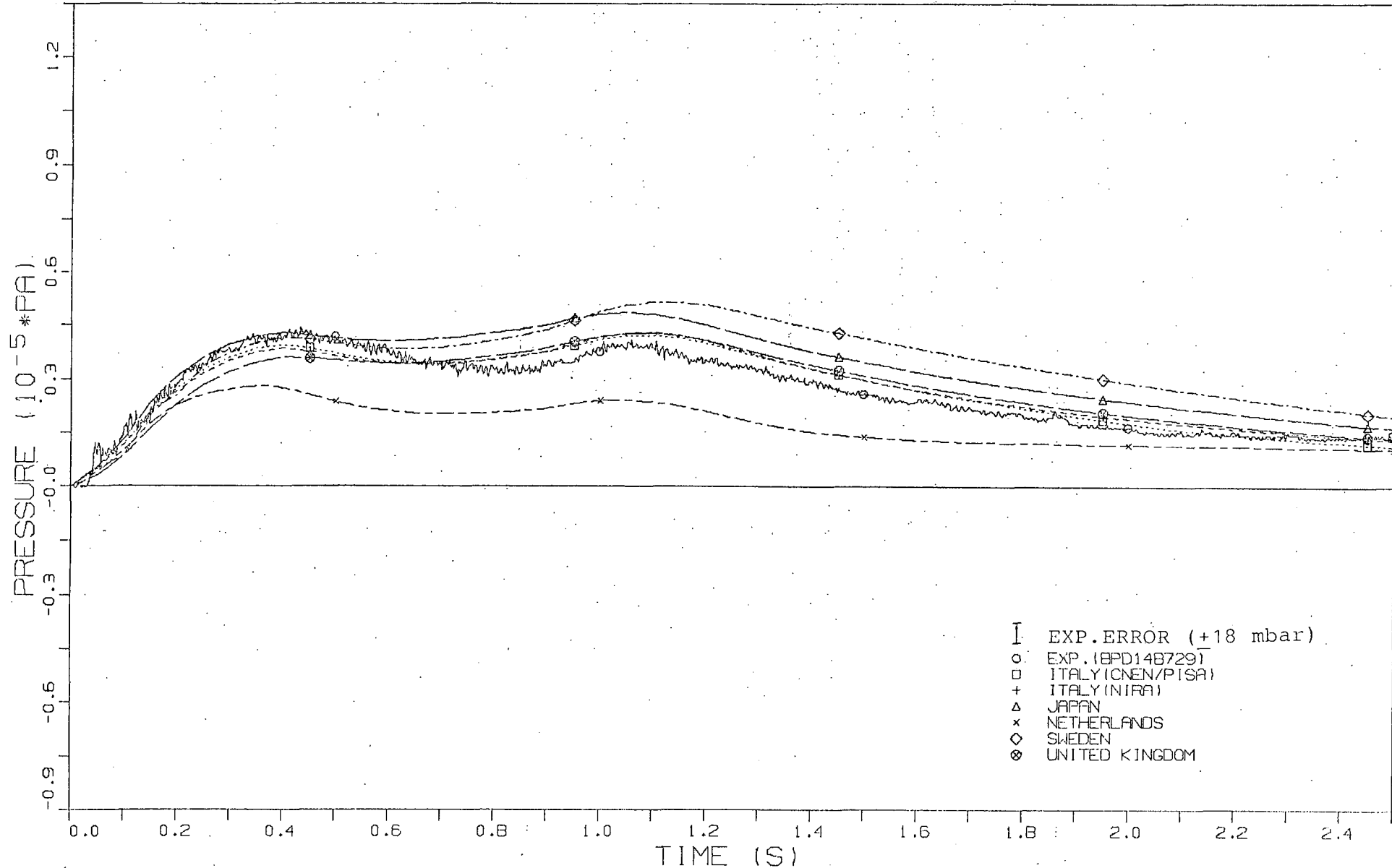


FIG. 29B HISTORY OF PRESSURE DIFFERENCE R7-R8



- Temperatures in rupture compartment R4 (figs. 30A, 30B and 31A, 31B):

At the bottom as well as in the middle of the compartment temperature breaks can be observed, which indicate the passage of large air bales what cannot be described by the programs. The steep rise to saturation temperature in the lower region (= rapid propagation of the steam-water-mixture) is calculated within a relatively small bandwidth disregarding 2 respectively 1 exception.

The calculational results of Germany are considerably lower than the experimental data, although compartment R4 is simulated by 3 nodes (hindered washing-out of air?). Results of Sweden correspond to the higher pressure calculated for R4.

- Temperatures in compartment R5 (figs. 32A, 32B and 33A, 33B):

The nearer the measuring point to vent Ü45, the sooner it is reached by the steam front (sharp rise delayed by 0.1 s). The rear part of the compartment not directly flown through, is reached later by the steam front (0.3 s). This temperature behaviour shows that there is a large portion of air which is not washed out (slow rise with breaks).

The results of participants who do not subdivide the compartment are approximately in the middle between both experimental curves. Participants using a finer nodalisation (Finland, Germany, Netherlands) calculate the temperature behaviour near the vent very well, however, their results for the rear part of the compartment fall considerably below the experimental results (percentage of air too high?). It is obvious that no program describes the propagation of the steam front correctly.

- Temperatures in compartment R7 (figs. 34A, 34B and 35A, 35B):

In compartment R7 in which the flow is mainly longitudinal, the dead-end effect is less pronounced.

Except in the initial phase (steam front) there is a good agreement between calculational and experimental results.

- Temperatures in compartment R8 (figs. 36A, 36B and 37A, 37B):

The arrival of a steam front can hardly be detected. Temperature rises slowly near the vent of R7, but faster than in the rest of the dead end space (additional temperature breaks caused by air bales).

The results obtained by the participants differ widely especially with respect to the dead end space and fall mainly above the experimental results.

- Temperature in dome compartment R9 (figs. 38A, 38B):

The measuring point located within the inner cylinder at appr. the level of vent Ü59B shows the washing of air bales containing little steam quality after a slight temperature rise until 0.7 s due to compression.

The calculational results of the participants with one node for R9 show a good agreement with the experimental results, while the other participants overpredicted this temperature.

- Temperature in compartment R6 (figs. 39A, 39B):

The air in compartment R6 is obviously only compressed.

The participants, except United Kingdom, predicted the temperature in compartment R6 higher than the experimental one. The results remain in a wide spreadband. The results of Australia, Canada, Italy (NIRA), Japan and United Kingdom are close to the experiment (all with 6-node simulation of the whole containment, i.e. 1 node for R6).

OECD-CSNI CONTAINMENT STANDARD PROBLEM NO.2 (TEST CASP2)

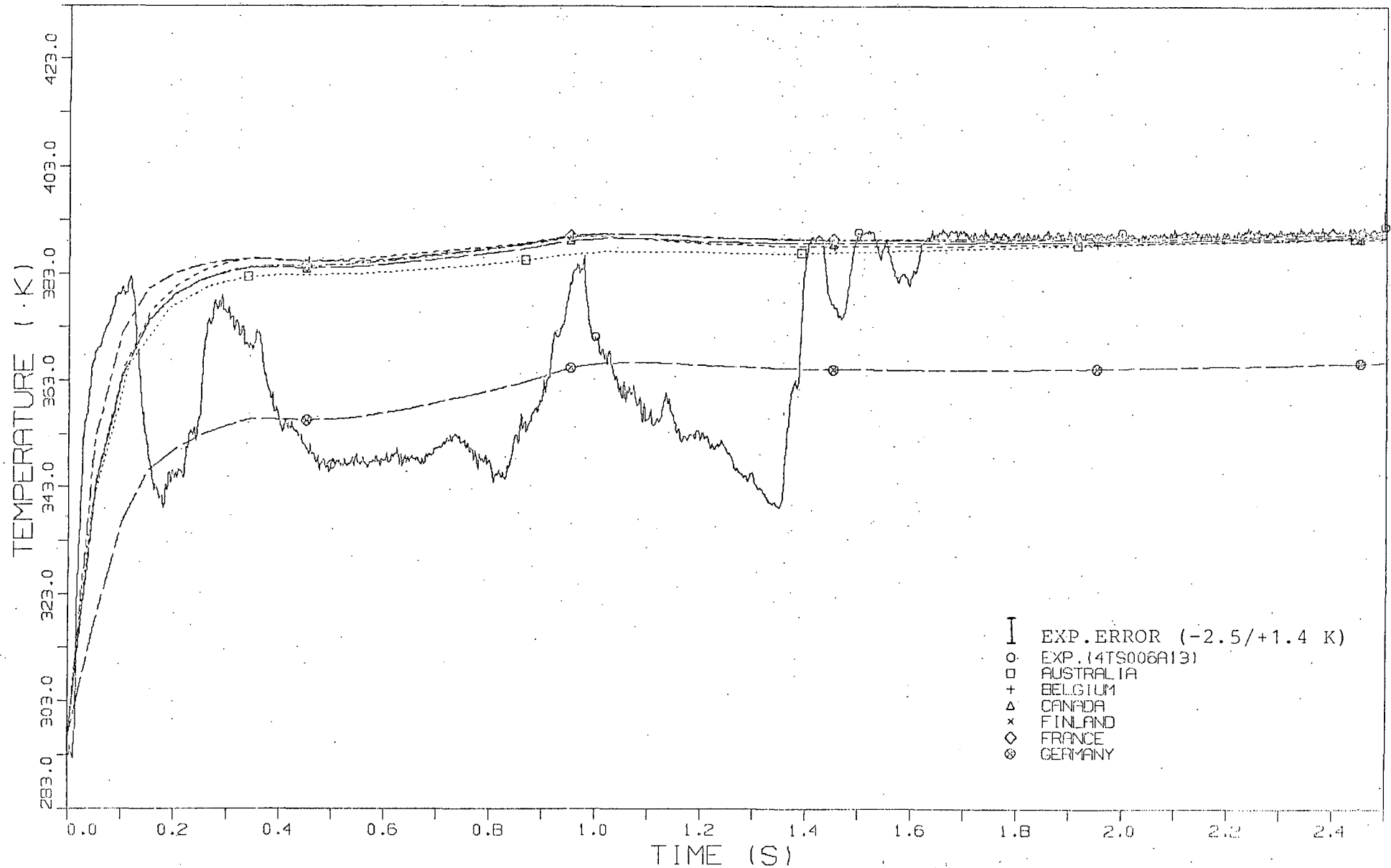


FIG. 30A TEMPERATURE HISTORY IN COMPARTMENT R4

OECD-CSNI CONTAINMENT STANDARD PROBLEM NO.2 (TEST CASP2)

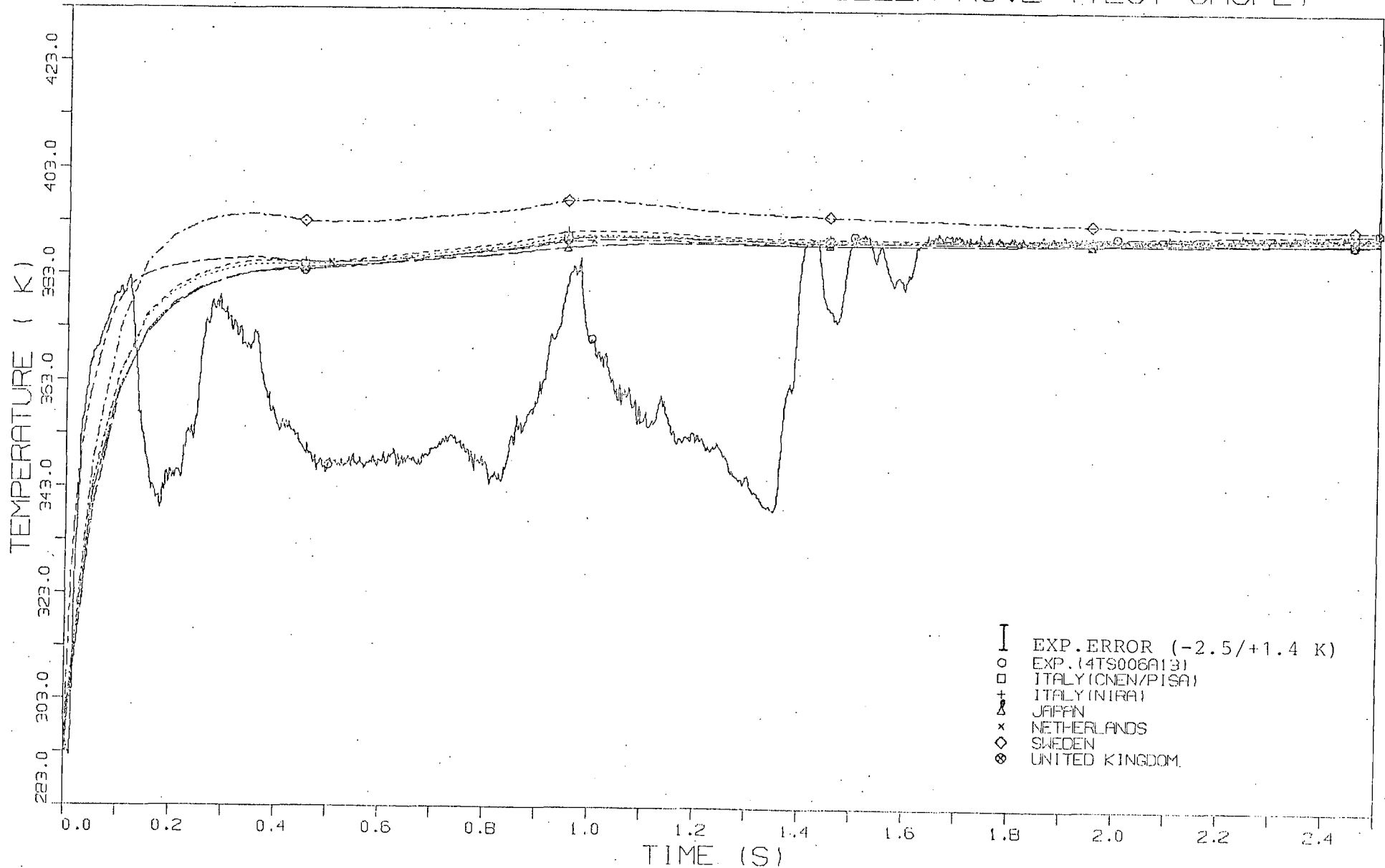


FIG. 30R TEMPERATURE HISTORY IN COMPARTMENT D1

OECD-CSNI CONTAINMENT STANDARD PROBLEM NO.2 (TEST CASP2)

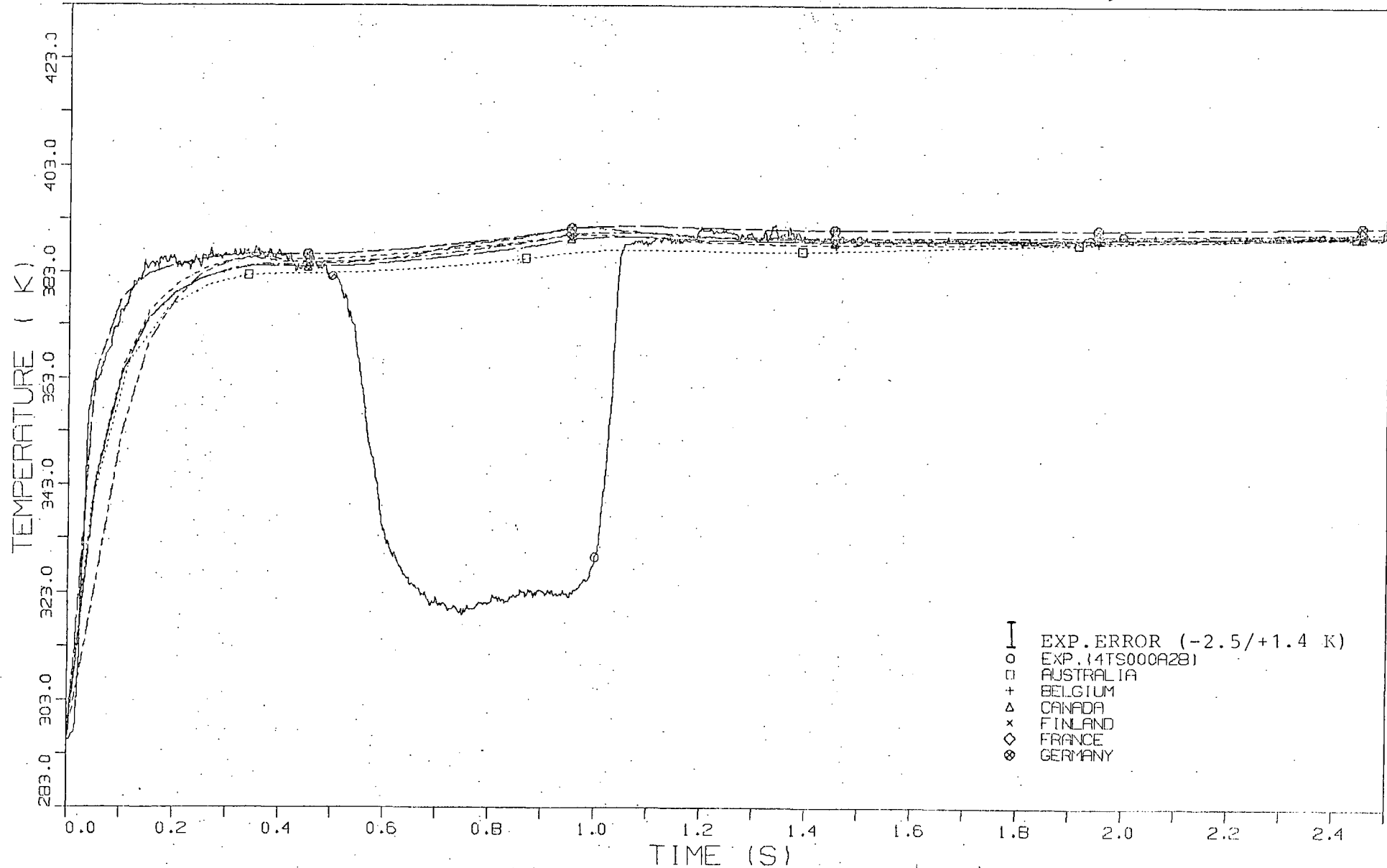


FIG. 31A - TEMPERATURE HISTORY IN COMPARTMENT R4

OECD-CSNI CONTAINMENT STANDARD PROBLEM NO.2 (TEST CASP2)

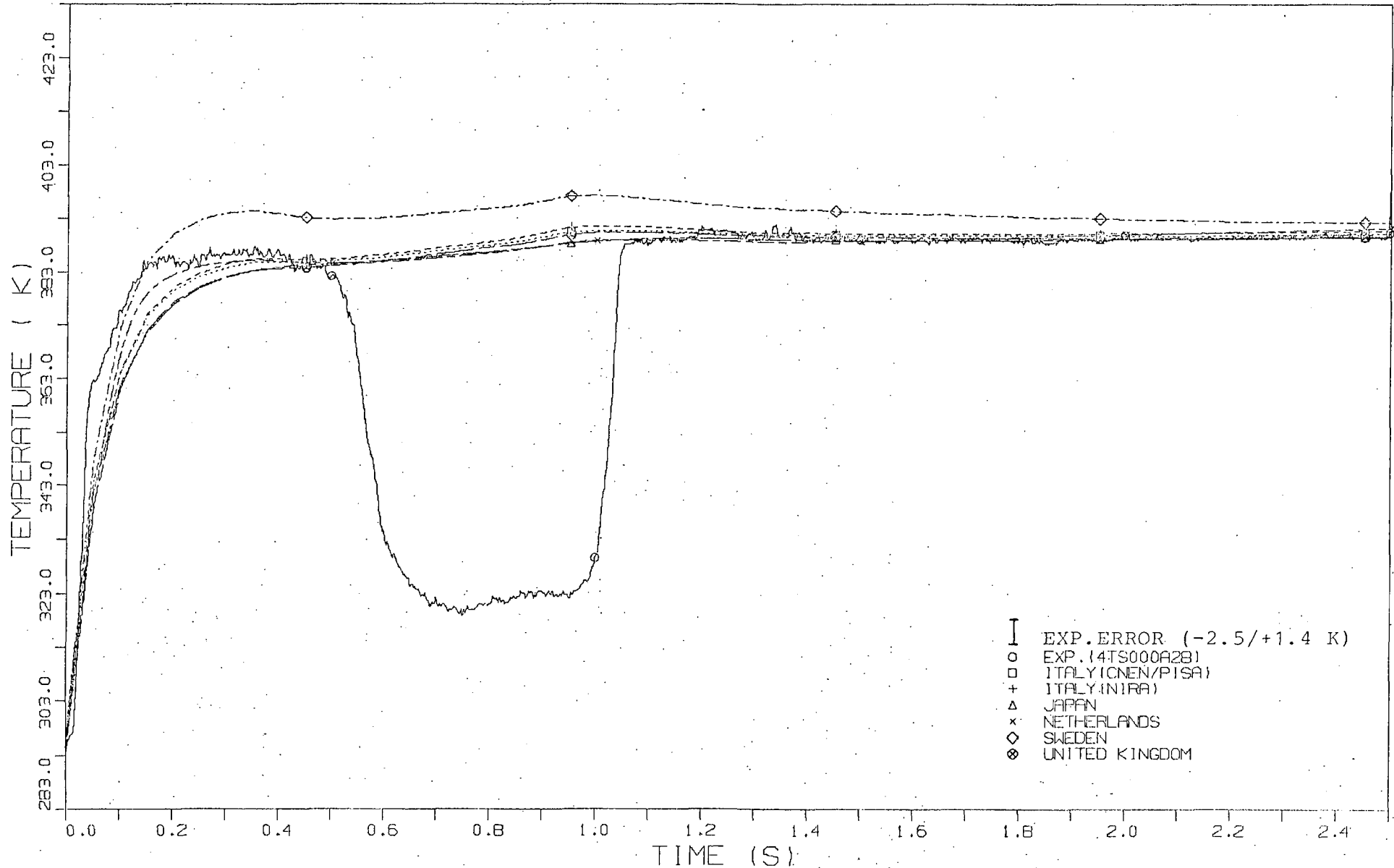


FIG. 31B TEMPERATURE HISTORY IN COMPARTMENT R4

OECD-CSNI CONTAINMENT STANDARD PROBLEM NO.2 (TEST CASP2)

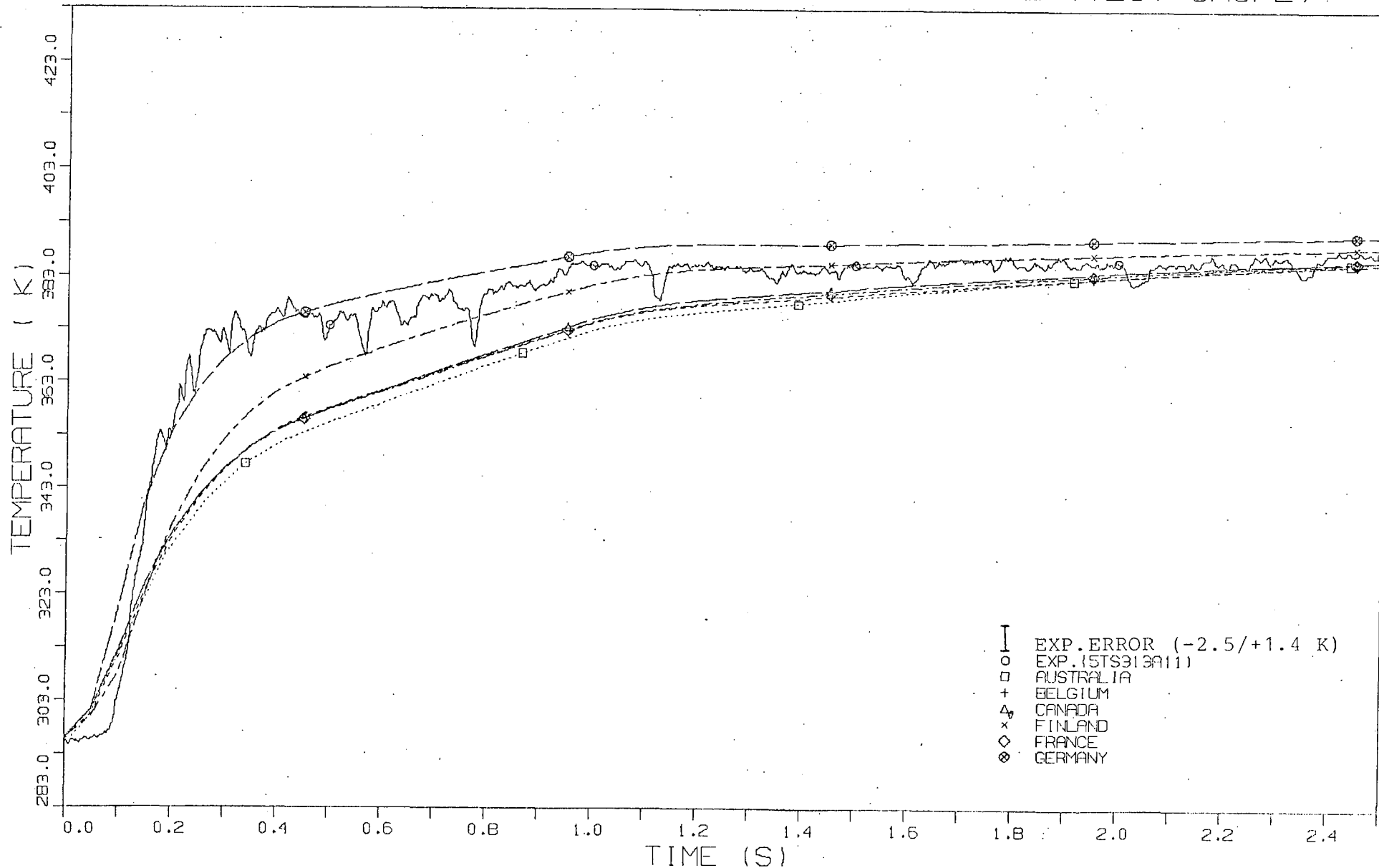


FIG. 32A . TEMPERATURE HISTORY IN COMPARTMENT R5

OECD-CSNI CONTAINMENT STANDARD PROBLEM NO.2 (TEST CASP2)

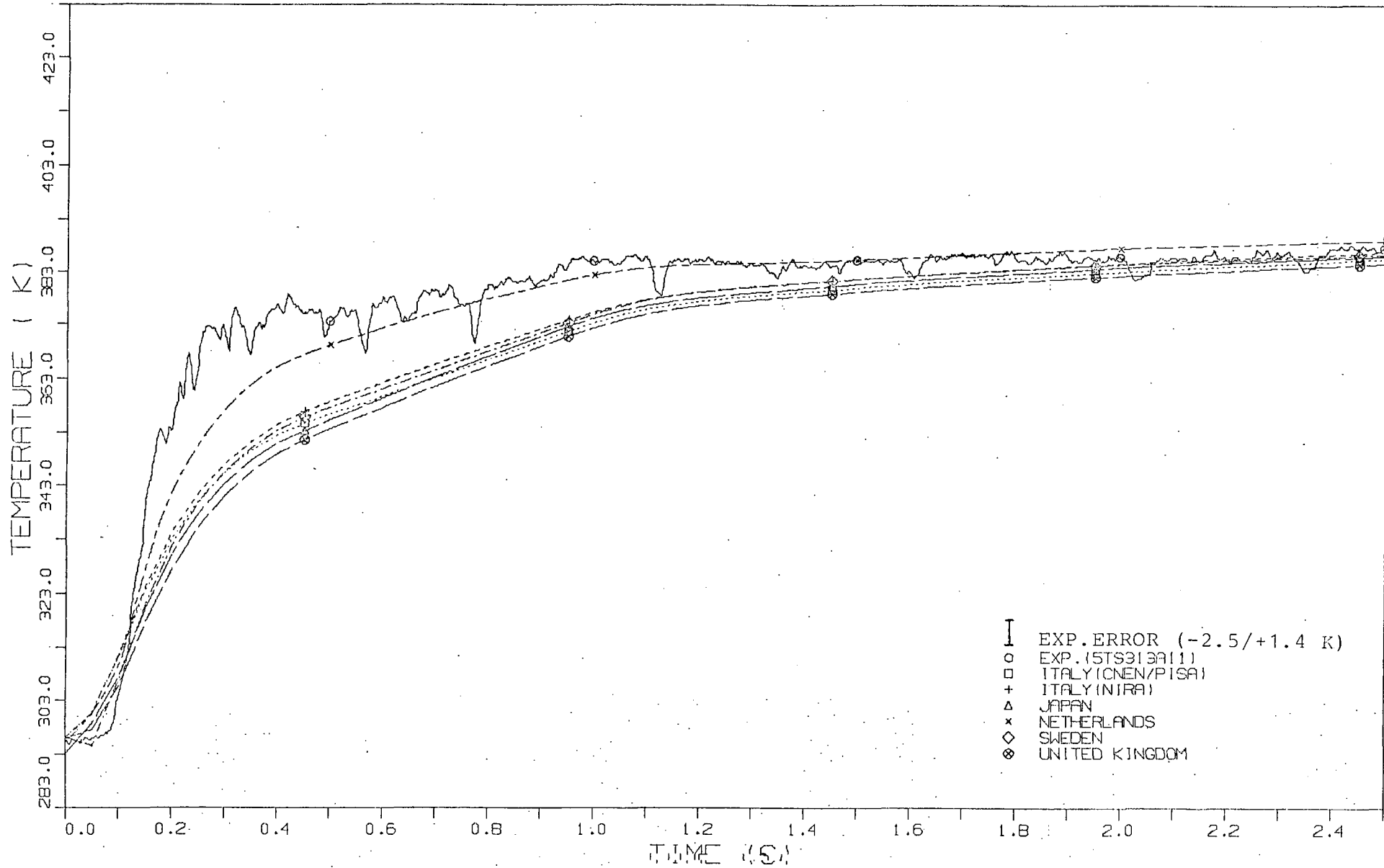


FIG. 32B TEMPERATURE HISTORY IN COMPARTMENT R5



OECD-CSNI CONTAINMENT STANDARD PROBLEM NO.2 (TEST CASP2)

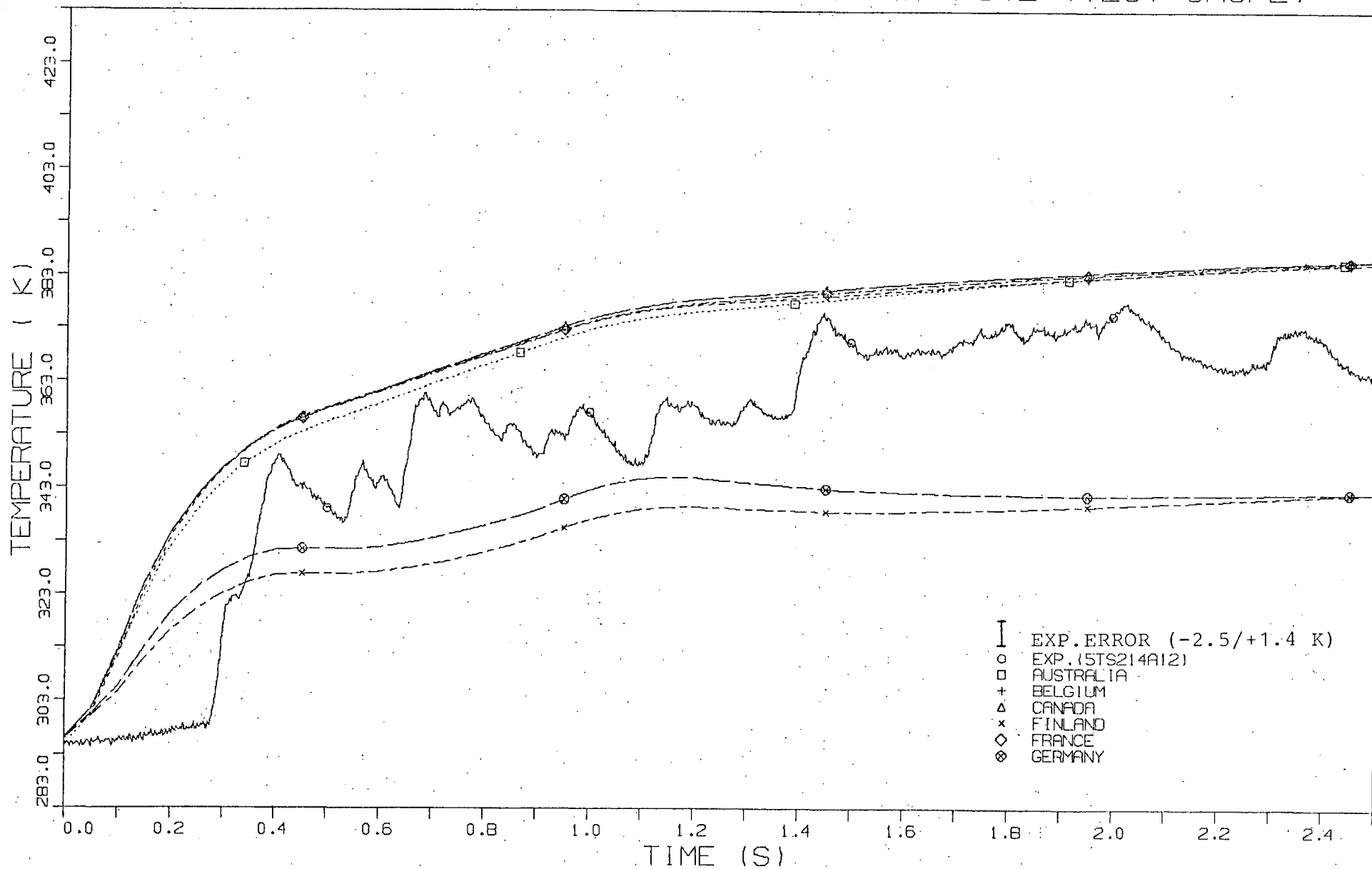


FIG. 33A TEMPERATURE HISTORY IN COMPARTMENT R5

OECD-CSNI CONTAINMENT STANDARD PROBLEM NO.2 (TEST CASP2)

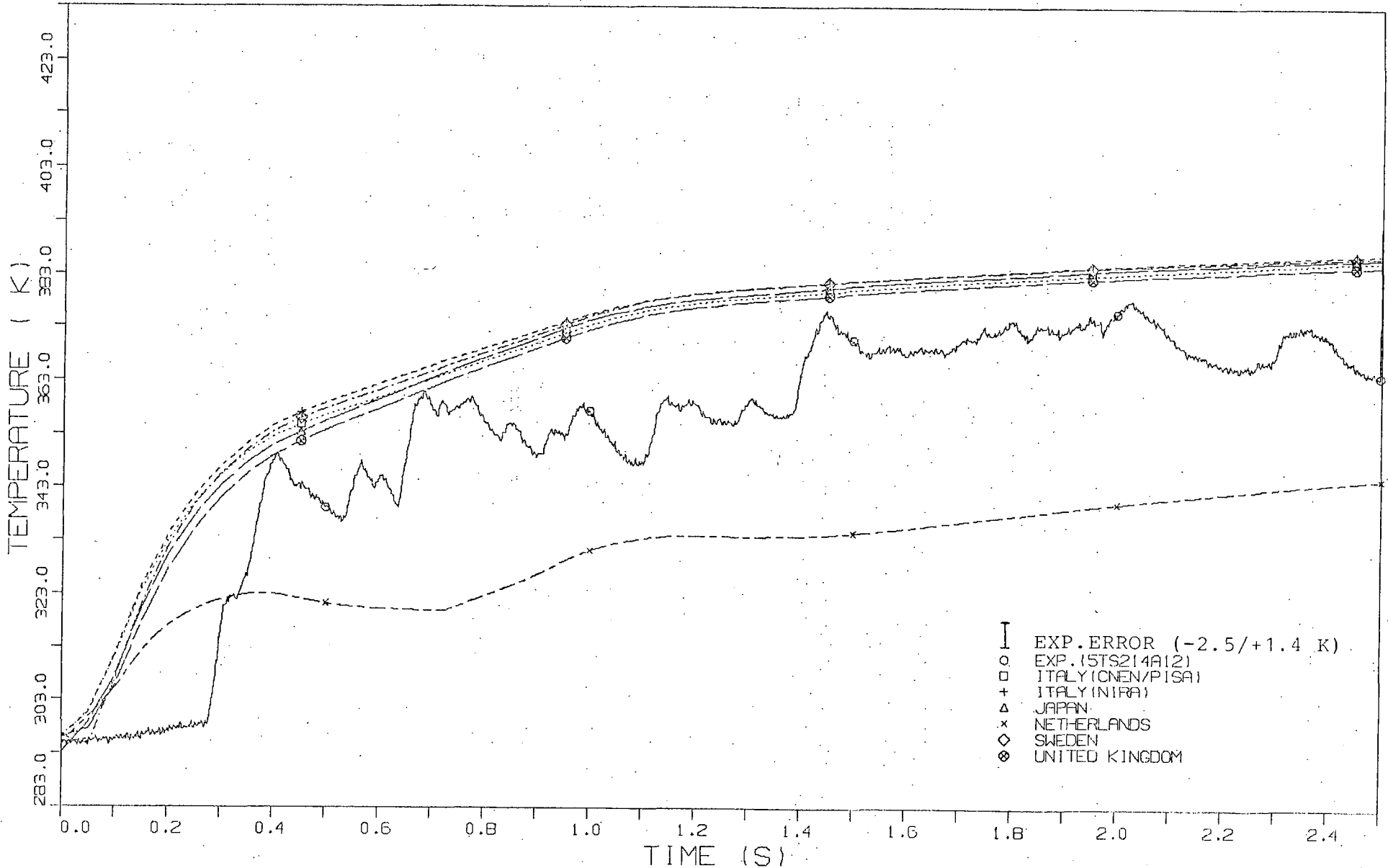


FIG. 33B TEMPERATURE HISTORY IN COMPARTMENT R5

OECD-CSNI CONTAINMENT STANDARD PROBLEM NO.2 (TEST CASP2)

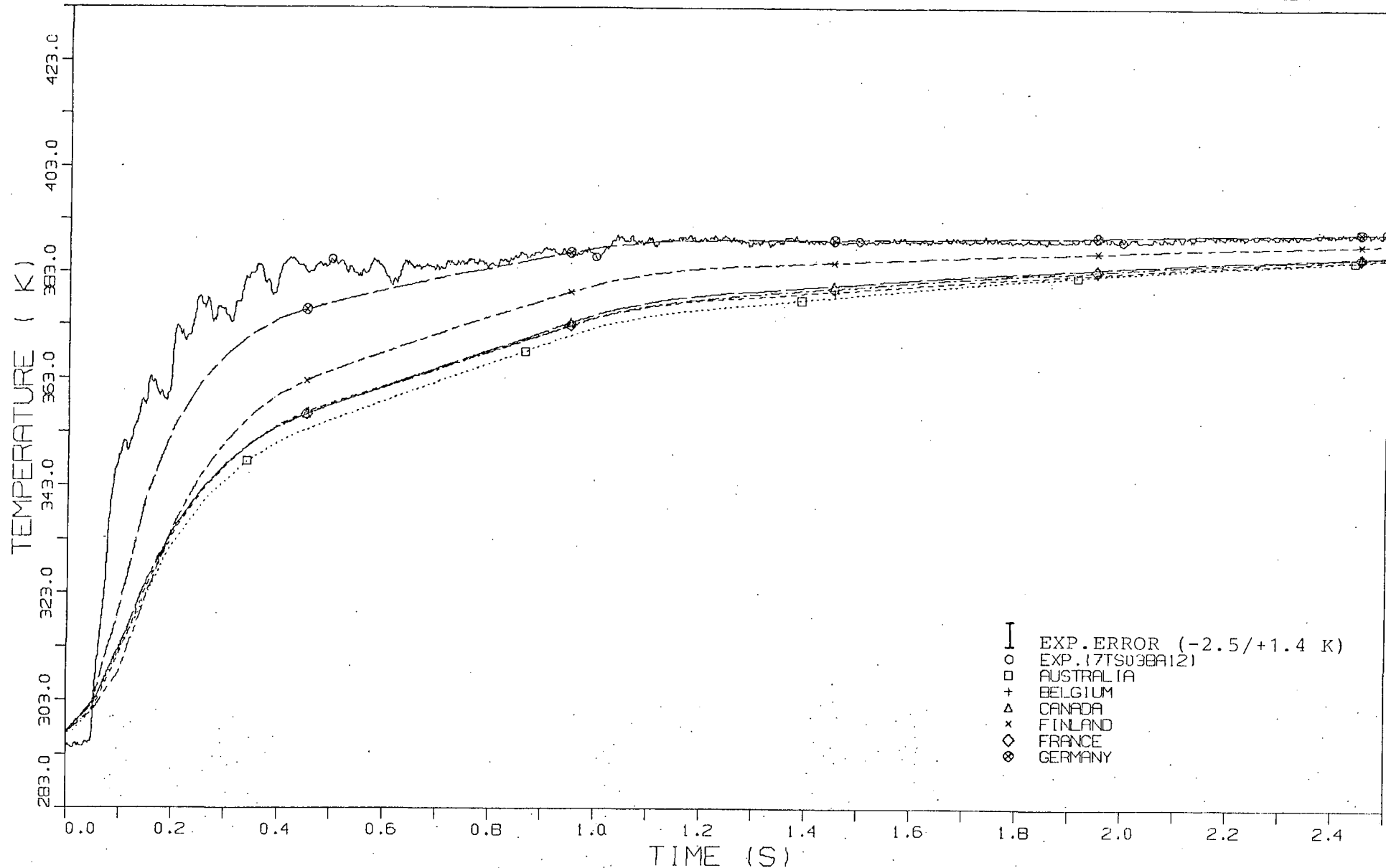


FIG. 34A . TEMPERATURE HISTORY IN COMPARTMENT R7

OECD-CSNI CONTAINMENT STANDARD PROBLEM NO.2 (TEST CASP2)

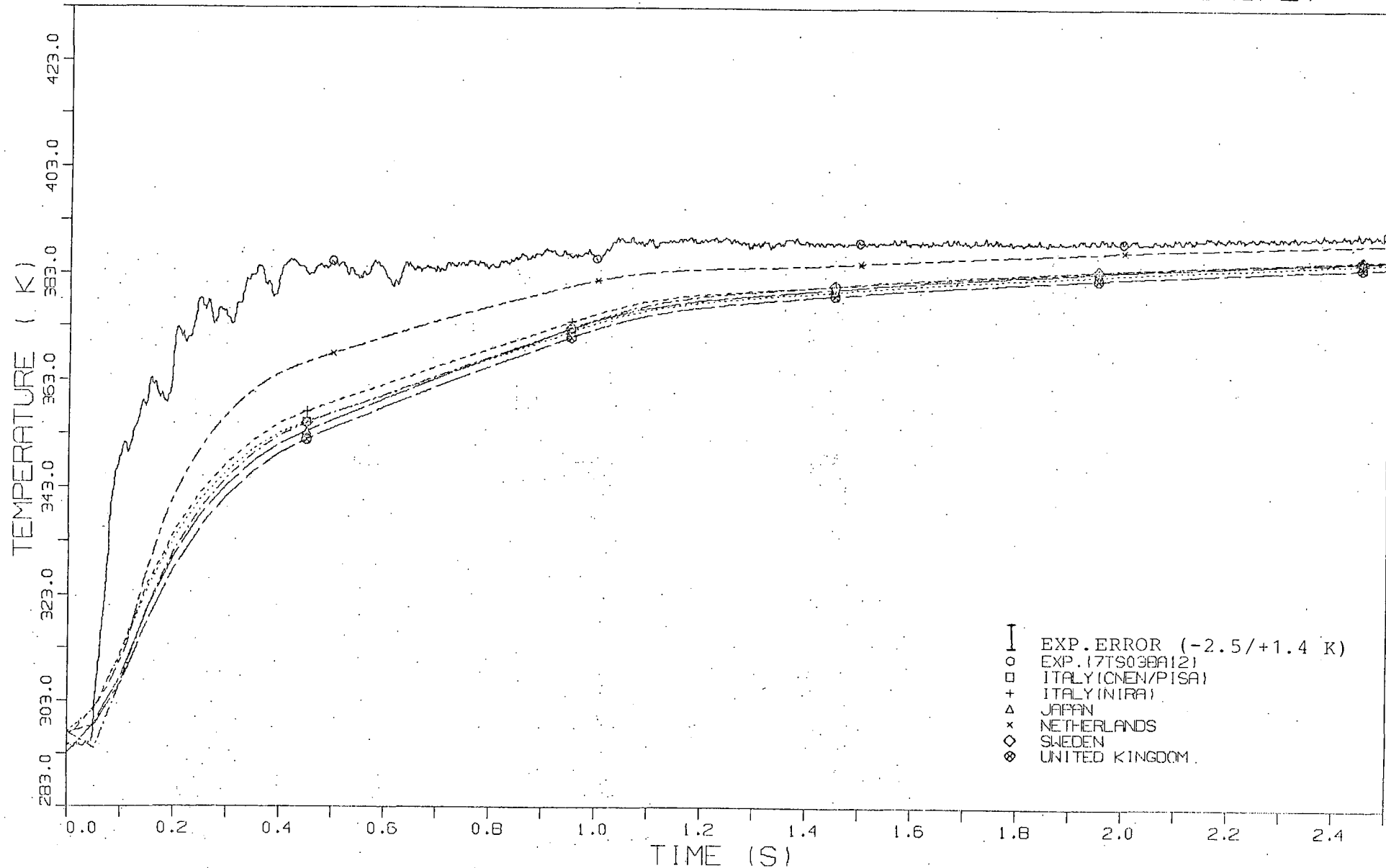


FIG. 3/8 TEMPERATURE HISTORY IN COMPARTMENT B7

OECD-CSNI CONTAINMENT STANDARD PROBLEM NO.2 (TEST CASP2)

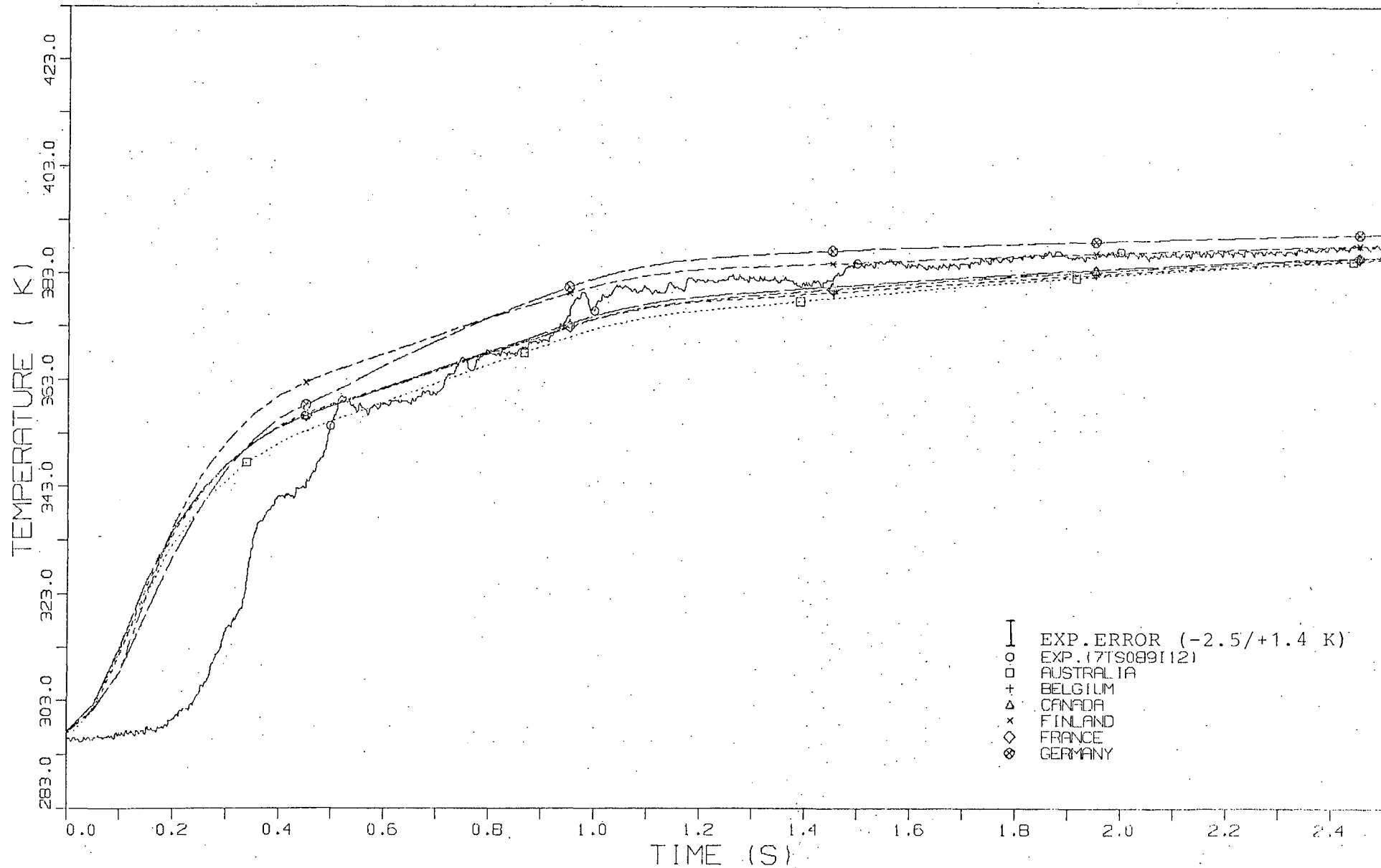


FIG. 35A , TEMPERATURE HISTORY IN COMPARTMENT R7

OECD-CSNI CONTAINMENT STANDARD PROBLEM NO.2 (TEST CASP2)

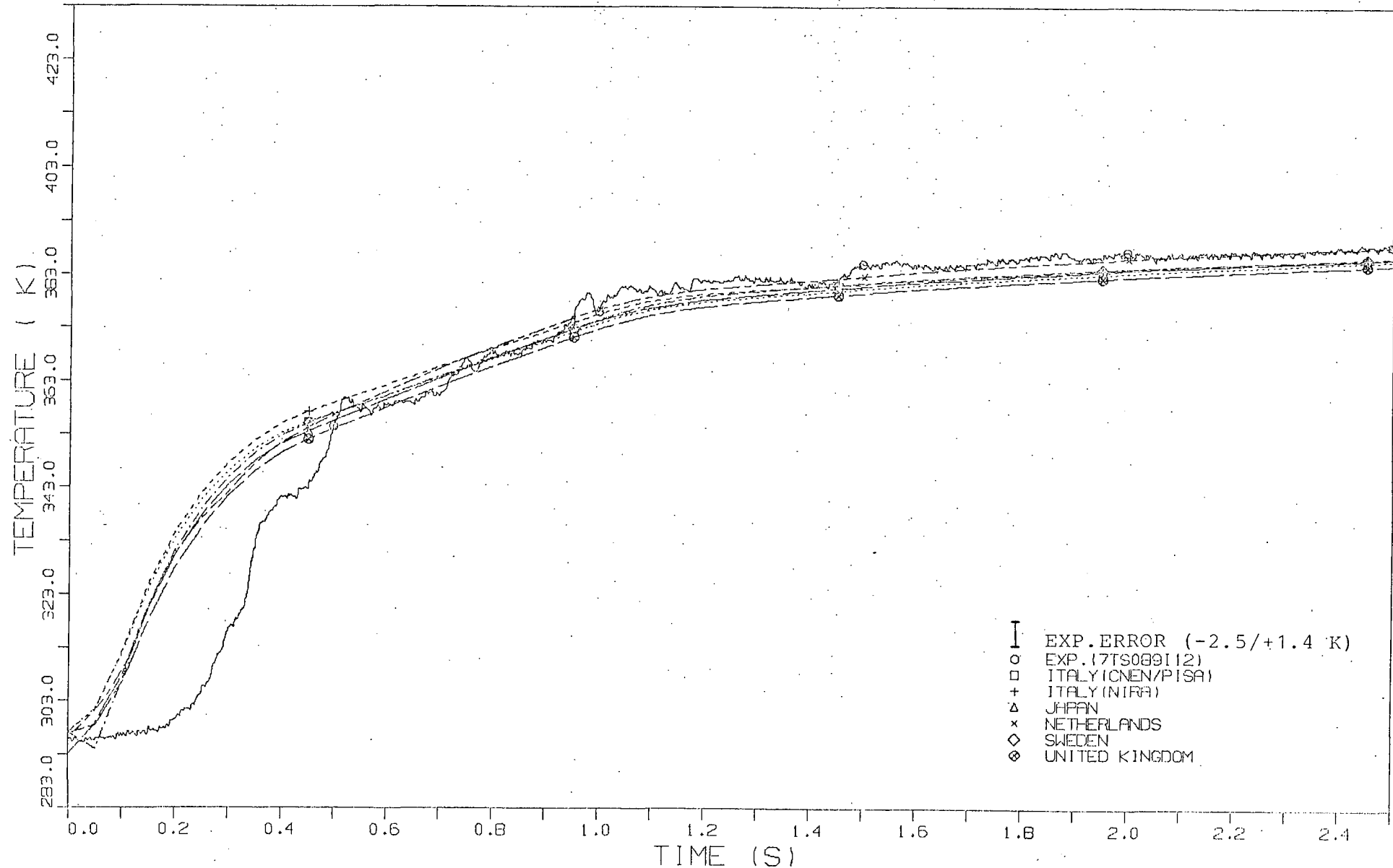


FIG. 35R TEMPERATURE HISTORY IN COMPARTMENT R7

OECD-CSNI CONTAINMENT STANDARD PROBLEM NO.2 (TEST CASP2)

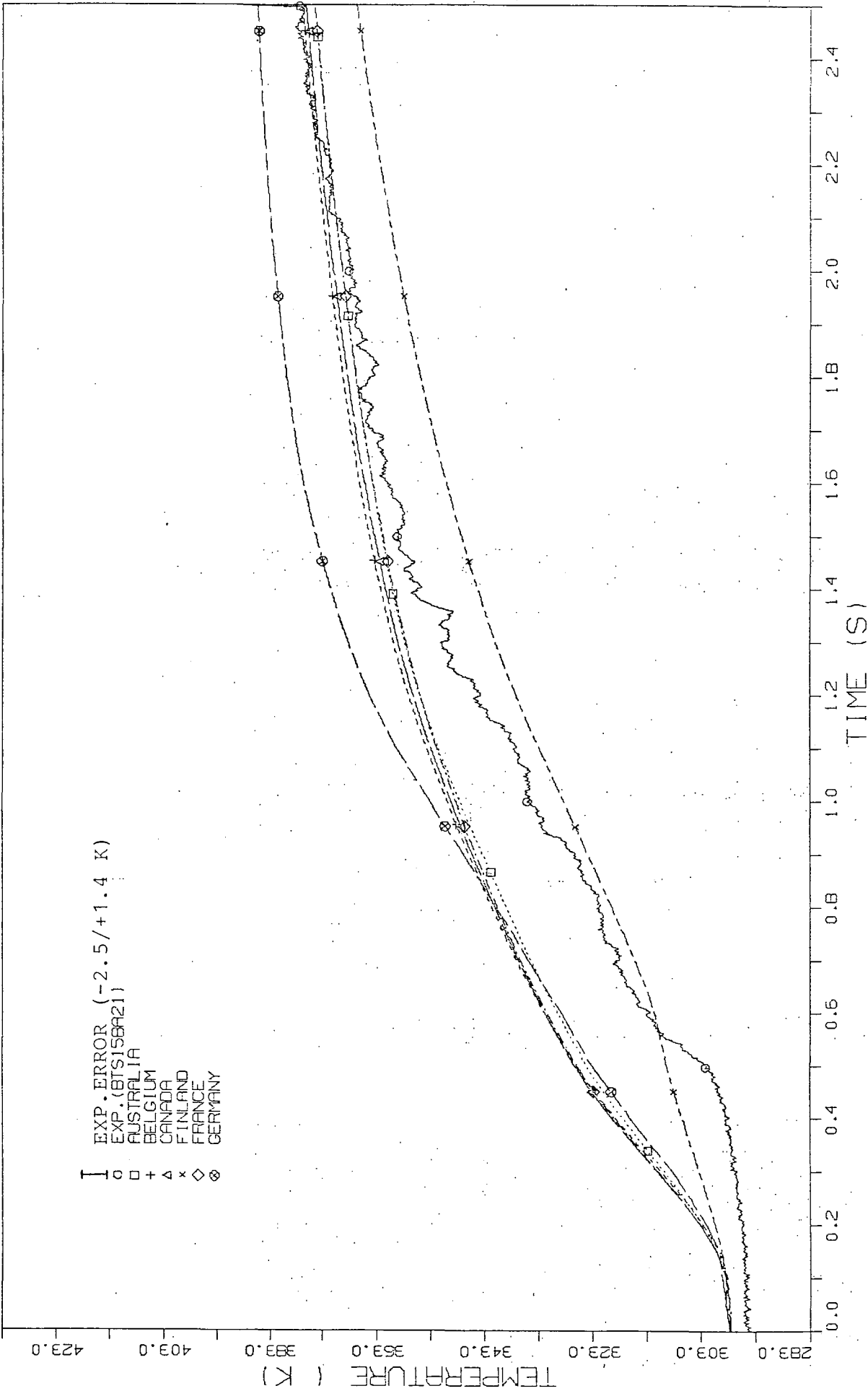


FIG. 36A TEMPERATURE HISTORY IN COMPARTMENT RA

OECD-CSNI CONTAINMENT STANDARD PROBLEM NO.2 (TEST CASP2)

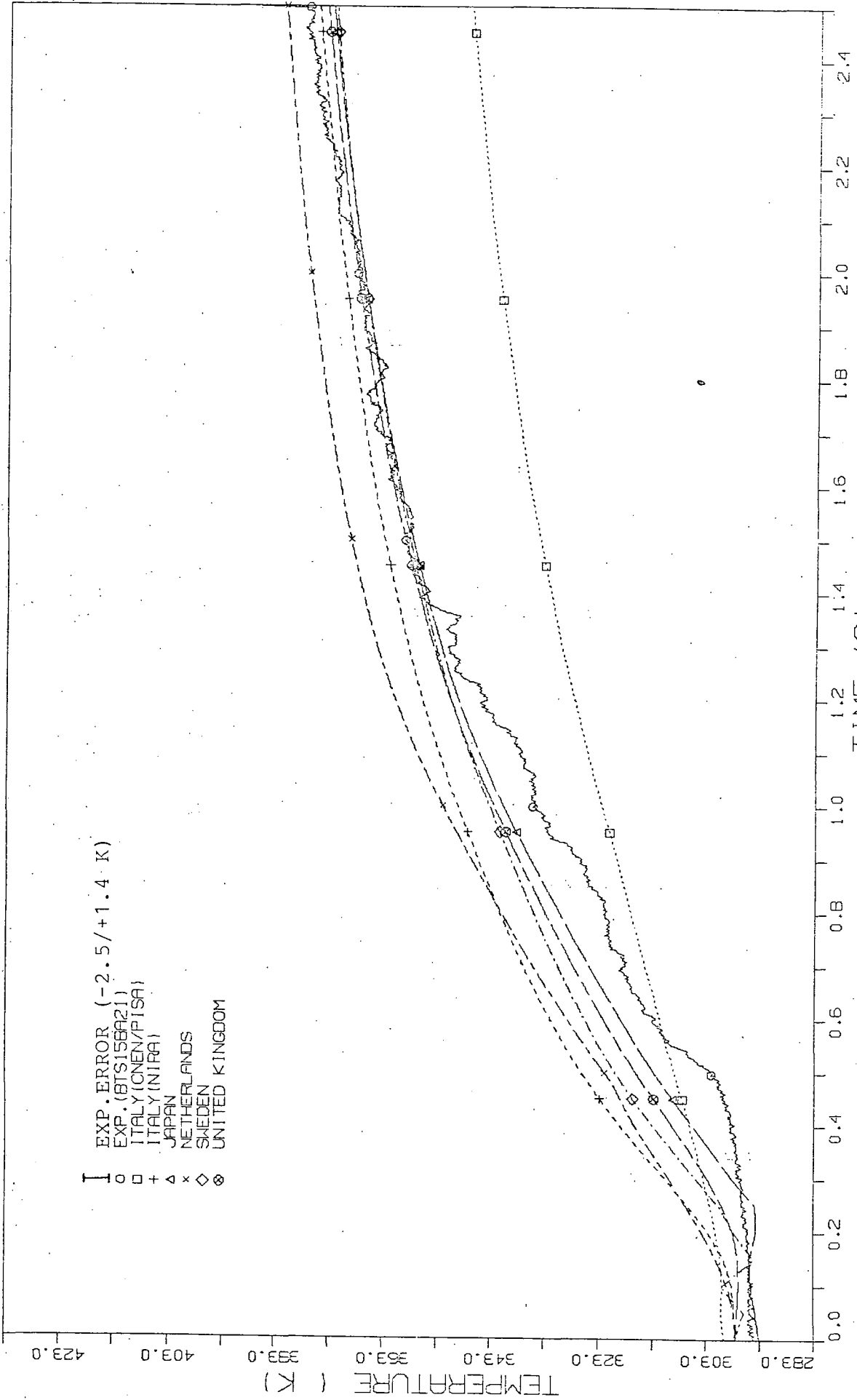


FIG 36B TEMPERATURE HISTORY IN COMPARTMENT 00



OECD-CSNI CONTAINMENT STANDARD PROBLEM NO.2 (TEST CASP2)

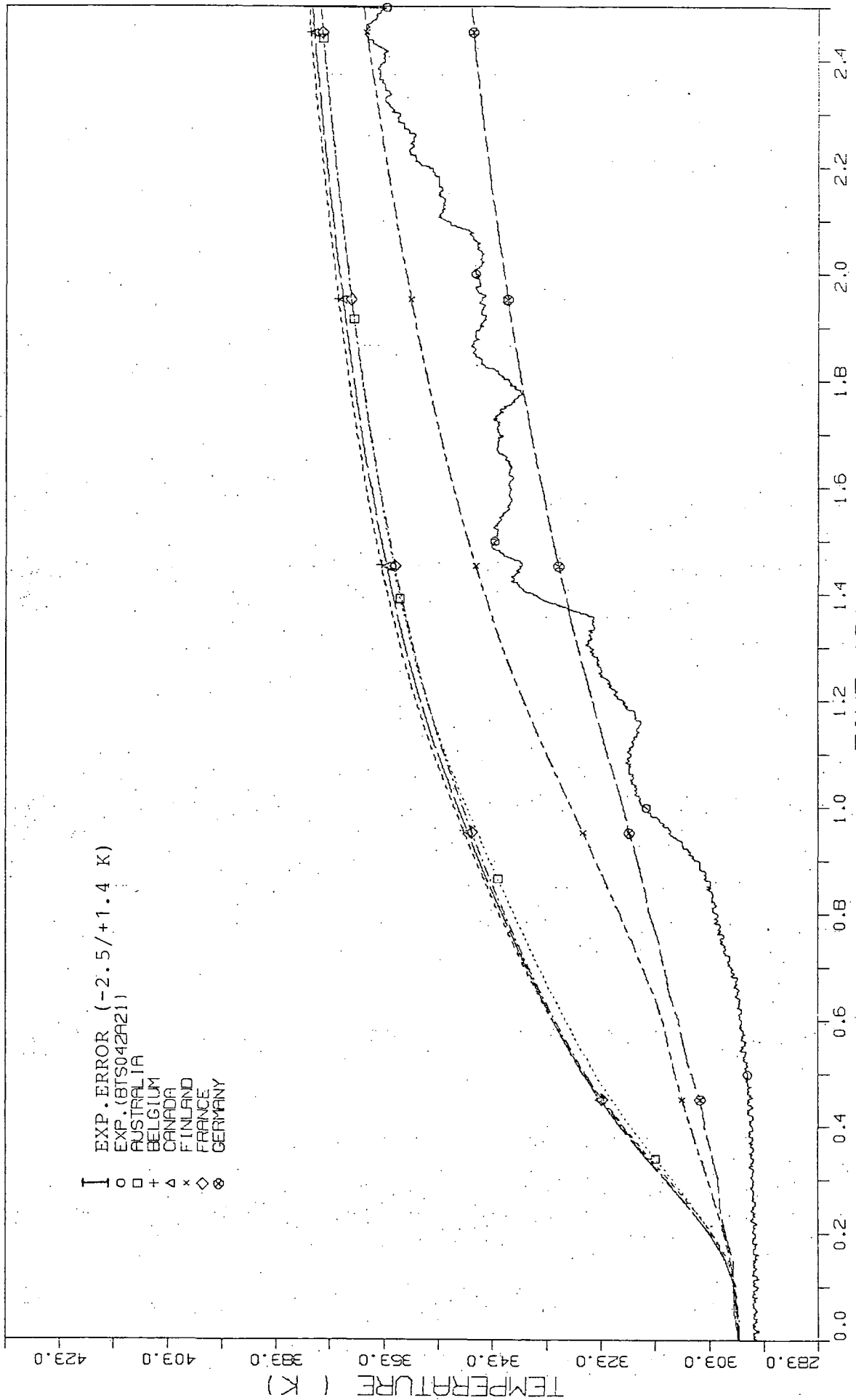


FIG. 37A . TEMPERATURE HISTORY IN COMPARTMENT R8

OECD-CSNI CONTAINMENT STANDARD PROBLEM NO.2 (TEST CASP2)

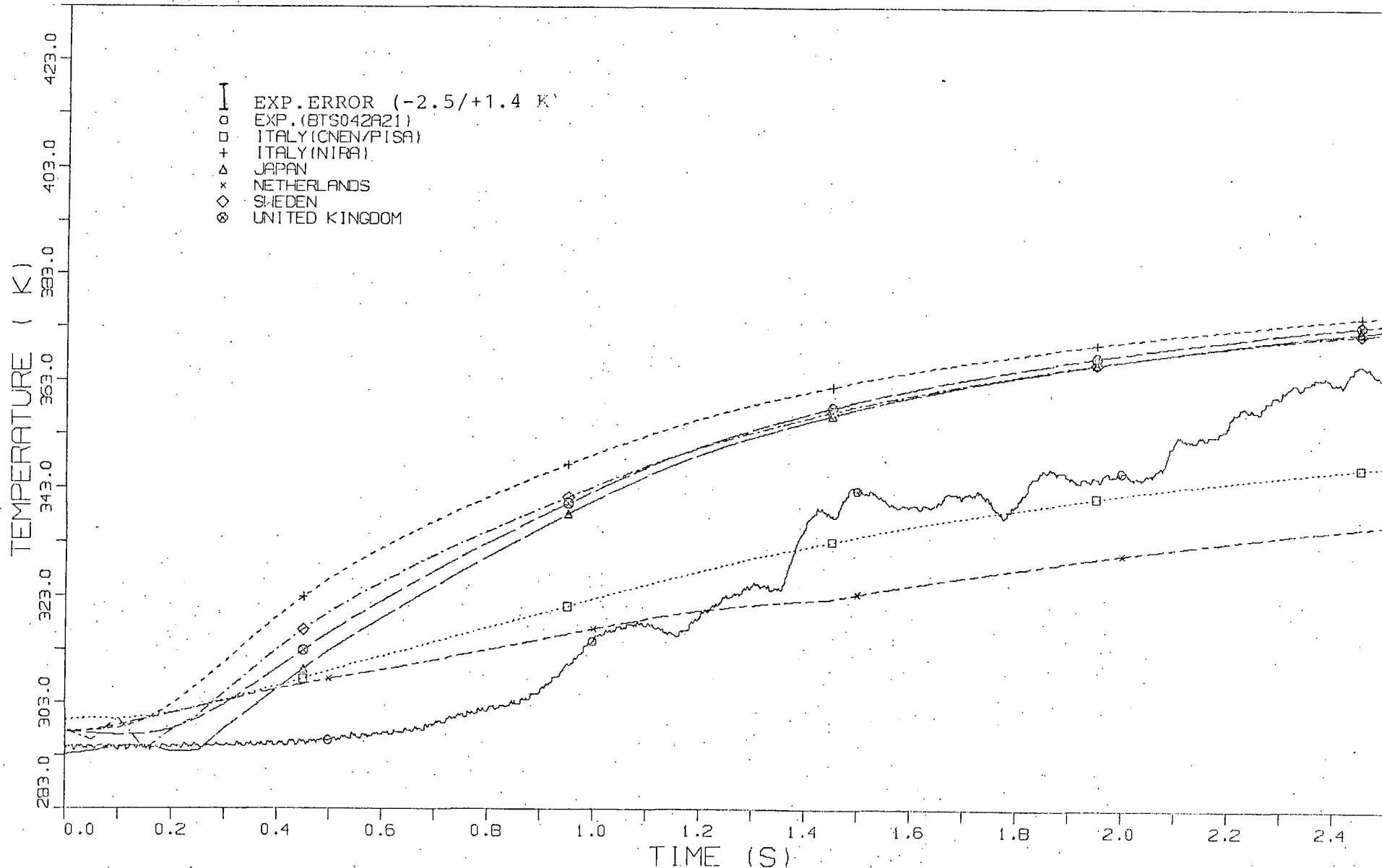


FIG. 37B TEMPERATURE HISTORY IN COMPARTMENT RO

OECD-CSNI CONTAINMENT STANDARD PROBLEM NO.2 (TEST CASP2)

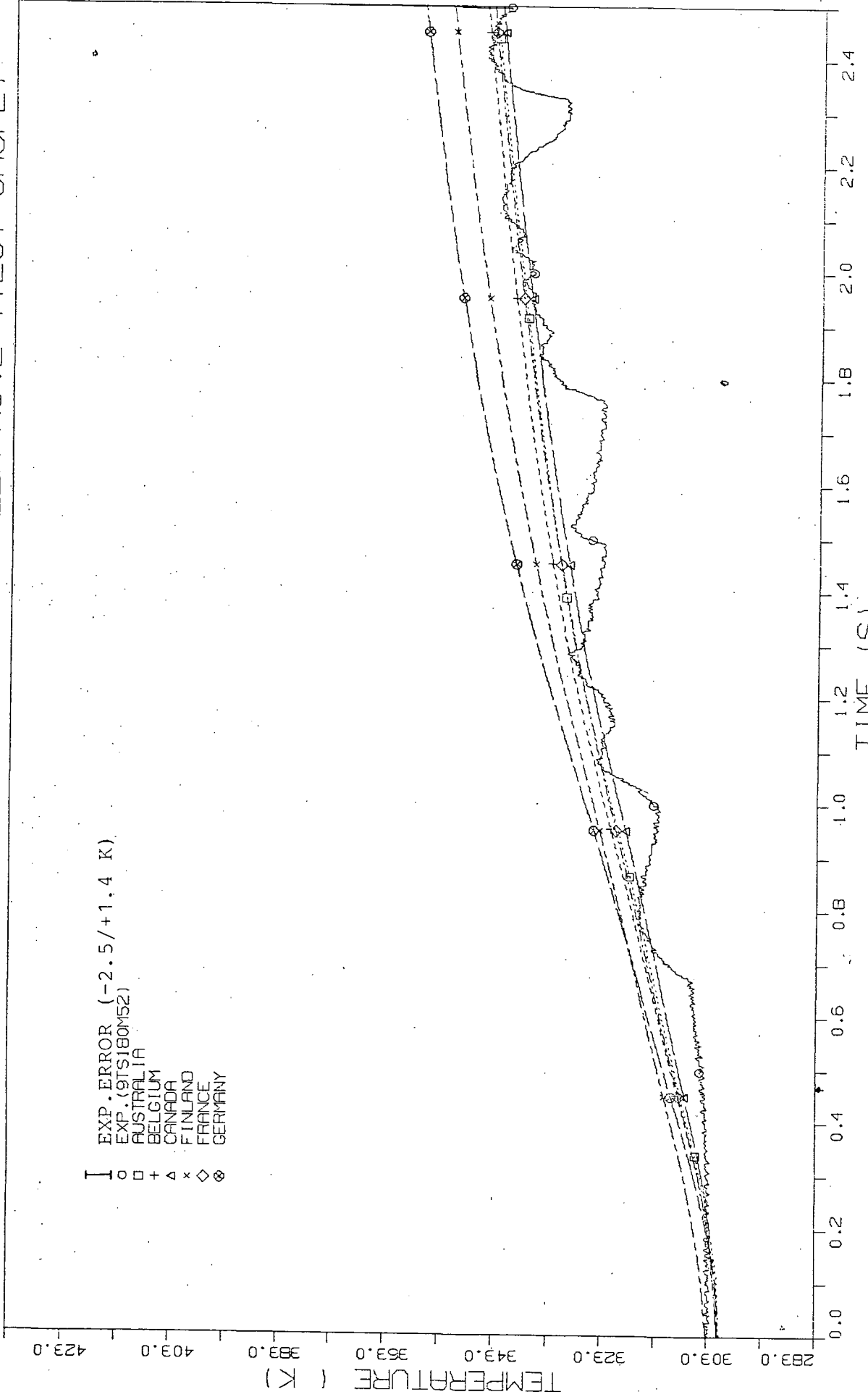


FIG. 38A . TEMPERATURE HISTORY IN COMPARTMENT R9

OECD-CSNI CONTAINMENT STANDARD PROBLEM NO.2 (TEST CASP2)

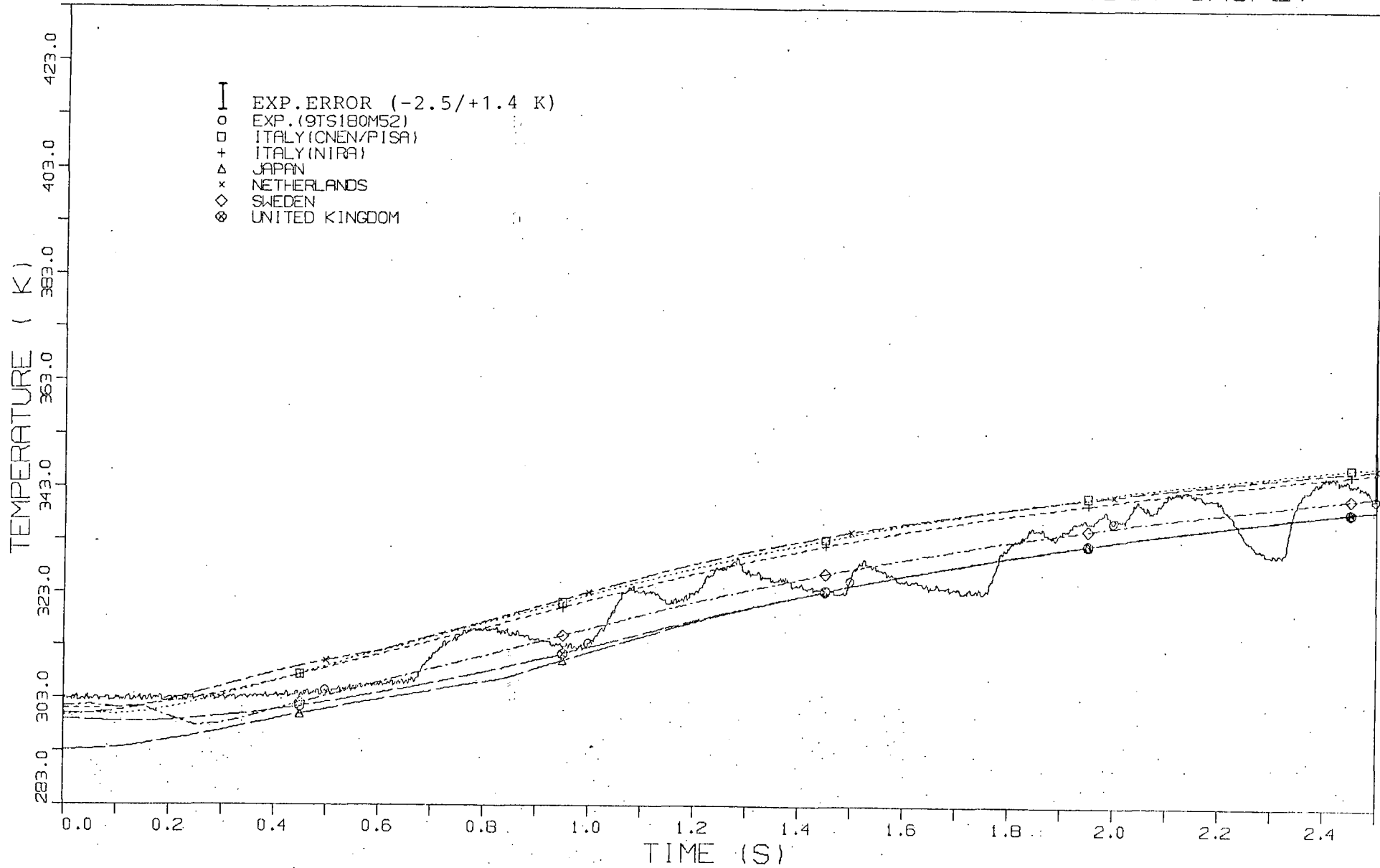


FIG. 38 B TEMPERATURE HISTORY IN COMPARTMENT R9

OECD-CSNI CONTAINMENT STANDARD PROBLEM NO.2 (TEST CASP2)

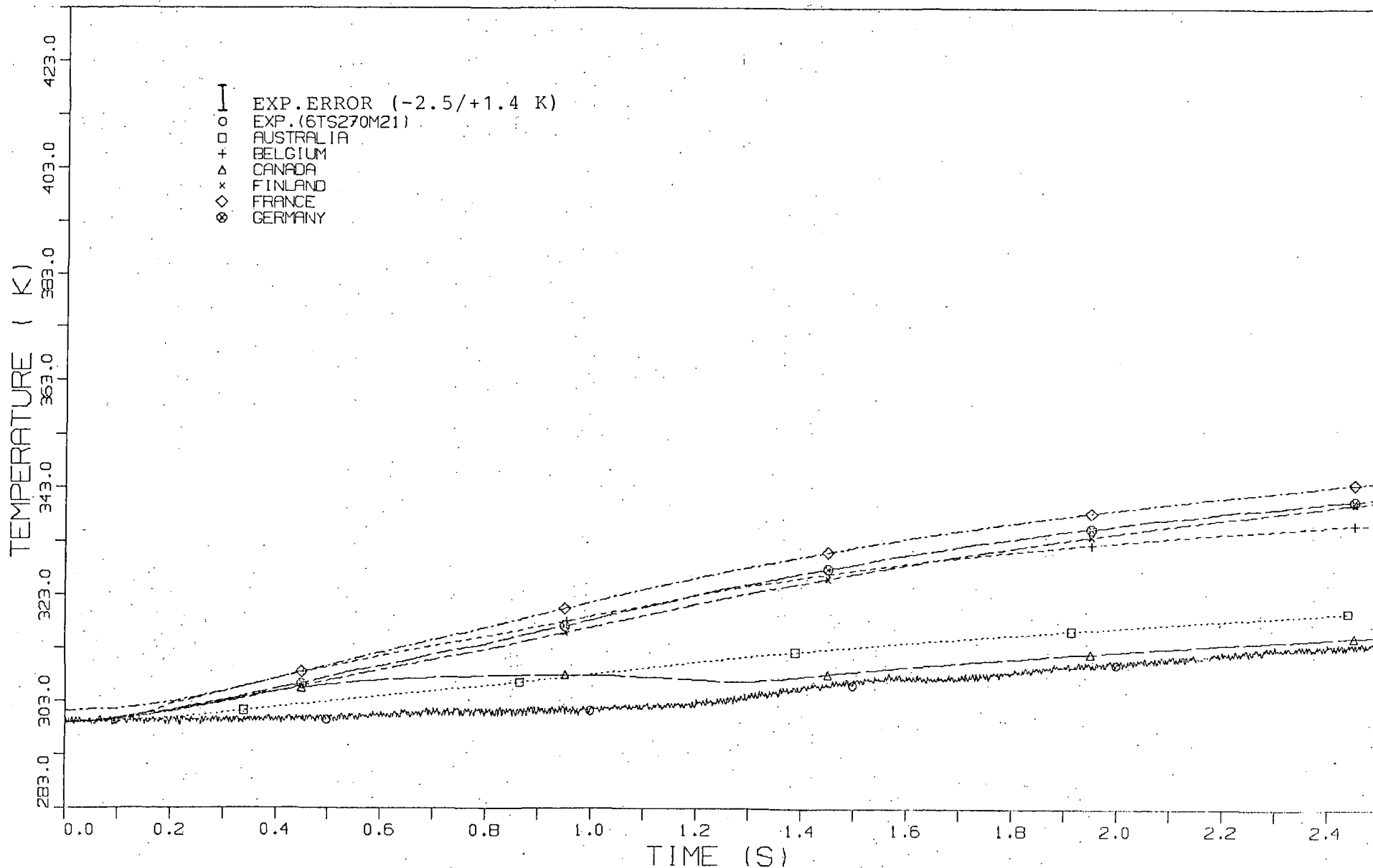


FIG. 39A. TEMPERATURE HISTORY IN COMPARTMENT R6

OECD-CSNI CONTAINMENT STANDARD PROBLEM NO.2 (TEST CASP2)

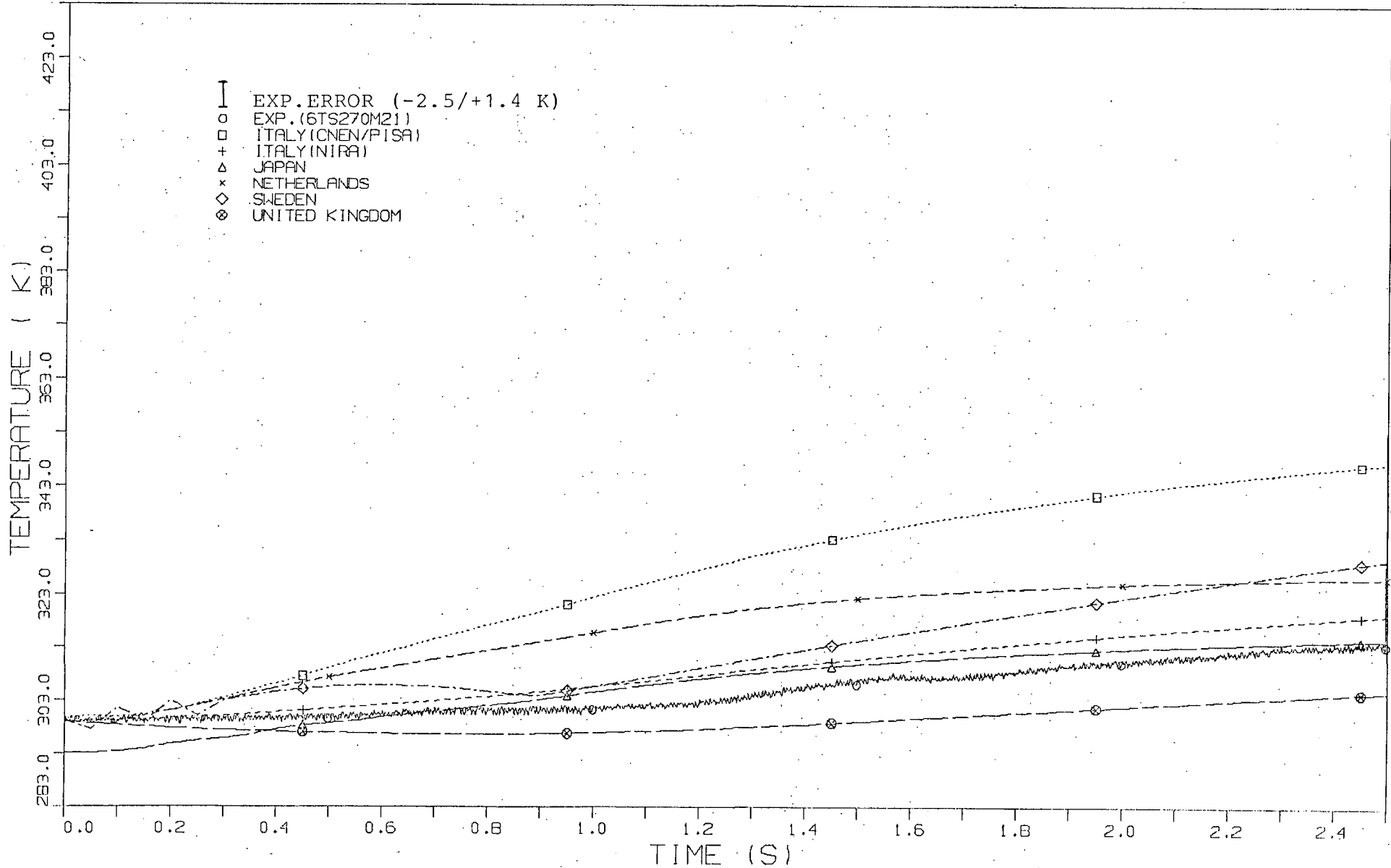


FIG. 39B TEMPERATURE HISTORY IN COMPARTMENT R6

### 3.5.3 Time interval 0 to 50 s

The calculated results for this time interval relatively good agree with the experimental results except 1 or 3 higher overestimations of the important total pressure behaviour. Because of the 1-zone simulation of the containment already in this time interval the results of Belgium are only compared with the experimental results of big dome compartment R9, which approach mean values for the whole containment still at best. In the comparative plots for pressure and temperature in compartment R9 (figs. 41A and 44A) the results of Finland (1-zone simulation) are included, although they are obtained for time interval 0 to 1000 s.

In the following selected variables are considered in more detail:

- Pressure in rupture compartment R4 (figs. 40A, 40B) and in dome compartment R9 (figs. 41A, 41B):

After more or less pressure equalization in the containment after approx. 4 s the experimental pressure behaviour in the individual compartments differs only slightly. At 33 s a maximum pressure occurs (3.95 bar) which is relevant to containment design.

As explained in chapter 3.1, the same scales as in the comparison report for the 1st Containment-SP are applied for the purpose of directly comparing within this report. With regard to total pressure history, which is to be considered here, it should hardly be disadvantageous to omit pressure range 1.0 to 2.0 bar.

The results of the majority of participants are within a spread band, which can be regarded as relatively narrow compared to the influence of several possible deviations from nominal values (see chapter 2.5.3.2). Except France, the participants overestimated these variables, particularly NIRA (Italy). About 6 participants are close to the experiment, however, two or three of them consider only an essentially thinner coating than is given in table 3 as a minimum.

- Temperature in rupture compartment R4 and in compartment R8 (figs. 42A, 42B and 43A, 43B):

After initially smaller deviations the temperatures in compartments R4

and R8 are essentially at saturation to the measured pressure, just like in compartments R5 and R7.

For compartment R4 the participants' results are close to the measuring results (+10K/-1K with an experimental error bandwidth of +1.4K/-2.5K), especially those of Italy (CNEN/Pisa) and France. The agreement between the ZOCO V (Australia), PRESCON-2 (Canada), PACO (Italy/NIRA) and CLAPTRAP II (U.K.) calculations (6-node simulation of the containment, i.e. one node for R8) and the measured data for compartment R8 may be regarded as very satisfactory, while the other participants except Netherlands (lumping R6, R8 and R9) underestimate this temperature after 2 s even if the pressure history is calculated well.

- Temperature in dome compartment R9 (figs. 44A, 44B):

At the measuring points to be computed in compartment R9 temperature rises somewhat differently and slowly caused by the high fraction of air. After appr. 25 s a temperature stratification starts to develop. At 50 s the temperature in the lower part of the inner cylinder is about 20K less than at the dome's ceiling.

The participants' results are considerably higher than the experimental results, especially in the phase of temperature increase. Temperature differences present in the experiment cannot be included into the computations, if e.g. compartment R9 is only simulated by one node.

- Temperature in dead end compartment R6 (figs. 45A, 45B):

After appr. 4 s the measuring point situated in the centre of the compartment indicates higher oscillations in temperature what can be attributed to equalization streams with different steam/air composition. This temperature corresponds to those in the lower part of the inner cylinder of compartment R9, but is on the average somewhat higher.

Partly, the deviations of the participants' results from the measured temperature history are considerable. The PACO (Italy/NIRA) calculations are in the mean close to experimental data. Higher underestimations can be observed from the results of the other participants who also simulate R6 by one node.



OECD-CSNI CONTAINMENT STANDARD PROBLEM NO.2 (TEST CASP2)

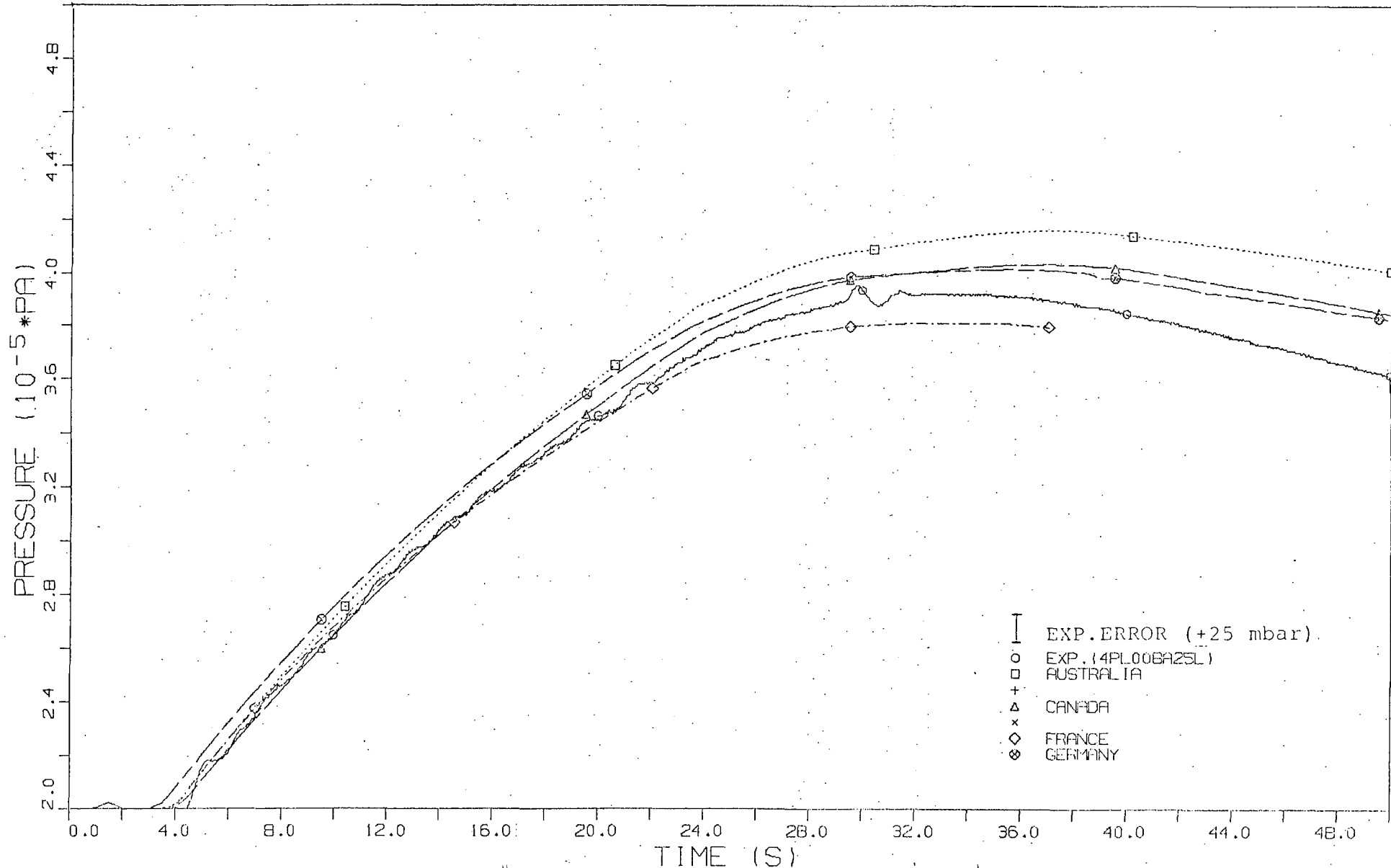


FIG. 40.A PRESSURE HISTORY IN COMPARTMENT R4

OECD-CSNI CONTAINMENT STANDARD PROBLEM NO.2 (TEST CASP2)

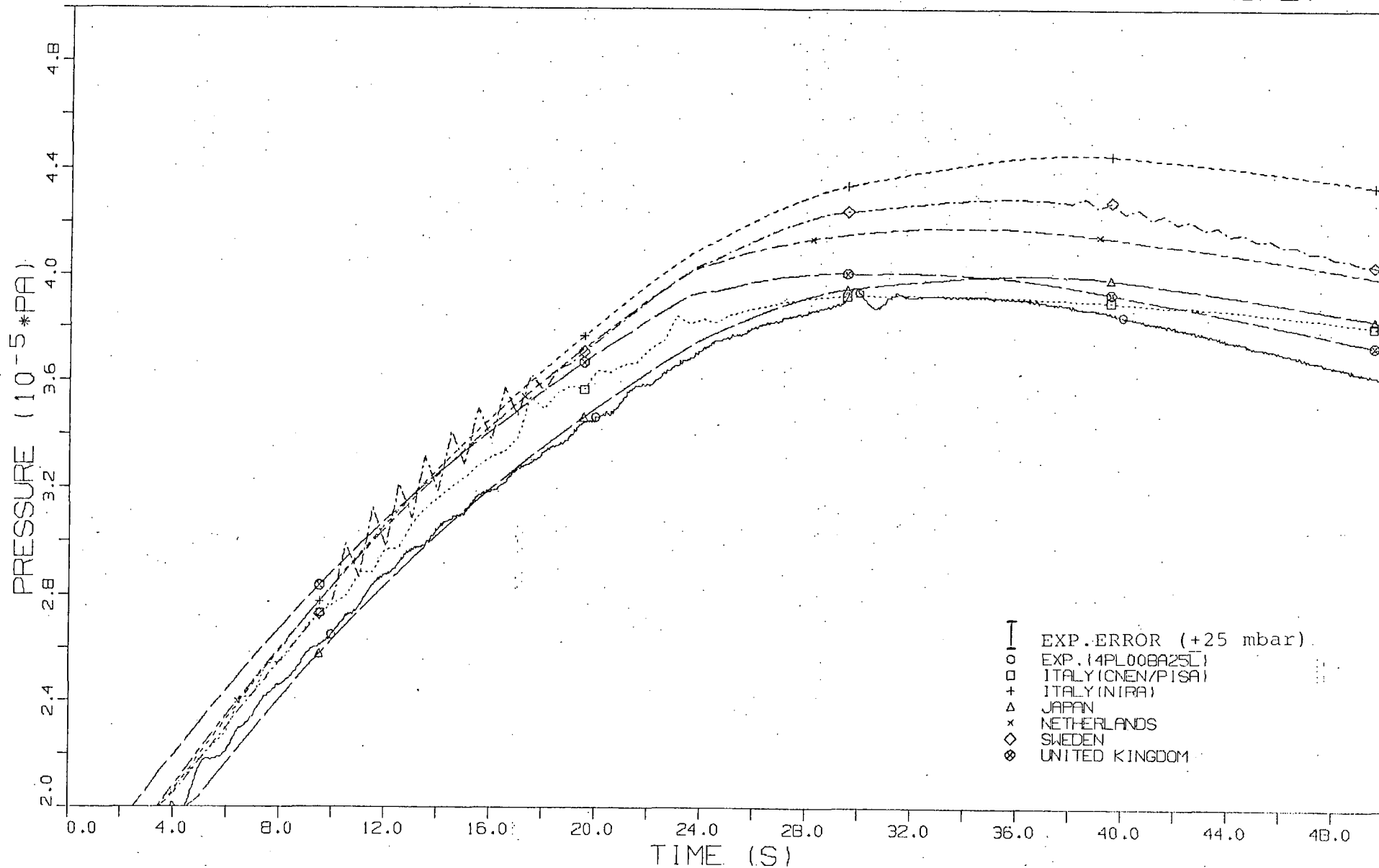


FIG. 40B PRESSURE HISTORY IN COMPARTMENT R4

OECD-CSNI CONTAINMENT STANDARD PROBLEM NO.2 (TEST CASP2)

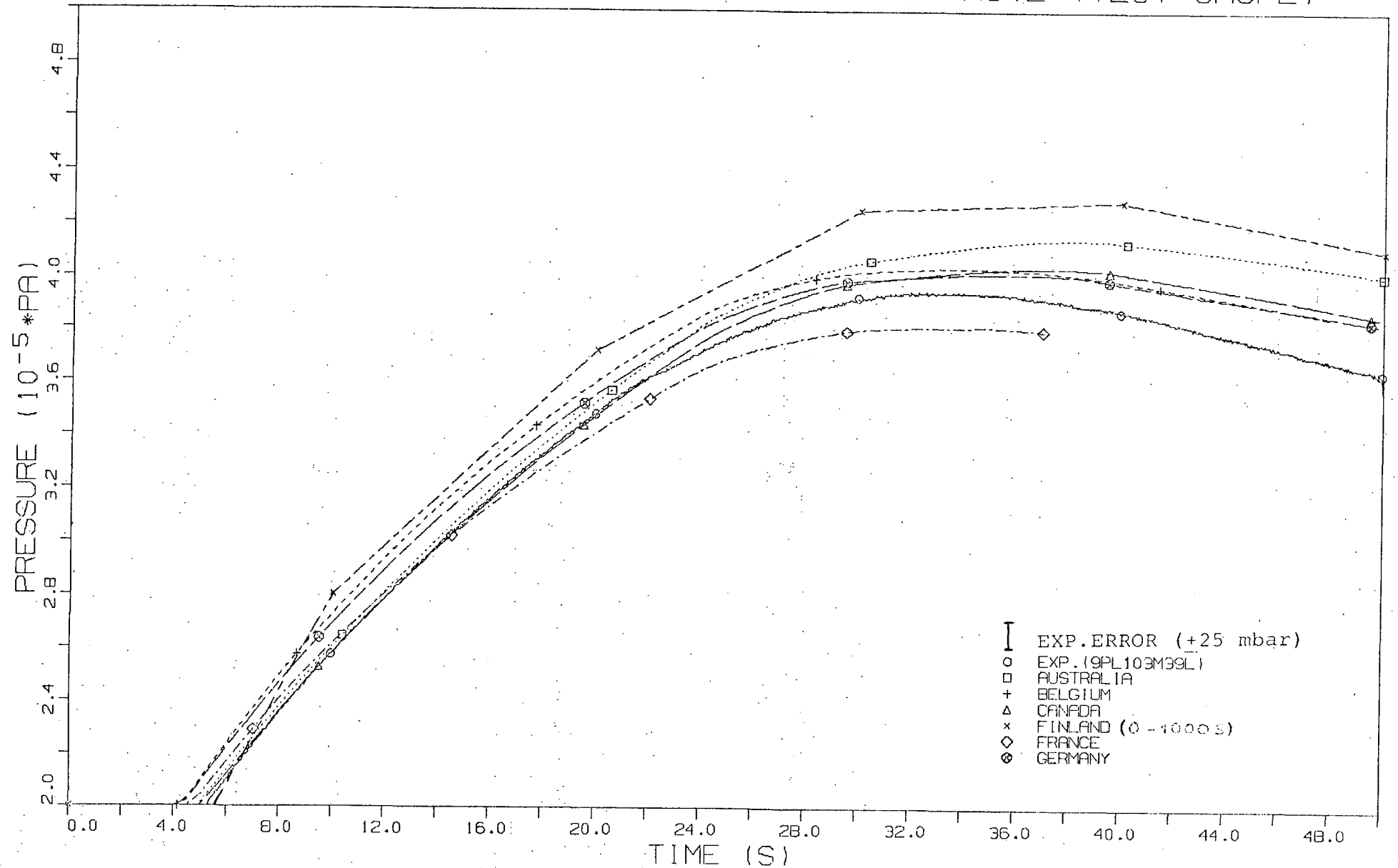


FIG. 4.1A PRESSURE HISTORY IN COMPARTMENT RA

OECD-CSNI CONTAINMENT STANDARD PROBLEM NO.2 (TEST CASP2)

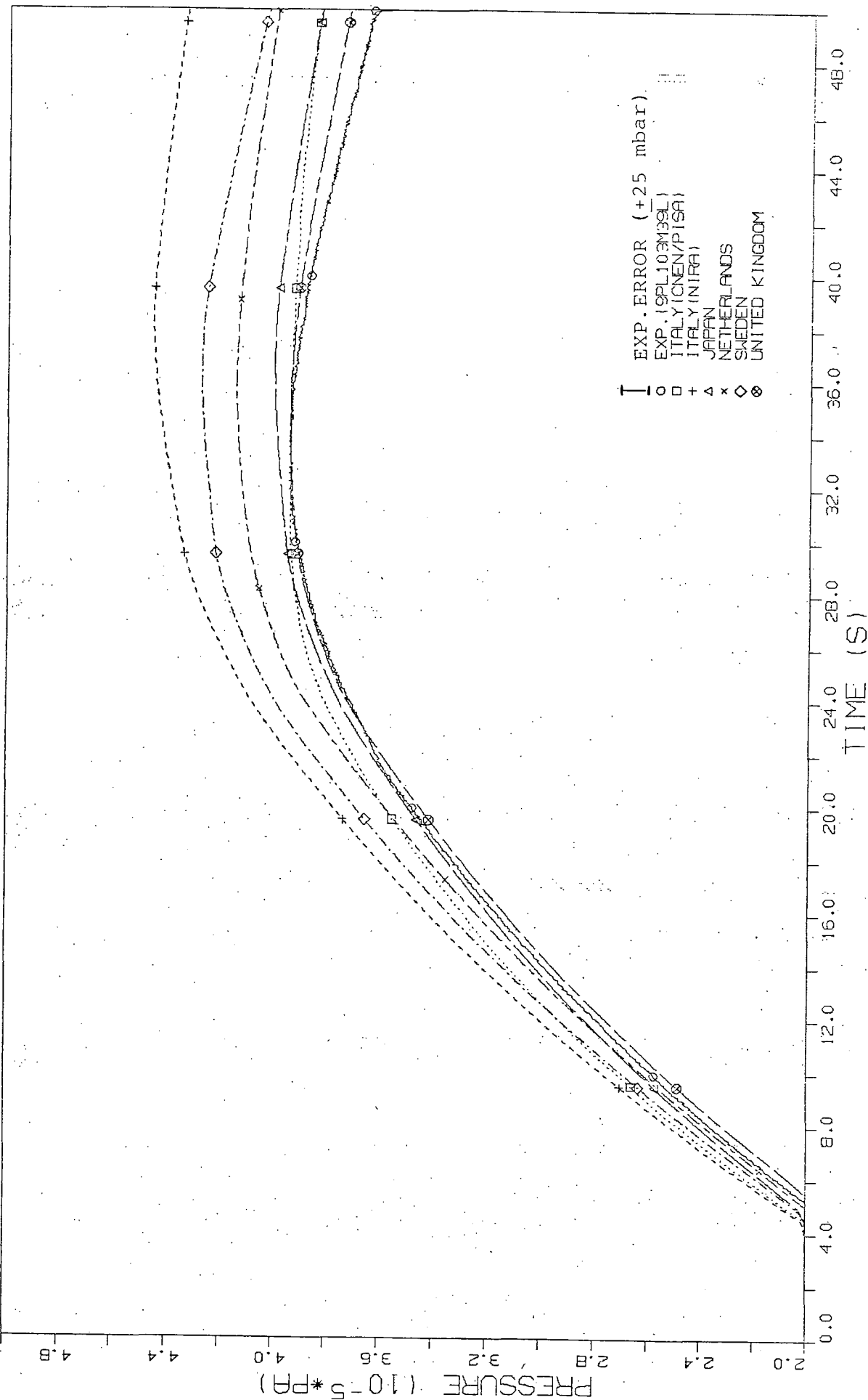


FIG. 41B PRESSURE HISTORY IN COMPARTMENT R9

OECD-CSNI CONTAINMENT STANDARD PROBLEM NO.2 (TEST CASP2)

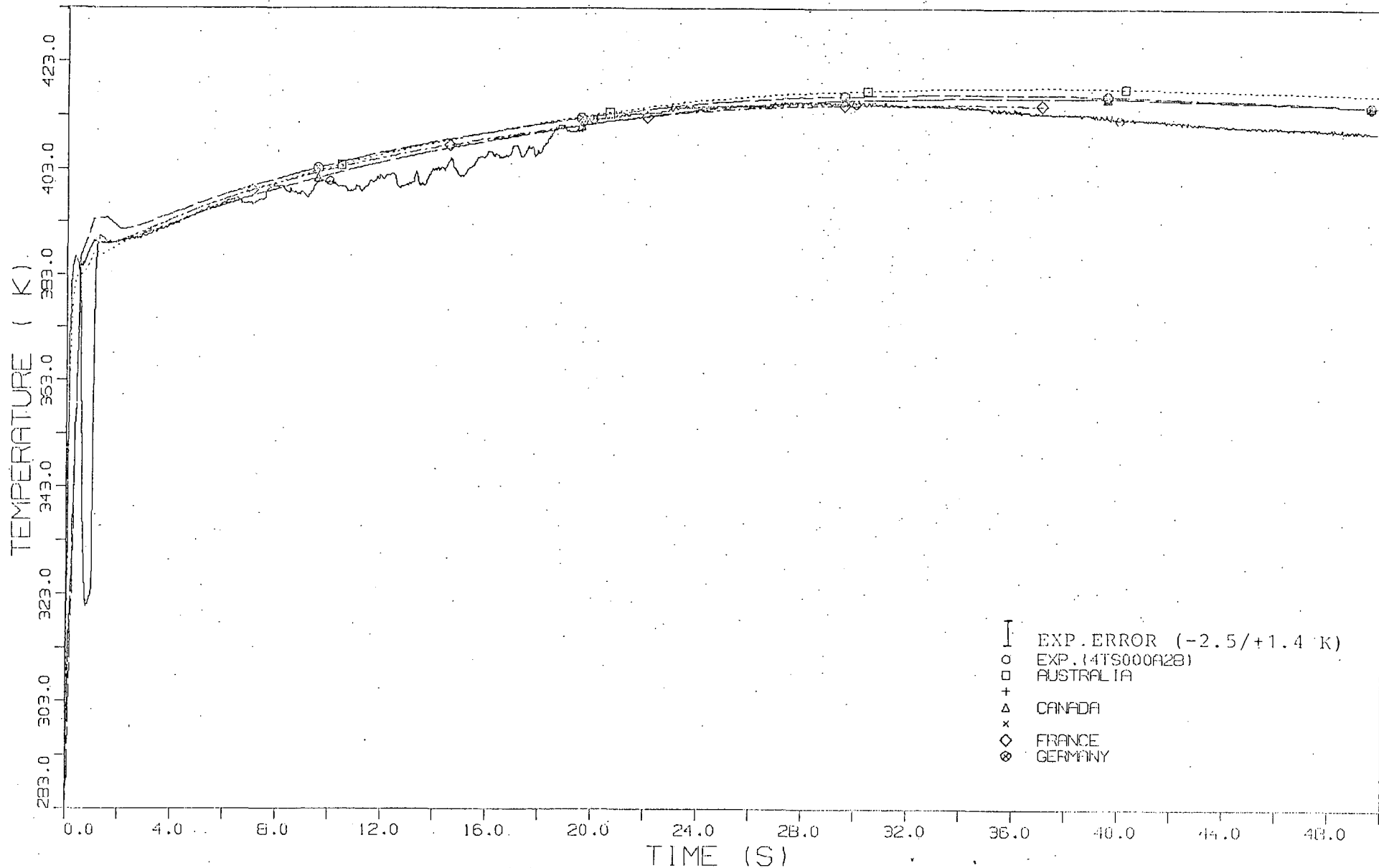


FIG. 42A TEMPERATURE HISTORY IN COMPARTMENT R1

OECD-CSNI CONTAINMENT STANDARD PROBLEM NO.2 (TEST CASP2)

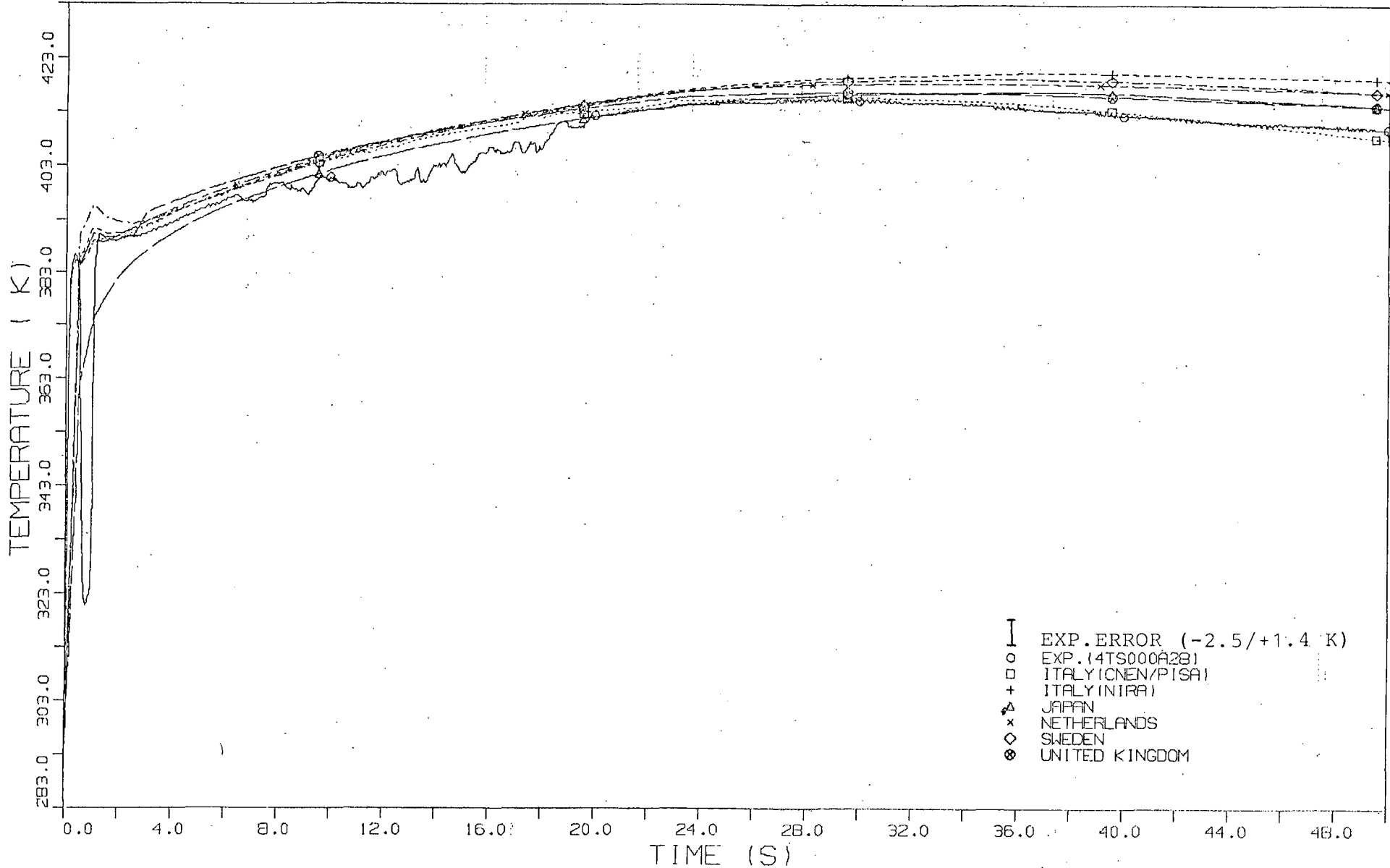


FIG. 42B TEMPERATURE HISTORY IN COMPARTMENT R4

OECD-CSNI CONTAINMENT STANDARD PROBLEM NO.2 (TEST CASP2)

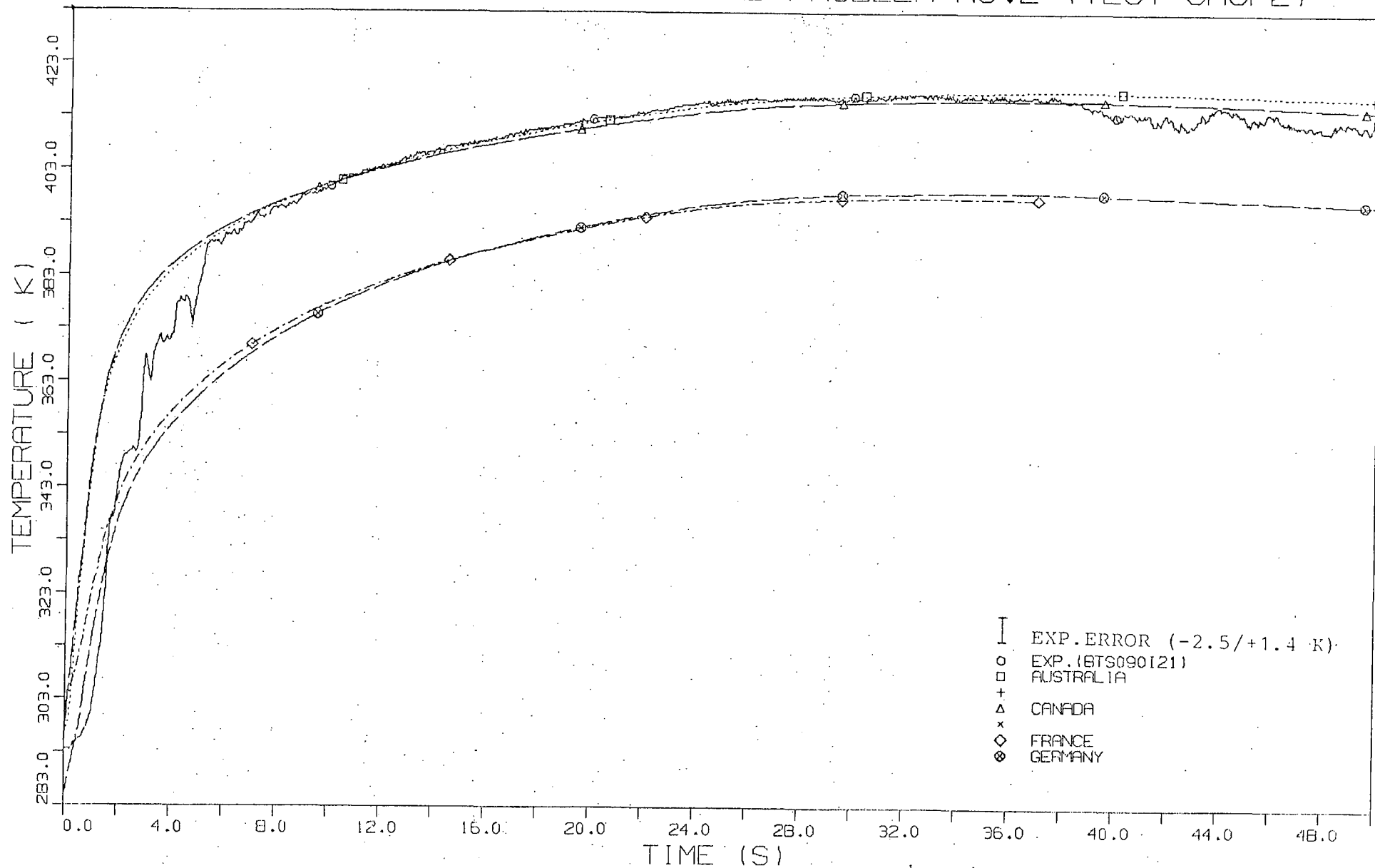


FIG. 43A. TEMPERATURE HISTORY IN COMPARTMENT RB

OECD-CSNI CONTAINMENT STANDARD PROBLEM NO.2 (TEST CASP2)

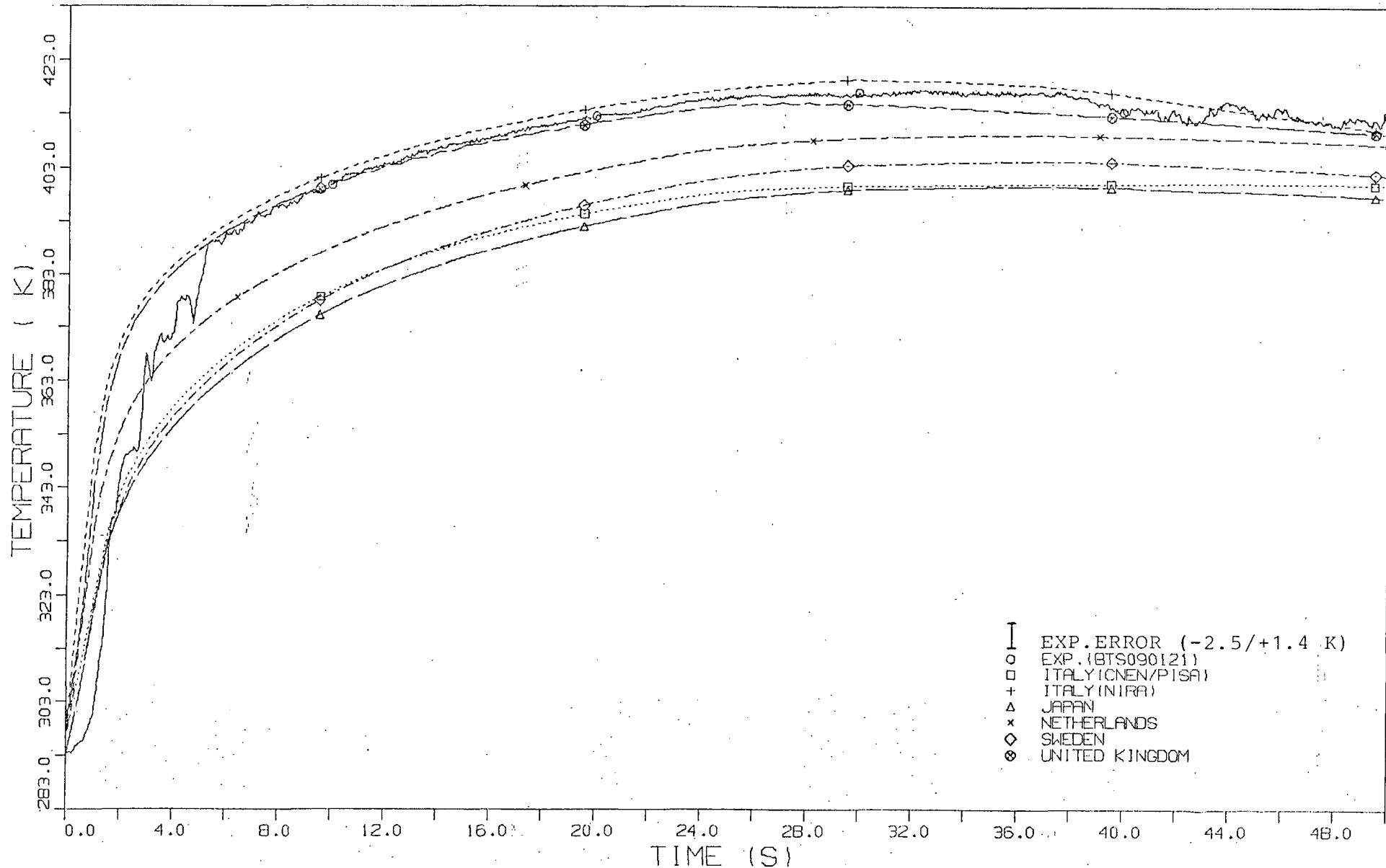


FIG. 43 B TEMPERATURE HISTORY IN COMPARTMENT R8



OECD-CSNI CONTAINMENT STANDARD PROBLEM NO.2 (TEST CASP2)

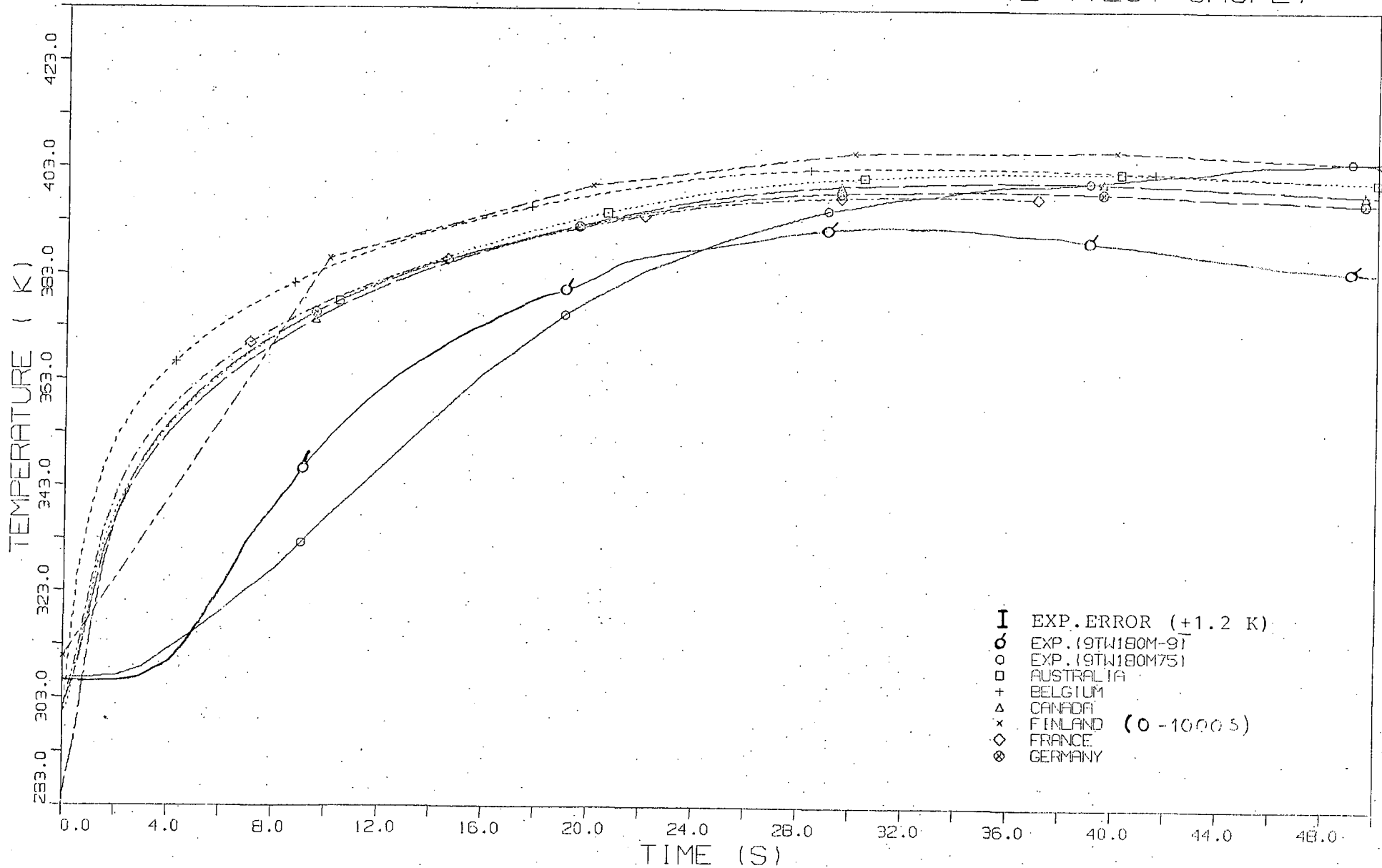


FIG. 44 A . TEMPERATURE HISTORY IN COMPARTMENT RA

OECD-CSNI CONTAINMENT STANDARD PROBLEM NO.2 (TEST CASP2)

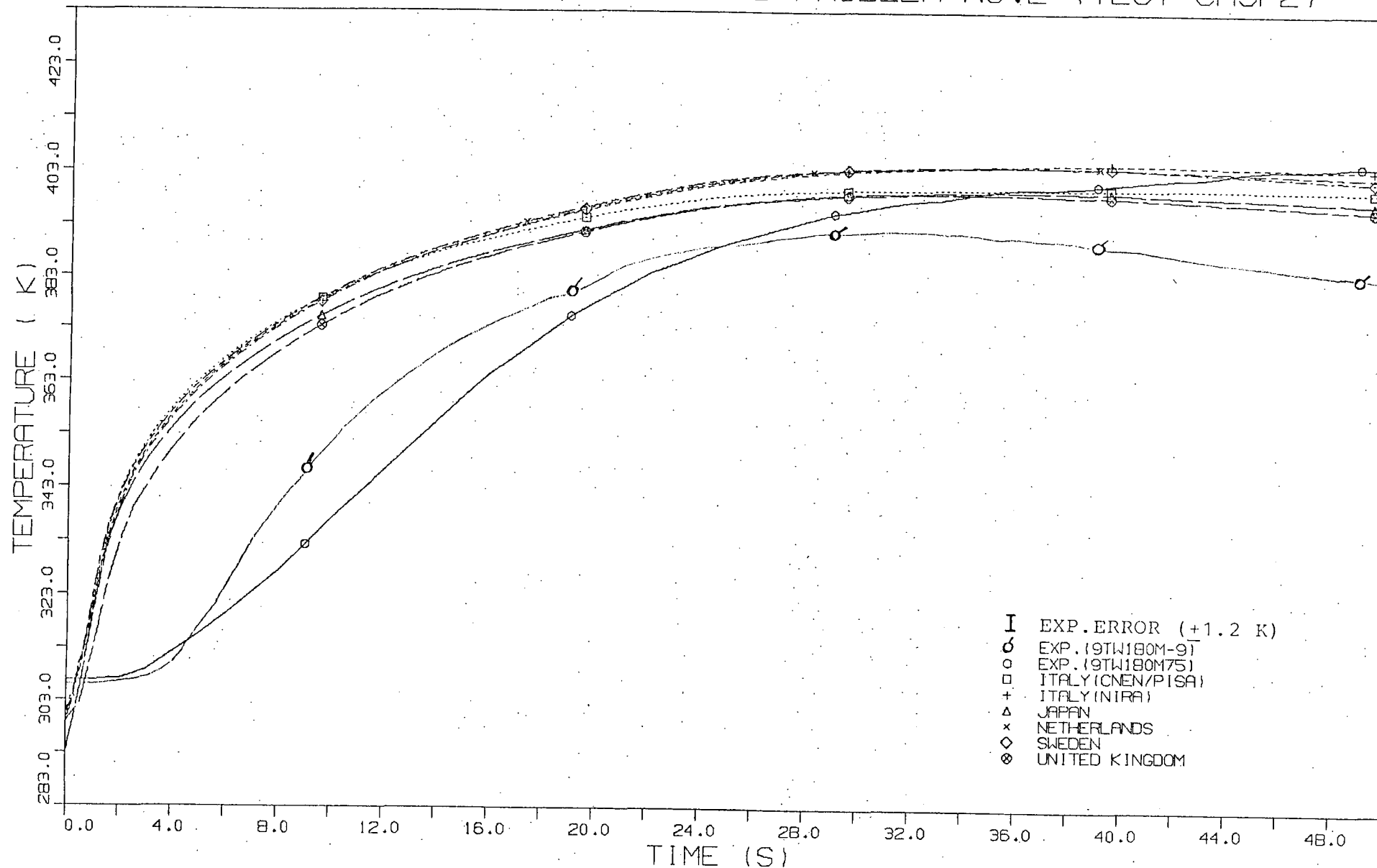


FIG. 44B TEMPERATURE HISTORY IN COMPARTMENT RA

OECD-CSNI CONTAINMENT STANDARD PROBLEM NO.2 (TEST CASP2)

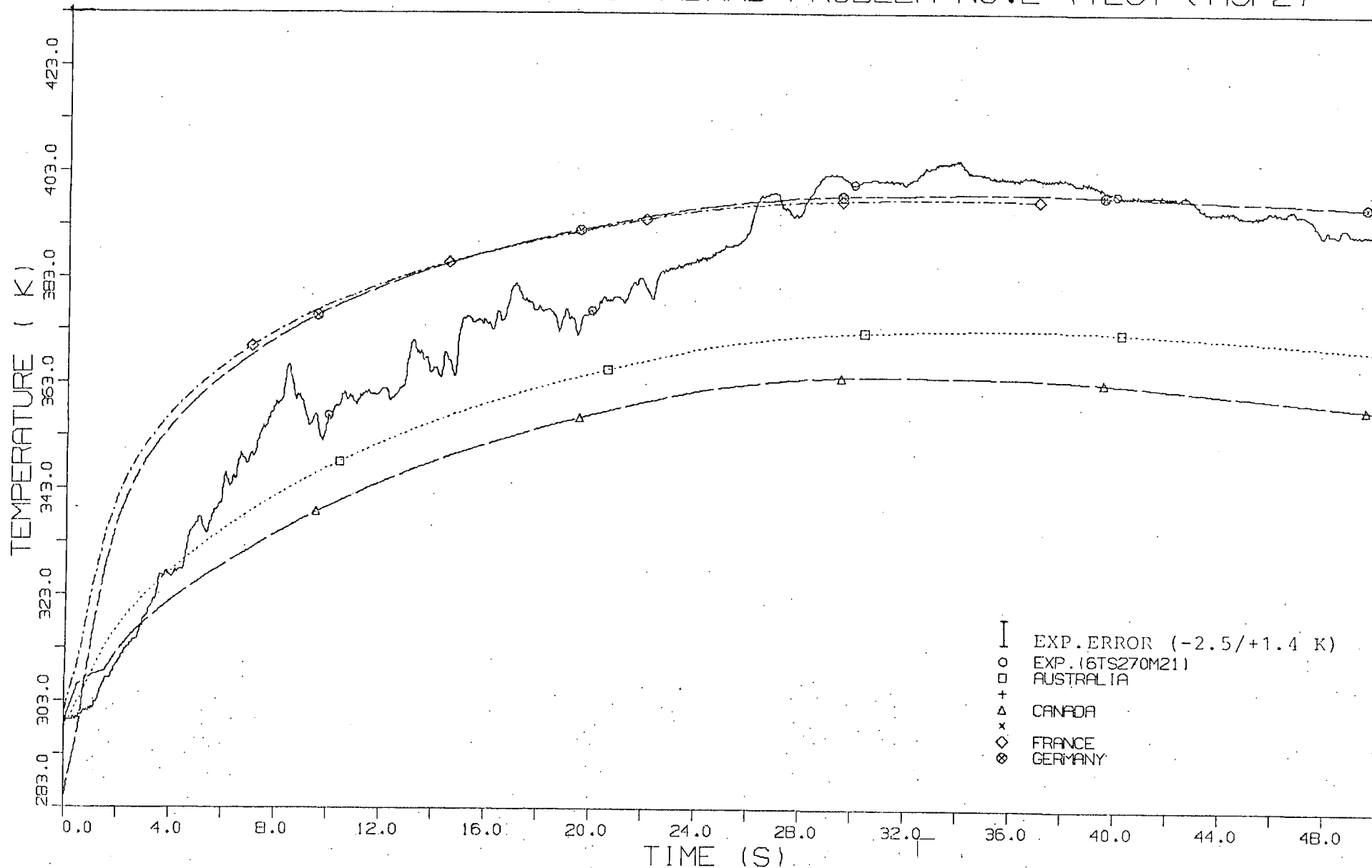


FIG. 45A TEMPERATURE HISTORY IN COMPARTMENT 10

OECD-CSNI CONTAINMENT STANDARD PROBLEM NO.2 (TEST CASP2)

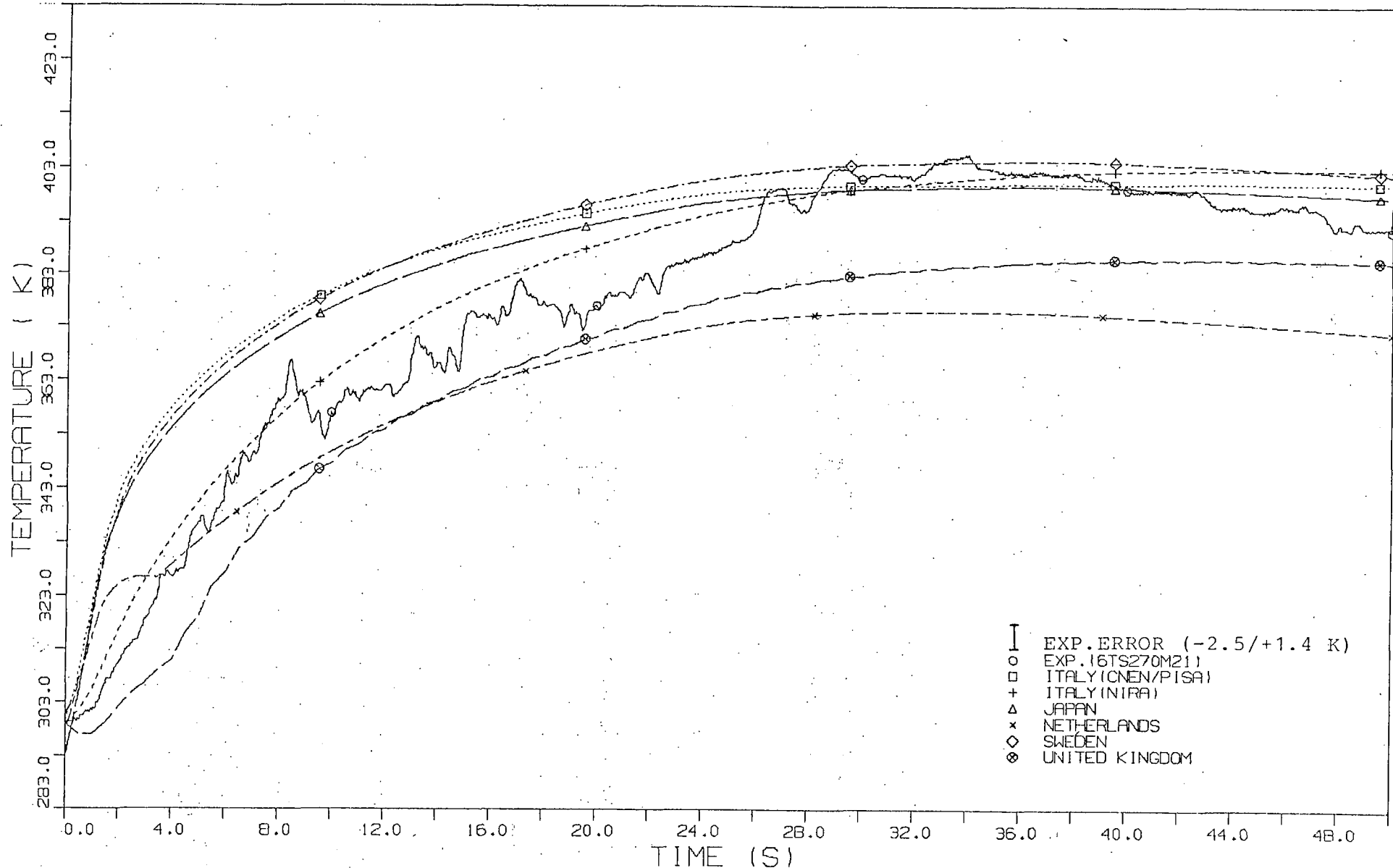


FIG.45B TEMPERATURE HISTORY IN COMPARTMENT R6

### 3.5.4 Time interval 0 to 1000 s

For this time interval Australia submitted two calculations with computer codes ZOCO V and ZOCO VI. The results of ZOCO V are only included in comparison plots because for each organization only one calculation shall be taken and the results of ZOCO V are considerably better than those of ZOCO VI. A few remarks shall be made on the individual results as follows:

- Pressure history in containment (figs. 46A, 46B):

After a maximum the pressure in the containment falls slowing down continuously due to cooling of the atmosphere.

With the exception of France and United Kingdom, pressure maximum is overpredicted by the participants. After pressure maximum calculational results on the average agree in course of the cooling process, but are mainly higher than experimental results. This systematic deviation can be explained by the influence of a possible leakage of the model containment on the total pressure built-up in the long term interval. Since there are no measured data available on the real leak tightness of the containment all calculations could not take this into account. The results of Germany come closest to the experiment. It may be interesting to quantify the influence of the uncertainty of data of the concrete coating acting more and more as heat conductive resistance (see also fig. 18).

- Temperature in containment (figs. 47A, 47B):

Pressure decrease is caused by heat transfer from the containment atmosphere to the concrete walls. Temperature stratification in the large dome compartment, which has started in time interval 0 to 50 s, is increasing. After about 250 s it has fully developed: Both of the depicted measuring points in R9 (bottom of inner cylinder, dome at the top) indicate a continuous, homogeneous cooling-down (constant difference of about 40K). Temperatures are the same at the same level in the annulus of R9 as in compartments R6 and R8, while in compartments R4, R5 and R7 temperature level is always somewhat higher.

Considering these substantial differences in temperature, a subdivision of the containment, for instance in 3 or 4 zones, seems to be more suitable than the 1-zone simulation. For a 1-zone simulation calculational results, as a matter of fact, should have to be compared with a temperature averaged volumetrically over the containment volume. Corresponding to the different pressure histories, temperatures obtained by the participants decrease and are on the average slightly above the middle of the two experimental curves. The temperature maximum in compartment R9 has been computed too early, but within a narrow range of 9K.

- History of water mass in containment (figs. 48A, 48B):

The considerable discrepancy between experiment and the narrow range of calculational results (corrected curve of Canada in App. 2) is mainly caused by the fact, that even after a longer time a substantial amount of condensed water is still adhering to the walls. It would result in a mean thickness of condensed film of about 0.85 mm (300 s) and 0.55 mm (1000 s), if we assume the difference between the mean value of the computed water mass and the measured sump-water to be homogeneously distributed on the total structural surface. Regarded as a pure heat conductive resistance, this film  $[(0.8 \text{ to } 1.3) \cdot 10^{-3} \text{ m}^2\text{K/W}]$  is not at all negligible compared to the concrete coating  $[(3.7 \text{ to } 4.3) \cdot 10^{-3} \text{ m}^2\text{K/W}]$ .

OECD-CSNI CONTAINMENT STANDARD PROBLEM NO.2 (TEST CASP2)

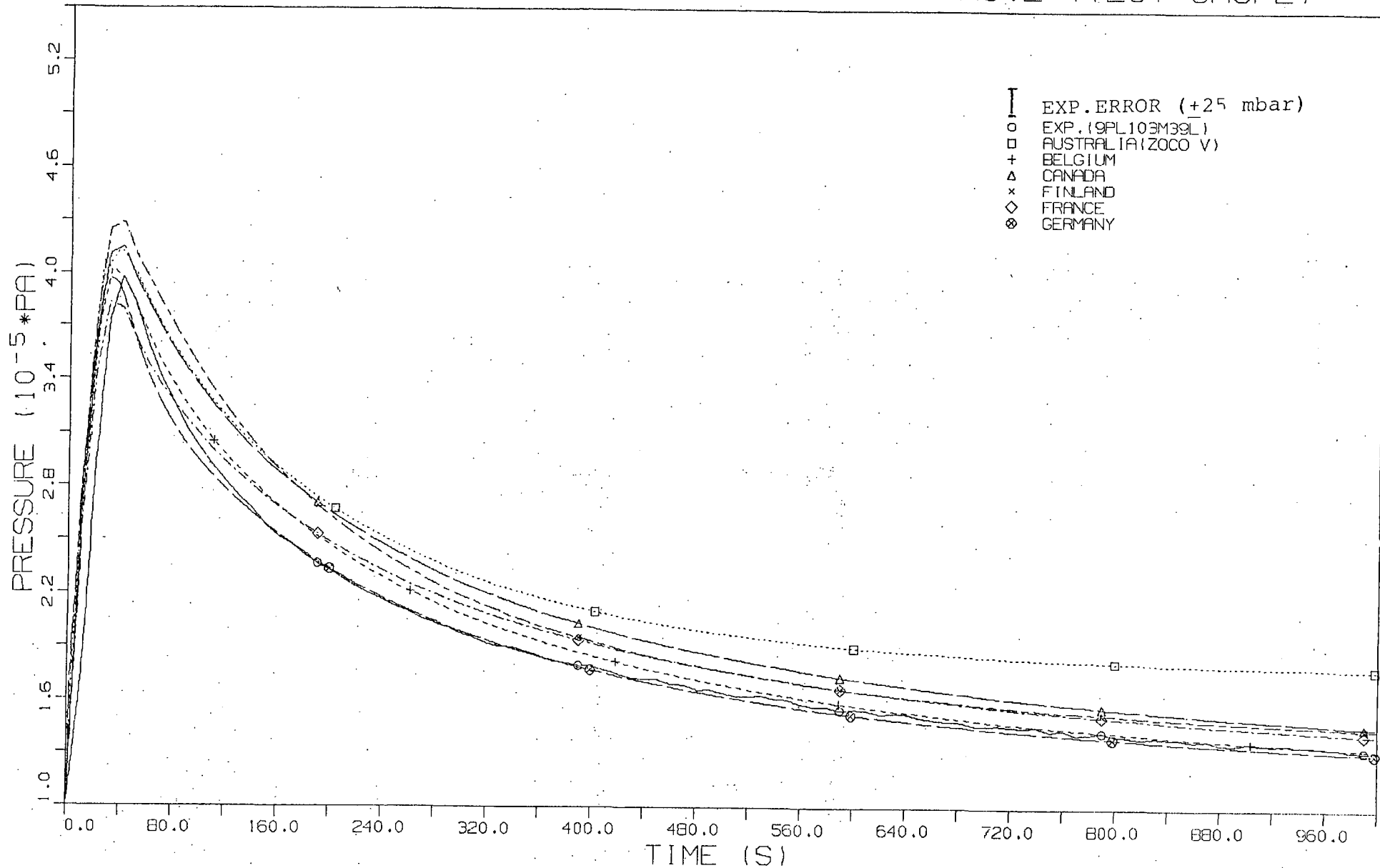


FIG. 46A PRESSURE HISTORY IN CONTAINMENT

OECD-CSNI CONTAINMENT STANDARD PROBLEM NO.2 (TEST CASP2)

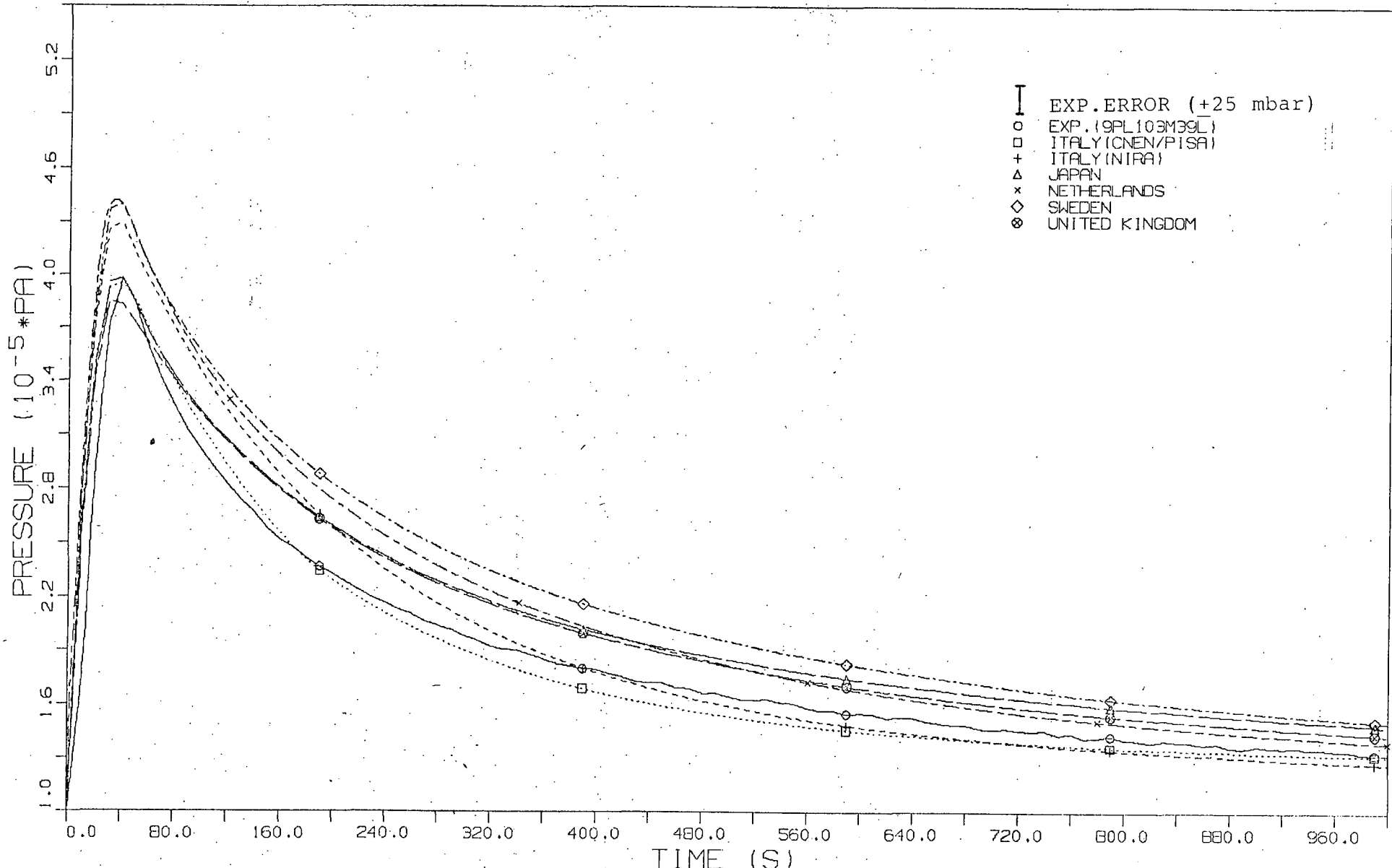


FIG. 46 B PRESSURE HISTORY IN CONTAINMENT



OECD-CSNI CONTAINMENT STANDARD PROBLEM NO.2 (TEST CASP2)

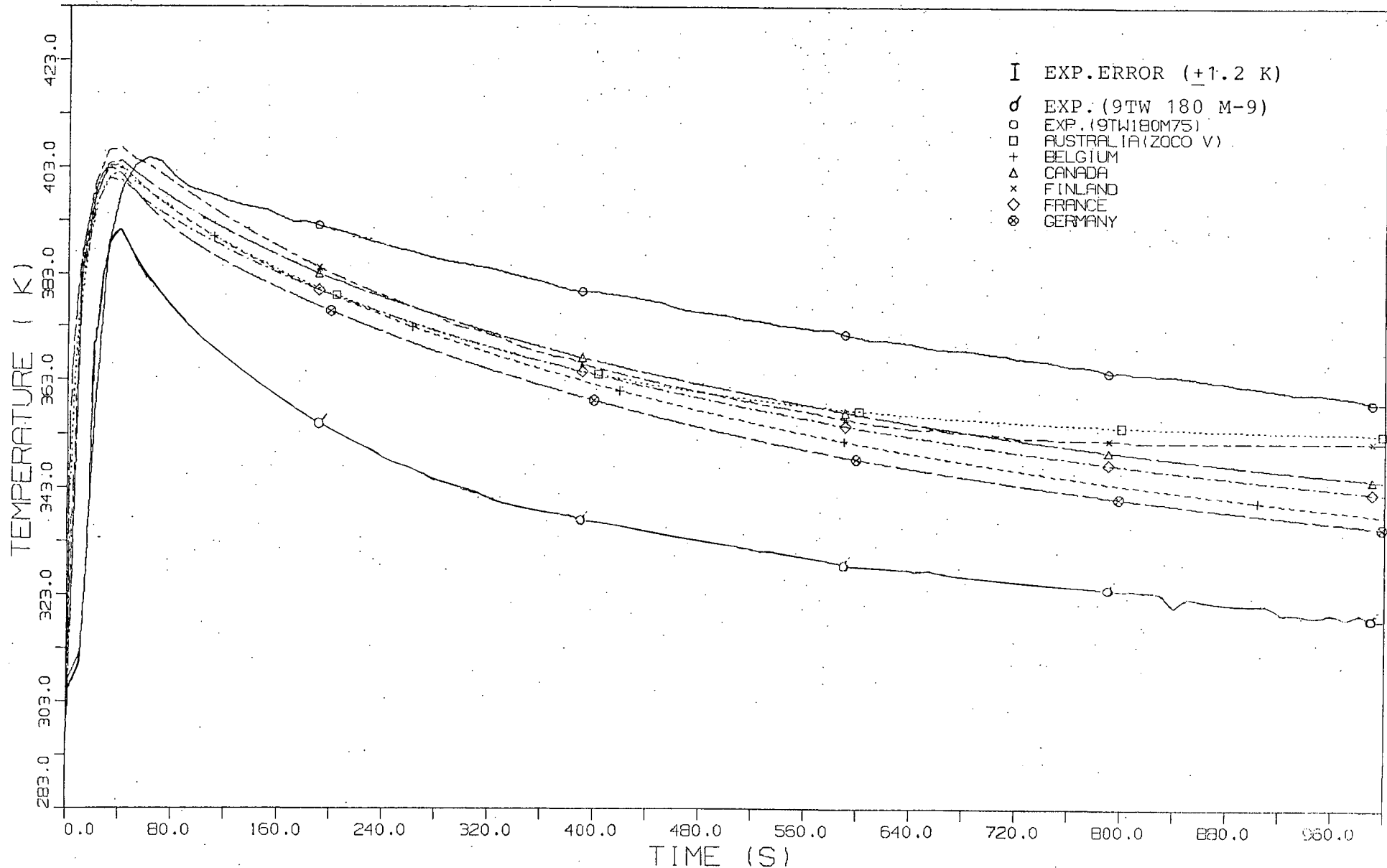


FIG. 47A TEMPERATURE HISTORY IN CONTAINMENT

OECD-CSNI CONTAINMENT STANDARD PROBLEM NO.2 (TEST CASP2)

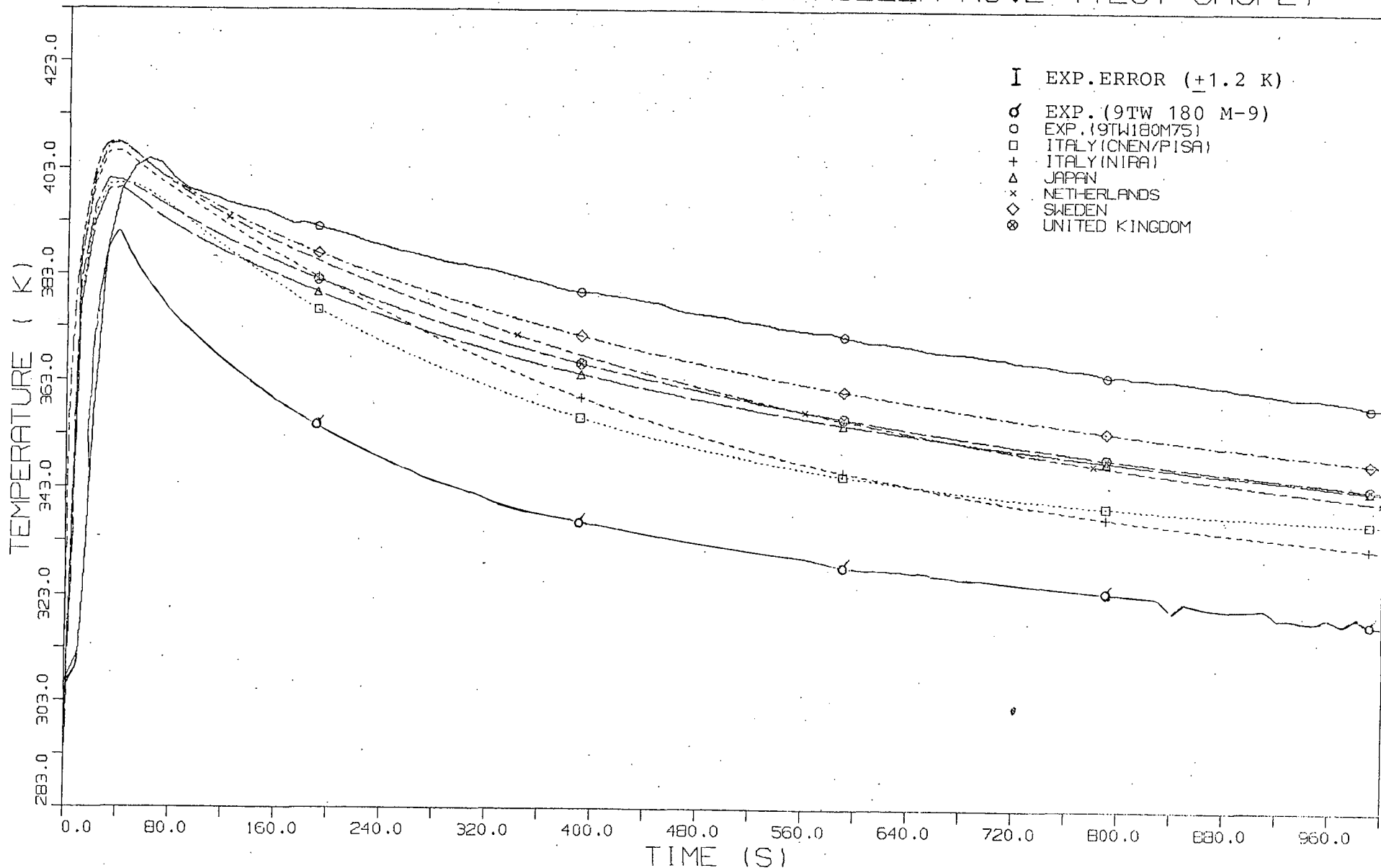


FIG. 47B TEMPERATURE HISTORY IN CONTAINMENT

OECD-CSNI CONTAINMENT STANDARD PROBLEM NO.2 (TEST CASP2)

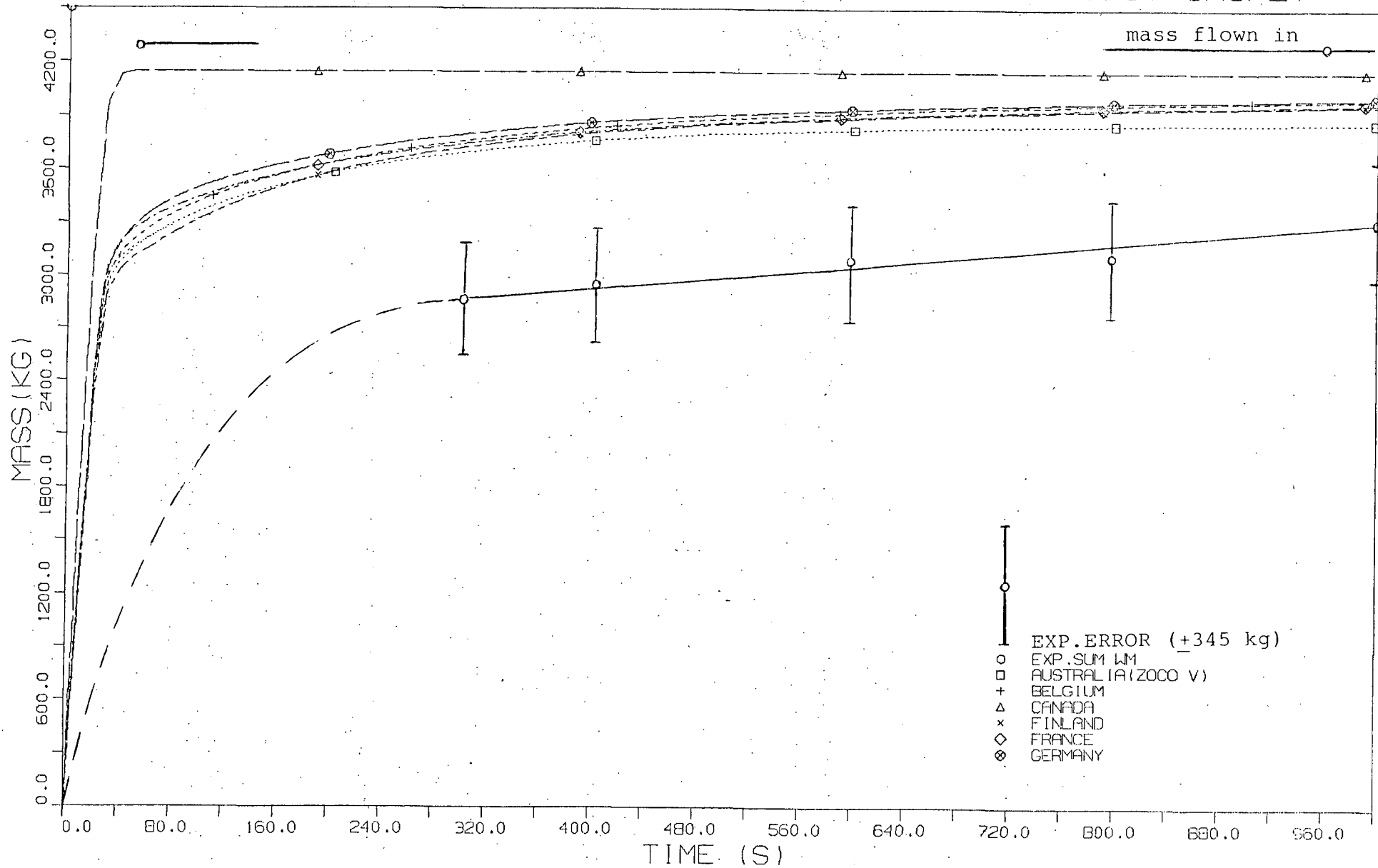


FIG. 48A HISTORY OF WATER MASS IN CONTAINMENT

OECD-CSNI CONTAINMENT STANDARD PROBLEM NO.2 (TEST CASP2)

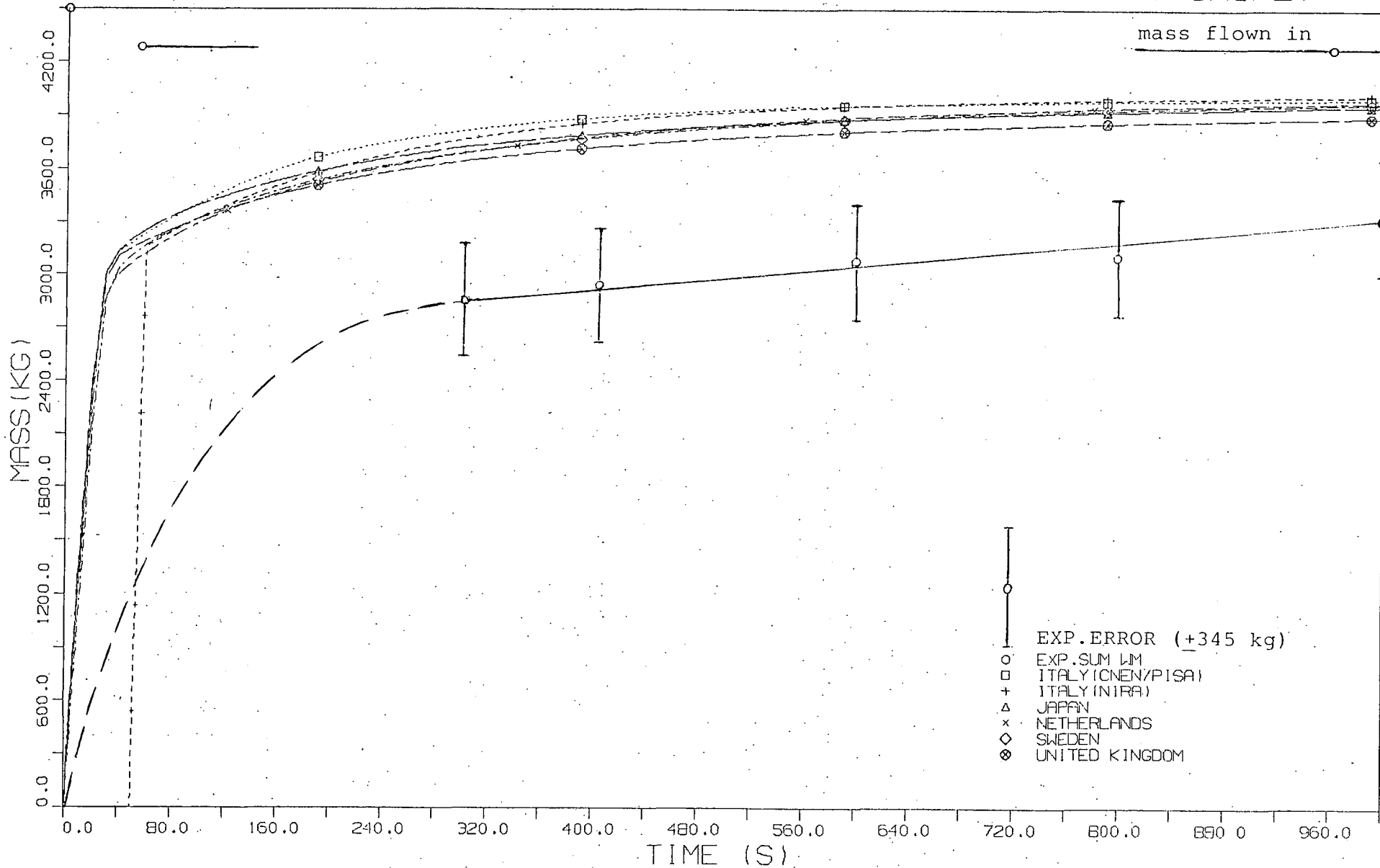


FIG. 48B HISTORY OF WATER MASS IN CONTAINMENT

### 3.6 Comparison of Remaining Specified Variables

The presentation of these variables is meant to facilitate the individual participant carrying out detailed analysis of possible deviations. Corresponding figures can be found in the preliminary comparison report /40/.

### 3.7 Measured Results of Non-specified Variables

- Alpha-block-measurements:

In order to determine long-term heat transfer, a so-called alpha-block was installed, each in the lower part of rupture compartment R4 and in the upper part of R9's annulus /6/.

- Alpha-disk measurements

So-called alpha-disks were installed in rupture compartment R4 (at the lower part) and in follow-up compartment R7 (mean compartment height at Ü78B) for the purpose of determining short-term heat transfer.

- Sump temperature and sump water mass:

As mentioned in chapter 3.3, the measured sump temperatures in connection with masses of sump water provide an indication for water transport conditions (carry-over, separation). High sump temperature indicates that sump water contains a larger portion of hot water, carried over respectively separated, and low sump temperature (see especially dead end compartment R6 at 300 s: 60 kg with 32 °C) shows that the share of water resulting from condensation at the colder structures predominates. However, it is difficult to easily quantify water transport from the mass of sump water at e.g. 300 s (first available measuring point). Particularly this results from unknown history of the condensed water added to the sump and relatively unknown temperature history of the condensate. In addition, conditions in the various compartments of the containment are very different.

From a relatively large constant mass of sump water (905 kg at 300 s) at high sump temperature in R4 it can be concluded that the sump water essentially originated from the rupture-site, respectively that condensation in the small compartment was low. In compartment R5 (outflow upwards, sump temperature somewhat below compartment temperature) water carried-over, and after 20 s some condensate, may have come to the bottom ( about 550 kg at 300 s). Probably the water in compartment R7 (room temperature  $\cong$  compartment temperature) separated during the long flow path, was washed into compartment R8 across the edge of vent Ü78B [3 cm(?) above bottom]. A relatively high sump temperature in compartment R8 already existing at the end

of blowdown confirms this, yet, also demonstrates that a some colder condensate is mixed in (at 300 s in R7: 10 kg; in R8: 430 kg). In the centre of R9 only condensate of low temperature can be found (at 300 s: 170 kg with 32 °C), which allows to conclude that no water was carried over upwards via vent Ü59B. It is surprising (gap?) that hotter water apparently arrived in the annulus of R9 (relatively high sump temperature of 55 to 80 °C and sump water mass of 760 kg at 300 s).

It is evident that a considerable amount of water was transported from the rupture compartment to other compartments. Therefore, e.g. the assumption of a zero carry-over surely contradicts the experimental results. The reason for this substantial difference between calculations and experiment obviously originates from the description of the process itself and from compensation with other assumptions. It seems necessary to improve, possibly in quantity, the description of the real conditions by way of suitable measurements, for instance, in project HDR.

- Static and dynamic measurements of pressure at the vents:

Because of the contraction a determination of the vent mass flow from these measurements is as uncertain as corresponding results from codes. From the measurements of the Pitot-tubes at Ü59B (flow upwards) and Ü 78B (flow downwards) one can possibly observe a short term reduction in dynamic pressure by a smaller amount of water carry-over and, consequently, lower acceleration losses from the water droplets.

### 3.8 Comparison with the Results of OECD-CSNI Containment Standard Problem No. 1

---

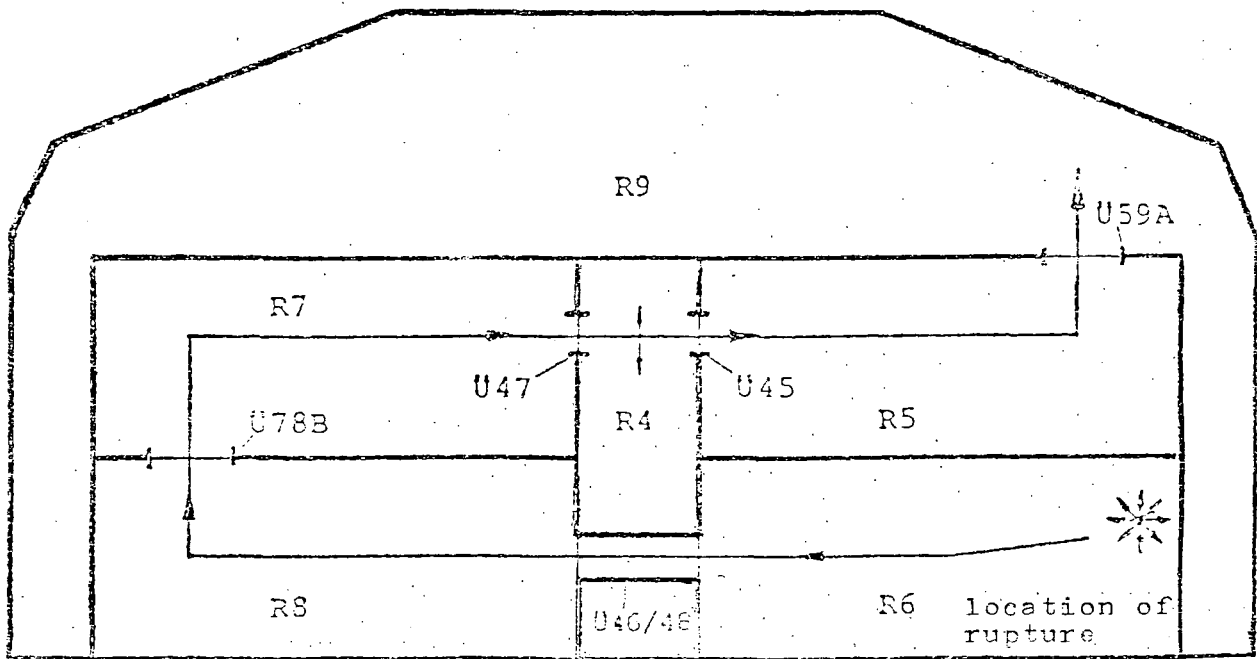
Test CASP2 (basis of the 2nd Containment SP, performed on September 21, 1979) and test D15 (basis of the 1st Containment SP, performed on December 20, 1977) both were conducted in model containment of Battelle-Institute within project RS 50 of BMFT. In both cases best-estimate post-calculations were performed (submittals due to May 1, 1979 resp. November 1, 1980). 12 organizations participated in the 1st and the 2nd Containment SP with 12 different computer codes and, partly, several modifications.

Therefore some comparisons are made possible between the 1st Containment SP and this 2nd Containment SP. In the following they are shortly reported.

#### 3.8.1 Compartment scheme and flow paths

The compartment scheme in test CASP2 (branched chain asymmetric in relation to flow paths, see fig. 49B) is different from the one in test D15 (chain-type arrangement of 6 subsequent compartments, see fig. 49A). The rupture is initiated in test D15 at the end of compartment R6 ( $\cong 41 \text{ m}^3$ ), in test CASP2 in the middle of the small compartment R4 ( $\cong 14 \text{ m}^3$ ). In both tests the vents were mainly orifices. Dimension of orifices, flow to and fro vents as well as through compartments are largely different for both tests.





Rupture compartment:

R6

Compartment chain:

R6 - R8 - R7 - R4 - R5 - R9

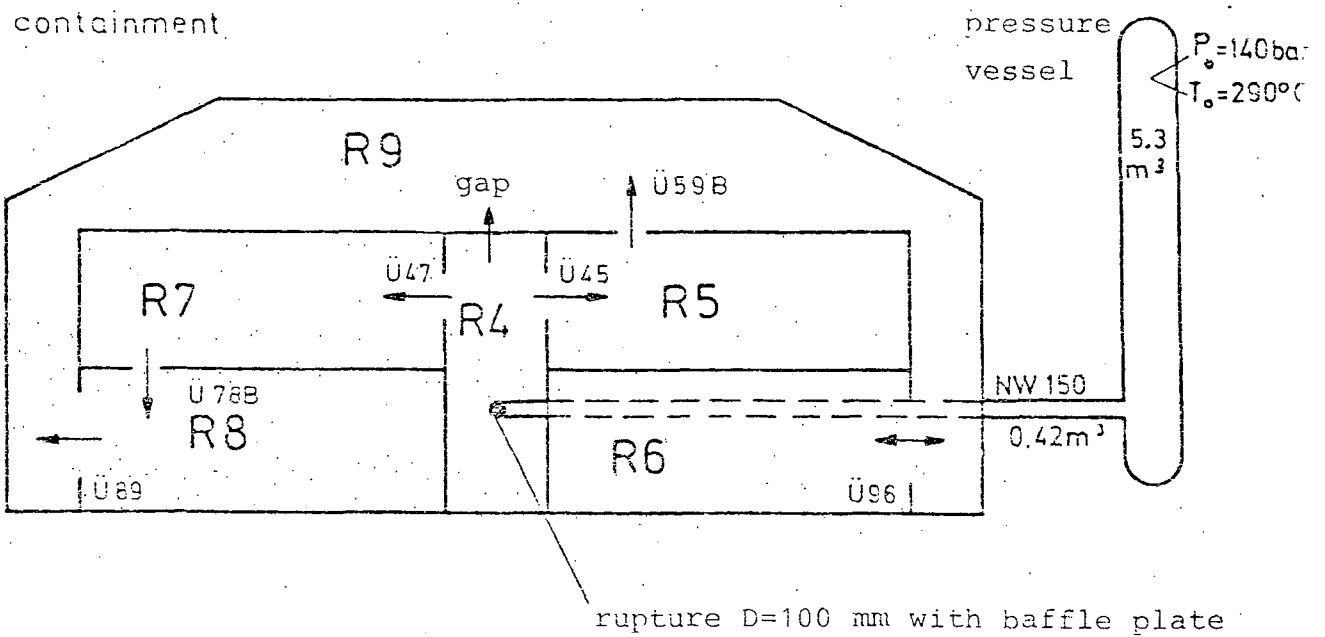
Flow areas:

U 46/48 } circular channel  
U 78B, U 47 } sharp-edged orifices  
U 45, U 59A }

Flow path:

R6 - U 46/48 - R8 - U 78B - R7 - U 47  
- R4 - U 45 - R5 - U 59A - R9

Fig. 10A: Scheme of the Compartment Chain and Associated Flow Paths (D15)



rupture compartment : R4

vents : U45, U47, U59B, U78B sharp-edged orifices  
U89, U96 wall holes

flow paths :

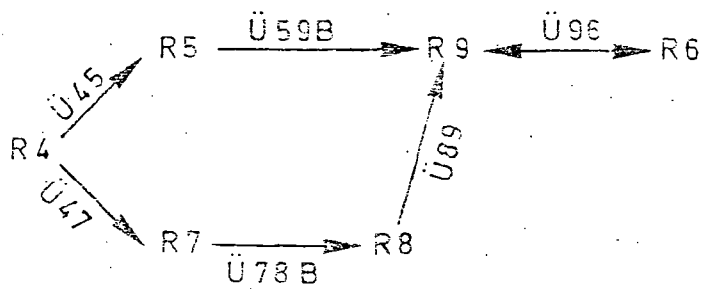


Fig.49B: Scheme of the Containment and Flow Paths (CASP2)

### 3.8.2 Boundary conditions

Contrary to the initial conditions (e.g. small difference between the mean values of initial temperature in the containment: for test D15: 8.9 °C; for test CASP2: 27.6 °C) the boundary conditions of the two tests differ essentially.

Figures 50A, 50B and 51A, 51B show in direct comparison the histories of the break mass flow rate with the associated error bands. The maximum mass flow rate into the containment in the vapour blowdown test D15 is equal to about 85 kg/s, while the two maxima in the water blowdown test CASP2 are at 405 kg/s (0.105 s) and 374 kg/s (0.92 s). In the short time interval the error bands of the two tests are approximately equal. In the long time interval they are in test CASP2 (end of blowdown at 50 s) only half of those in test D15 (end of blowdown at 70 s).

The histories of specific enthalpy of break mass flow with the associated error bands for both tests and different time intervals are compared in figs. 52A, 52B and 53A, 53B. In test D15 up to about 3 s vapour (high specific enthalpy of 2750 kJ/kg) flows from the break into the containment, then until 40 s water-vapour-mixture (minimum spec. enthalpy 1240 kJ/kg) and finally again pure vapour. In the water blowdown test CASP2 up to about 23 s saturated water respectively two-phase mixture with low quality (mean value of spec. enthalpy 1250 kJ/kg), after that two-phase mixture and from about 40 s on pure vapour (spec. enthalpy 2730 kJ/kg) flows into the containment.

The error band in test D15 is small in the short time interval. In test CASP2 up to 0.3 s it is greater (for example +9 %/-2.2 % of measured value). However, during the two-phase flow the error band in both cases is of the same order.

Besides the mass flown in [at blowdown end: 4075 kg (CASP2), 1310 kg (D15)] the amount and history of the total energy up to a certain moment flown in have a considerable influence on the pressure built-up. The figs. 54 and 55 show the great differences between water and vapour blowdown. The ratio of the total enthalpy flown in for tests CASP2 and D15 is equal to about 2.3 at time 2.5 s and about 2.4 at the maximum pressure in containment (33 s and 40 s).



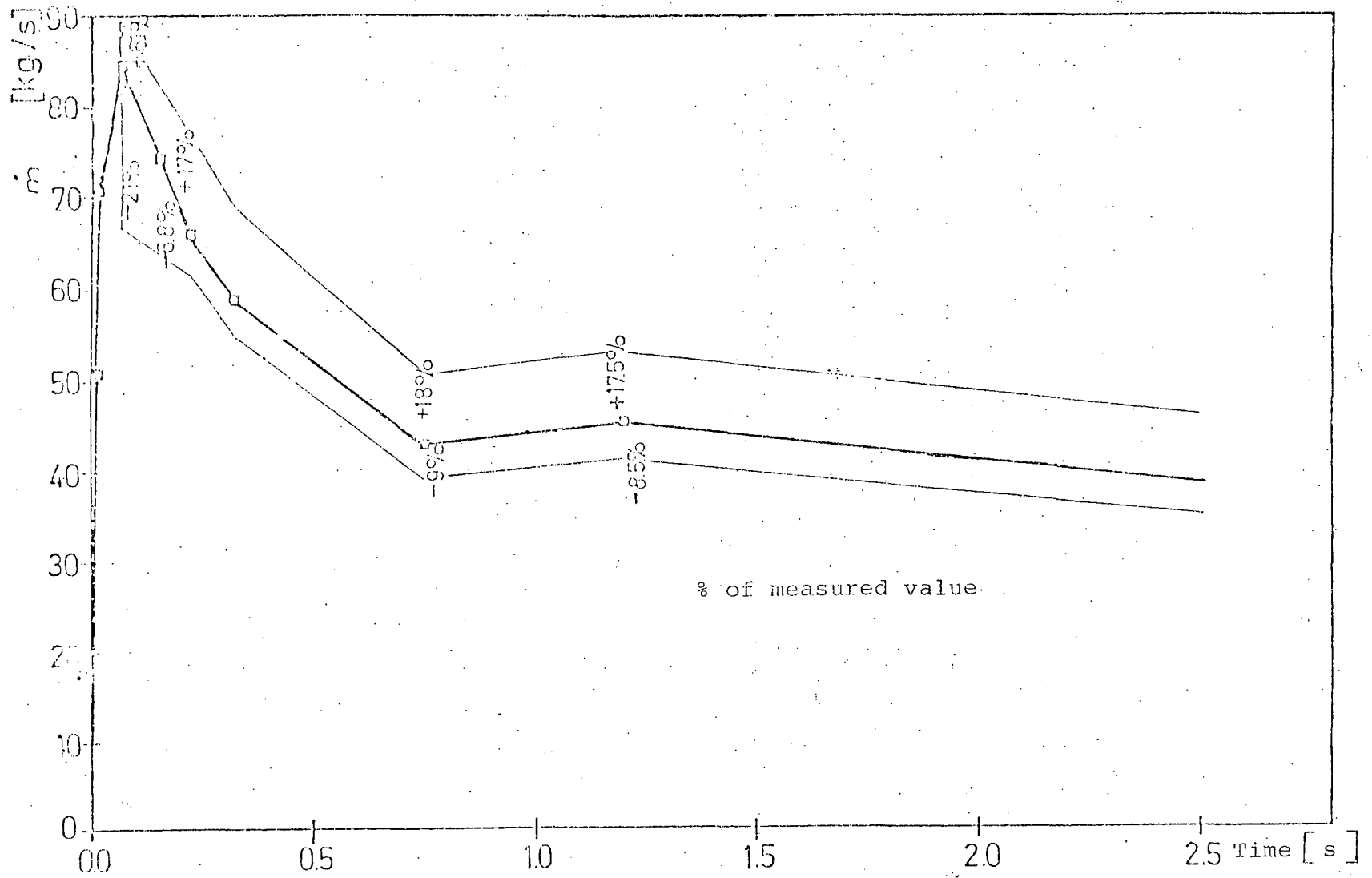


Fig.50A: Break mass flow  $\dot{m}$  with error band (D15/0-2.5s)

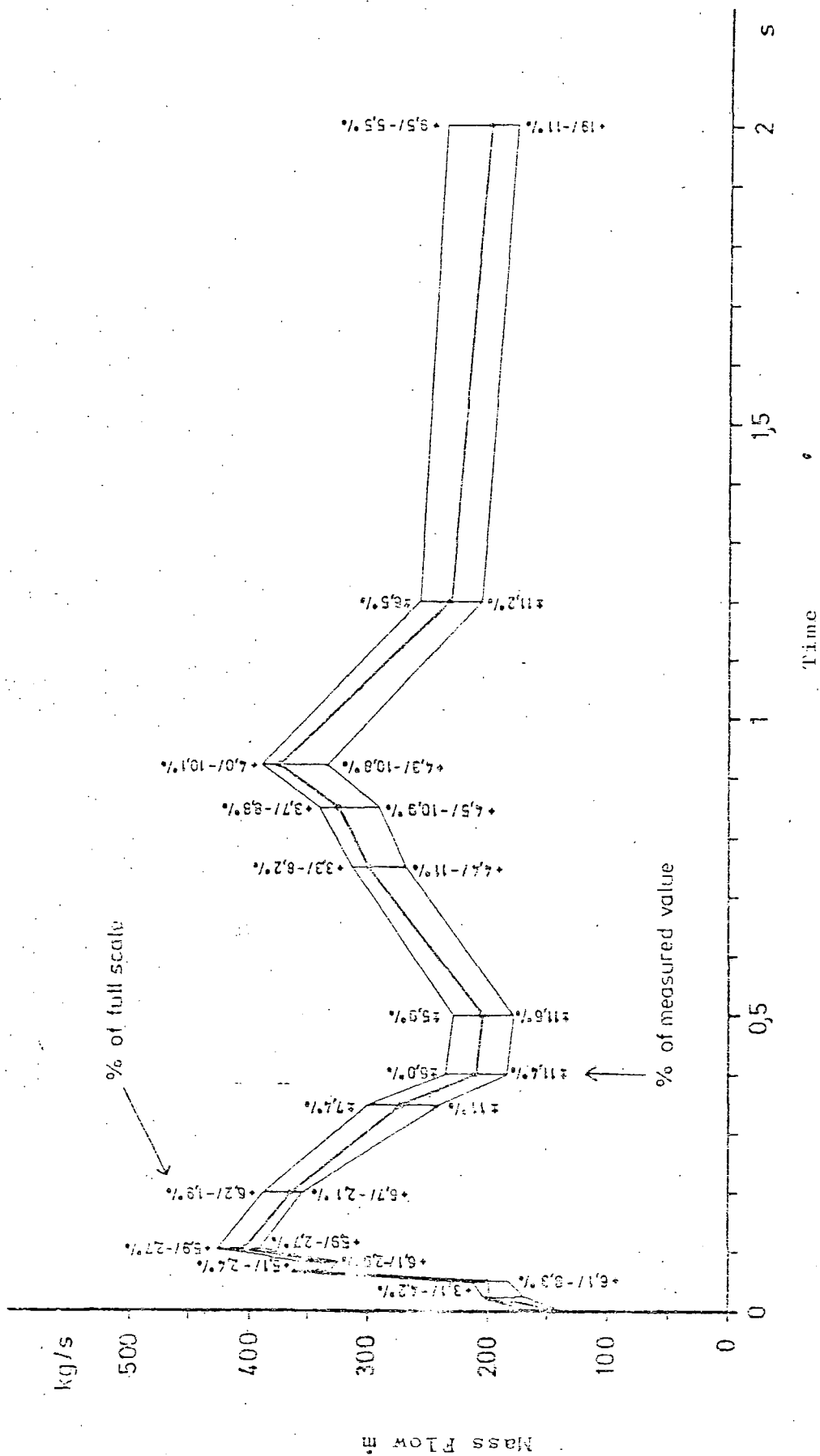


Fig. 50B: Break mass flow in with error band (CASP2/0-2s)

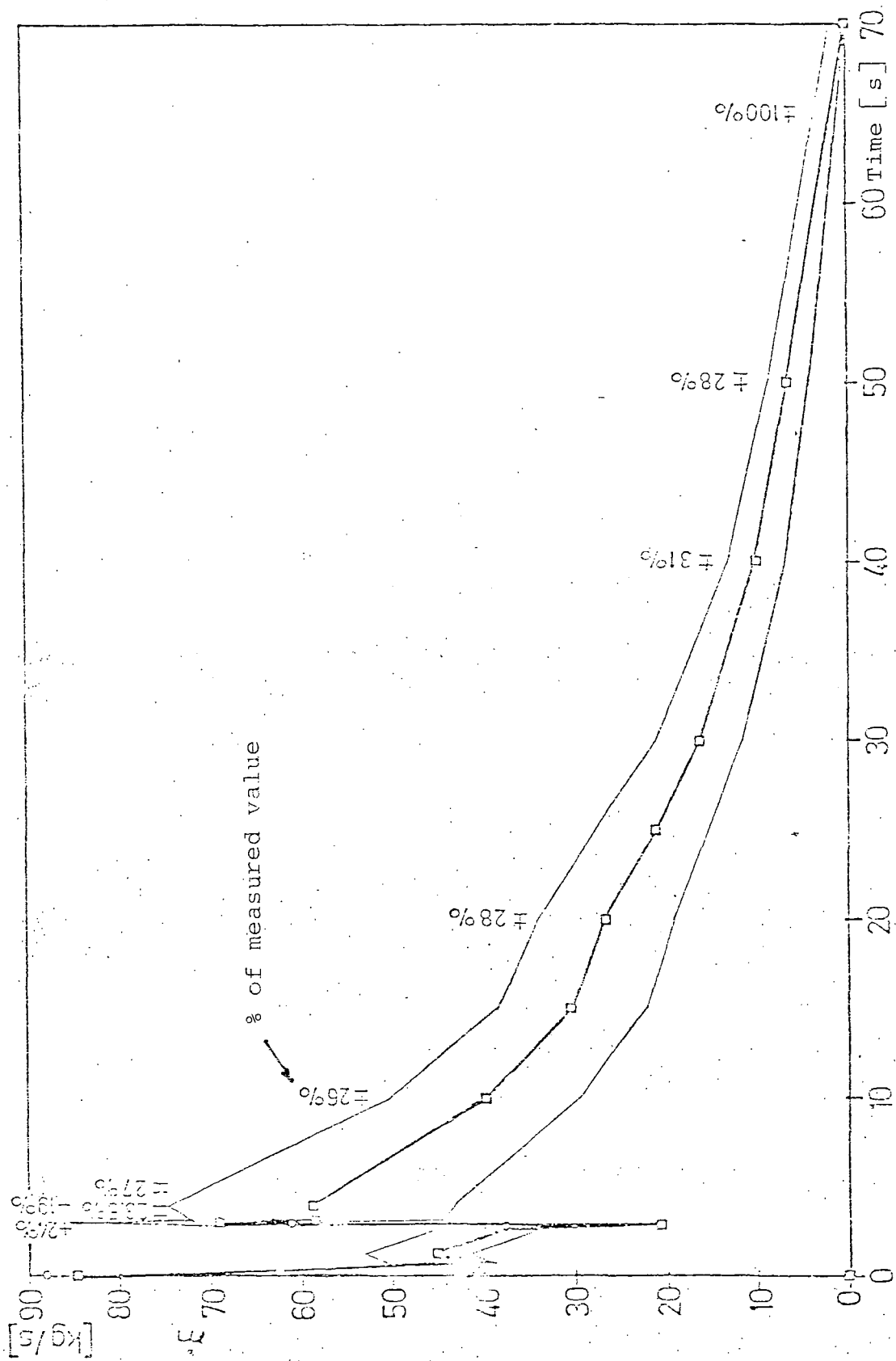


Fig. 51A: Break mass flow  $\dot{m}$  with error band (D15/0-70s)

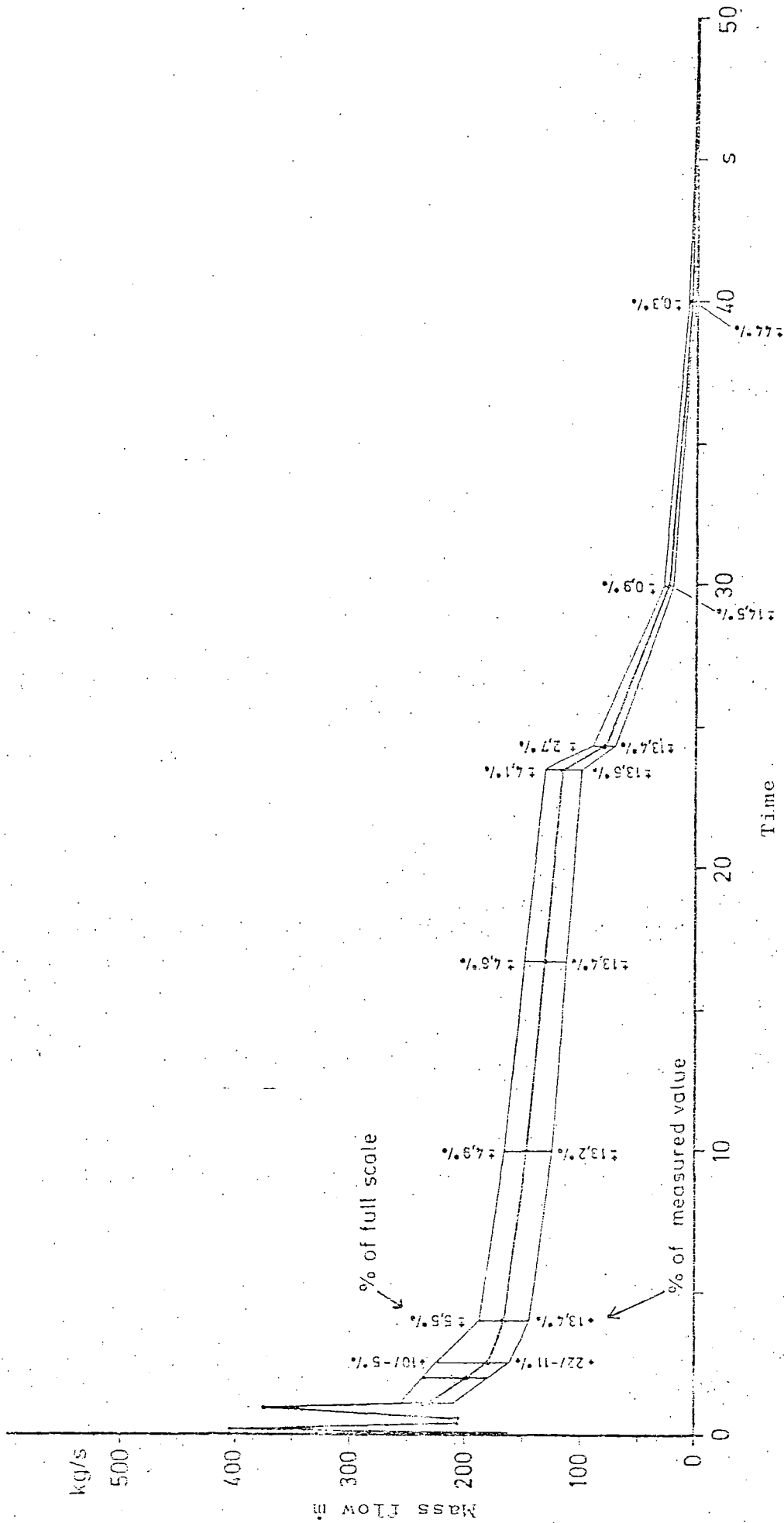


Fig. 51B: Break mass flow  $\dot{m}$  with error band (CASP2/0-50s)



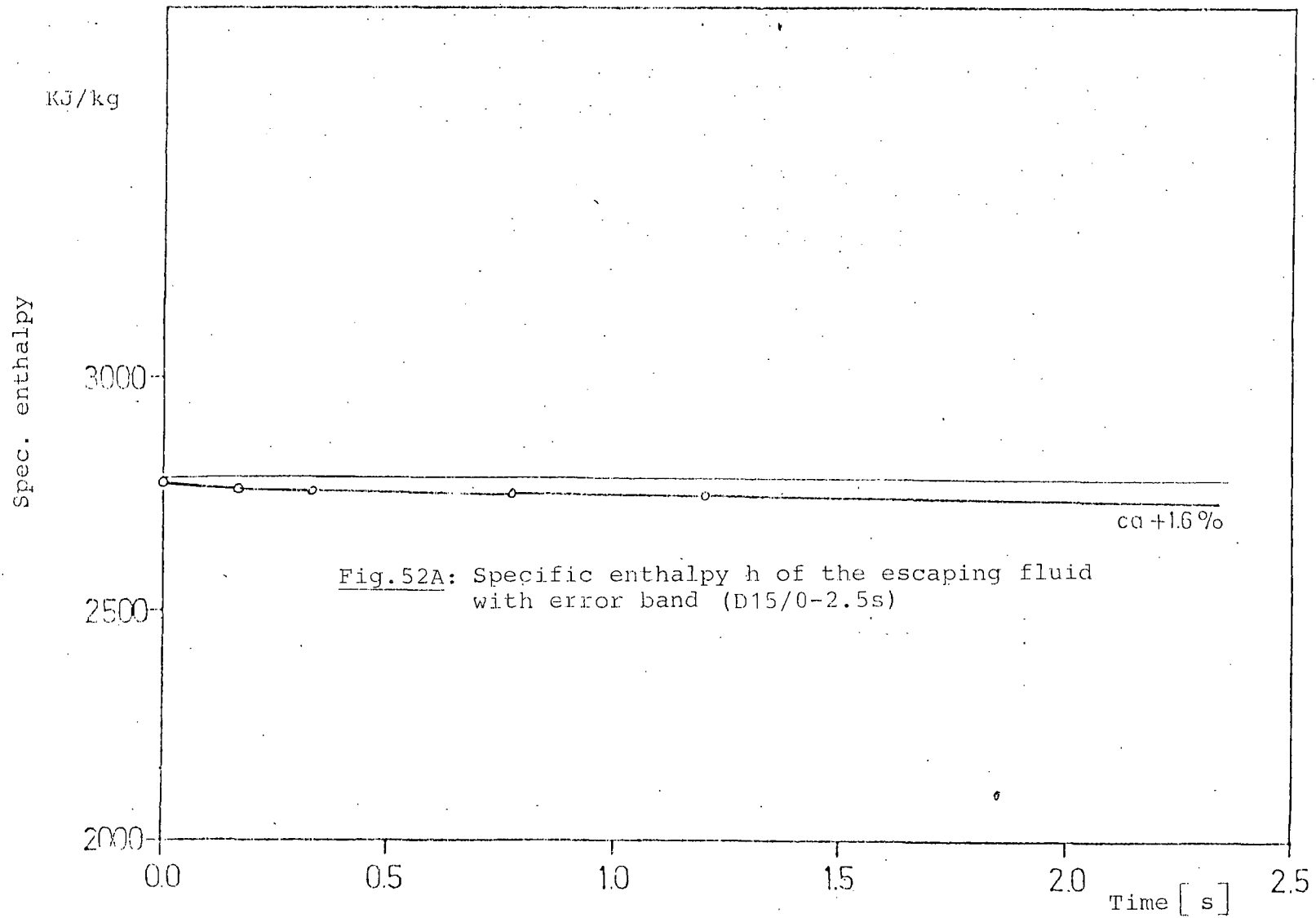


Fig.52A: Specific enthalpy  $h$  of the escaping fluid with error band (D15/0-2.5s)

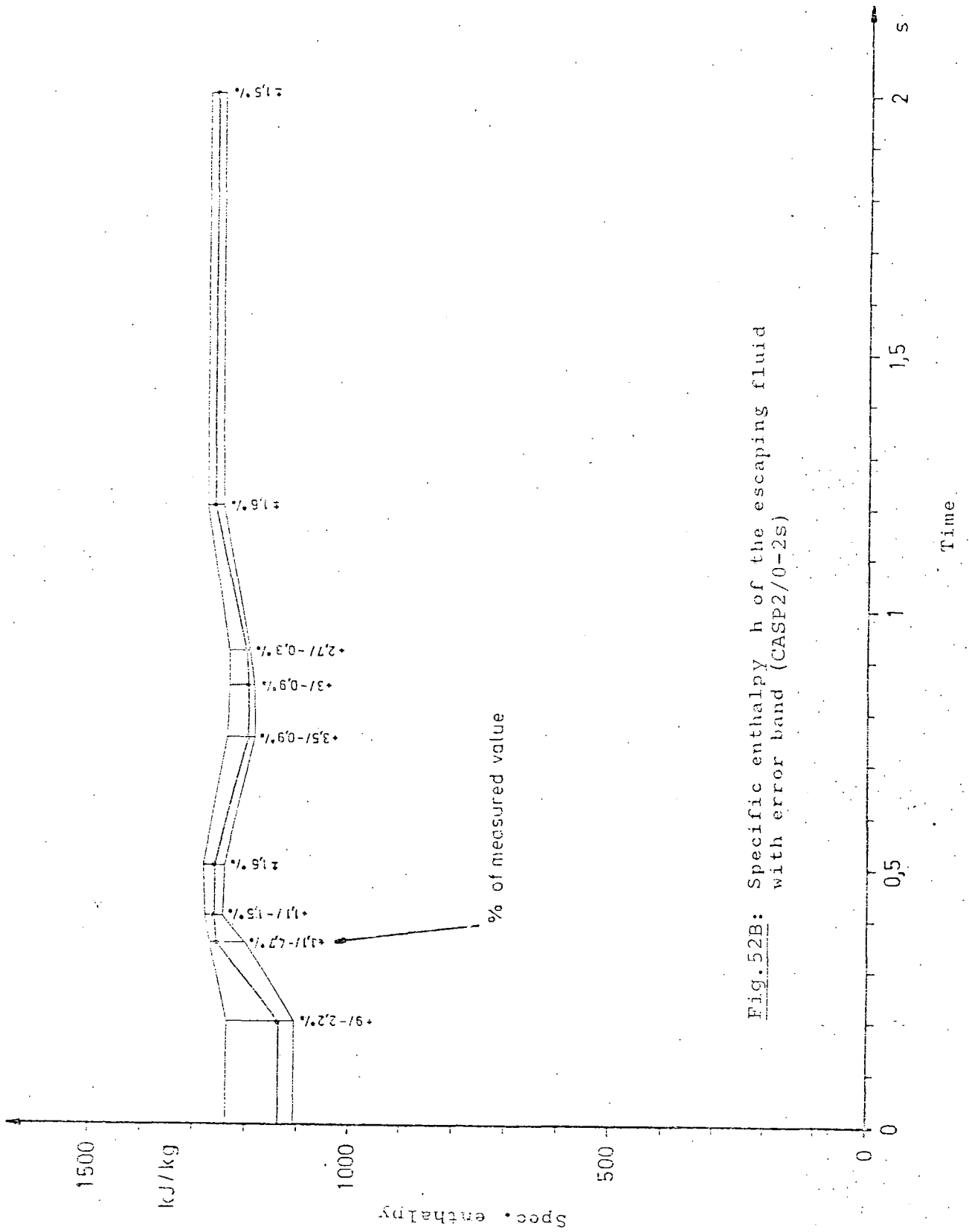


Fig. 52B: Specific enthalpy  $h$  of the escaping fluid with error band (CASP2/0-2s)

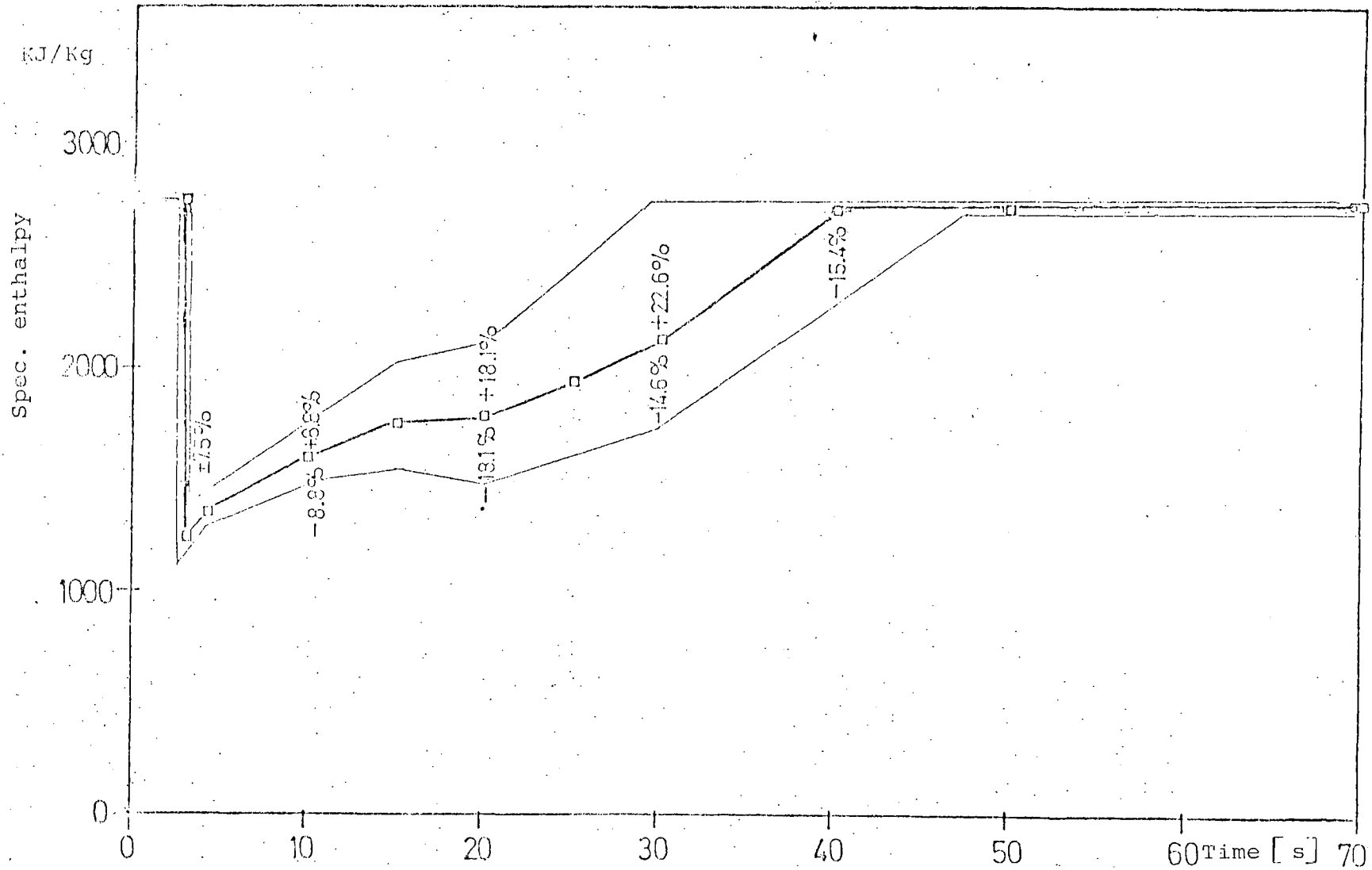


Fig. 53A: Specific enthalpy  $h$  of the escaping fluid with error band (D15/0-70s)

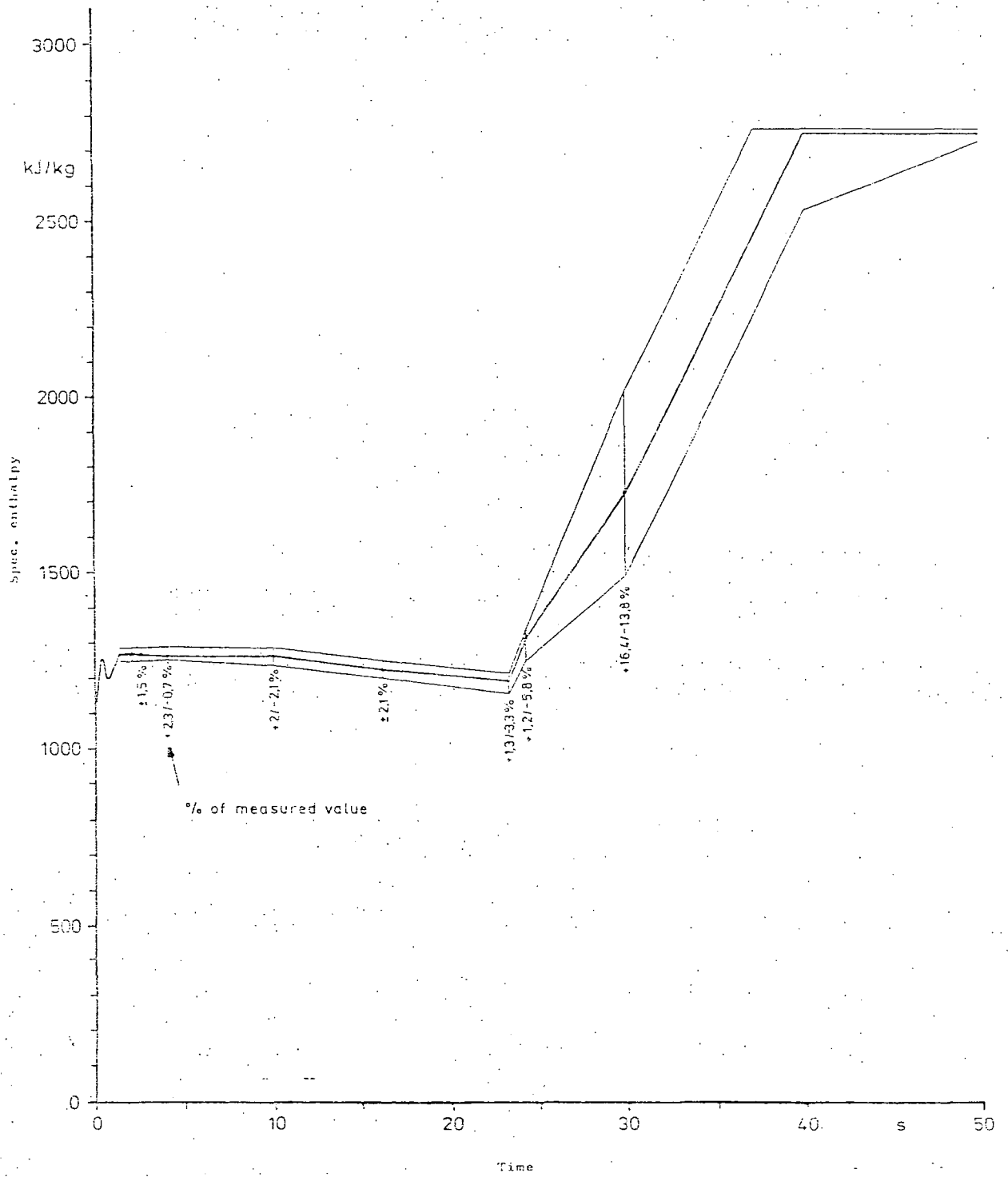


Fig.53B: Specific enthalpy  $h$  of the escaping fluid with error band (CASP/0-50s)

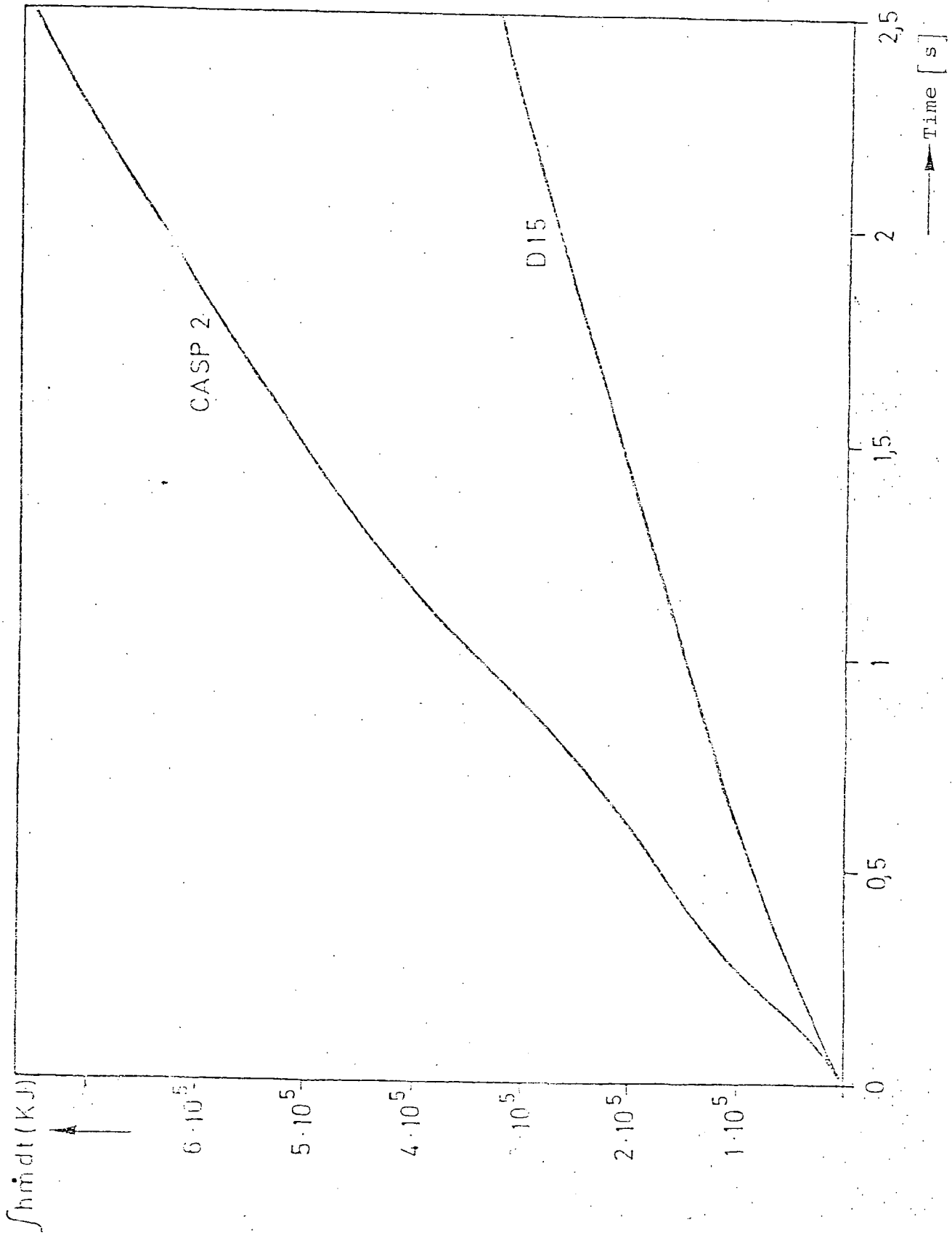


Fig. 54: Total enthalpy flown in (0 - 2.5s)

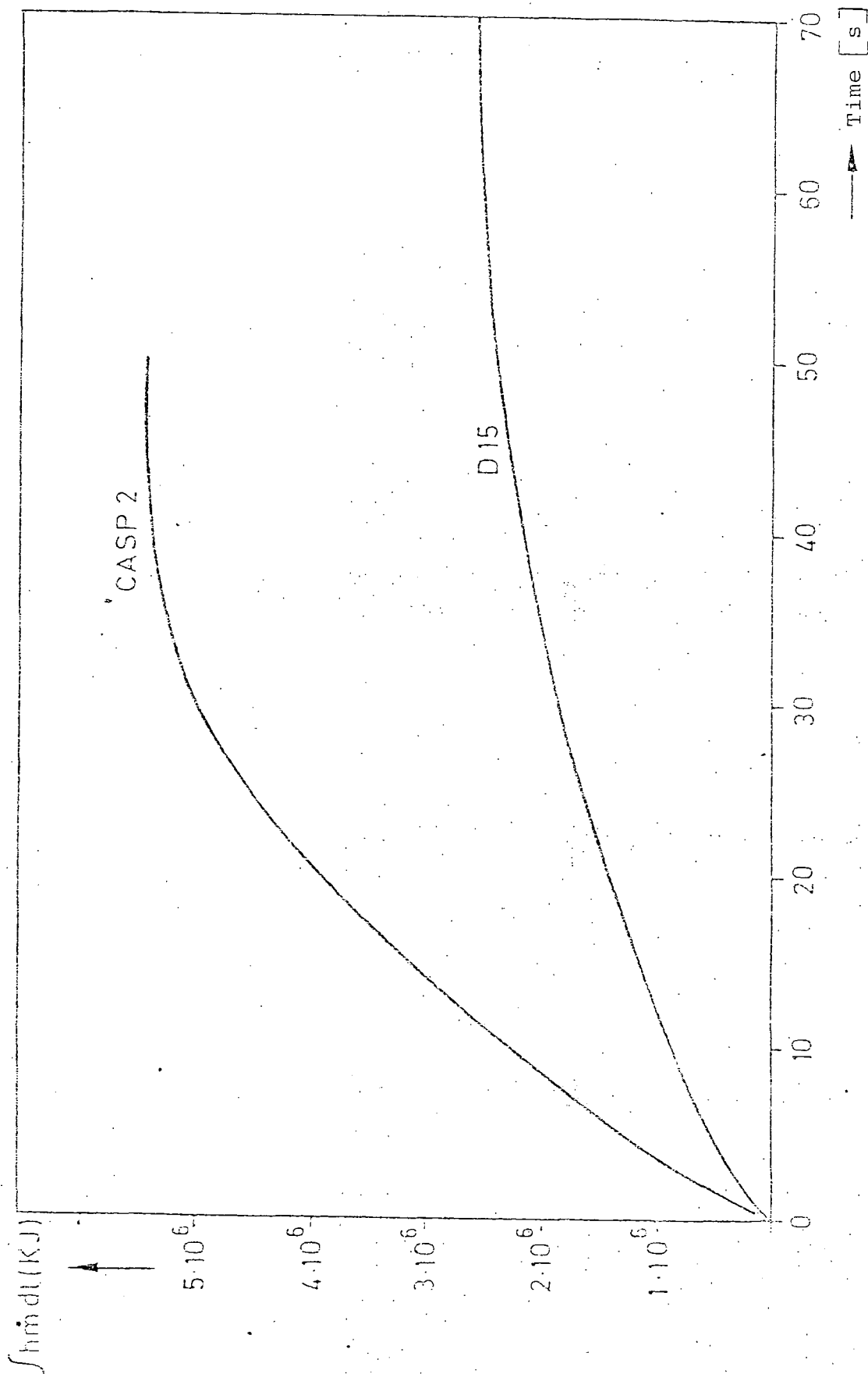


Fig.55: Total enthalpy flown in (0 - 70s)

### 3.8.3 Comparison of important characteristic variables

In the following, results for important characteristic variables of the two SP are directly compared. The results of participants, who calculated the experiment with essential higher deviation than the majority of participants, and the small experimental error bands [ $\pm(0.02 \div 0.03)$  bar] are not considered. Relative values for pressure are related to the pressure built-up of the experiment, and for the differential pressures to the experimental values.

- Time interval 0 to 2.5 s:

For test D15 the maximum pressure in the rupture compartment R6 (exp. value: 1.53 bar) was calculated by the participants within a margin of 0.12 bar (22.6 %) and with a maximum deviation of +0.09 bar (17.0 %). The corresponding values for test CASP2 are (2nd maximum in rupture compartment R4, exp. value: 1.81 bar): 0.25 bar (30.9 %), +0.18 bar (22.2 %) (see figs. 56A and 56B).

While the experimental curve for the pressure history in the large dome compartment R9 for test D15 is approximately in the middle of the calculational bandwidth, the pressure increase for test CASP2 is mainly overpredicted (figs. 57A and 57B). More details at the time 2.5 s are given in the following table:

Variable	D15	CASP2
$P_{R9exp.}$	1.32 bar	1.55 bar
calculational bandwidth	0.25 bar 78 %	0.13 bar 24 %
maximum deviation (calculation-experiment)	-0.14 bar -44 %	+0.14 bar +25 %

The next table gives the results for the maximum of the highest differential pressure (figs. 58A and 58B) and for the maximum of the differential pressure between the rupture compartment and the 1st follow-up compartment (figs. 59A and 59B).

Variable	D15	CASP2
$\Delta P_{R6-R9}$ or $\Delta P_{R6-R8}$ or R4-R9 exp. R4-R5 exp.	0.49/0.27 bar	0.62/0.33 bar
calculational bandwidth	0.09/0.12 bar 18 %/44 %	0.28/0.21 bar 45 %/64 %
maximum deviation (calculation-experiment)	-0.05/-0.12 bar -10 %/-44 %	-0.27/-0.21 bar -44 %/-64 %



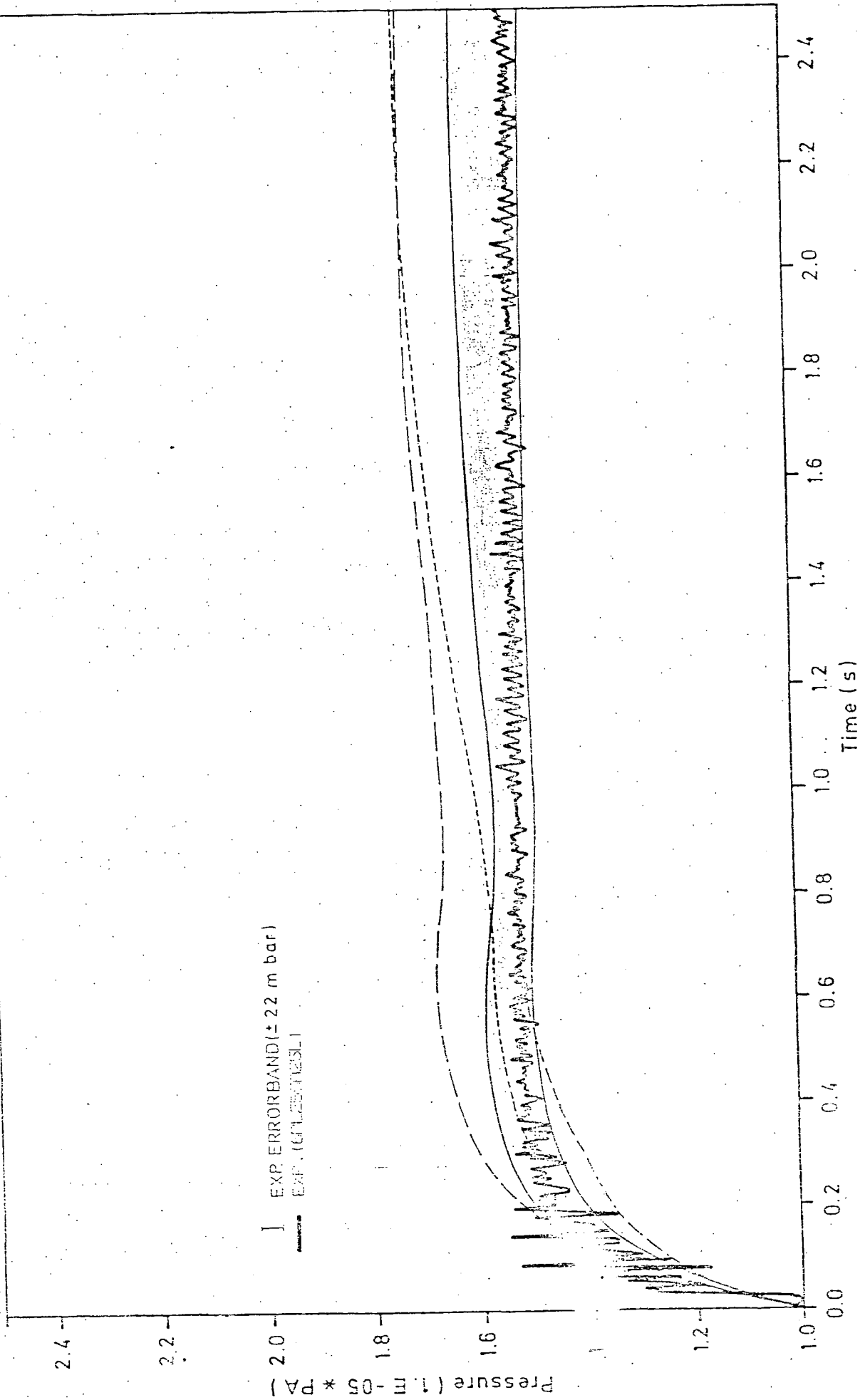


FIG. 56A: PRESSURE HISTORY IN COMPARTMENT R6

OECD-CSNI CONTAINMENT STANDARD PROBLEM NO.2 (TEST CASP2)

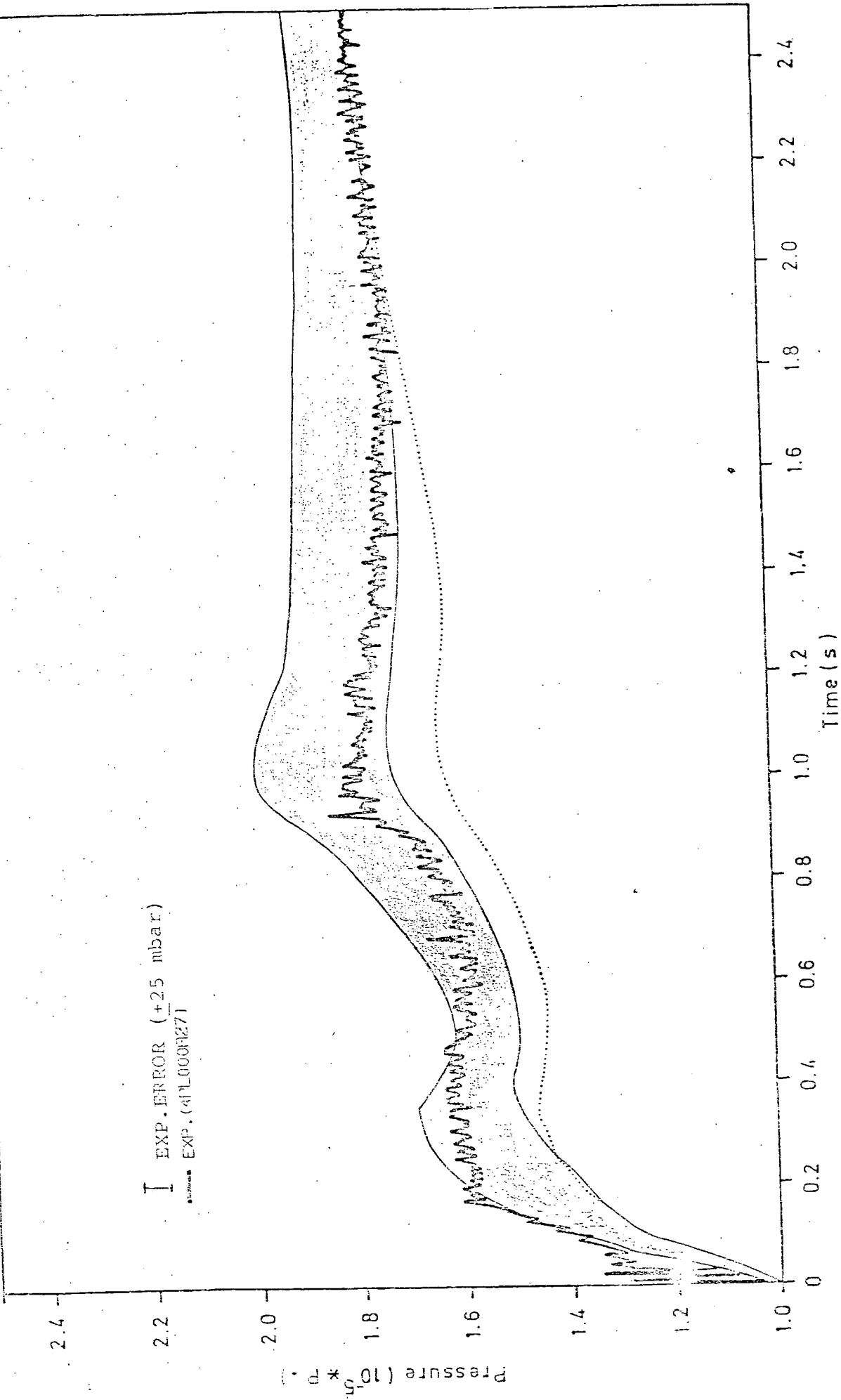


FIG. 56B : PRESSURE HISTORY IN COMPARTMENT R4

OECD-USSM CONTAINMENT STANDARD PROBLEM NO.1 (BATTELLE-TEST D15)

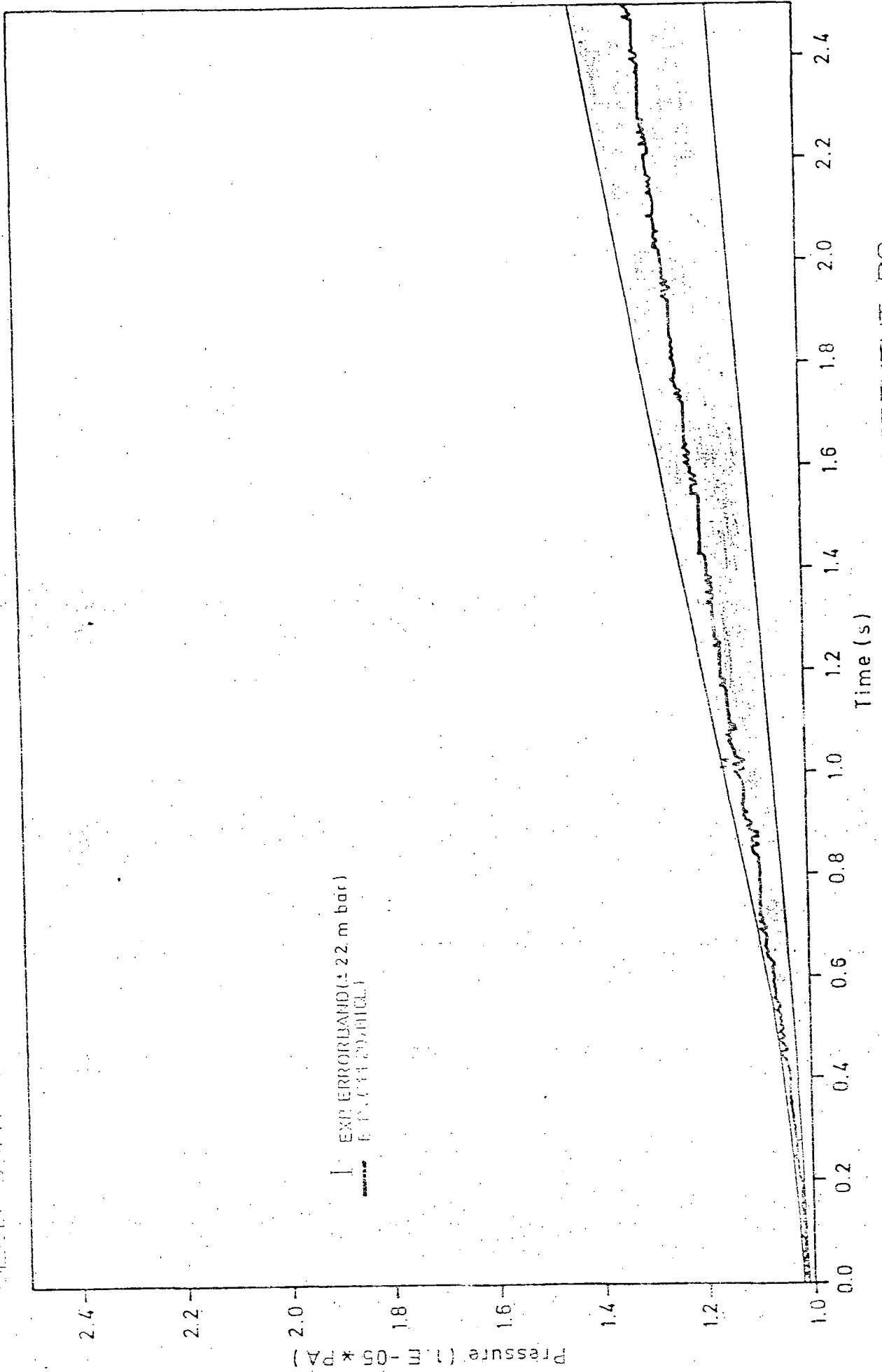


FIG. 57A: PRESSURE HISTORY IN COMPARTMENT R9

OECD-CSNI CONTAINMENT STANDARD PROBLEM NO.2 (TEST CASP2)

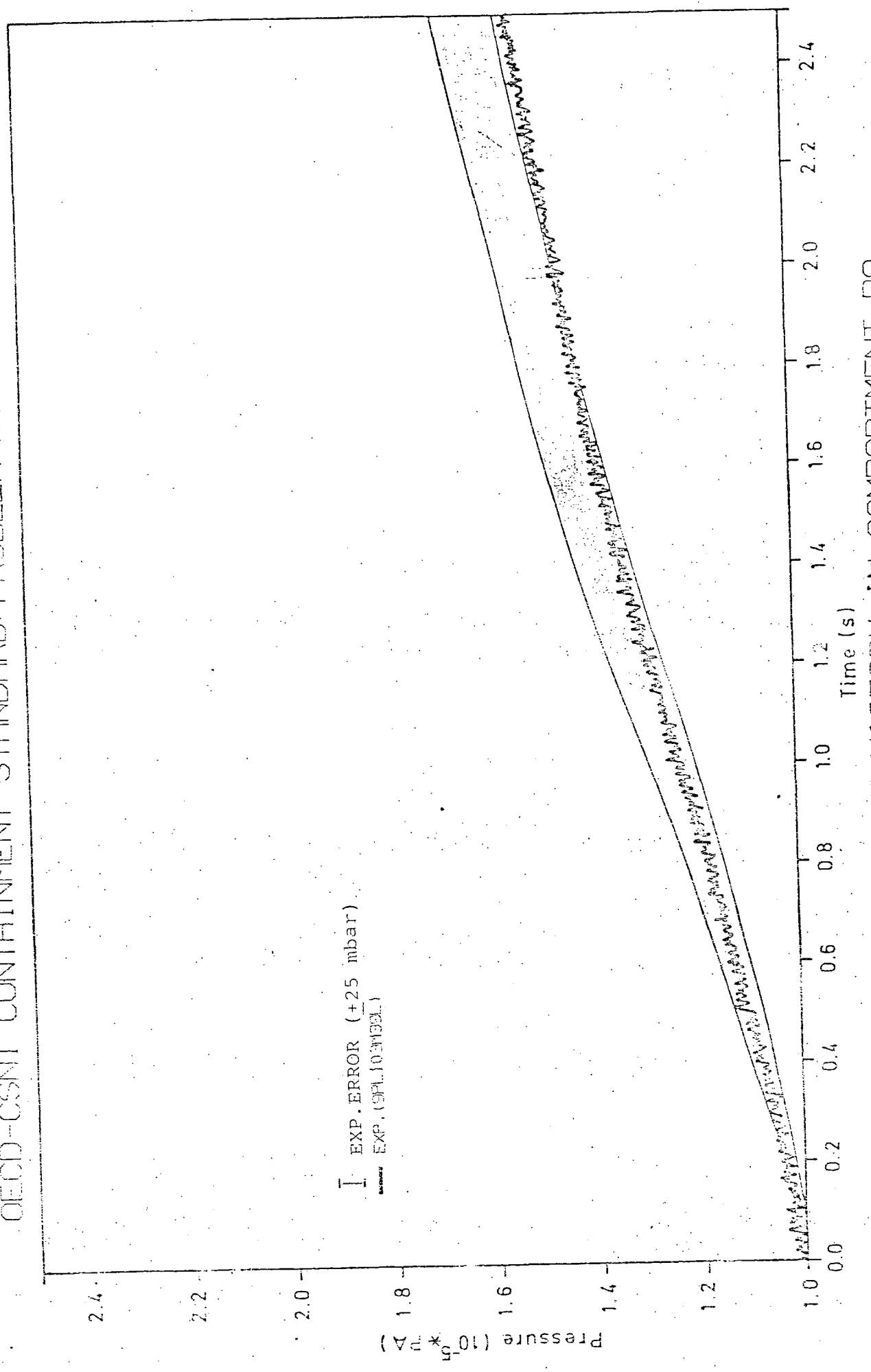


FIG. 57B : PRESSURE HISTORY IN COMPARTMENT R9

OIECD-CSNI CONTAINMENT STANDARD PROBLEM NO. 1 (BATTELLE-TEST D15)

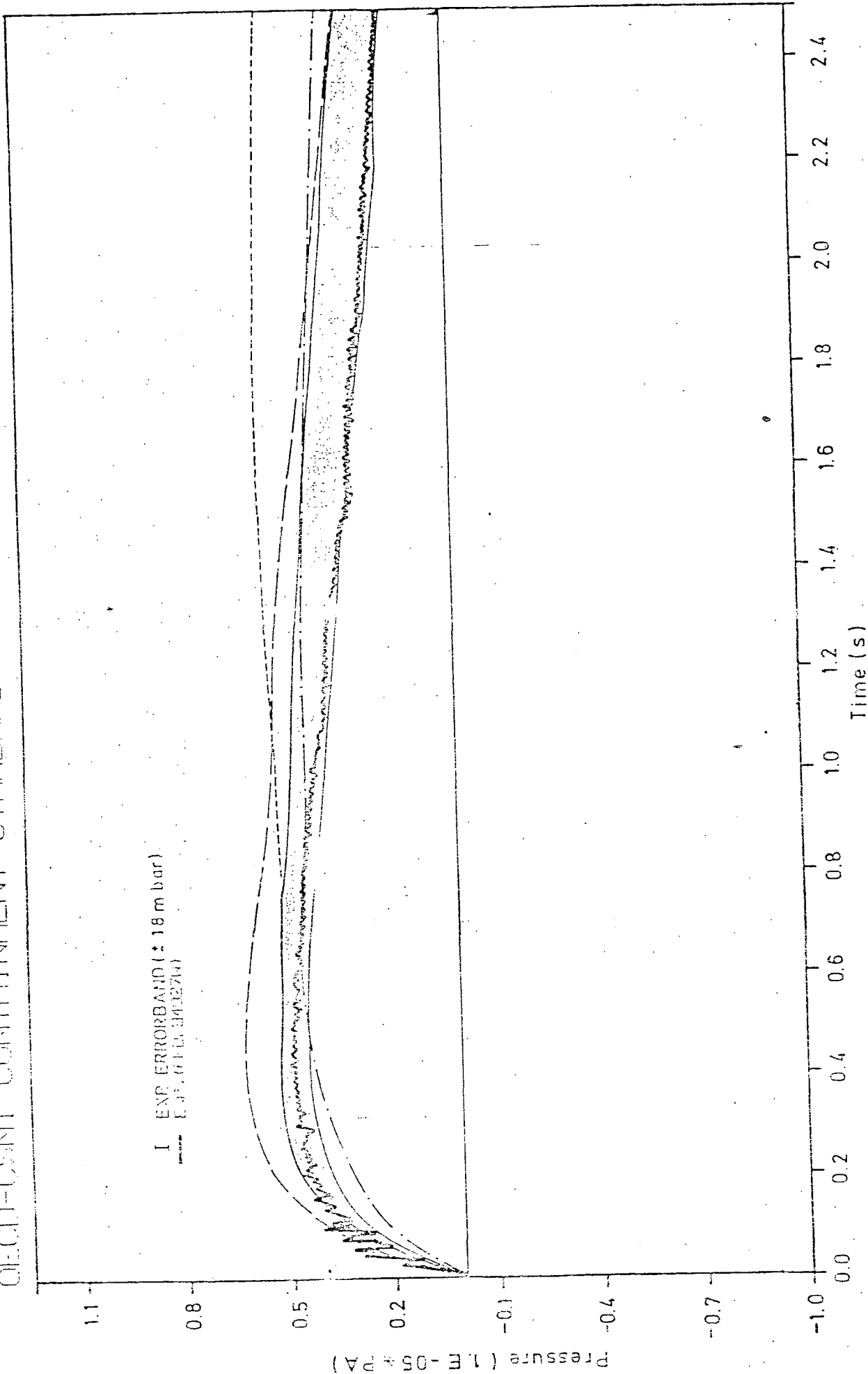


FIG. 58A: HISTORY OF PRESSURE DIFFERENCE R6-R9

OECD-CSI CONTAINMENT STANDARD PROBLEM NO.2 (TEST CASP2)

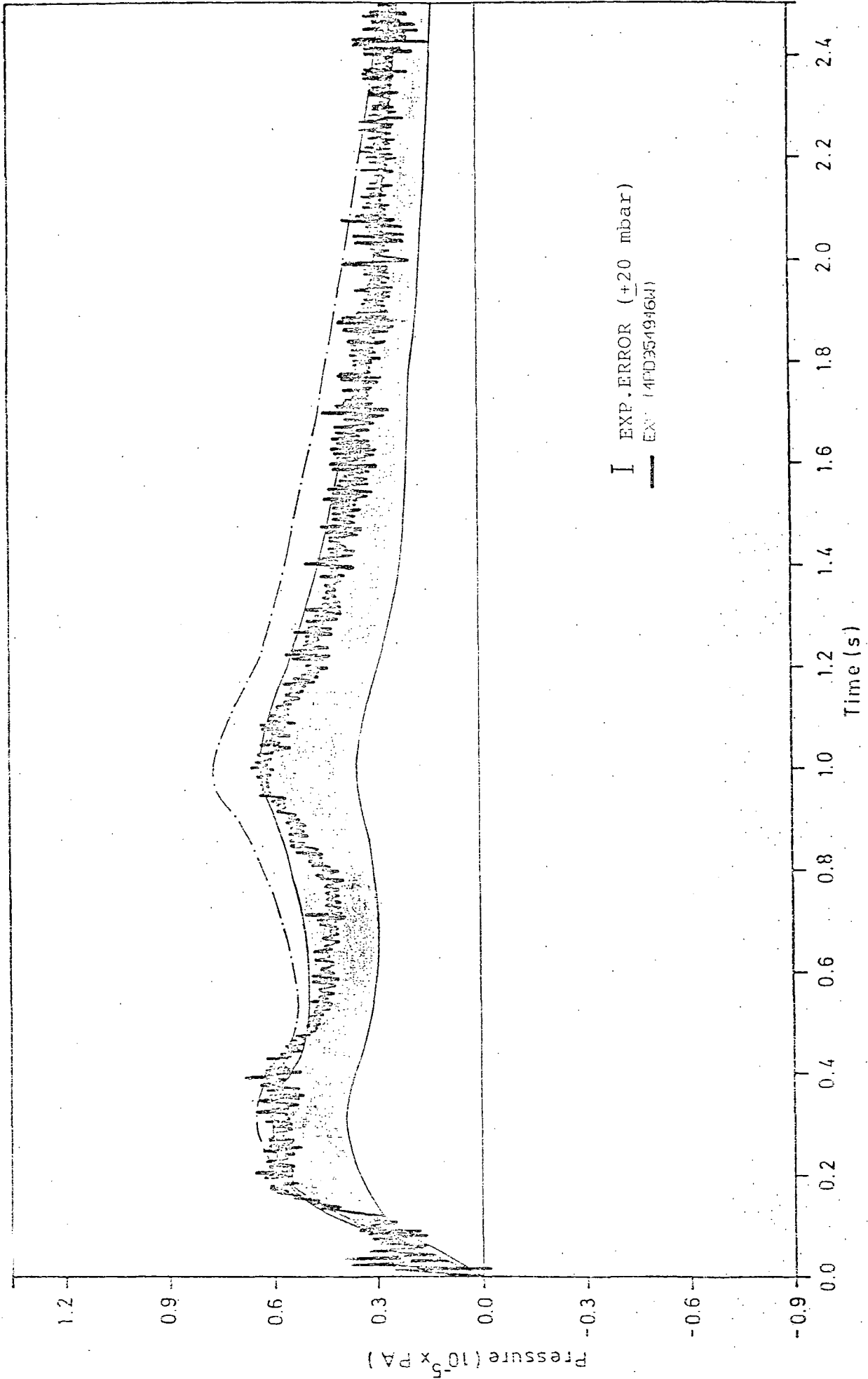


FIG. 58B: HISTORY OF PRESSURE DIFFERENCE R4-R9

DECTRON CONTAINMENT STANDARD PROBLEM NO. 1 (BATTELLE-TEST D15)

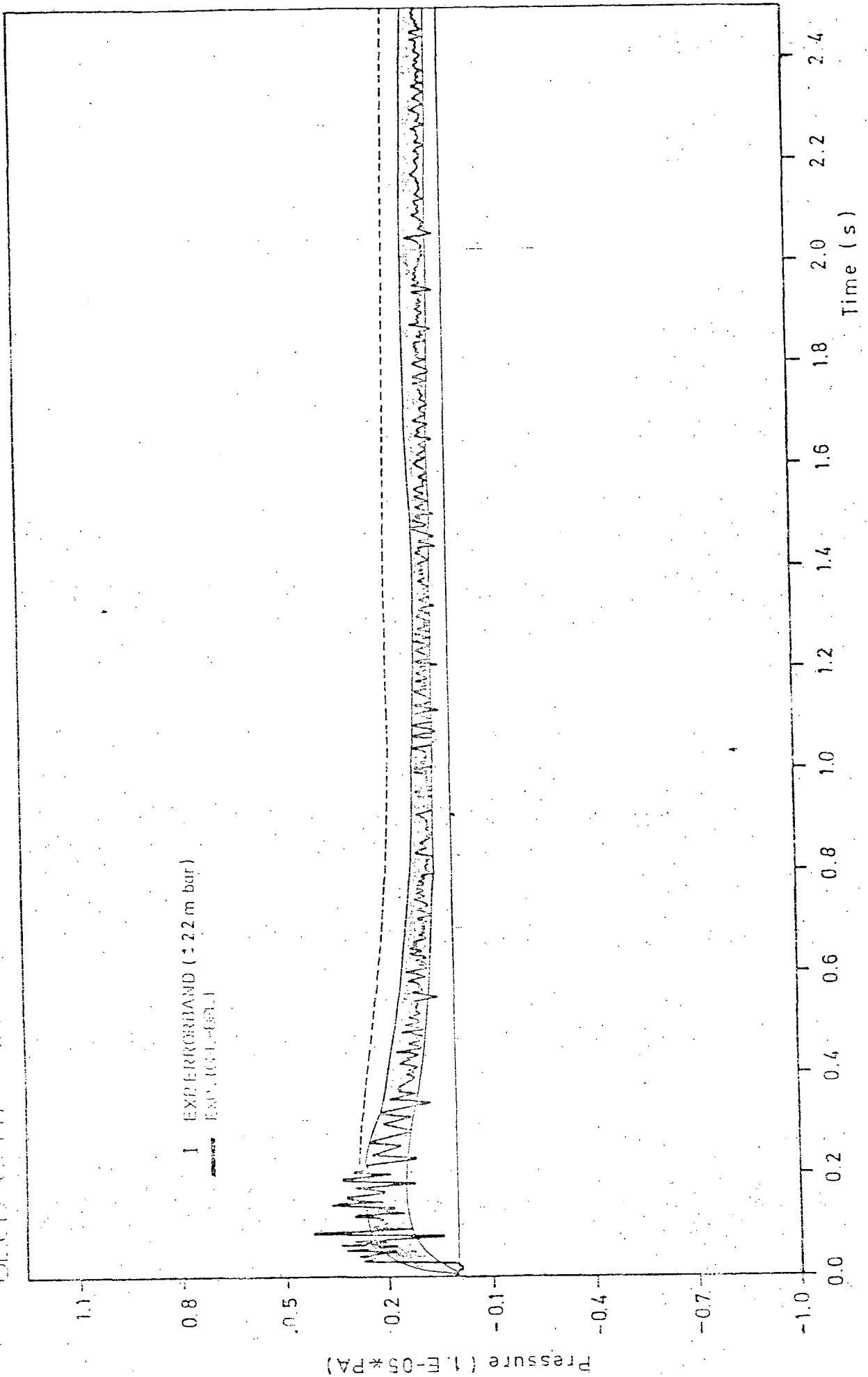


FIG. 59A: HISTORY OF PRESSURE DIFFERENCE RG-RB

(HEAD-CONTAINMENT STANDARD PROBLEM NO.2 (TEST CASP2))

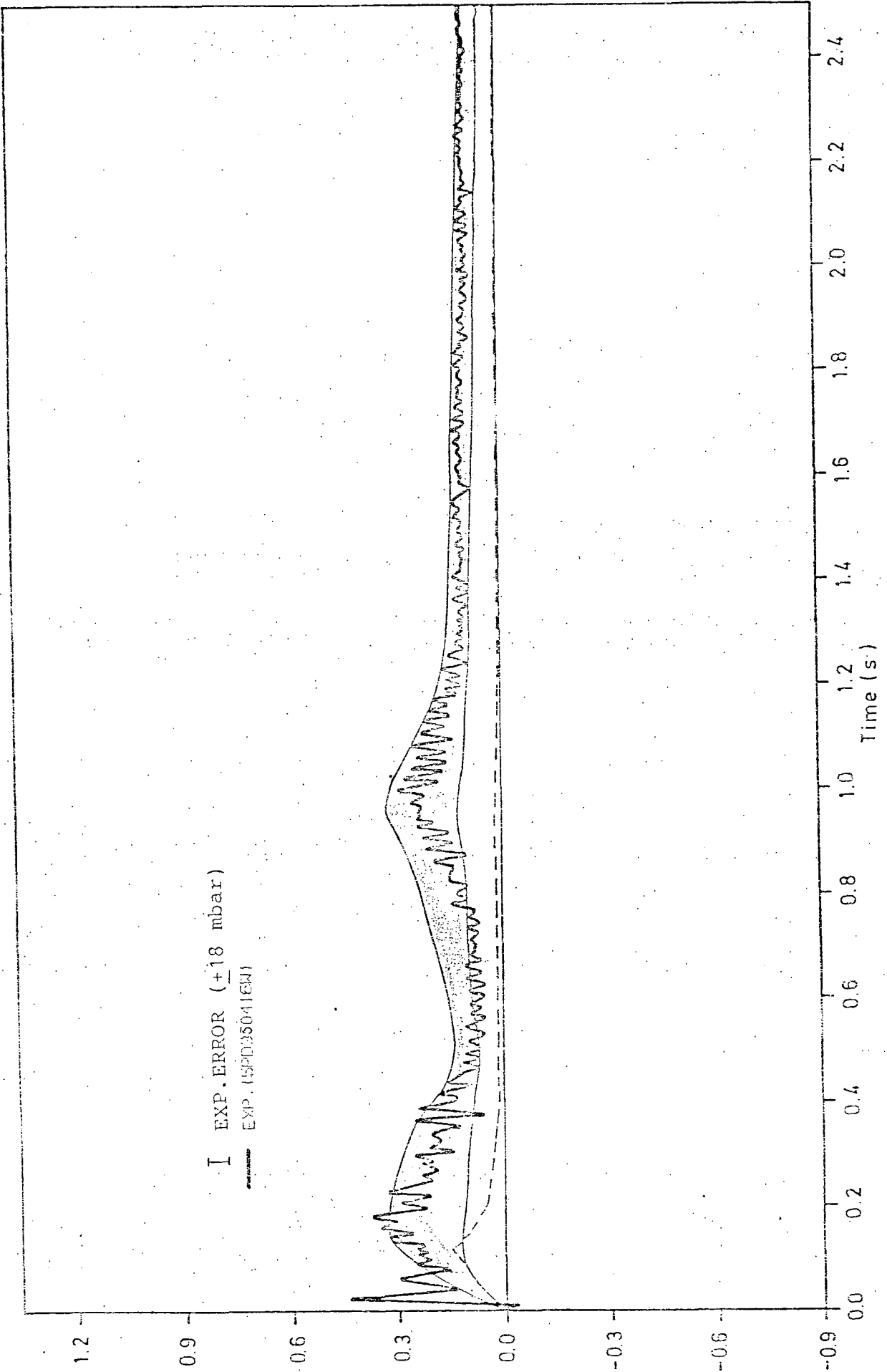


FIG. 59B: HISTORY OF PRESSURE DIFFERENCE R4-R5



- Time interval 0 to 50 s:

The measured maximum pressure in test CASP2 (3.95 bar) is considerably higher than in test D15 (2.08 bar). The ratio of the maximum pressure built-up CASP2 : D15 amounts to 2.7. It is somewhat higher than the ratio of the total enthalpy flown into the containment up to the respective maximum pressure (2.4), because the heat absorption of the concrete walls in test D15 is greater than in test CASP2. This may be caused by the longer time period up to maximum pressure (D15: 40 s; CASP2: 33 s), the slightly higher surface area/volume-ratio (D15: 1.93; CASP2: 1.77) and the lower initial temperature of the structures (D15: 9 °C; CASP2: at least 18.2 °C) in test D15.

The maximum pressure for test D15 is calculated by the participants within a margin of 0.58 bar (54 % of measured pressure built-up). The maximum deviations amount to +0.49 bar (45 %) and -0.09 bar (-18 %) (fig. 60A). The scatter band of calculations for test CASP2 is equal to 0.48 bar (16 %). The maximum deviations amount to +0.34 bar (12 %) and -0.14 bar (-5 %) (fig. 60B).

These values and the histories of the most important variables indicate that the scatter bandwidths of the calculations respectively the maximum deviations between calculations and experiment at the 2nd Containment-SP (water blowdown, single branched chain) on the average are of the same amount as at the 1st Containment-SP (vapour blowdown, single chain). This positive result is certainly caused by the experiences from the 1st Containment-SP.



OECD-CSNI CONTAINMENT STANDARD PROBLEM NO. 1 (BATTELLE-TEST D15)

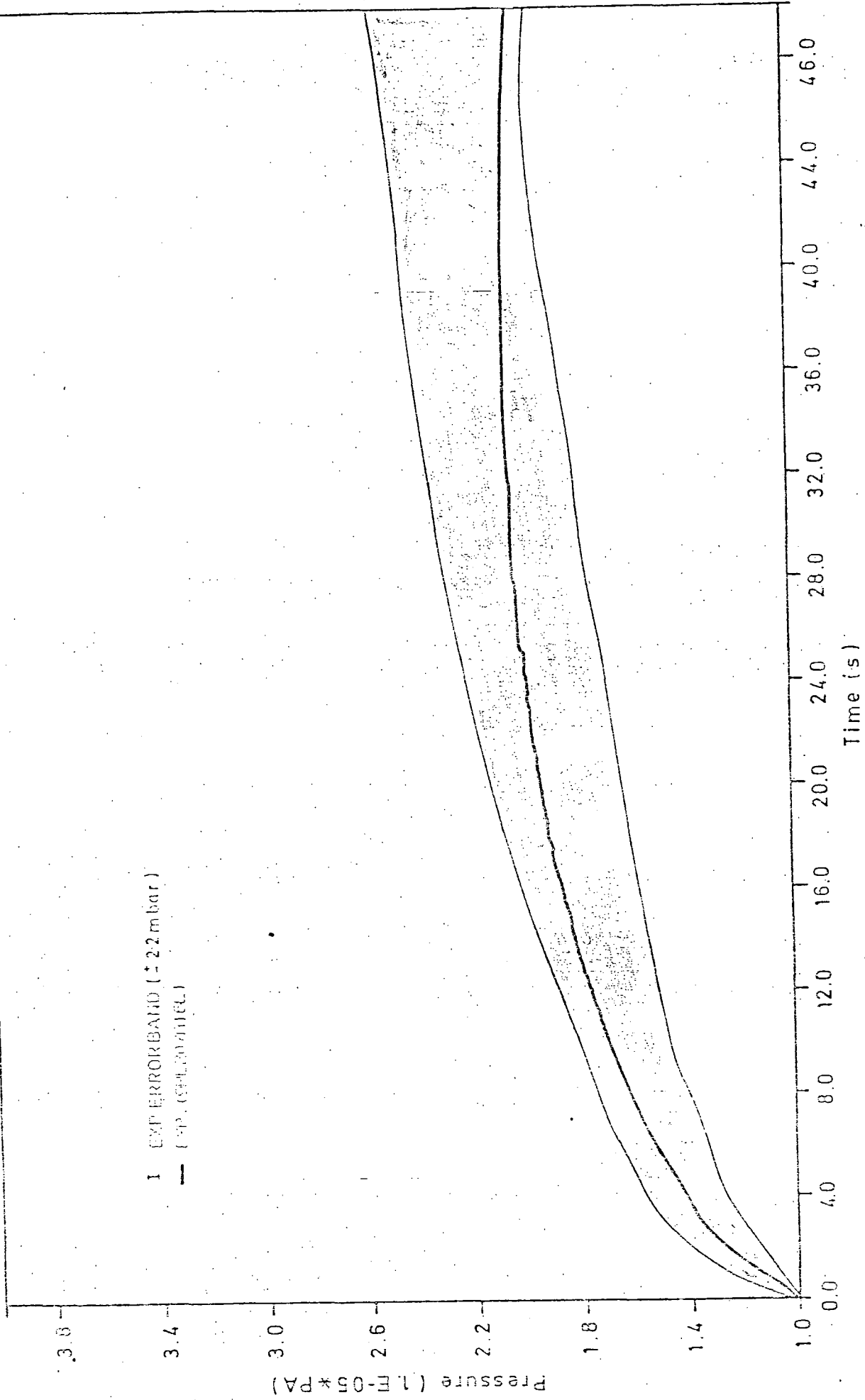


FIG. 60A: PRESSURE HISTORY IN COMPARTMENT R9

OECD-CSNI CONTAINMENT STANDARD PROBLEM NO.2 (TEST CASP2)

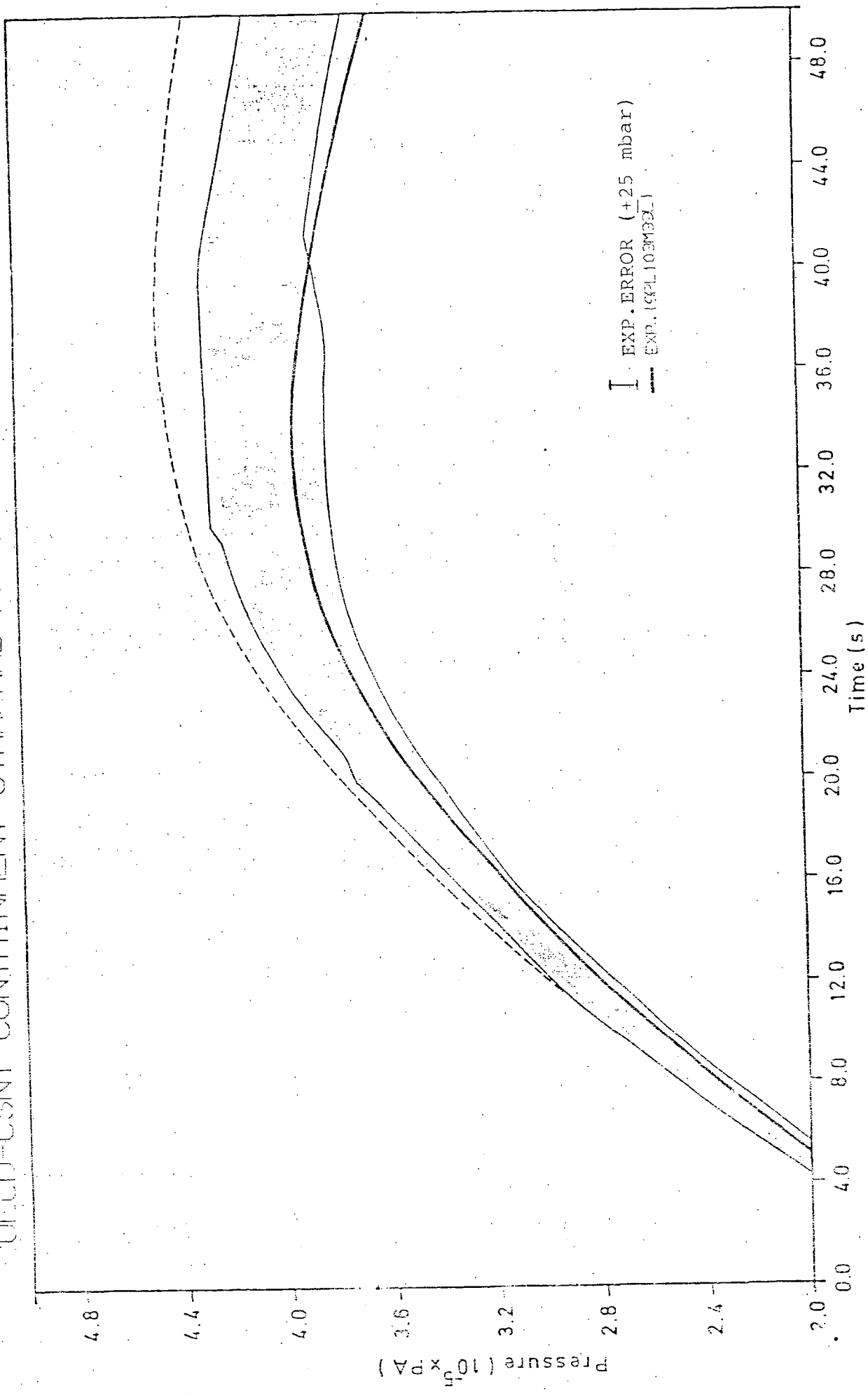


FIG. 60B : PRESSURE HISTORY IN COMPARTMENT R9

#### 4 ABSTRACT AND CONCLUSIONS

While the relatively simple test D15 (steam-blowdown, simple chain of compartments) was taken as a basis for the 1st Containment-SP, conditions of test CASP2 (water blowdown, branched chain) at this 2nd Containment-SP have been closer to Design Basis Accident Conditions of a PWR. Aim of test CASP2 was to investigate histories of pressures, pressure differences, temperatures and water masses in a model containment after break of a water line. Because of the small rupture compartment and the arrangement of compartments in a branched chain it is evident, that water transport had an increased influence on the results.

12 organizations from 11 countries have participated in this second CSNI-Containment Standard Problem. 12 different codes and additional code modifications were used to analyse processes within model containment. The calculations were to be performed with the nominal, measured initial and boundary conditions on best-estimate basis as an "open" international SP.

Errors for variables measured in containment are as a rule small and mostly within the oscillatory margins of the measured values. Boundary conditions as determined from measurements and input for the SP-calculations have smaller error bands in this test than in test D15. In view of the considerable influence on variables to be calculated for the containment, error bands are still relatively high for certain time periods. As already discussed at the workshops for the 1st Containment-SP the related measurement technique should be improved.

Quantitative results concerning the effects of possible deviations from nominal values were found for some important input data. The relatively high amount of influence on calculational results will be reduced on the one hand when the more or less unknown systematic errors could be separated, but will be increased on the other hand when regarding all statistical errors. Assuming nearly compensation means that these effects are about as high as the scatter bandwidths of the calculational results.

The bandwidths of the open results are on the average equal the bandwidths of the blind results and of the results of the 1st Containment-SP. Related to the more difficult problem in comparison with the 1st Contain-

ment-SP and the possible effects of uncertainties of input data the agreement between calculations and experiment can generally be considered as quite satisfactory.

Because of the effects of uncertainties of input data quantitative statements render more difficult. However, some observations shall be summarized partly in repetition of the conclusions for 1st Containment SP:

- Time interval 0 to 2.5 s:

In general the results of the participants are within a "calculational error band". The mean values of the calculational results for the pressure built-up deviate in part systematically from the experiment (-0.05 to +0.09 bar). For the pressure differences between compartments, the maximum absolute deviations of calculational results from the experiment are between -0.27 and +0.14 bar.

- Time interval 0 to 50 s:

With three exceptions the participants predicted the maximum pressure in the containment within a small bandwidth between 3.81 and 4.16 bar (mean value: 4.02 bar; exp. result:  $3.95 \pm 0.03$  bar).

- Time interval 0 to 1000 s:

In most of the calculations long term pressure is overpredicted, which seems to indicate that the experimental results might be influenced by a leakage of the containment.

- The deviations, which are partly considerable, between calculational results and the experiment can be explained by code handling (choice of options, input parameters, nodalization) and by the analytical models themselves. For example, concerning the influence of the heat transfer to or from structures (dead ends, steam front propagation, vertical temperature stratification), the nodalization seems to be not sufficiently fine, especially in most calculations for the long term.

- It is to recommend to study thoroughly the reasons for deviations between calculations and experiment. This task being individual and beyond the scope of this report, should be done by each participant for his own after exchange of experiences at the workshop. It should be advisable to include the suggested systematic error consideration to be able to better quantitatively interpret the results.

- Some important physical phenomena were described in connection with simplified models by different input parameters partly defined disadvantageously (water transport: for example water carry-over factors from 0 to 1; heat transfer: for example heat transfer coefficients from 1300 to 15 000 W/(m<sup>2</sup>K) in the rupture compartment, from 100 to 2000 W/ (m<sup>2</sup>K) in dome compartment during the short time interval; orifice flow: for example discharge coefficient from 0.6 to 1.2). It is difficult to detect a connection between input parameter and quality of the results, because the different influences are hardly separable and have to a certain degree a compensating effect on the calculational results. It seems to be advisable to improve the physical simulation of these phenomena (e.g. based on tests with defined test conditions and improved instrumentation).
- Friction- and acceleration-losses of the two-phase flow are often taken into account by constant compressible or incompressible discharge coefficients. Thus, in connection with the usual description of water transport by homogeneous models momentum losses were described by a mass flow correlation.
- It is to be assumed that subdivision of walls had an influence on the calculational results. In order to examine this problem more closely, the CSNI Benchmark Problem on containment codes should be taken into account.
- It is recognizable, that the quality of calculational results depended on the experience from the first Containment-SP and the knowledge of the individual code user and developer about the previous similar tests in the same model containment.
- Although SP should preferably be performed on best-estimate basis, it is to note, that some participants rather tried to obtain "conservative" results.
- Even after this 2nd Containment-SP it is difficult to draw quantitative conclusions with respect to the achievable accuracy of predictions of thermo-fluiddynamic effects within a real full pressure containment. Especially, it seems to be beneficial to perform a further Containment-SP based on a water blowdown test in the large-scale HDR-facility and planned within the German SP-activity for mid of 1982.

REFERENCES

- / 1/ Battelle-Institut, Frankfurt  
Projekt RS 50 - Investigation of the Phenomena Occurring Within  
a Multi-Compartment Containment After Rupture of the Primary  
Cooling Circuit in Water-Cooled Reactors  
Specification of the Containment Standard Problem Experiment CASP2  
Techn. Bericht BF-RS 50-42-11, September 1979
- / 2/ G. Hellings  
German Standard Problem No. 3 (2nd Containment Standard Problem):  
Water Line Rupture in a Branched Compartment Chain  
Specification  
GRS, August 1979
- / 3/ GRS-letter of December 19, 1979  
referring to continuation of 2nd Containment Standard Problem
- / 4/ Battelle-Institut, Frankfurt  
Project RS 50: Initial Conditions, Break Mass Flow and Specific  
Enthalpy from Experiment CASP2  
(German Standard Problem No. 3)  
Techn. Bericht BF-RS 50-42-12-2, November 1979
- / 5/ T. Kanzieiter  
Projekt RS 50  
Quick Look Report Experiment D16/CASP2  
(German Standard Problem No. 3)  
Techn. Bericht BF-RS 50-30-D16-2 (English version), March 1980
- / 6/ T. Kanzieiter  
Projekt RS 50: Ergänzende Versuchsdokumentation D16/CASP2  
(Deutsches Standard-Problem Nr. 3)  
Techn. Bericht BF-RS 50-32-D16  
Battelle-Institut, Frankfurt, März 1980
- / 7/ Letter of July 9, 1980, •  
"Second Containment Standard Problem,  
Gap Size R4/R9 in RS 50 Experiment D16/CASP2"  
T. Kanzieiter, Battelle-Institut, Frankfurt



- / 8/ W. Winkler  
2nd Containment Standard Problem:  
Experimental Data of Test D16/CASP2  
(Battelle Model Containment)  
GRS, Garching; July 14, 1980
- / 9/ H. Karwat, D.L. Nguyen, W. Winkler  
Containment Standard Problem No. 2:  
Results of "Blind" Predictions Submitted by International Participants  
GRS, November 1980
- /10/ W. Winkler  
Comparison Report on OECD-CSNI Containment Standard Problem  
No. 1: "Steamline Rupture Within a Chain of Compartments"  
CSNI Report No. 41, May 1980
- /11/ "Hütte". Des Ingenieurs Taschenbuch  
Band 1, Theoretische Grundlagen  
28. Auflage, Berlin 1955
- /12/ W. Erdmann  
Fehlerbetrachtungen zum Standard-Problem-Versuch CASP2  
GRS-A-617 (Juni 1981)
- /12a/ W. Erdmann  
Vergleich der gerechneten Ergebnisse zum RS 50 CASP2-Versuch  
mit den Meßdaten und Nachrechnung  
GRS-A-502. September 1980
- /13/ W. Winkler, G. Mansfeld  
Containment Standard-Problem  
Untersuchungen zu den Rand- und Anfangsbedingungen des  
Standard-Problem-Versuchs D10 und des Wiederholungsversuchs D15  
(Battelle-Modell-Containment)  
GRS-A-111, Februar 1978
- /14/ GRS-letter of July 23, 1980 on  
"OECD-CSNI Containment Standard Problem No. 2"

- /15/ P.G. Holland and J. Marshall  
The Use of ZOCO V and ZOCO VI in the Containment Analysis  
Standard Problem No. 2  
AAEC (Australia), October 1980
- /16/ D. Brosche  
"ZOCO V - a computer code for the calculation of time- and space-  
dependent pressure distributions in reactor containments"  
Nucl. Eng. Design, 23 (1972), pp. 239-272
- /17/ G. Mansfeld  
"ZOCO VI - ein Rechenprogramm zur Berechnung von zeitlichen und  
örtlichen Druckverteilungen in Volldrucksicherheitsbehältern wasser-  
gekühlter Kernreaktoren. Programmbeschreibung"  
MRR-P-14, Dezember 1974  
LRA, TU München
- /18/ E.J. Stubbe  
OECD-CSNI Containment Standard Problem No. 2  
Open analysis of the Battelle-Frankfurt water line rupture in a  
branched compartment chain  
Brief description of the computational models  
Report PE/TC 260 A (26.2.80), revision of December 1980  
Tractionel Engineering (Belgium)
- /19/ E.J. Stubbe, J. Robeyns, A. Danguy (Tractionel)  
TRAP: computer codes for the evaluation of the pressure tran-  
sients in the subcompartments (TRAP-SCO) and the containment  
(TRAP-CON) of a reactor plant following a high energy line break  
Proceedings of the ENS/ANS International Topical meeting on nuclear  
power reactor safety  
Brussels, October 1978, Vol. III p. 2168
- /20/ W.M. Collins  
PRESCON-2 Simulation of the OECD/CSNI Containment Analysis  
Standard Problem No. 2  
AECL (Canada), October 1980

- /21/ Short Report of the Finnish OECD-CSNI Containment Standard Problem No. 2 Calculations, ("Open" Problem Calculations Using RELAP4/MOD6 and VTT's Version of CONTEMPT LT/026)  
VTT (Finland); October 28, 1980
- /22/ A. Mattei, A. Sonnet / F. Herber  
O.E.C.D.-C.S.N.I. Open Containment Standard Problem No. 2  
Pressure Distribution Within the Containment Following a Pipe Break  
French Short Report  
CEA/EDF (France); October 30, 1980
- /22a/ A. Mattei, A. Sonnet / D. Roy  
Containment Standard Problem No. 2  
Pressure Distribution Within the Containment Following a Pipe Break  
French Short Report ("blind" Results)  
CEA/EDF (France)
- /23/ W. Erdmann, M. Tiltmann  
OECD-CSNI Containment Standard Problem  
Postcalculation With COFLOW and CONDRU for the RS-50-D16-CASP2  
Experiment  
GRS-A-593 (April 1981), F.R. Germany
- /24/ G. Mansfeld  
Zum instationären Druckaufbau in Volldrucksicherheitsbehältern  
wassergekühlter Kernreaktoren nach einem Kühlmittelverlustunfall  
Dissertation  
Techn. Universität München, Juli 1977
- /25/ F. Cassano, A.M. Gorlandi, M. Marchi, M. Mazzini, F. Oriolo,  
R. Romanacci  
OECD-CSNI Containment Standard Problem No. 2:  
Calculation Using ARIANNA-0 and CONTEMPT-LT 26 Computer Codes  
RP 422 (80)  
University of Pisa /CNEN (Italy)
- /26/ A.M. Gorlandi et alii  
"ARIANNA-0: Un codice di calcolo per l'analisi del transitorio  
termo-fluidodinamico in sistema di contenimento compartimentati"  
Atti Ist. Impianti Nucleari, RP 423 (80), Pisa 1980

- /27/ W.J. Mings  
"Version 26 Modifications to the CONTEMPT-LT Program"  
SRD-83-76, April 1979
- /28/ B. Chiantore, R. Monti, A. Pennese  
OECD-CSNI Containment Standard Problem No. 2  
Comparison With PACO Code Calculations  
Report L-28000 -XX-000-004, 28/10/80  
NIRA (Italy)
- /29/ OECD-CSNI Containment Standard Problem No. 1  
Comparison with PACO code calculations;  
by B. Chiantore, A. Pennese, May 10, 1979;  
presented at Garching, September 17th to 19th 1979
- /30/ I. Takashita, Y. Kukita, and K. Namatame  
JAERI Analysis on the CSNI Containment Analytical Standard  
Problem No. 2  
JAERI (Japan), October 1980
- /31/ RELAP4/MOD5: A Computer Program for Transient Thermal-  
Hydraulic Analysis of Nuclear Reactors and Related Systems"  
ANCR-NUREG-1335  
Aerojet Nuclear Company, September 1976
- /32/ J.P. A. van den Bogaard, A. Woudstra  
Calculational Results of OECD-CSNI Containment Standard  
Problem No. 2 by Means of a Modified ZOCO-V Code  
Memo No. 1.082.16 - GR 23, February 1980  
ECN (Netherlands)
- /33/ ZOCO-V - Ein Rechenmodell zur Berechnung von zeitlichen und  
örtlichen Druckverteilungen in Reaktorsicherheitsbehältern
- /34/ J.E. Marklund Calculations performed on "OECD-CSNI Containment  
Standard Problem No. 2" with COPTA SKI-B14/80 (DRAFT),  
80-11-27 Studsvik (Sweden)

- /35/ J.E. Marklund, A. Johansson Model description of containment program COPTA-6 AE-RD-105, 1979-07-12
- /36/ W.H.L. Porter OECD-CSNI Containment Standard Problem 2 - Open UK Submission Using CLAPTRAP WR/HTSG/P(80) 134, 3 June 1980 UKAEA, AEEW (United Kingdom)
- /37/ W.H.L. Porter CLAPTRAP - A Code for Calculating Pressure Transients in Total Containments Enclosing a Breached Water Reactor Circuit AEEW-R 965, 1977
- /38/ W.H.L. Porter CLAPTRAP II - A Code for Calculating Pressure Transients in the Interconnected Compartments of a Total Containment Enclosing a Breached Water Reactor Circuit AEEW-R 1108, March 1977
- /39/ E. Stubbe  
Summary Report  
Informal meeting of the international participants in the blind exercise for the 2nd Standard Problem (D16/CASP2)  
GRS (Garching), January 16th, 1981; Tractational Brussels, February 1981; SINDOC(81) 132,
- /40/ D.L. Nguyen  
Comparison Report on OECD-CSNI Containment Standard Problem No. 2: "Waterline Rupture in a Branched Compartment Chain"  
CSNI Report No. 65 (Draft), May 1981
- /41/ W. Erdmann  
Scientific Secretary's Report for the Comparison Workshop for CASP2 (25-26 May 1981)  
SINDOC(81) 134, July 1981
- /42/ OECD-NEA Paris  
Summary of Conclusions and Recommendations from the Workshop on the Comparison of Results for CSNI Containment Standard Problem No. 2 (CASP2) held at GRS, Garching, Federal Republic of Germany, 25th-26th May, 1981; SEN/SIN(81)22, drafted June 1981



---

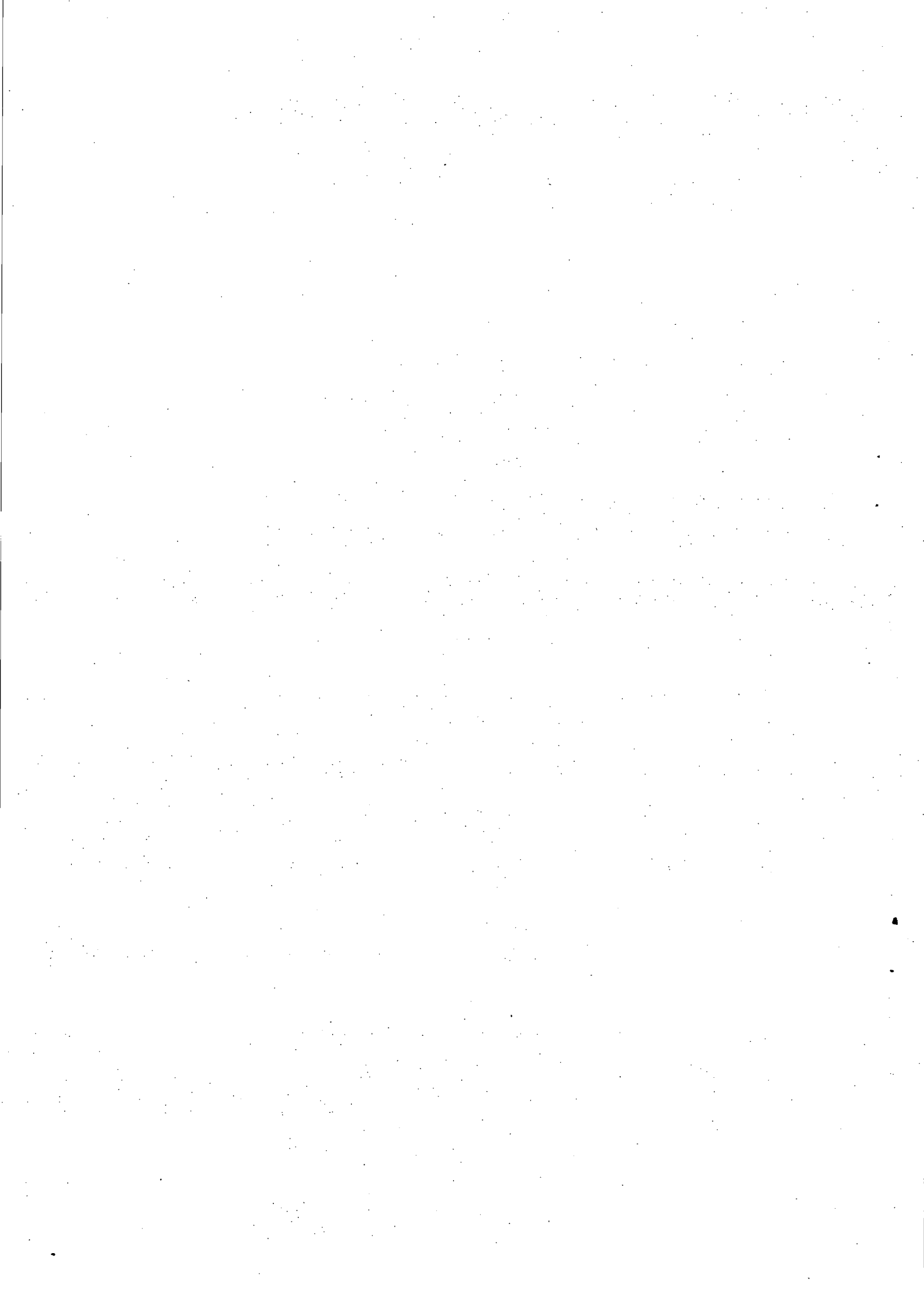
Gesellschaft für Reaktorsicherheit (GRS) mbH

CONTAINMENT STANDARD PROBLEM No. 2

Results of "Blind" Predictions  
Submitted by International Participants

November 1980

H. Karwat, TU München  
D. L. Nguyen, GRS  
W. Winkler, GRS



On occasion of the Workshop for the discussion of the results of the first CSNI-Containment Standard Problem held in September 1979 the Federal Republic of Germany offered the second Containment Standard Problem experiment to serve also as a basis for the 2nd CSNI-Containment Standard Problem. Several participants decided to submit within short deadlines "blind" predictions based on given technical boundary conditions of the experiment. Officially the 2nd CSNI-Containment Standard Problem is considered to be an "open" SP. The complete experimental data report has been distributed in April 1980. The deadline for submission of "open" predictions was set for November 1, 1980. The workshop to discuss the results of the 2nd CSNI-Containment SP is envisaged May 1981.

In order to shorten the time for participants, which submitted "blind" analytical results, an informal occasion has been established to discuss these contributions in December 1980\*. The following paper is a rough compilation of a comparison of "blind" contributions submitted before the release of the complete experimental data reports. This paper will not replace the preliminary comparison report to be produced before the CSNI-workshop planned for May 1981. It merely serves as a discussion basis for the forthcoming informal meeting.

November 1980

---

\* (shifted to January 1981)



## 1. PARTICIPATION

Table 1 lists the countries, institutions, and main contributors which submitted "blind" predictions based on the Specification-Report /1/ and some additional information distributed with a letter, dated Dec. 19, 1979 (Winkler/wvo). 6 institutions made use of 7 different computer codes to study the problem within the requested 3 characteristic time intervals. Table 2 gives more detailed information about main assumptions (nodalizations, choice of governing parameters for flow resistance, water transport, and heat transfer processes to be selected by the code user), the available computer and necessary computation time to perform calculations.

---

/1/ G. Hellings, German Standard Problem No. 3  
(2nd Containment Standard Problem):  
Water Line Rupture in a Branched Compartment Chain,  
Specification by GRS, August 1979

Country (Organization)	Contributor	Computer Code	Time Interval (s)
Belgium (Tractionel)	E.I. Stubbe	TRAP-SCØ	0 - 2.5
		TRAP-CØN	0 - 50
			0 - 1000
Finland (VTT)	H. Holmström, E. Pekkarinen	RELAP4/MOD6	0 - 2.5
		CONTEMPT-LT/026	0 - 1000
France (CEA/EDF)	A. Mattei, A. Sonnet/ D. Roy	GRUYER	0 - 2.5
			0 - 50
			0 - 1000
Netherlands (ECN)	J.P.A. van den Bogaard, A. Woudstra	ZOCO V (modif.)	0 - 2.5
			0 - 50
			0 - 1000
United Kingdom (UKAEA, AEEW)	W.H.L. Porter	CLAPTRAP II	0 - 2.5
			0 - 50
		CLAPTRAP I	0 - 1000
United States (USNRC/EG&G)	S. Fabric/ C.R. Broadus	BEACON/MOD3	0 - 2.5

Table 1 : Participants and Codes

Table 2: Important features and input parameters of codes

A = surface area  
 $C_D$  = discharge coefficient  
 $E_k$  = kinetic energy  
 H = total enthalpy  
 htc = heat transfer coefficient

$m_A$  = air mass  
 $m_V$  = vapour mass  
 n = number of orifices  
 R = compartment  
 t = time

V = volume  
 $\Delta P$  = pressure difference  
 $\zeta$  = pressure loss coefficient  
 $\epsilon_W$  = water carry-over factor, carry over coefficient (France)

$\Delta T$  = temperature difference  
 $c_w$  = water carry-over fraction  
 E = energy into containment  
 $T_0$  = initial temperature

COUNTRY	COMPUTER CODE	TIME INTERVAL (s)	NUMBER OF NODES	WATER TRANSPORT	ORIFICE FLOW		HEAT TRANSFER TO STRUCTURES		COMPUTER	COMPUTER TIME (s)	OTHER REMARKS
					concept	coefficients	correlation acc. to... [htc:W/(m <sup>2</sup> K)]	coating thickness			
BELGIUM	TRAP-SCØ	0-2.5	6	$c_{w4-7}=0.5$ $c_{w7-8}=0.9$ $c_{w8-9}=0.5$ f. rest; $c_w=0,2$	Fauske critical flow model, frictionless flow without inertial effects	$C_D=1.0$	no (specific enthalpy input reduced by 0 to 7.5%)		IBM370/3031	56	param. stud. for: water entrainm., energy reduct.
	TRAP-CØN	0-50 0-1000	1	-	-	-	t < 23.5s: Tagami, E=2xreal energy htc <sub>concrete</sub> =0.4 htc <sub>steel</sub> t > 23.5s: Uchida htc <sub>max, steel</sub> = 2400	0.2 mm		24,6	2 stratified regions of equal temperature; flashing fraction at break 90% = 10% of released fluid to sump; param. stud. for: flashing, coating 1 mm, htc = 1300
Finland	RELAP4/MOD 6	0-2.5	Ø(R5,R7:2; R4,R6,R8, R9:1)	no	compressible single stream flow with mom. flux; homogeneous equilibrium model f. predicting critical flow; $\zeta$ from Idel'chik	$\zeta_{4-7,4-5}=2.85$ $\zeta_{7-8,5-9}=2.85$ $\zeta_{8-9}=2.77$ $\zeta_{9-6}=2.81$ $\approx C_D=0.6$	40xDittus-Bölder (liqu. forc. conv.) [R4:10000,R5:3000/100, R7:3000,R8:2000,R9:90, R6:40]	0.7 mm	CDC-CYBER 170	66	$E_k \neq 0$ complete separation of phases with same temperatures
	CONTEMPT-LT/026 (mod.)	0-1000	1	9(R4,R5,R7:2 R6,R8,R9:1) rev. calc.	-	-	f.R9:Uchida - f. rest: 0-25s: 45.4→10000 lin. incr. 25-50s:10000 50-1000s:Uchida		IBM370/168	276	complete separation of phases with different temperatures

Table 2 (continued)

France	GRUYER	0-2.5	5 (R4, R5, R7, R8:1; R6+R9:1)	$\epsilon_{w4-5}=0.5$ $\epsilon_{w4-7}=0.5$ $\epsilon_{w5-9}=0.25$ $\epsilon_{w8-9}=0.25$ $\epsilon_{w7-8}=0.75$	steady state adiabatic flow; isentropic expansion, no friction and gravity; non-frozen model	$C_{D4-5}, C_{D4-7} = 1.2$ $C_{D5-9}, C_{D7-8} = 1.1$ $C_{D8-9} = 1.05$	ECOTRA	0.7 mm $\left[ \lambda=0.6 \left( \frac{t}{W} \right) \right]$ W/(mK)	IBH30-33	37	$E_k \neq 0$
		0-37	4 (R4, R5, R7:1; R6+R8+R9:1)	$\epsilon_{w4-5}=0.5$ $\epsilon_{w4-7}=0.5$ $\epsilon_{w5-9}=0.25$ $\epsilon_{w7-9}=0.75$	$C_{D4-5}, C_{D4-7} = 1.2$ $C_{D5-9} = 1.1$ $C_{D7-9} = 1.1$						
		0-1000	1	-	-	-				$t < 50s : 1300$ $t > 50s : htc = 1.5(\Delta T)^{1/3}$ and Uchida for warmer walls; $11.3 + 454 \left( \frac{m}{V} \right) f$ . colder walls	
Netherlands	7000 V (mod.)	0-2.5	11 (R4 :3; R5, R7, R8 :2; R6, R9 :1)	$\epsilon_w(R4A) = 0.01$ f. rest: $\epsilon_w = 0.5$	onedimensional steady state incompr. flow	$C_D = 1$	Henderson and Marchello	1.2 mm	CYBER-175	292	$E_k = 0$
		0-50								-	
		0-1000	1	-	-	-				2492	
United Kingdom	CLAPTRAP II	0-2.5	6	$\epsilon_w = 0.03$	homogeneous, slip, adiabatic flow	$C_D = 1$	$htc = \frac{128}{n} \sum \left[ \frac{\Delta P \cdot A}{\sqrt{2/3}} \right]^{0.4}$ but $\geq 150$ ; add. component f. R4: $htc = 5.48 \times 10^{-7} \left( \frac{1}{V} \frac{\partial H}{\partial t} \right)^{1.62}$	0.8mm	4-70	3180 (0-70s) from SP1	$E_{kin} \neq 0$
		0-50								-	
	CLAPTRAP I	0-1000	1	-	-	-				$t < 45s : htc = 8571$ $t > 45s : htc = 100$	
United States	BEACON/MOD 3	0-2.5	136 2D-cells +2 regions (R6, R9)	yes	1D-meshes, orifices (6)	formlosses, equivalent flow area	analogy between heat and mass transfer	yes	CDC-176	7200	under developmental checkout, $E_{kin} \neq 0$

$\epsilon_w = \frac{\text{transportable}}{\text{total}}$  mass of water in node

$C_w = \frac{\text{water flow quality}}{\text{homog. upstream node quality}}$

## 2. CHARACTERISTIC FEATURES OF THE EXPERIMENT

The initial conditions and the technical boundary condition "mass- and enthalpy-flow" are given in tables 3 and 4. Figs. 1 and 2 give the break-mass flow in [kg/s] with associated error bands as given by the Battelle-Institute while Figs. 3 and 4 show the corresponding information on the specific enthalpy of the discharged fluid. Specific feature is the occurrence of two subsequent peaks in the flow discharge rates observed at  $\sim 0.1$  and  $\sim 0.9$  sec.

Additionally a gap between compartments R4 and R9 has been formed which was not specified before the test. A rough sketch of the gap is given in Fig. 5. In order to preserve a common comparison basis a recommendation was given to all participants in the "blind" exercise, to disregard the formation of the gap and perform calculations according the specified flow scheme.

Furthermore some preheating occurred within the center and the dome due to a small leakage before the specified test started leading to some deviations in the initial conditions of the containment as indicated in table 5.

GRS has performed some COFLOW-calculations indicating the effects of uncertainties associated with some boundary conditions on the results of calculations. Fig. 6 shows the calculated pressure built-up for compartment R4 for nominal energy discharge rates (curve A) together with the results based on the upper bound of uncertainties in energy discharge (curve B) and the lower bound (curve C). Additionally the two pressure peaks are illustrated by arrows indicating the estimated influence of the unspecified gap on the measured pressure built-up. Had the gap not existed the first and second peak might have been raised corresponding to the magnitude of these arrows based on the measured curve with gap. Fig. 7 shows the corresponding results for a selected pressure difference (R4-R9) while Fig. 8 indicates that short term calculations for nominal conditions, for upper, and lower bound of energy discharge rates over-predict the pressure increase within the main compartment R9.

Similar studies have been made for the time interval 0-50 sec. For this period of the experiment the main uncertainties are associated with the

heat soakage by structures coated with paintings of variable properties and are additionally associated with initial conditions of the containment atmosphere. More details can be found in /2/. Fig. 9 gives a selected result of a parametric study indicating the effect of coating thickness (+ = upper bound of M = mass flow, H = enthalpy, T = initial temperature; - = lower bound of V = volume, AW = surface area).

---

/2/ W. Erdmann,

Fehlerbetrachtungen zum Standard-Problem-Versuch CASP2,  
GRS-A-617 (Juni 1981)

Table 3: Initial Conditions Prior to Blowdown

Pressure Vessel and Piping:

$p_0$	=	141.0 bar	
$T_1$	=	288.3°C (level A)	} pressure vessel (mean temperature: $T_m = 289.3°C$ )
$T_2$	=	288.5°C (level B)	
$T_3$	=	293.1°C (level C)	
$T_4$	=	295.3°C (level D)	
$T_5$	=	292.3°C (level E)	
$T_6$	=	286.1°C (level F)	
$T_8$	=	288.1°C (circulating pump)	} pipe, dia. 150 mm*)
$T_9$	=	290.8°C (rupture site)	
$T_{10}$	=	286.6°C (near gate valve)	
$m_{BO}$	=	3995 kg (pressure vessel)	} initial fluid mass
$m_{RO}$	=	315 kg (pipe)	

Containment:

$P_{CO}$	=	1.0 bar	
$T_{R4}$	=	23.5°C	} mean values of compartments R4 to R9, volumetric average for whole containment: $T_{CO} = 27.6°C$
$T_{R5}$	=	23.0°C	
$T_{R6}$	=	26.0°C	
$T_{R7}$	=	24.0°C	
$T_{R8}$	=	24.5°C	
$T_{R9}$	=	30.5°C (centre and dome)	
$T_{R9a}$	=	25.0°C (annulus)	
$f_r$	=	100 % (relative atmospheric humidity)	

\*) These values were obtained with two gauges of the plant instrumentation located at the two pipe ends. Values measured with the standard experimental instrumentation, however, indicate an inhomogeneous temperature distribution in the pipe within the temperature range from 255 to 290°C.

Table 4 : Break mass flow and specific enthalpy

D16/CASP2

Time (s)	Mass flow (kg/s)	Temperature (°C)	Density (kg/m <sup>3</sup> )	Spec. enthalpy (kJ/kg)
0	0	260	795	1134
0.004	52	260	784	1135
0.005	145	260	784	1135
0.028	200	260	784	1135
0.056	200	260	784	1135
0.067	340	260	784	1135
0.086	335	260	784	1135
0.105	405	260	784	1135
0.200	368	260	784	1135
0.350	270	283	715	1255
0.400	210	282	640	1260
0.500	205	281	600	1260
0.750	300	272	764	1195
0.850	324	272	764	1195
0.920	374	273	763	1201
1.20	230	281	580	1263
2.00	200	280	530	1267
2.50	180	279	500	1267
4.00	165	275	430	1261
10.00	145	268.5	310	1266
16.33	130	261	300	1225
23.50	115	252.5	255	1195
24.30	78	250	125	1323
30.00	25	207	20	1737
40.00	3	156	3	2752
50.00	0	152	2.7	2748

integral mass outflow : 4075 kg  $\pm$  55 kg



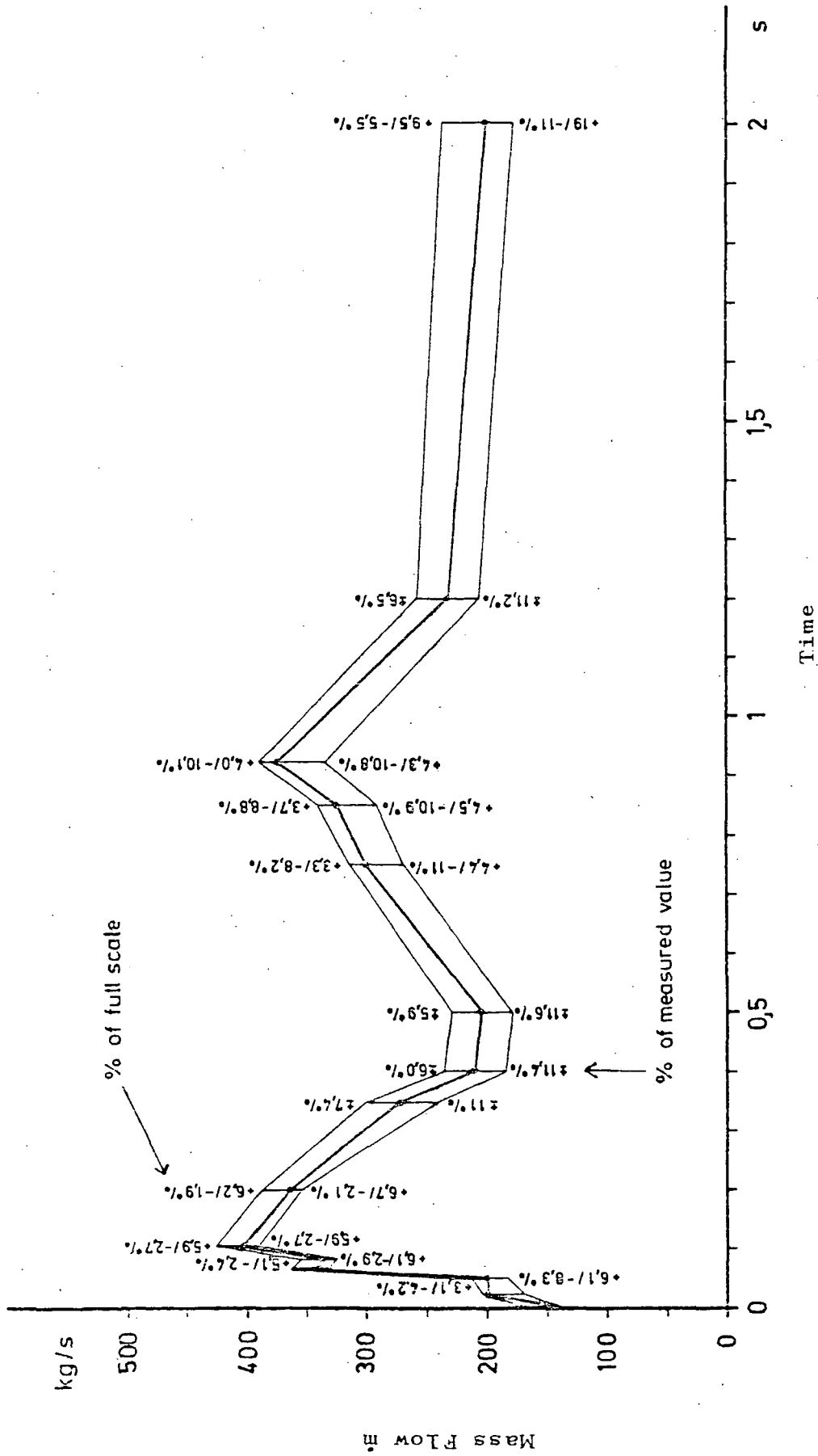


Fig. 1: Break mass flow  $\dot{m}$  with error band (experiment D16/CASP2)

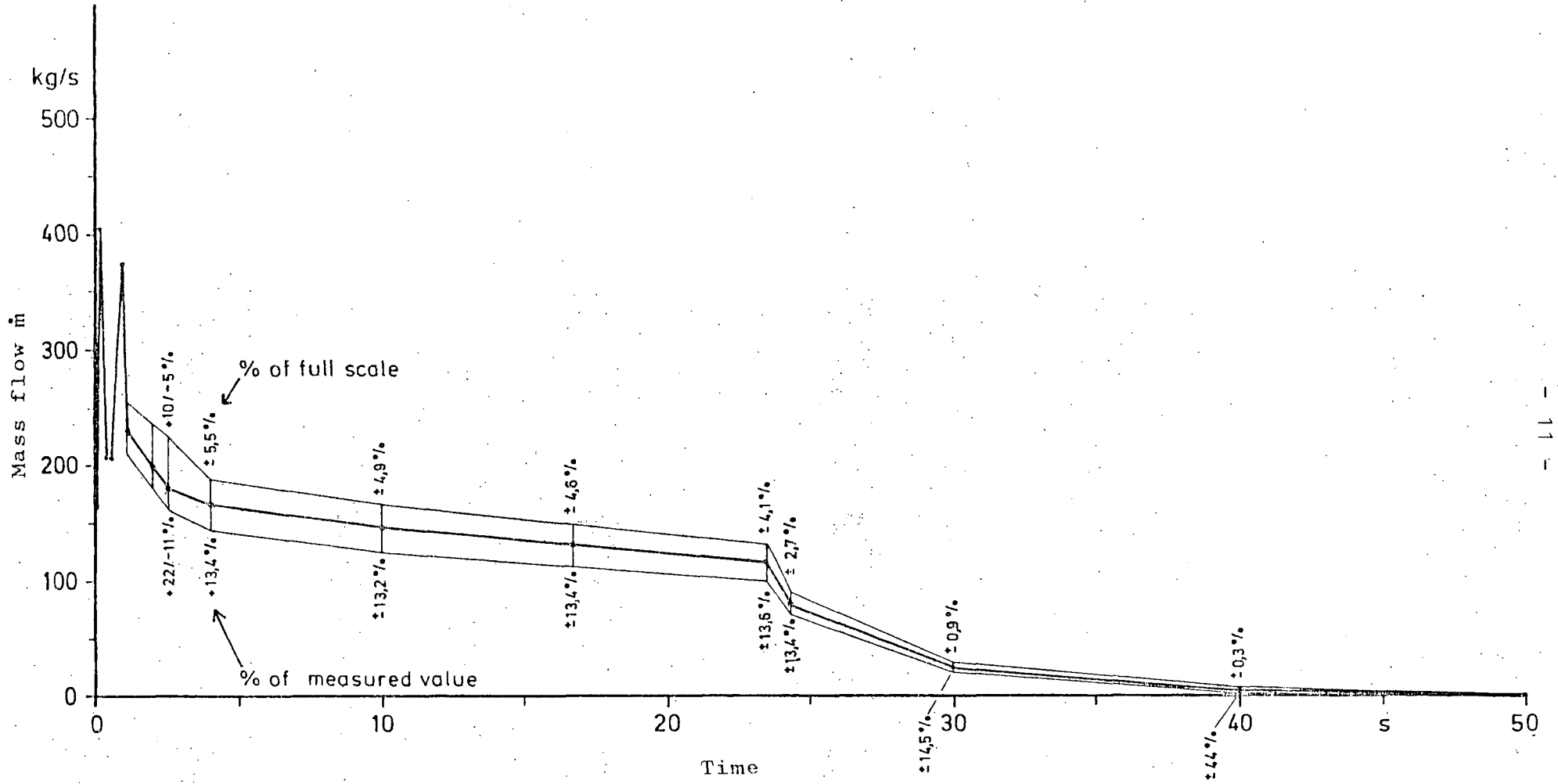


Fig. 2: Break mass flow  $\dot{m}$  with error band (experiment D16/CASP2)

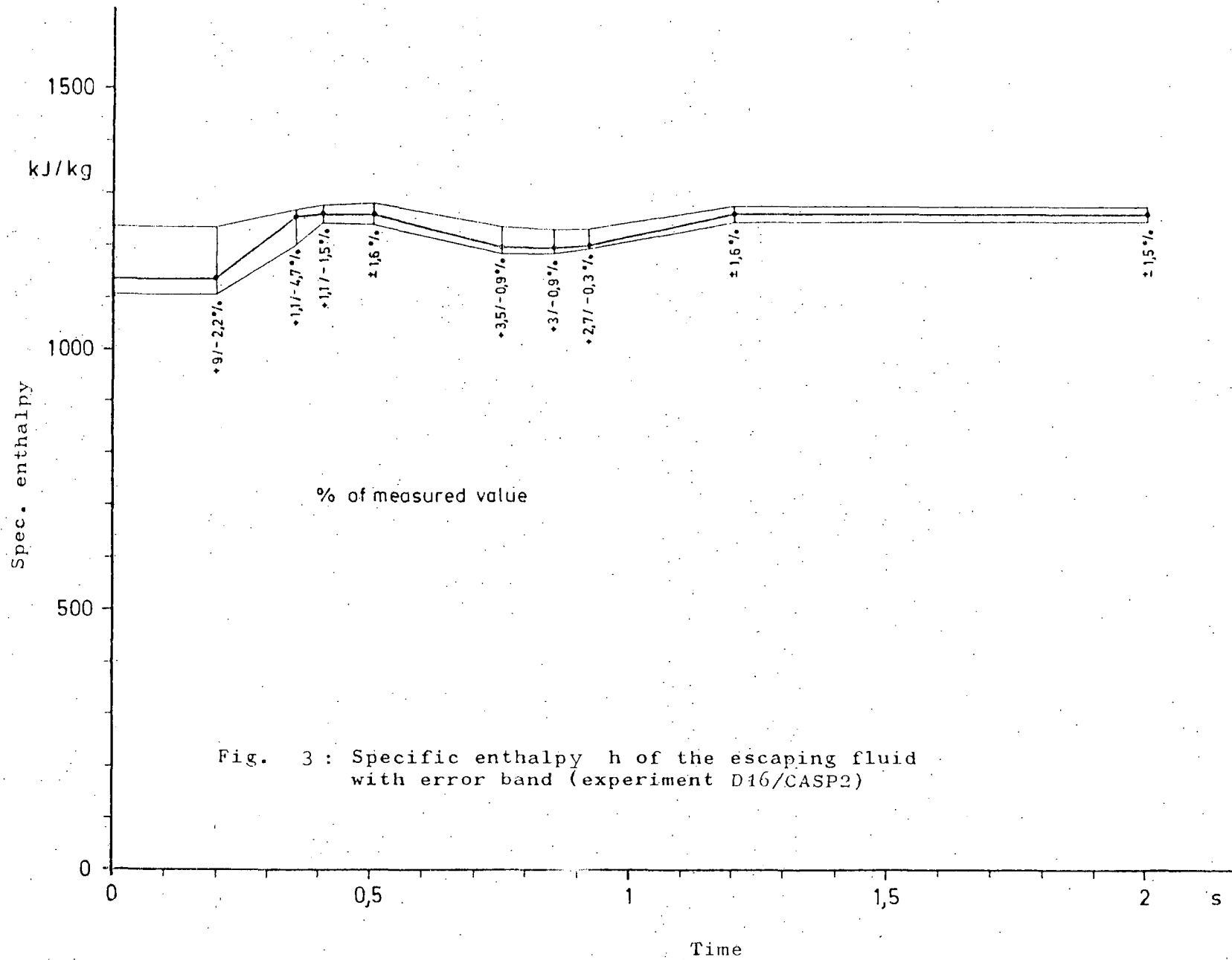


Fig. 3 : Specific enthalpy  $h$  of the escaping fluid with error band (experiment D16/CASP2)

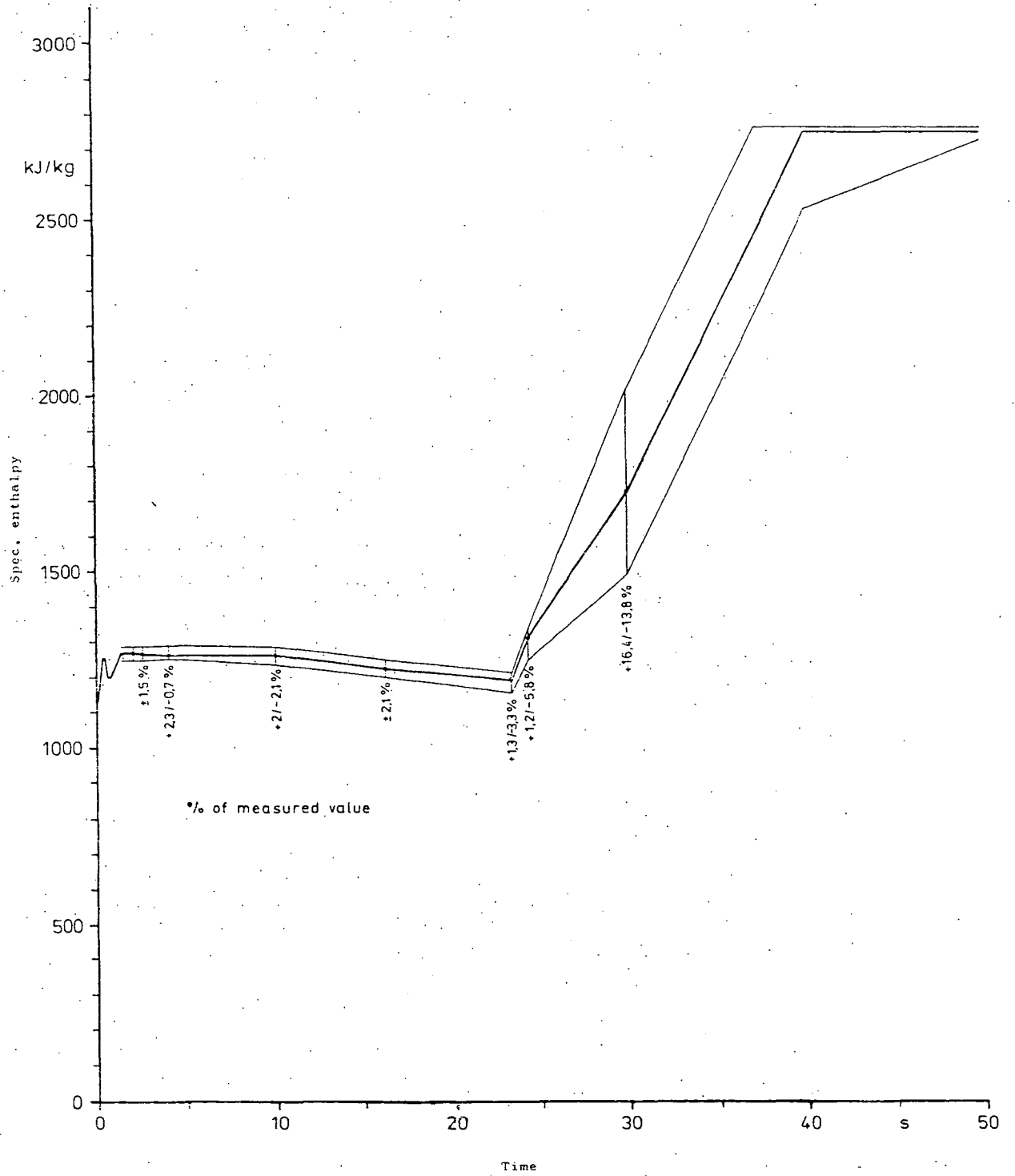
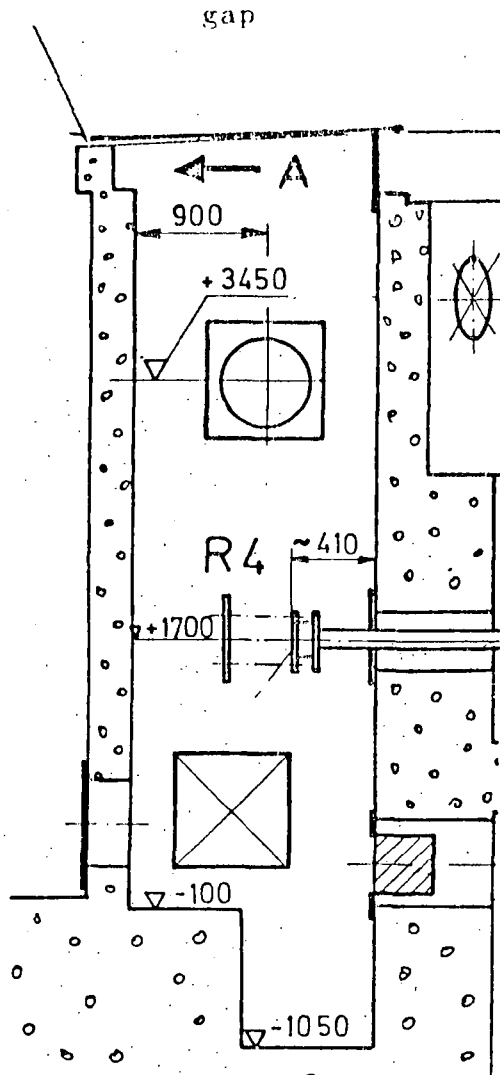


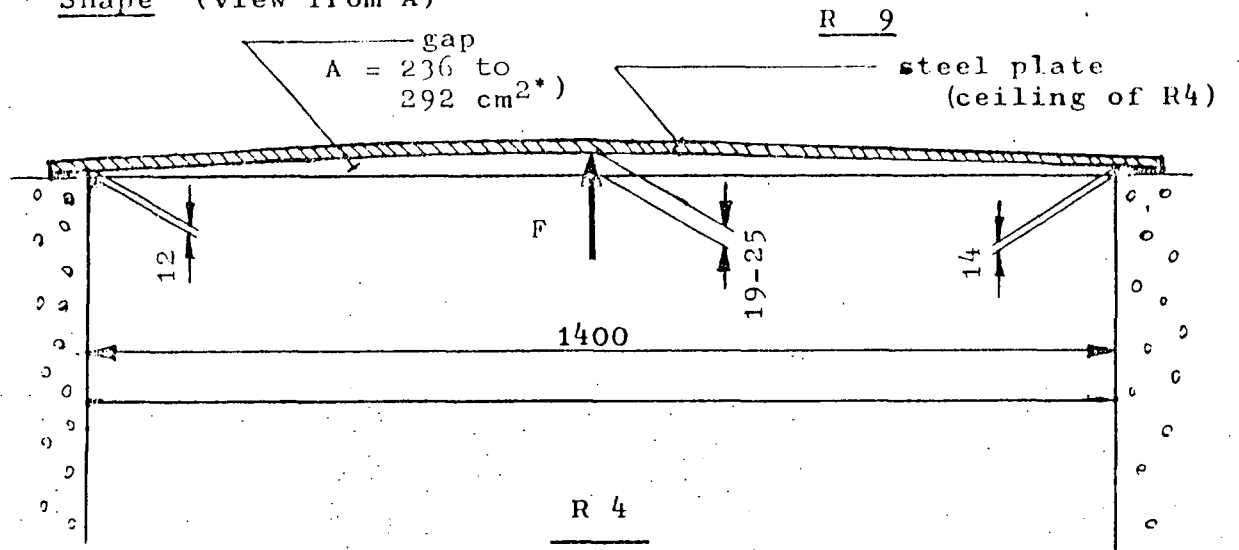
Fig. 4: Specific enthalpy  $h$  of the escaping fluid with error band (experiment D16/CASP2)

Position



scale 1 : 50

Shape (view from A)



scale 1 : 10

- \*) 19 mm (236 cm<sup>2</sup>) without load acting on ceiling of R4
- 25 mm (292 cm<sup>2</sup>) maximum gap (load 30 ≥ kN)

Fig. 5 : Gap between compartments R4 and R9 after partial failure of a sealing (measures in mm)

Table 5: Initial temperatures in containment

Noninsulation of and some leakage from the high pressure pipe within the containment caused some preheating of the containment. The lowest/highest measured temperatures within the compartments were:

$$T_{R4} = 18,6/26,2^{\circ}\text{C}$$

$$T_{R5} = 21,6/27,8^{\circ}\text{C}$$

$$T_{R7} = 21,6/24,2^{\circ}\text{C}$$

$$T_{R8} = 22,0^{\circ}\text{C}$$

$$T_{R9} = 25,2/32,9^{\circ}\text{C}$$

$$T_{R9a} = 18,2/29,7^{\circ}\text{C}$$

$$T_{R6} = 26,6^{\circ}\text{C}$$

## 2<sup>ND</sup> CONTAINMENT STANDARD PROBLEM (CASP 2)

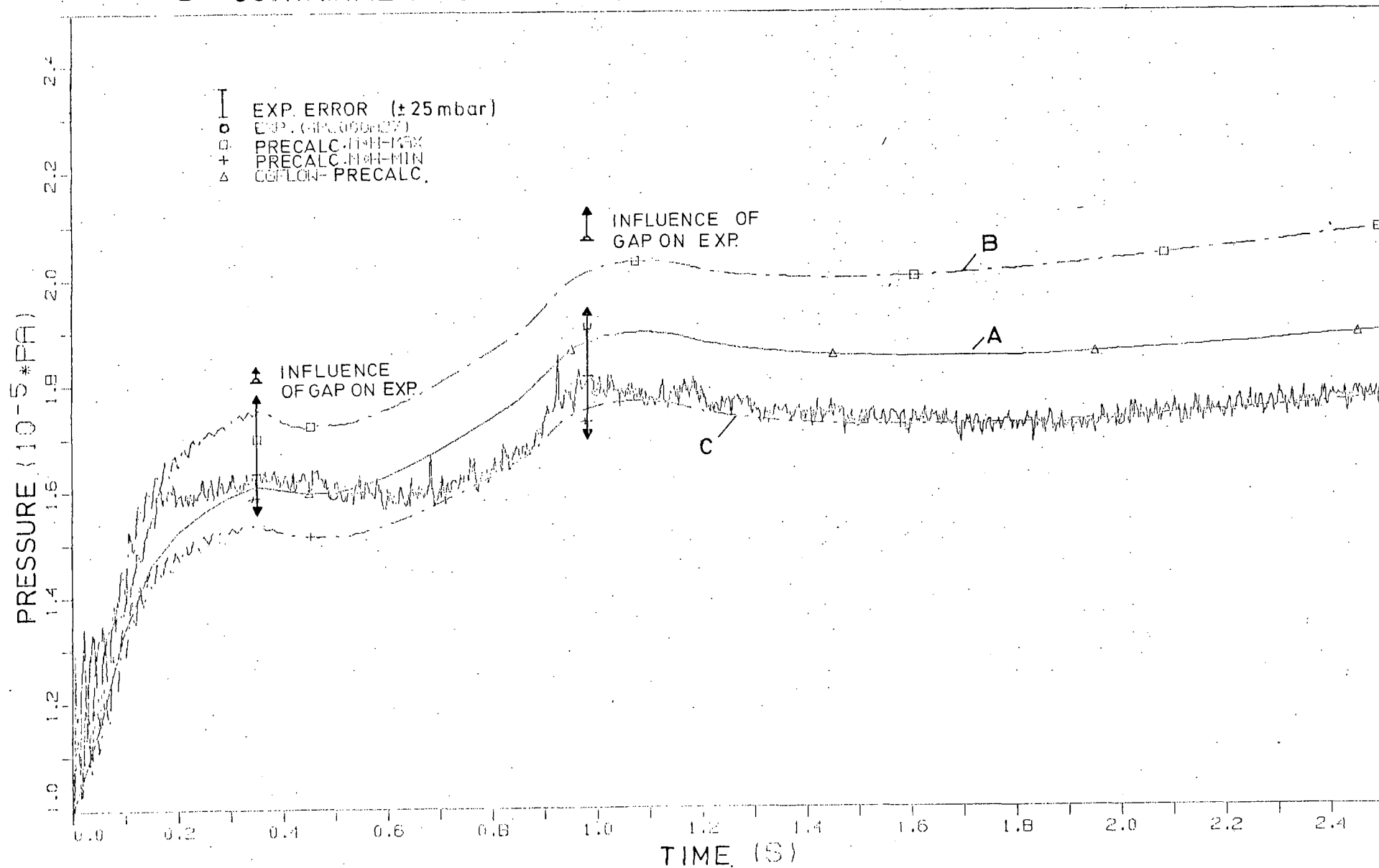


FIG. 6 : PRESSURE HISTORY IN COMPARTMENT R 4

## 2<sup>ND</sup> CONTAINMENT STANDARD PROBLEM (CASP 2)

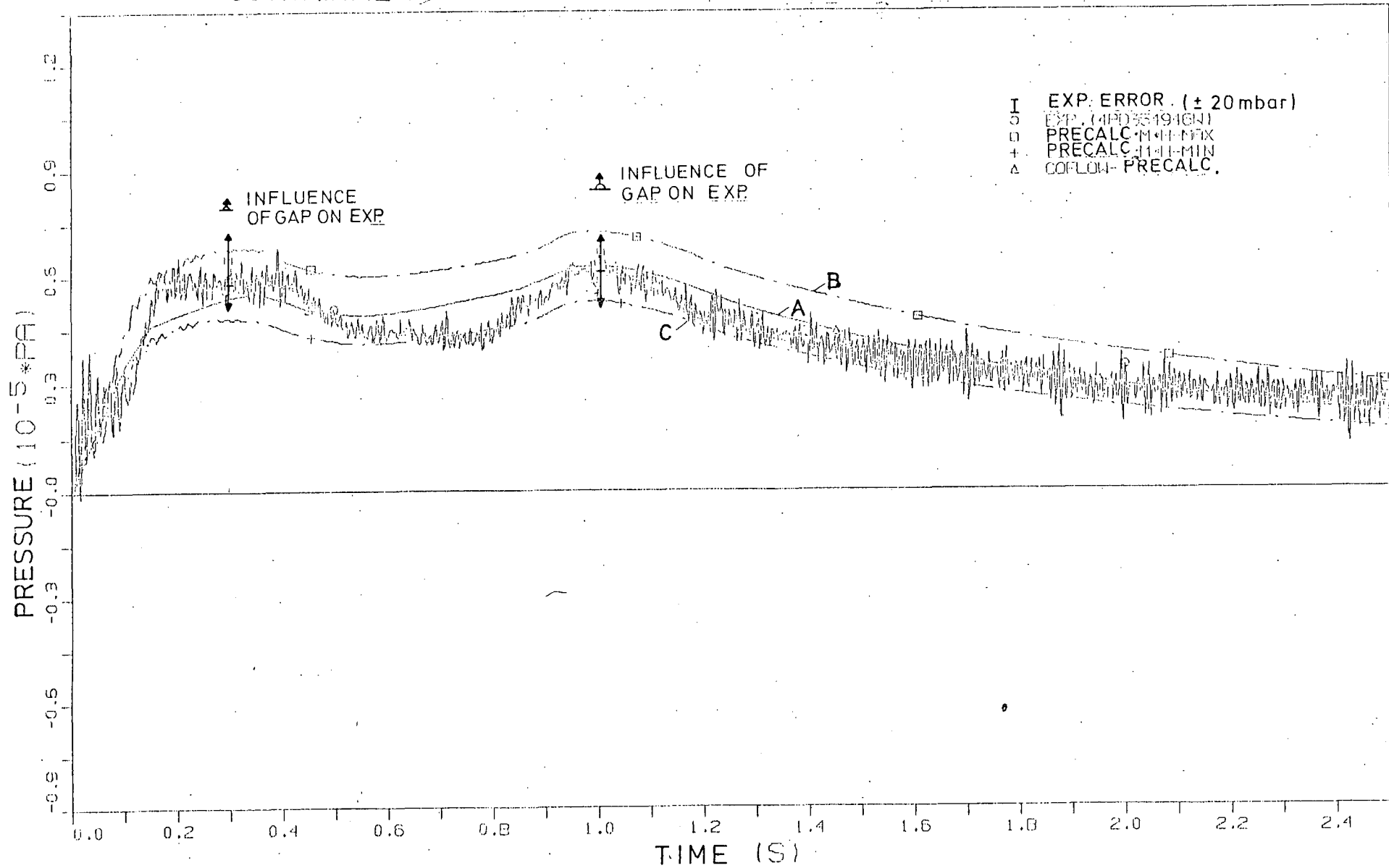


FIG. 7: HISTORY OF PRESSURE DIFFERENCE R4 - R9



# 2<sup>ND</sup> CONTAINMENT STANDARD PROBLEM (CASP 2)

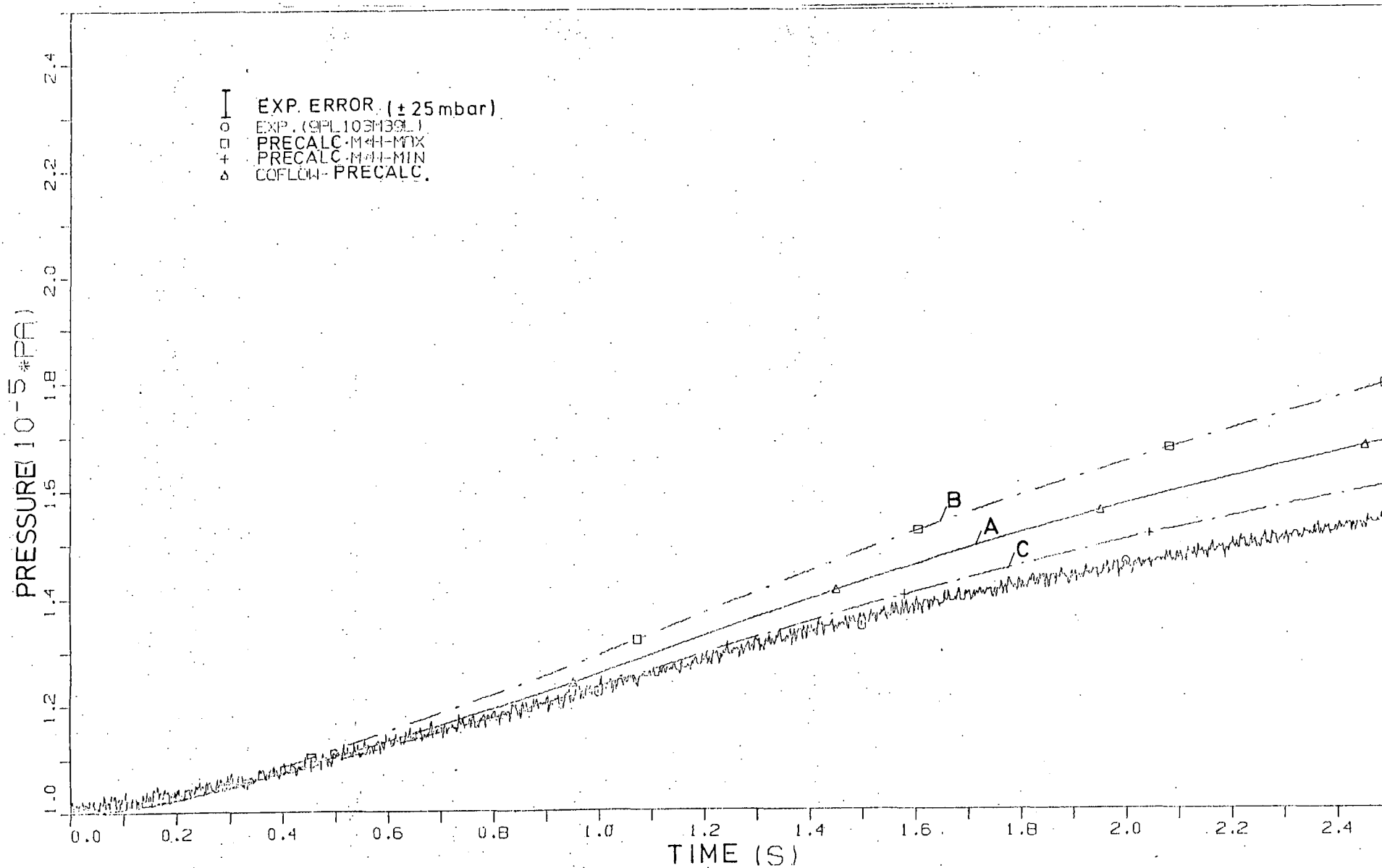


FIG. 8 : PRESSURE HISTORY IN COMPARTMENT R-9

# 2<sup>ND</sup> CONTAINMENT STANDARD PROBLEM (CASP 2)

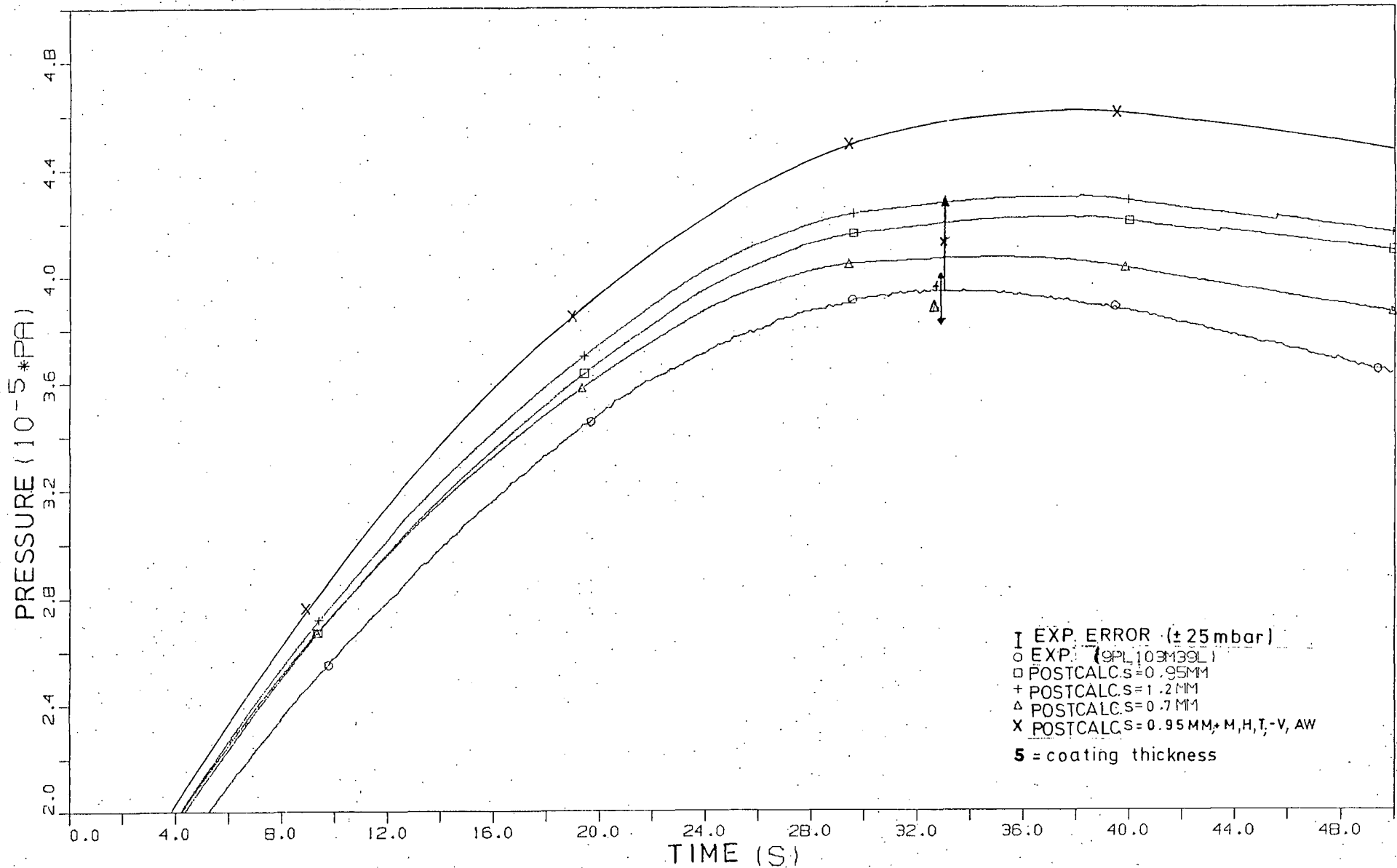


FIG. 9: PRESSURE HISTORY IN COMPARTMENT R 9

### 3. RESULTS OF THE PARTICIPANTS

Table 6 summarizes the main results of some important characteristic parameters obtained for the time intervals 0-2.5 s and 0-50 s. Calculated pressure built-up in compartment R4 (where the energy discharge occurred), for the main compartment R9, and pressure differences R4-R9 and R4-R5 in the vicinity of the energy discharge are listed with respect to its absolute maximum. Additionally the time of maximum is compared with the corresponding experimental observation. The error-band of the measurements and the possible effect of the unspecified gap are given as well.

More details can be found in the following figures. Figs. 10-15 represent plots of all results obtained for pressure built-up versus time within the specified 6 compartments R4, R5, R6, R7, R8 and R9. Figs. 10 and 11 indicate in magnitudes the possible effect of the gap on the measured pressure-maxima if the gap had not existed. The magnitude of the estimated general error bands of the pressure measurements  $\pm 25$  mbar is indicated as magnitude on each plot.

Country	Computer Code	Time Interval 0 - 2.5 s												Time Interval 0 - 50 s		
		P <sub>R4</sub>				P <sub>R9</sub>	ΔP <sub>R4-R9</sub>				ΔP <sub>R4-R5</sub>				P <sub>max</sub>	
		1st Max.		2nd Max.		t=2.5s	1st. Max.		2nd Max.		1st Max.		2nd Max.		P(bar) t(s)	t(s)
		P(bar)t(s)	P(bar)t(s)	P(bar)	P(bar)t(s)	P(bar)t(s)	P(bar)t(s)	P(bar)t(s)	P(bar)t(s)							
Belgium	TRAP-SCØ	1.54	0.35	1.76	1.05	1.68	0.46	0.35	0.48	0.95	0.18	0.15	0.16	0.95	-	-
	TRAP-CØN	-	-	-	-	-	-	-	-	-	-	-	-	-	3.77	33.5
Finland	RELAP4/MOD6	1.50	0.47	1.74	1.15	1.62	0.42	0.35	0.47	1.05	0.14	0.10	0.02	0.95	-	-
	CONTEMPT-LT/026	-	-	-	-	-	-	-	-	-	-	-	-	-	4.53	40.0
Finland *	RELAP4/MOD6	1.60	0.35	1.88	1.10	1.61	0.54	0.35	0.63	1.00	0.25	0.15	0.20	0.95	-	-
France	GRUYER	1.53	0.35	1.76	1.05	1.63	0.45	0.35	0.49	1.00	0.16	0.15	0.20	0.95	3.81	33.5
Netherlands	ZOCO V (modif.)	1.52	0.35	1.74	1.10	1.63	0.41	0.35	0.40	1.00	0.14	0.10	0.14	0.95	4.14	36.0
United Kingdom	CLAPTRAP II	1.62	0.35	2.02	1.10	1.53	0.57	0.35	0.80	1.00	0.29	0.15	0.19	0.95	4.20	37.5
United States	BEACON/MOD3	1.76	0.35	2.01	1.00	2.02	0.62	0.30	0.59	0.95	0.35	0.15	0.37	0.95	-	-
Experiment D16/CASP2		1.63	0.35	1.81	0.97	1.55	0.59	0.3	0.62	1.0	0.33	0.17	0.23	1.02	3.95	33.0
± Error		±0.025		±0.025		±0.025	±0.02		±0.02		±0.018		±0.018		±0.025	
+ Influence of Gap		+0.03		+0.061		-0.01	+0.02		+0.036		+0.0		+0.007		-	

Table 6: Important characteristic variables

\* calculation revised March 20, 1980

## 2<sup>ND</sup> CONTAINMENT STANDARD PROBLEM (CASP2)

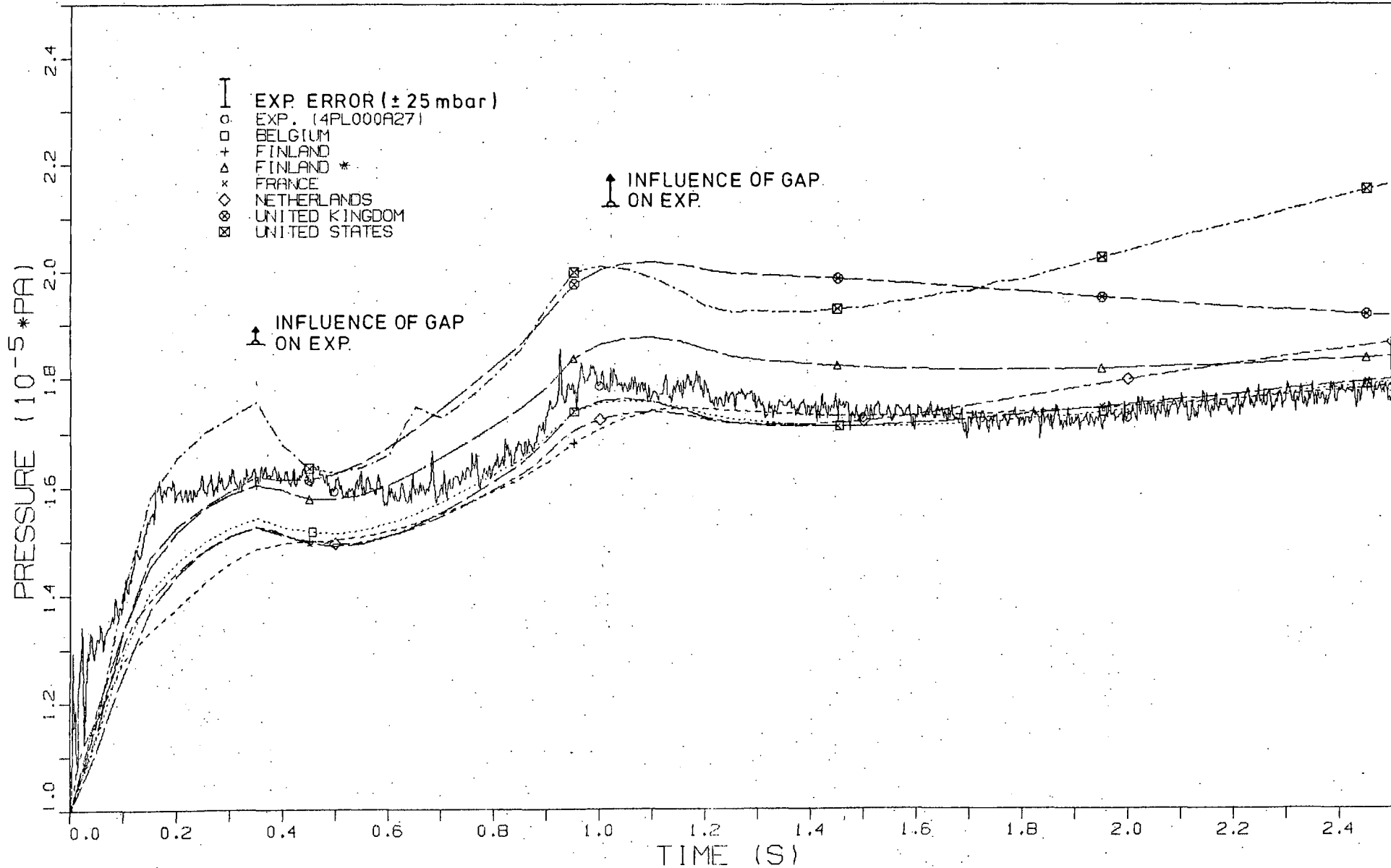


FIG. 10 PRESSURE HISTORY IN COMPARTMENT R4

## 2<sup>ND</sup> CONTAINMENT STANDARD PROBLEM (CASP2)

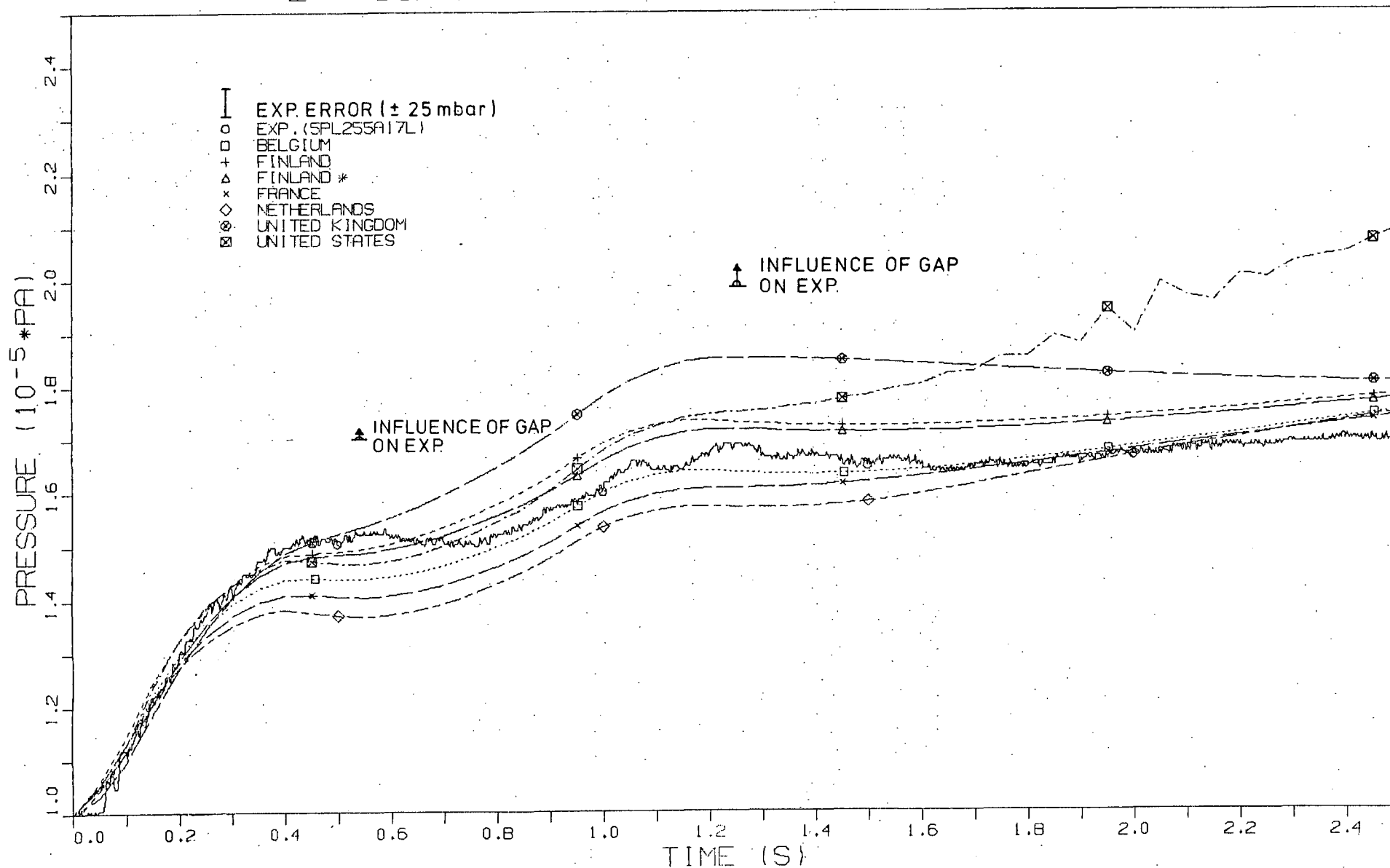


FIG. 11 PRESSURE HISTORY IN COMPARTMENT R5

# 2ND CONTAINMENT STANDARD PROBLEM (CASP2)

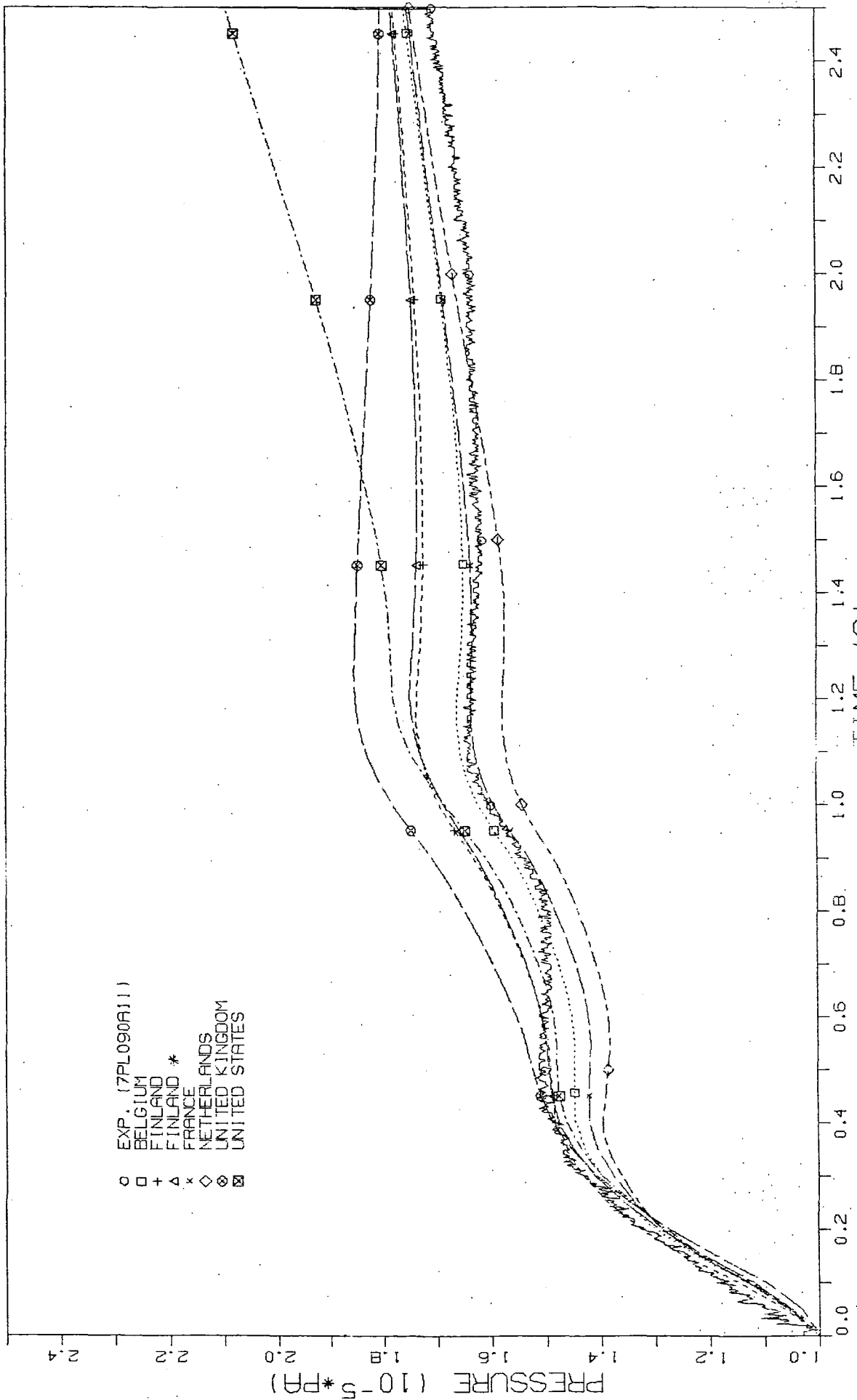


FIG. 12 PRESSURE HISTORY IN COMPARTMENT R7

# 2ND CONTAINMENT STANDARD PROBLEM (CASP2)

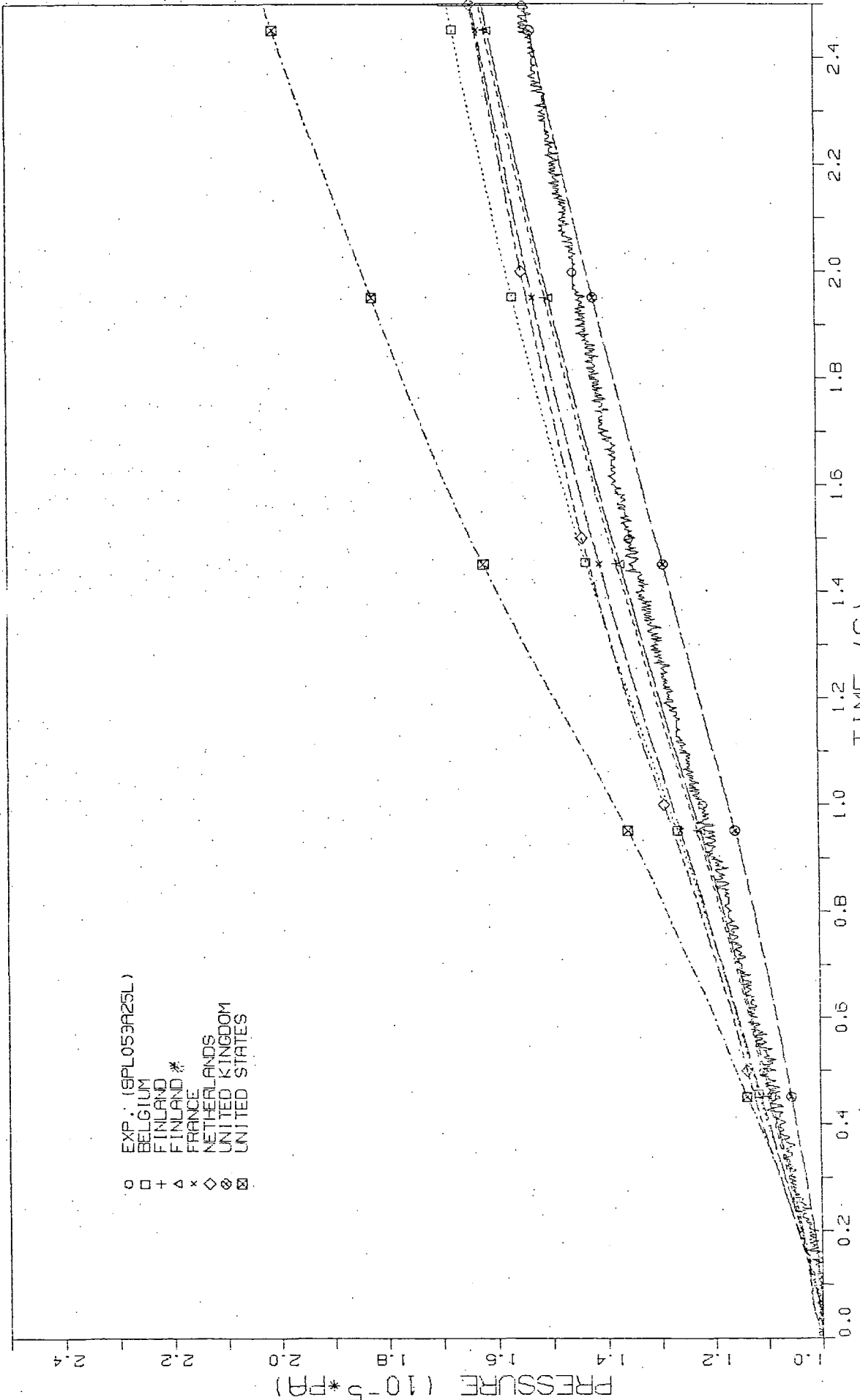


FIG. 13 PRESSURE HISTORY IN COMPARTMENT RB



# 2ND CONTAINMENT STANDARD PROBLEM (CASP2)

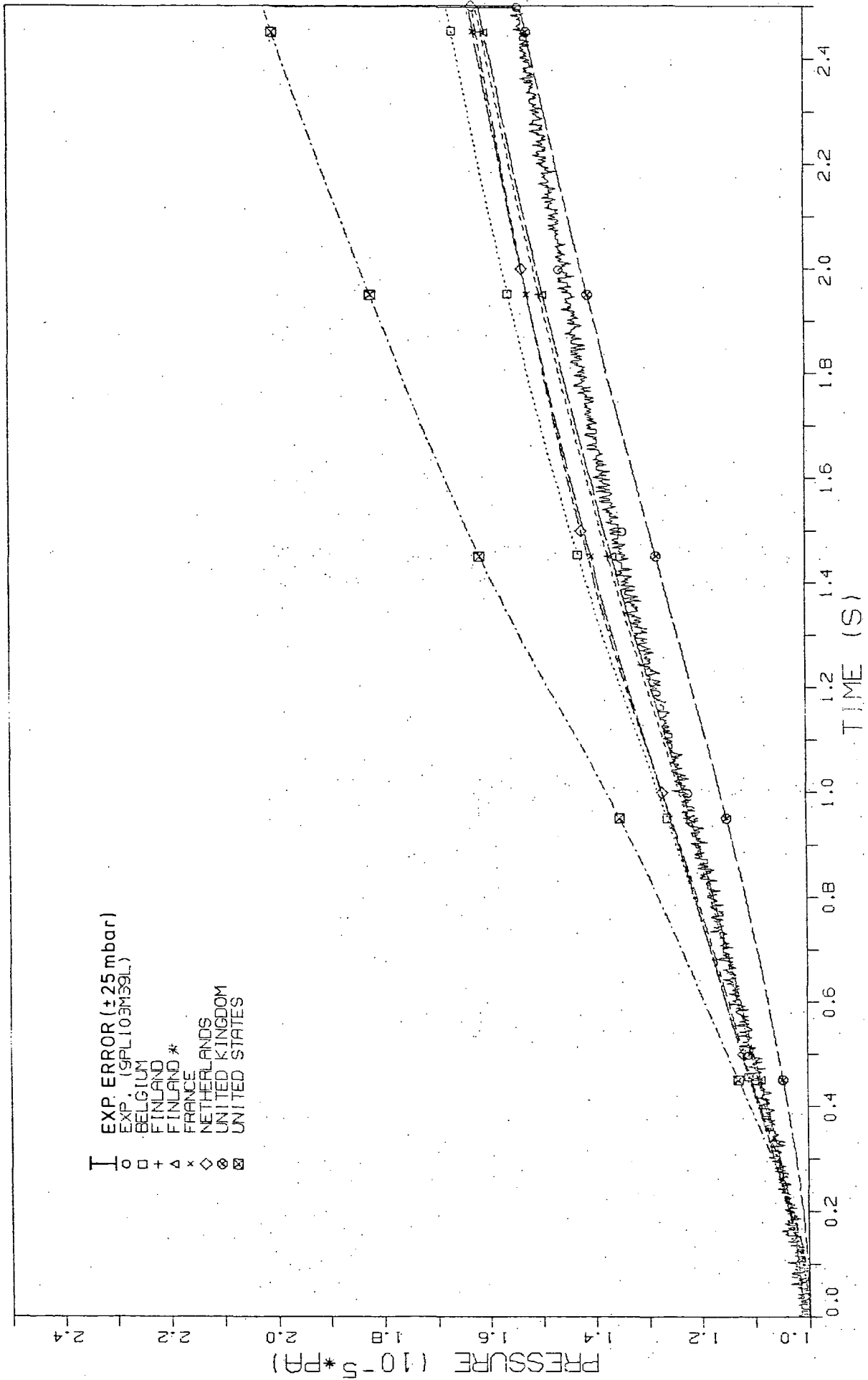


FIG. 14 PRESSURE HISTORY IN COMPARTMENT R9

# 2ND CONTAINMENT STANDARD PROBLEM (CAS2)

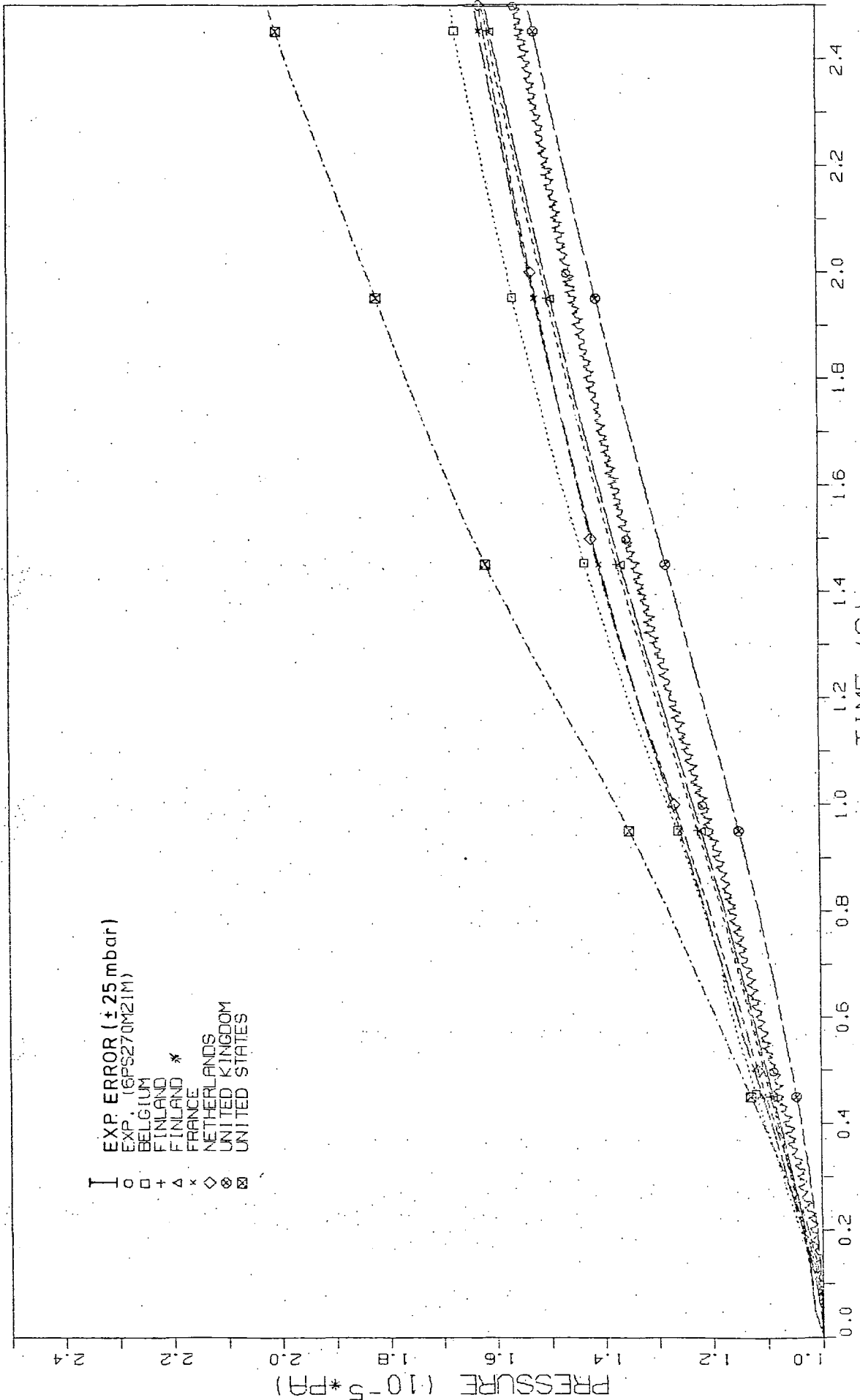


FIG. 15 PRESSURE HISTORY IN COMPARTMENT R6

Figs.16-22 give a comparison of measured pressure-differences between associated compartments and corresponding calculated results of the participants. The magnitude of the possible gap influence on the maximum values of measured pressure differences (if the gap had not occurred) is indicated in Figs. 16, 17, 18 and 19. Possible error bands of pressure differences measurements are given by the Battelle-Institute to be of a magnitude of  $\pm 18$  mbar as given on the plots.

# 2<sup>ND</sup> CONTAINMENT STANDARD PROBLEM (CASP2)

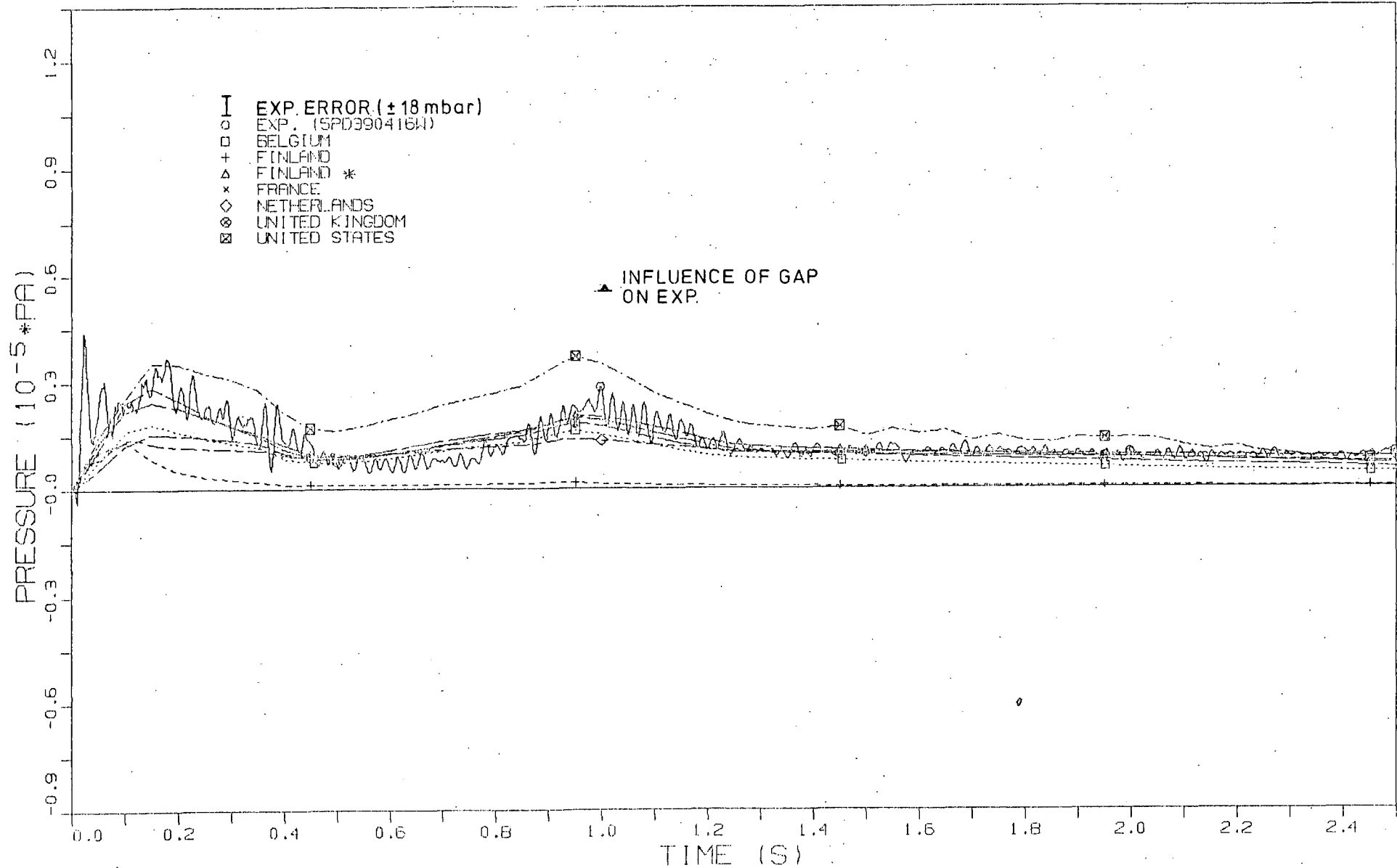


FIG 16

HISTORY OF PRESSURE DIFFERENCE R4-R5

## 2<sup>ND</sup> CONTAINMENT STANDARD PROBLEM (CASP2)

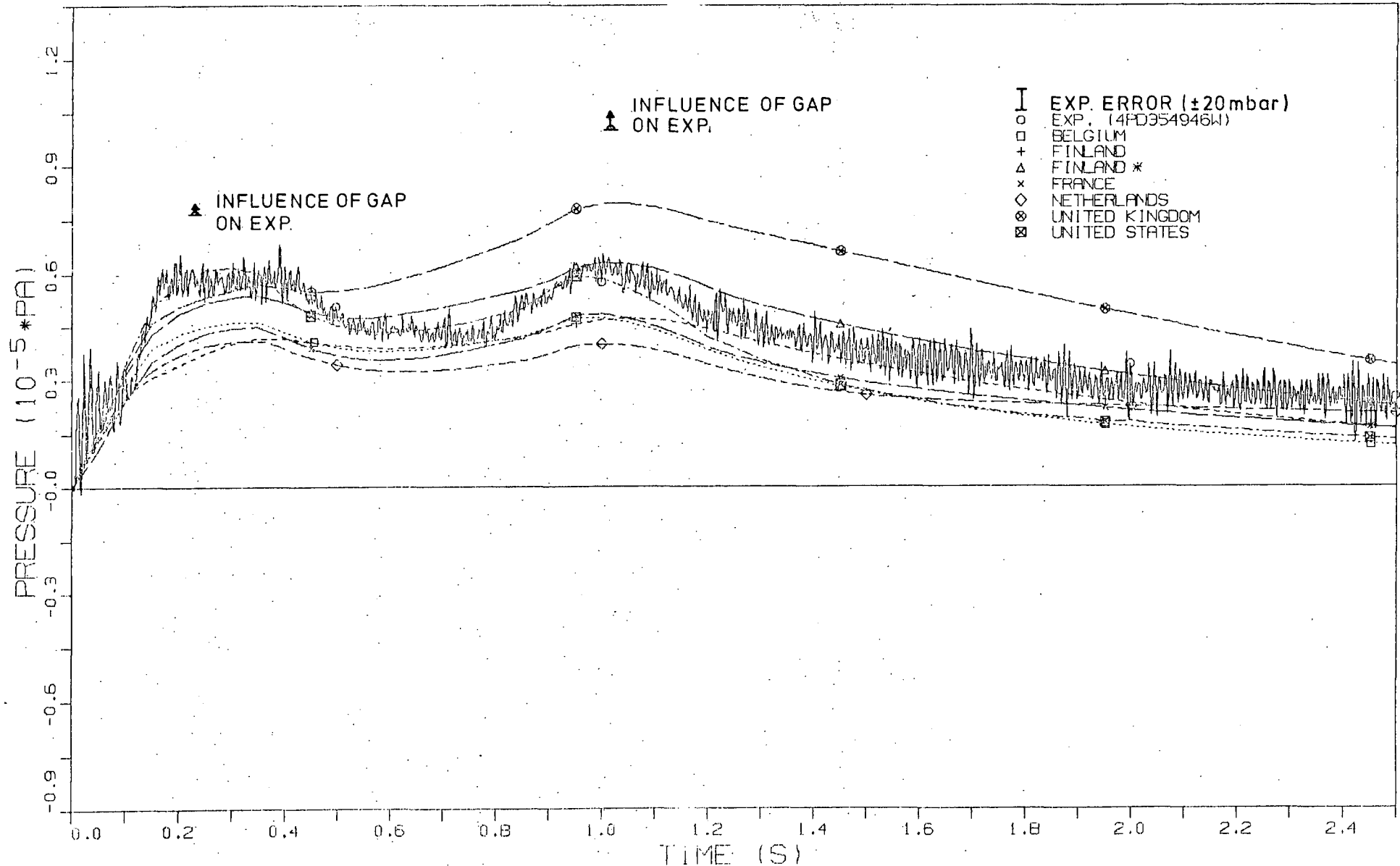


FIG. 17 HISTORY OF PRESSURE DIFFERENCE R4-R9

# 2ND CONTAINMENT STANDARD PROBLEM (CASP2)

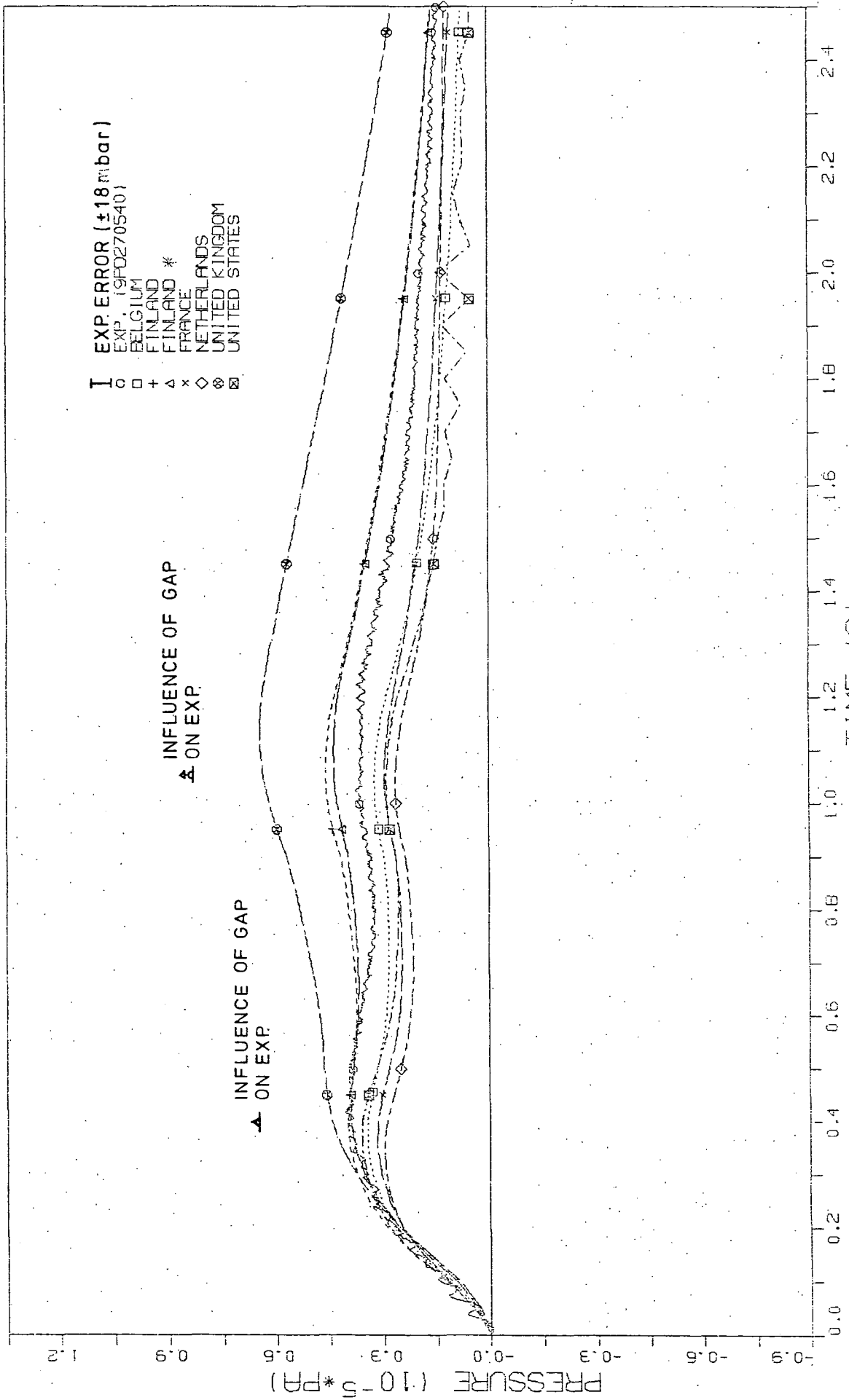


FIG 18 HISTORY OF PRESSURE DIFFERENCE R5-R9

# 2<sup>ND</sup> CONTAINMENT STANDARD PROBLEM (CASP2)

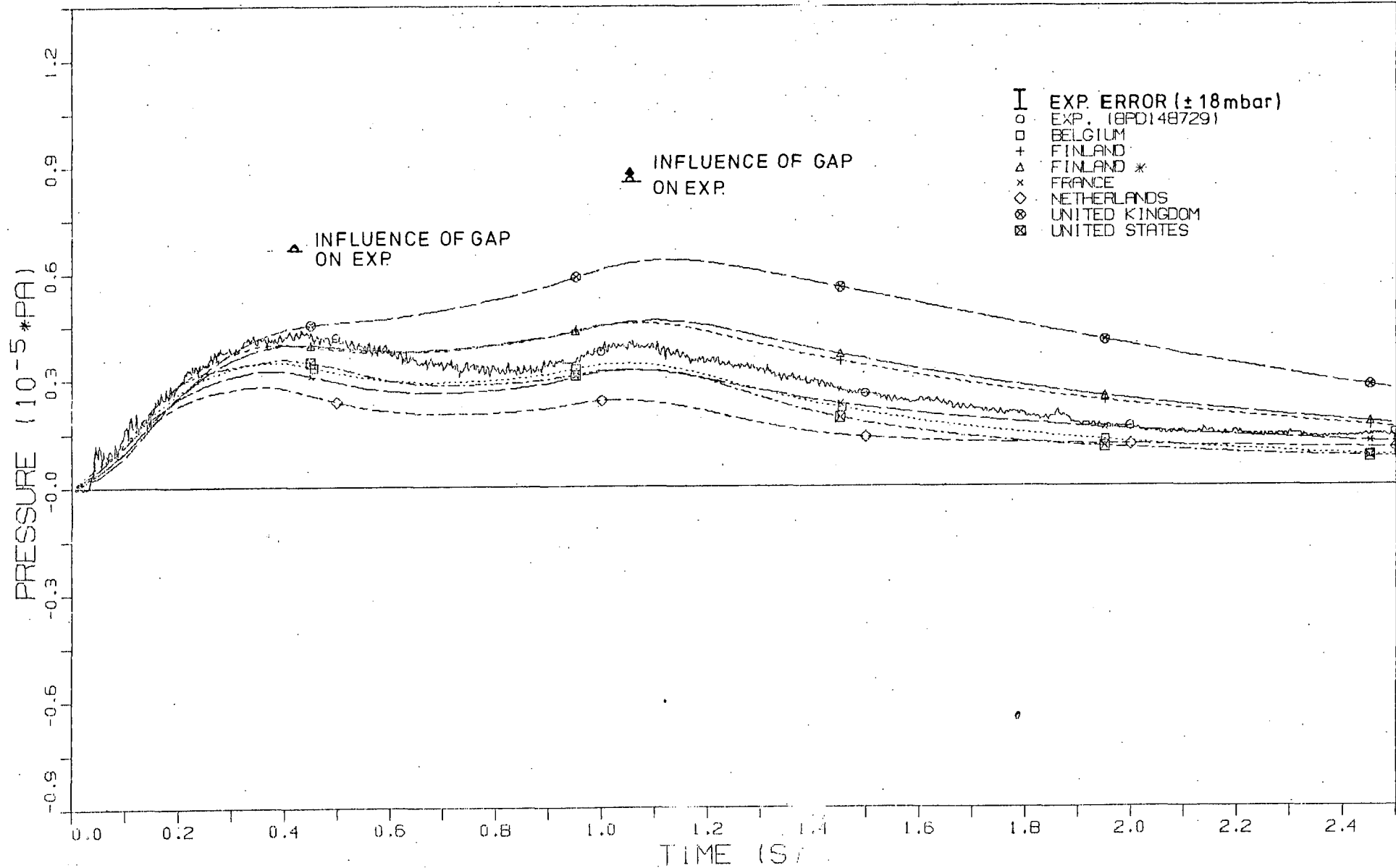


FIG.19

HISTORY OF PRESSURE DIFFERENCE R7-R8

# 2ND CONTAINMENT STANDARD PROBLEM (CASP2)

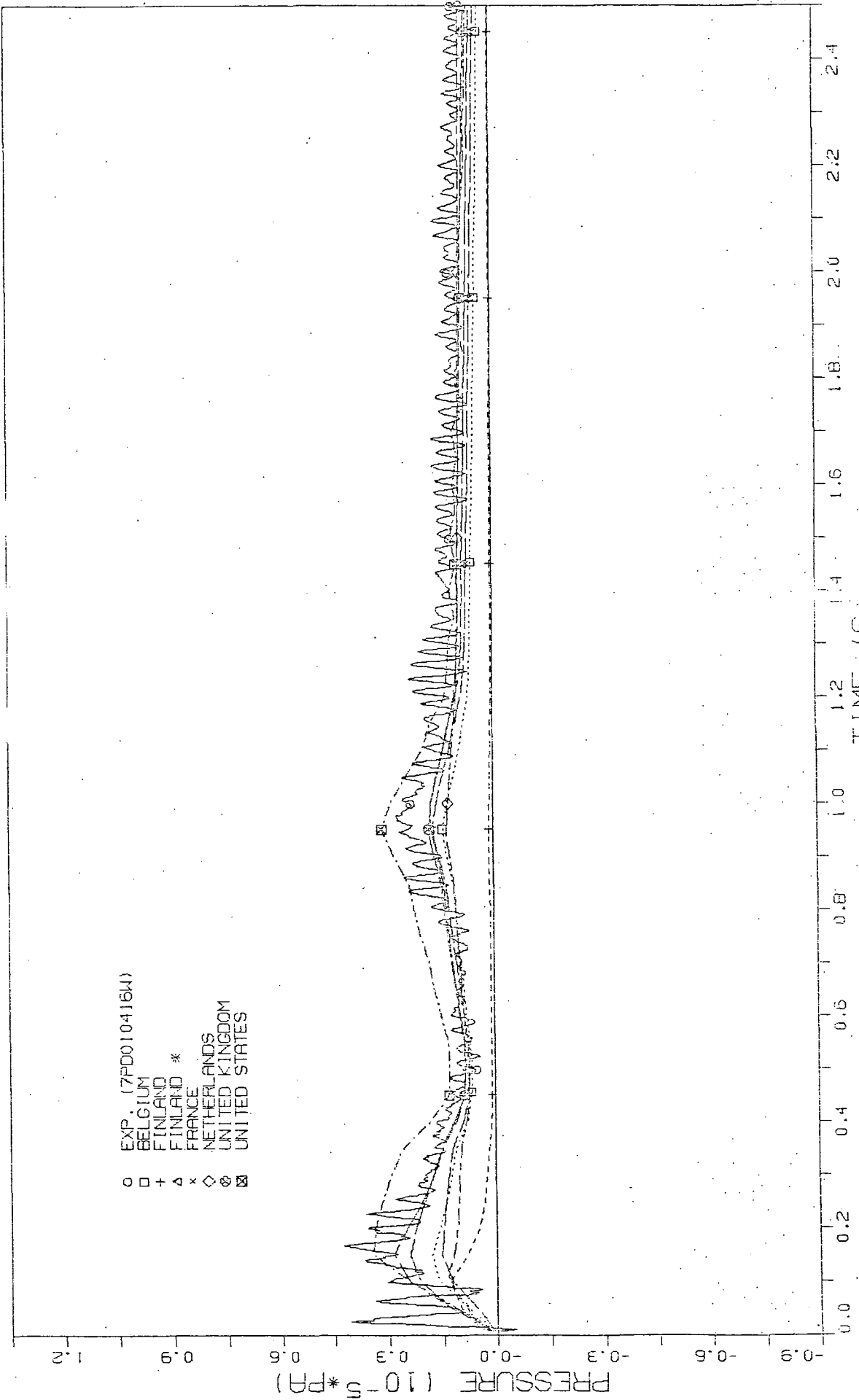


FIG 20 HISTORY OF PRESSURE DIFFERENCE R4-R7



# 2<sup>ND</sup> CONTAINMENT STANDARD PROBLEM (CASP2)

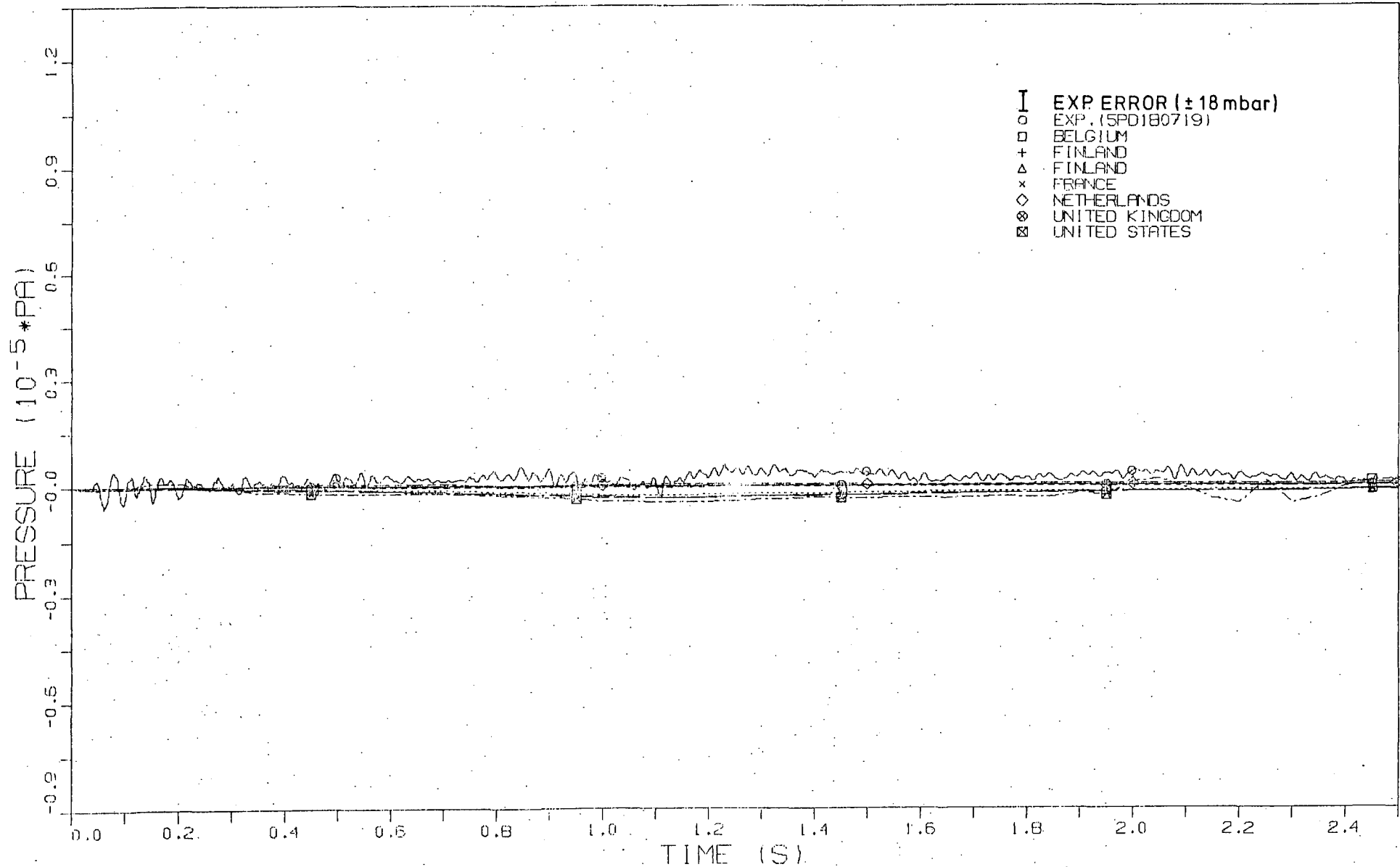


FIG. 21 HISTORY OF PRESSURE DIFFERENCE R5-R7

2ND CONTAINMENT STANDARD PROBLEM (CASP2)

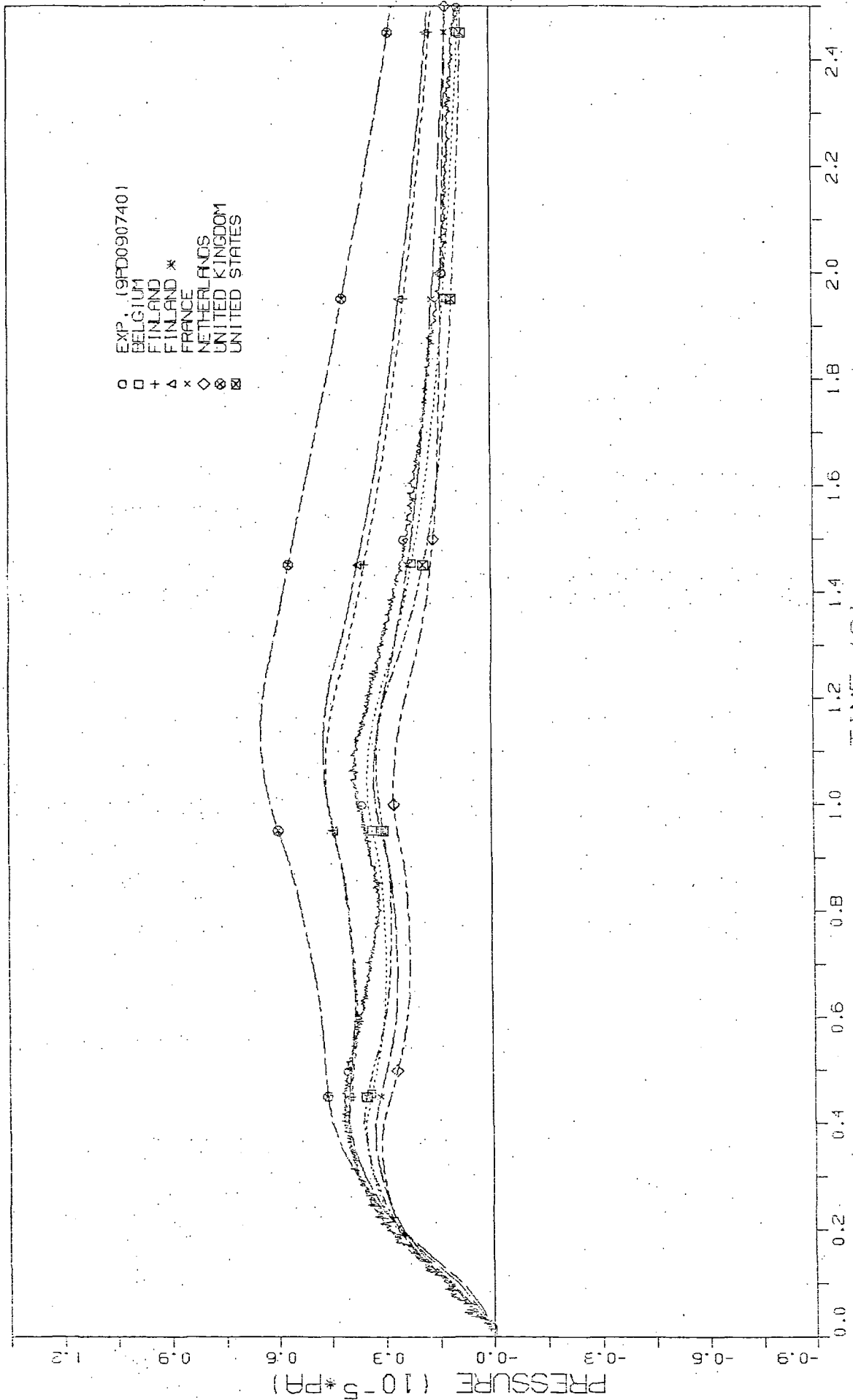


FIG. 22 HISTORY OF PRESSURE DIFFERENCE R7-R9

Figs. 23-36 give a variety of comparisons of measured temperature-time-histories with corresponding calculated curves for the time interval 0-2.5 s for all 6 compartments. As temperature distribution within compartments is quite heterogeneous compared to measured pressure distributions within each compartment care must be given when measured and calculated temperatures are compared. The results of calculations strongly depend on the applied nodalisation scheme.

## 2<sup>ND</sup> CONTAINMENT STANDARD PROBLEM (CASP2)

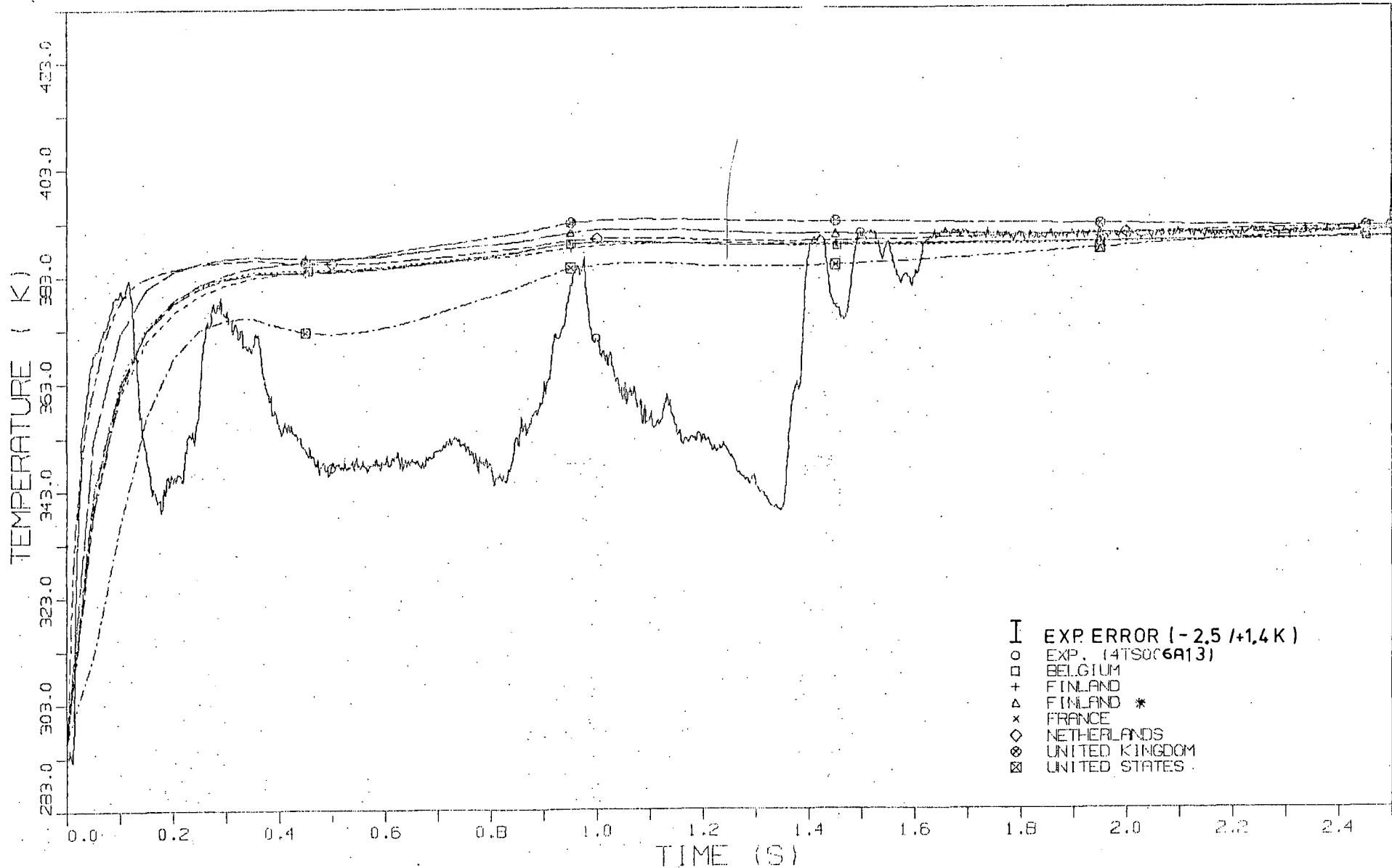


FIG. 23

TEMPERATURE HISTORY IN COMPARTMENT R4

2<sup>ND</sup> CONTAINMENT STANDARD PROBLEM (CASP2)

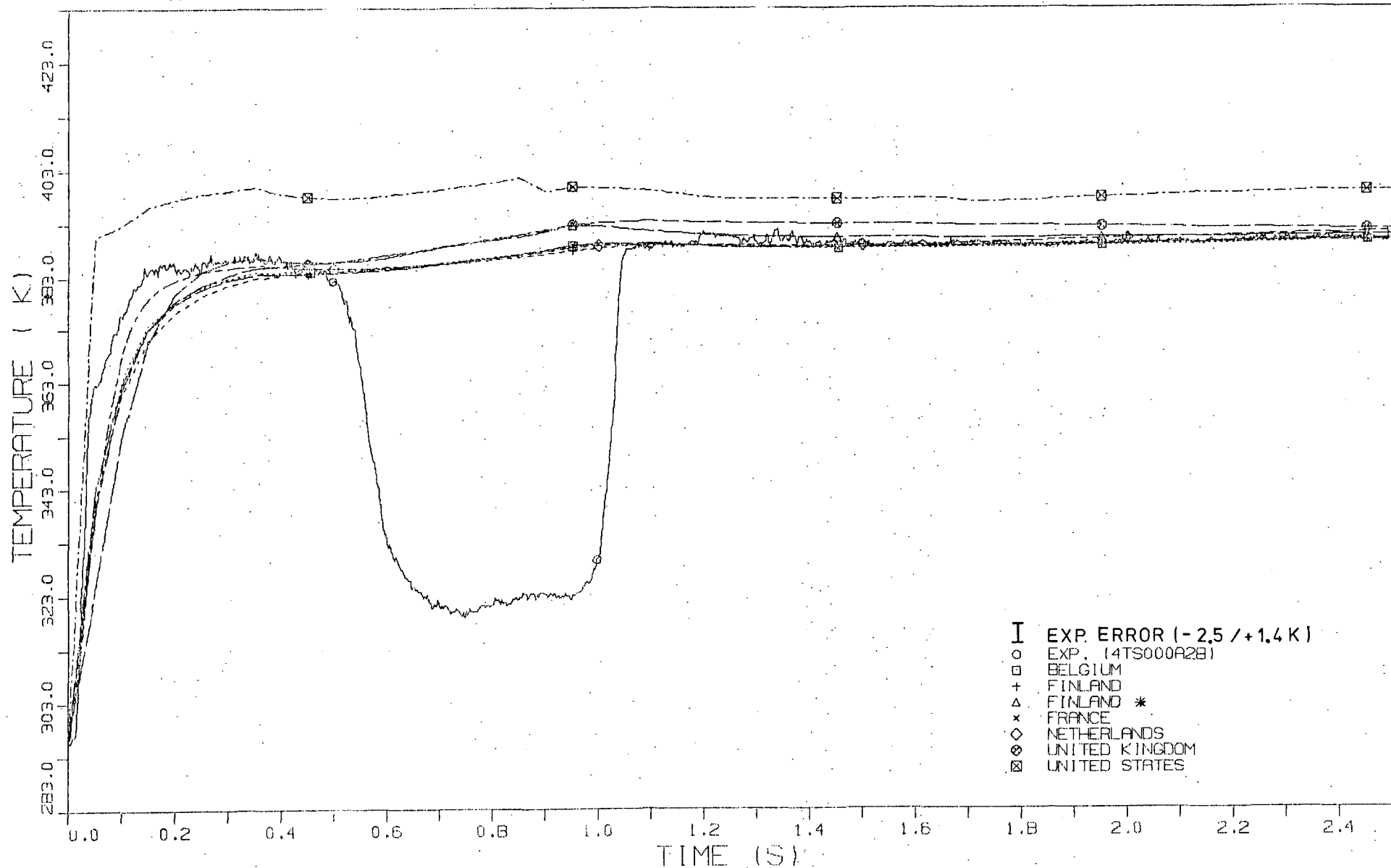


FIG. 24 TEMPERATURE HISTORY IN COMPARTMENT R4

2<sup>ND</sup> CONTAINMENT STANDARD PROBLEM (CASP2)

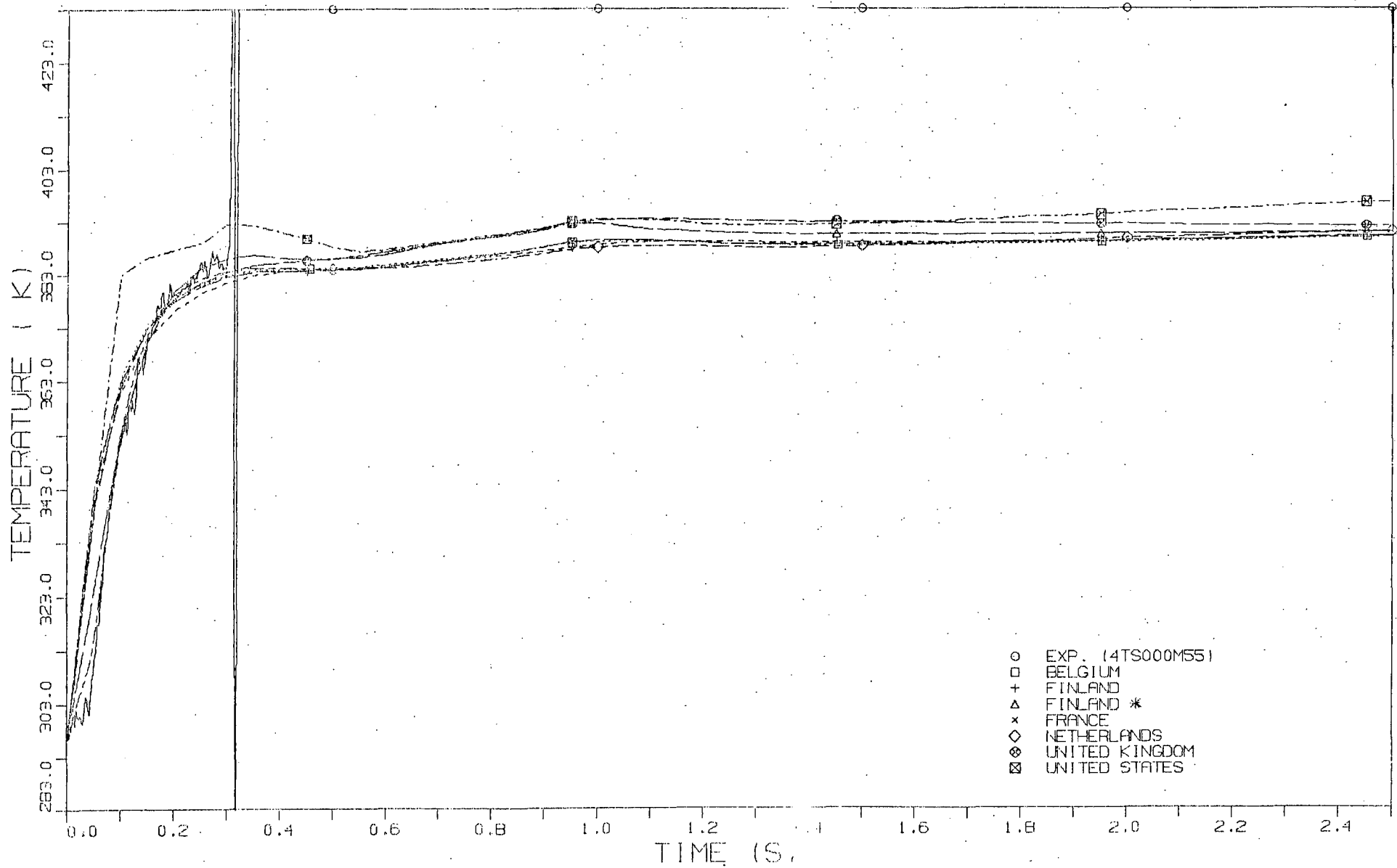


FIG 25

TEMPERATURE HISTORY IN COMPARTMENT R4

2<sup>ND</sup> CONTAINMENT STANDARD PROBLEM (CASP2)

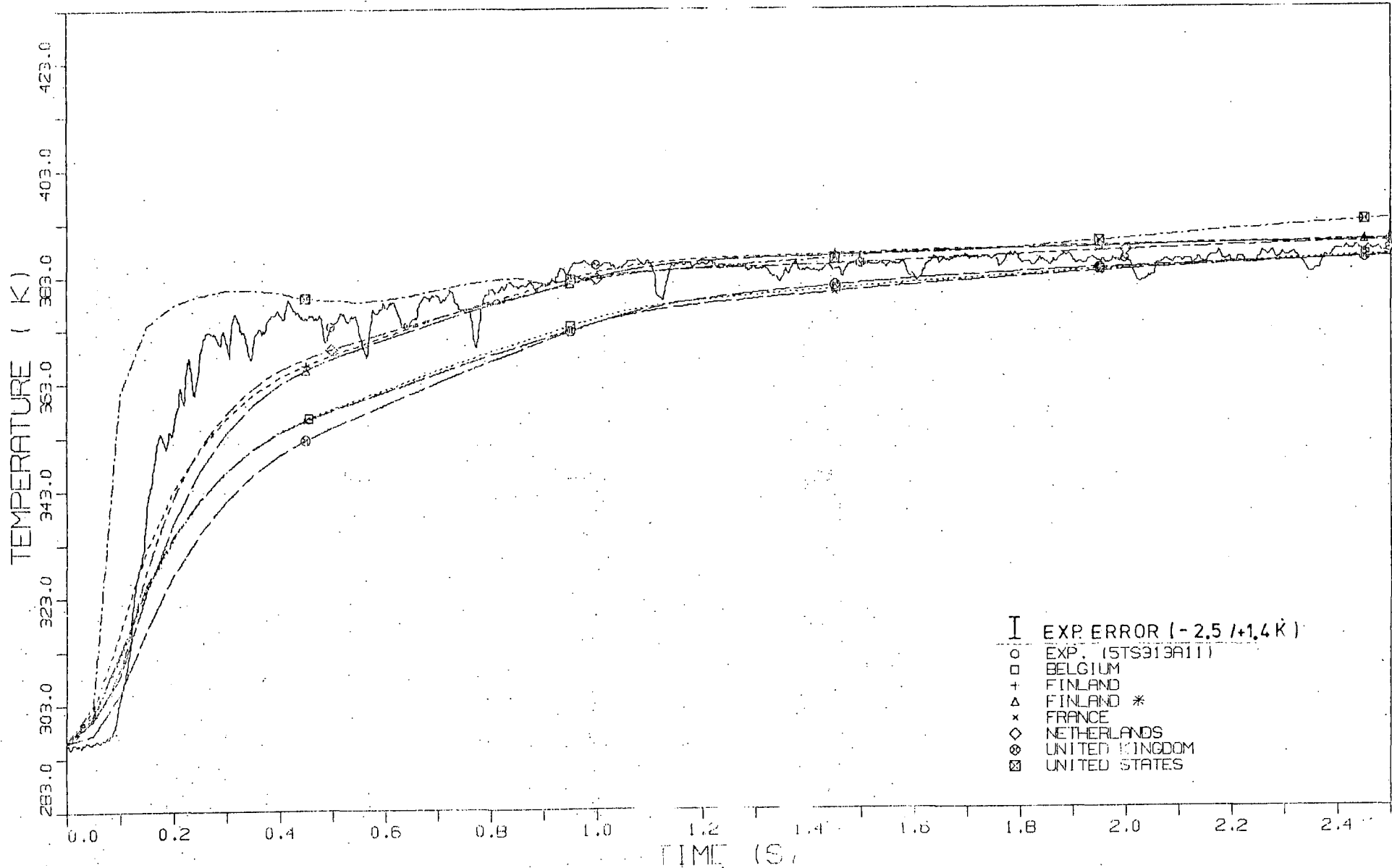


FIG. 26 TEMPERATURE HISTORY IN COMPARTMENT R5

2ND CONTAINMENT STANDARD PROBLEM (CASP2)

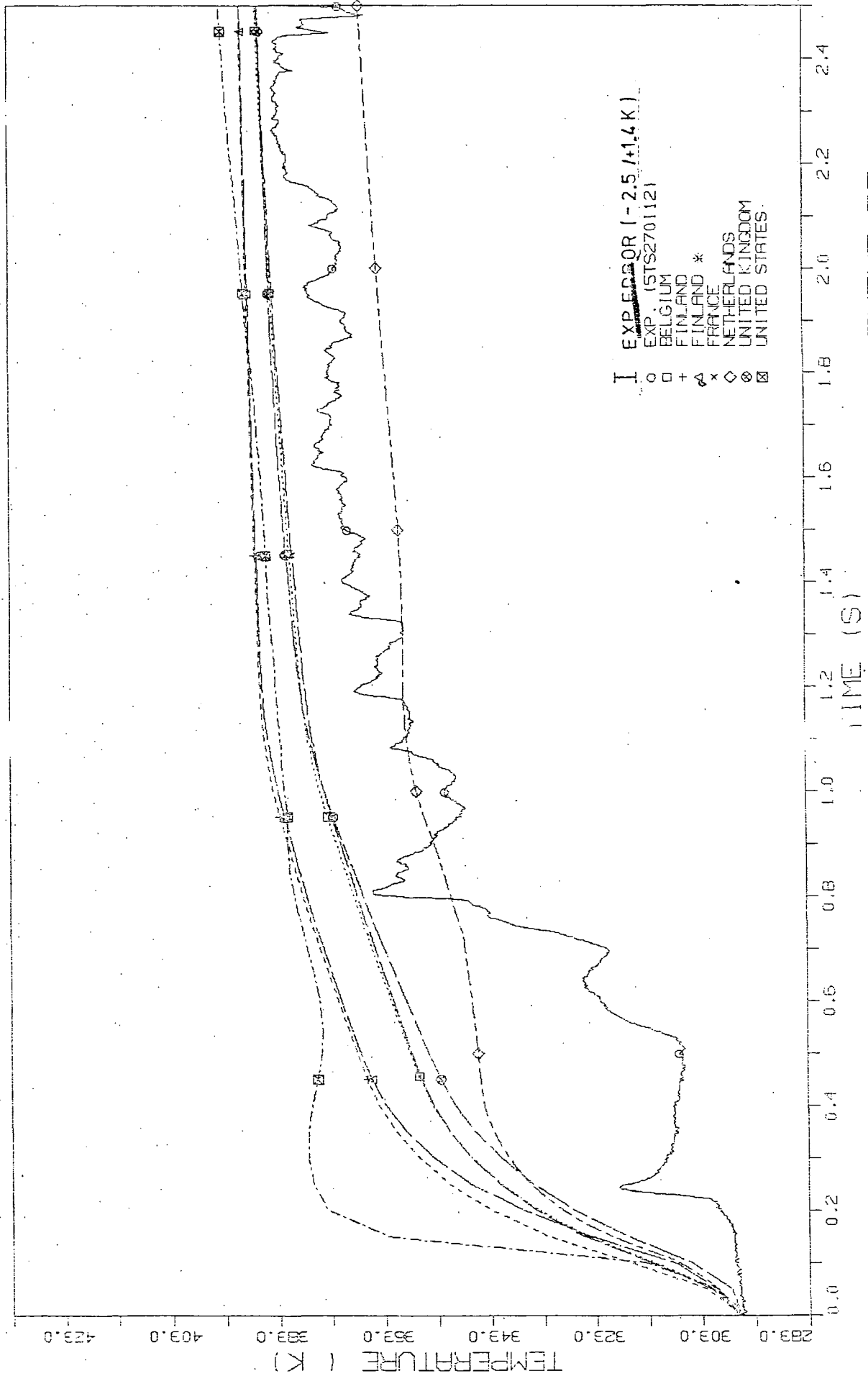


FIG 27 TEMPERATURE HISTORY IN COMPARTMENT R5



2<sup>ND</sup> CONTAINMENT STANDARD PROBLEM (CASP2)

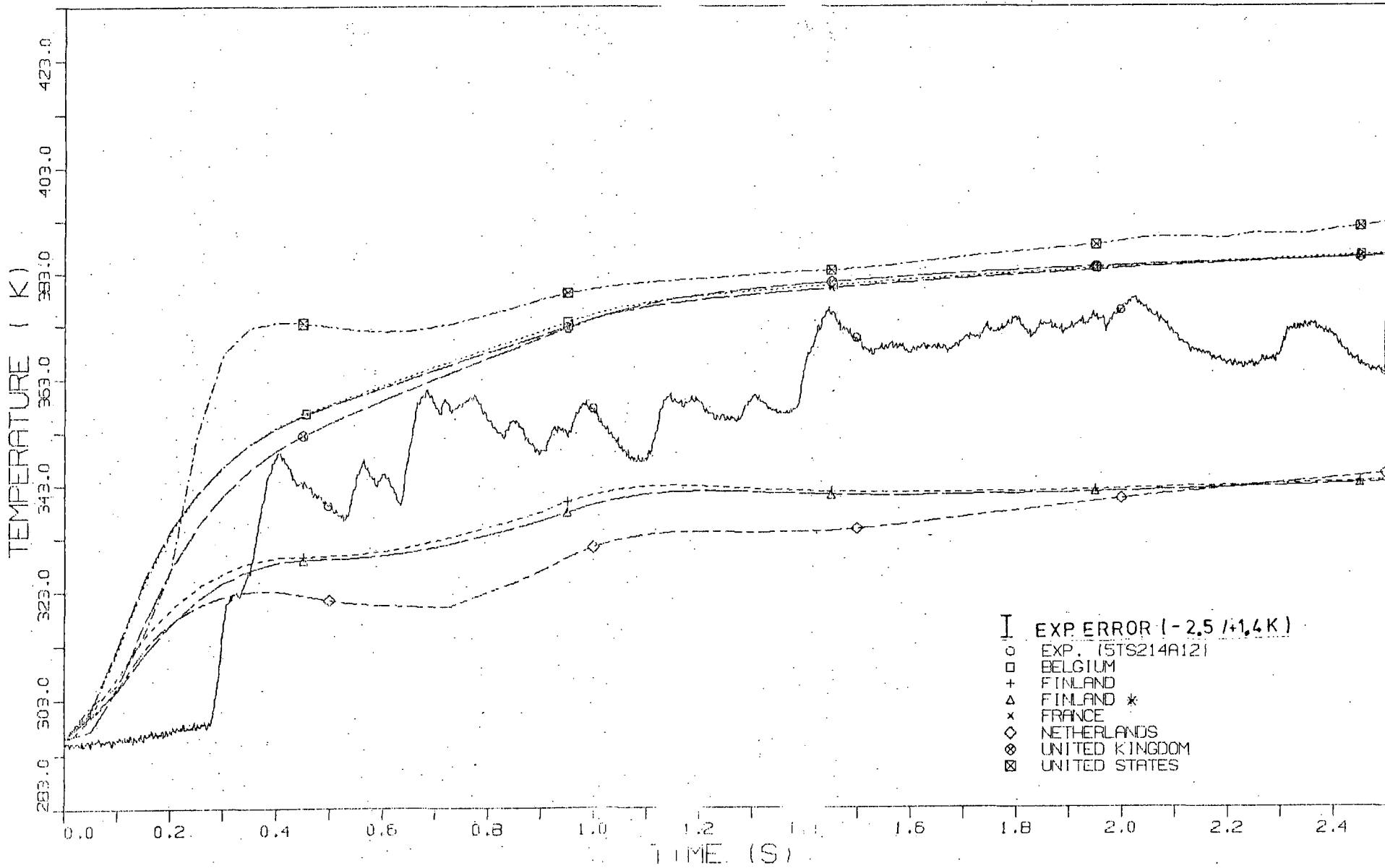


FIG. 28

TEMPERATURE HISTORY IN COMPARTMENT R5

2ND CONTAINMENT STANDARD PROBLEM (CASP2)

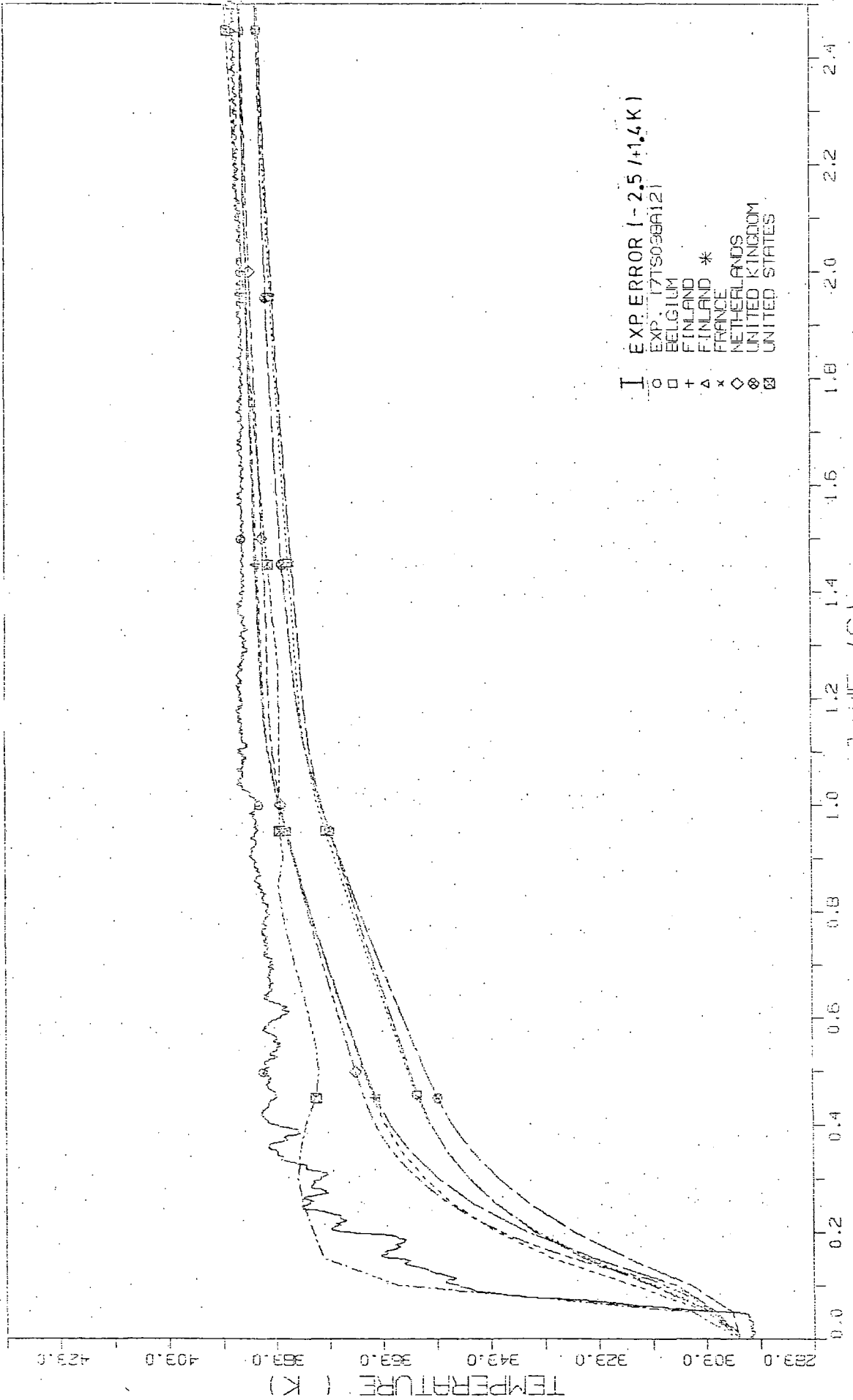


FIG. 29 TEMPERATURE HISTORY IN COMPARTMENT R7

# 2<sup>ND</sup> CONTAINMENT STANDARD PROBLEM (CASP2)

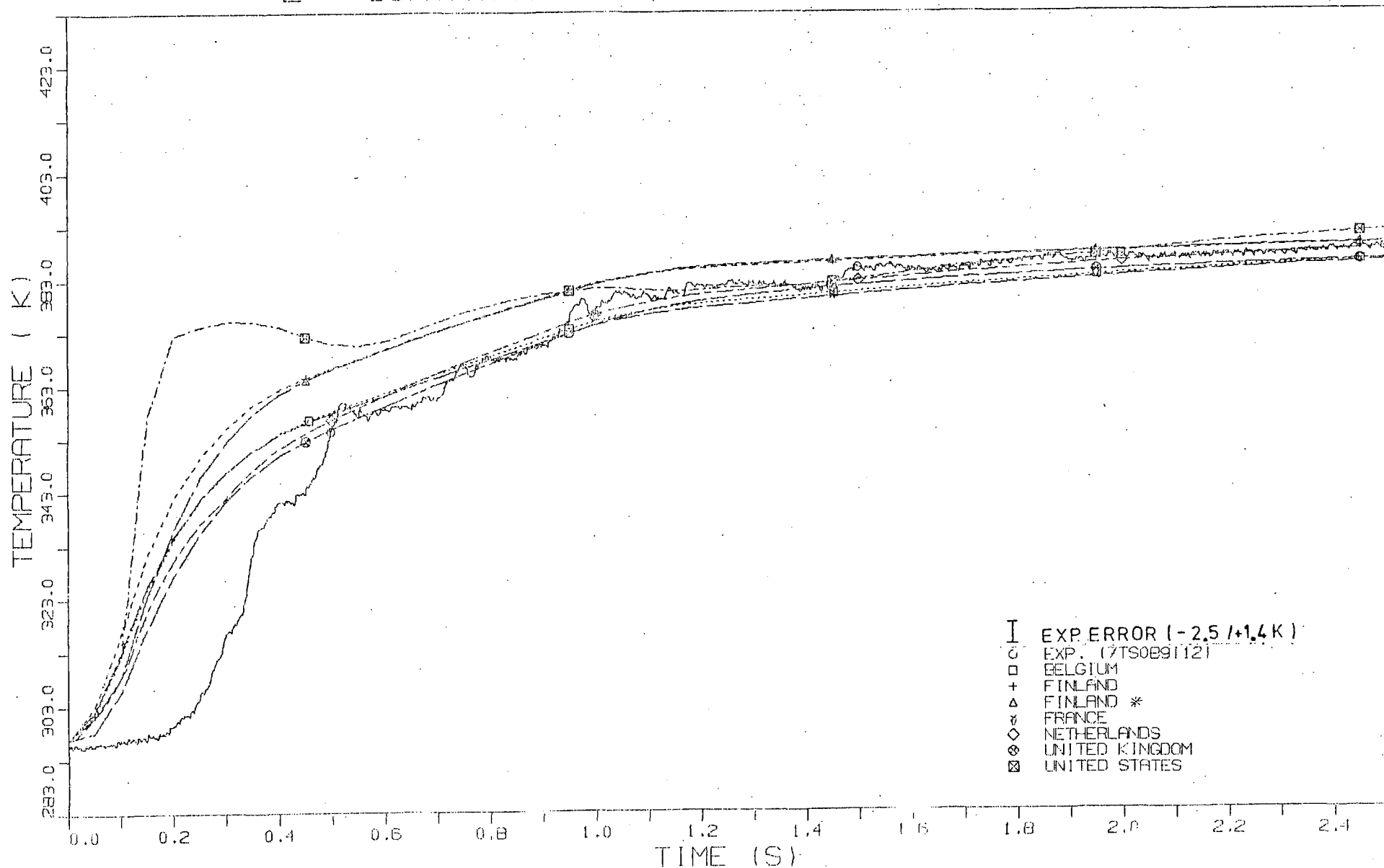


FIG. 30

TEMPERATURE HISTORY IN COMPARTMENT R7

# 2<sup>ND</sup> CONTAINMENT STANDARD PROBLEM (CASP2)

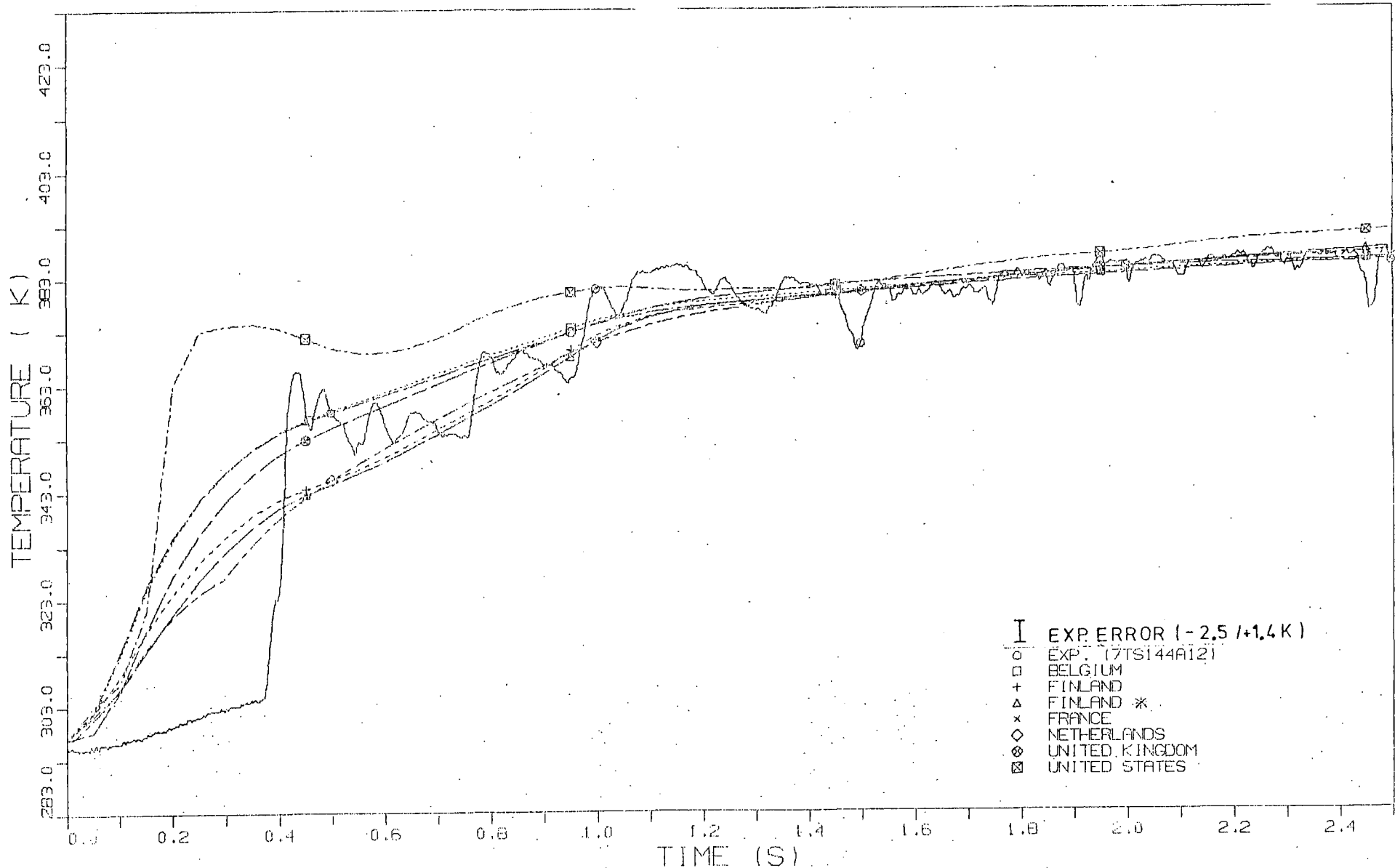


FIG. 31. TEMPERATURE HISTORY IN COMPARTMENT R7

# 2ND CONTAINMENT STANDARD PROBLEM (CASP2)

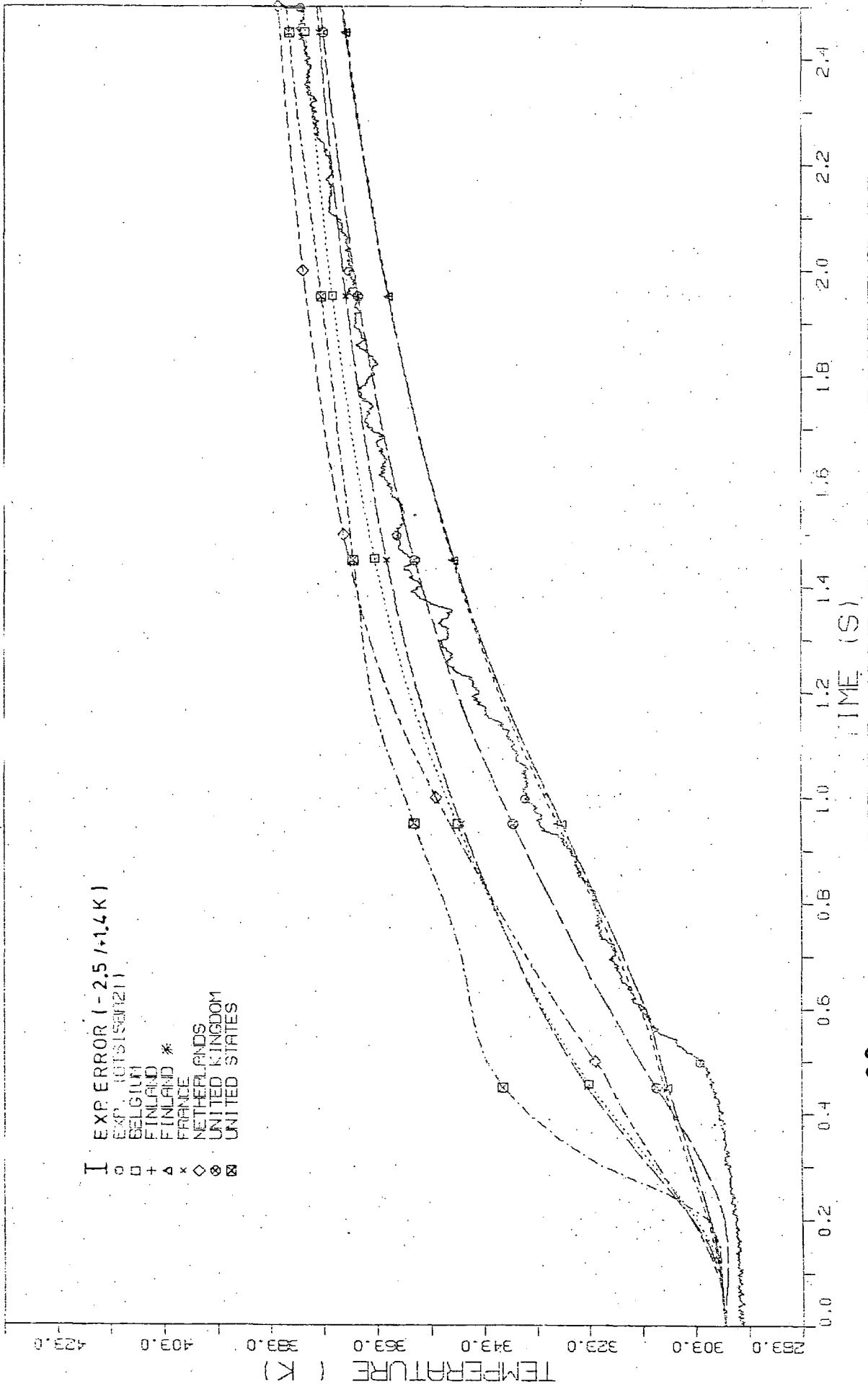


FIG. 32 TEMPERATURE HISTORY IN COMPARTMENT RB

2ND CONTAINMENT STANDARD PROBLEM (CASP2)

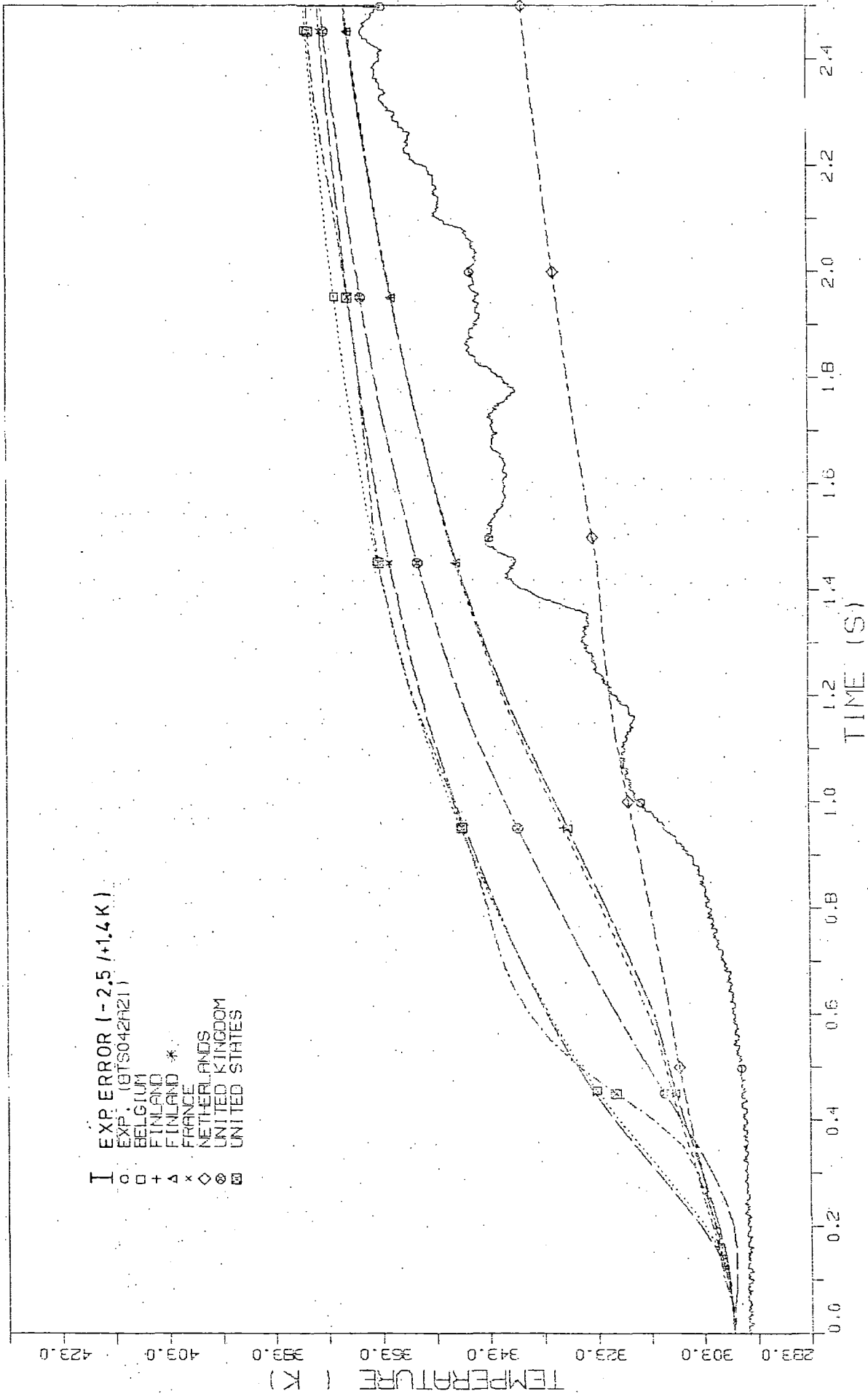


FIG 33 TEMPERATURE HISTORY IN COMPARTMENT RB

2ND CONTAINMENT STANDARD PROBLEM (CASP2)

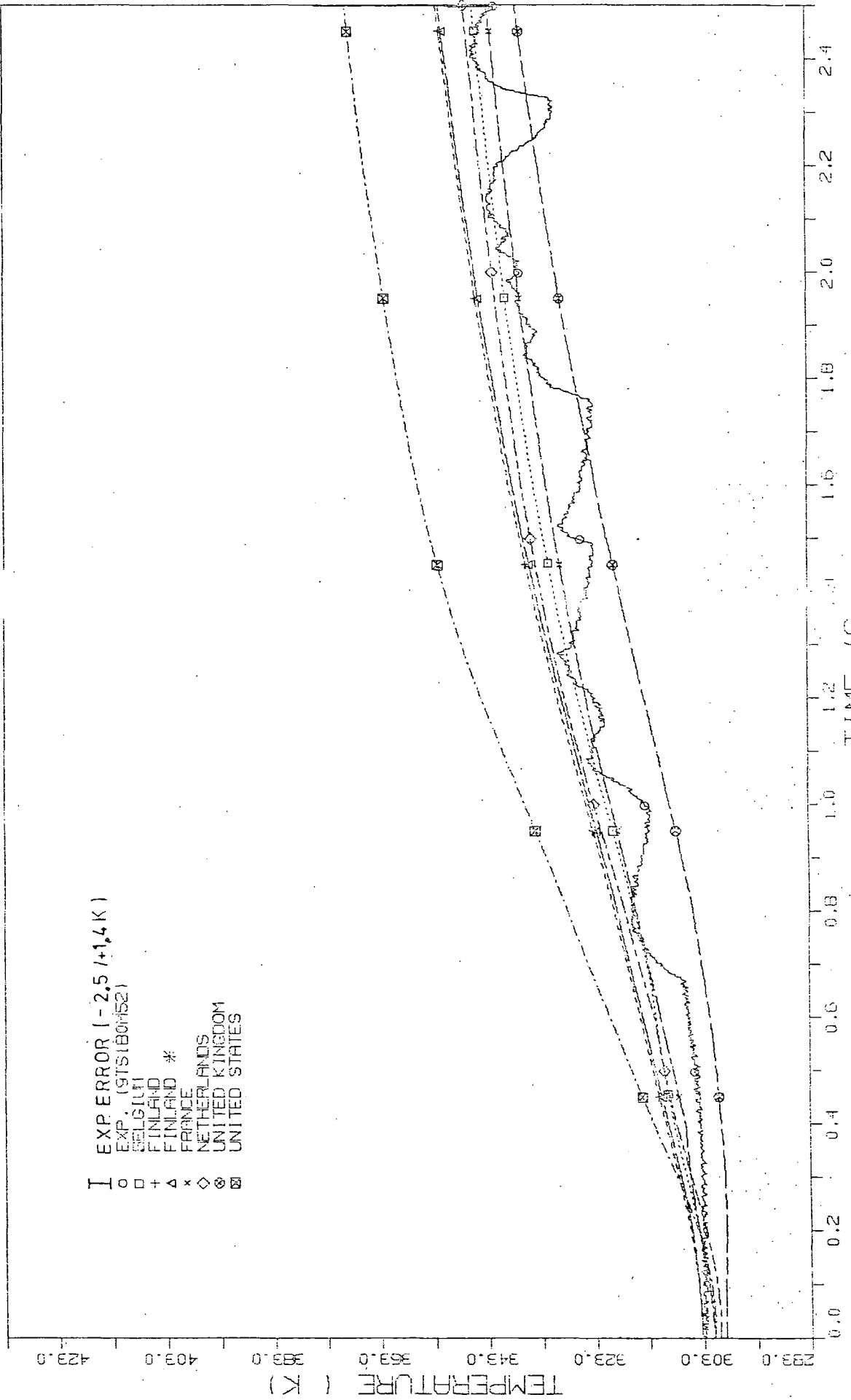


FIG. 34 TEMPERATURE HISTORY IN COMPARTMENT R9

# 2ND CONTAINMENT STANDARD PROBLEM (CASP2)

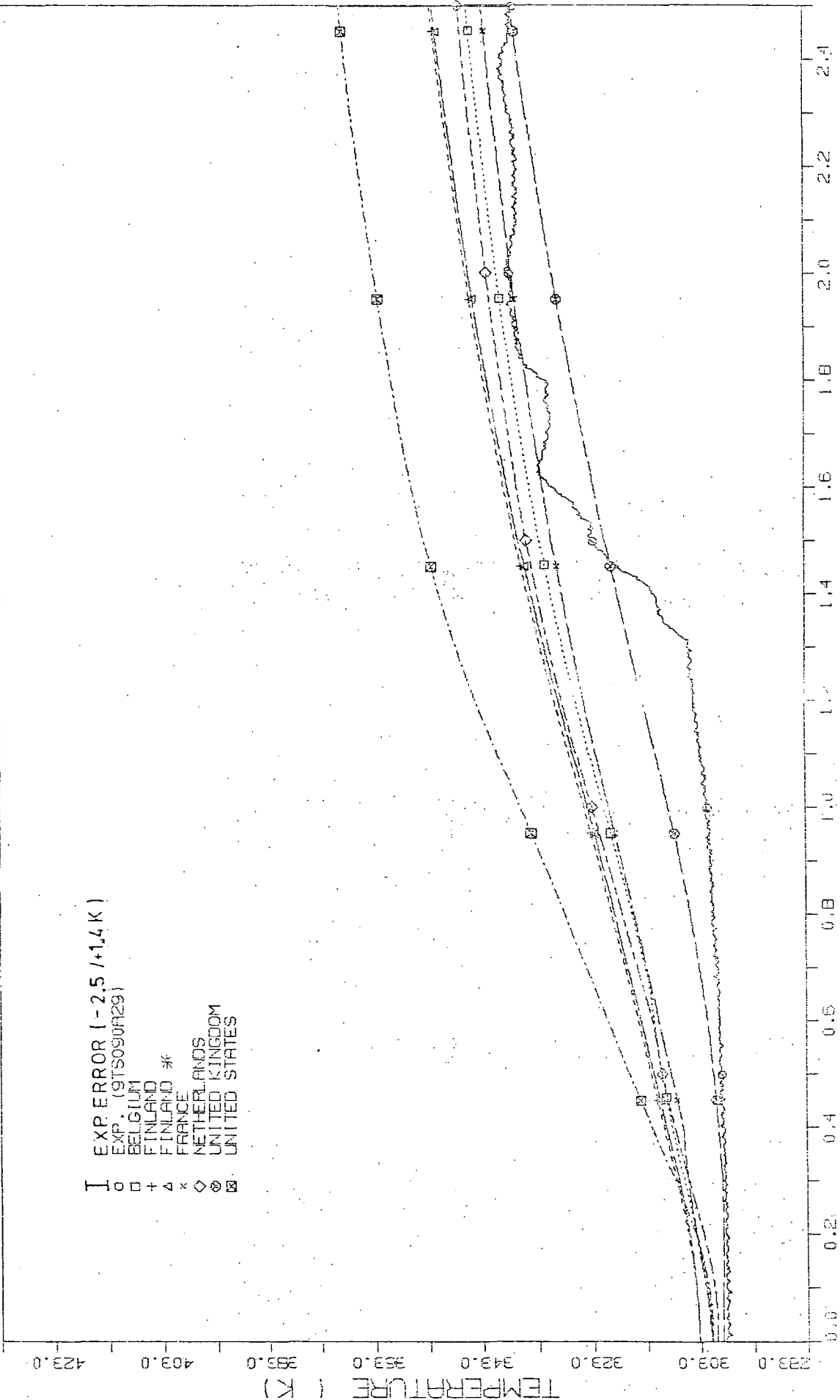


FIG 35 TEMPERATURE HISTORY IN COMPARTMENT R9



# 2ND CONTAINMENT STANDARD PROBLEM (CAS2)

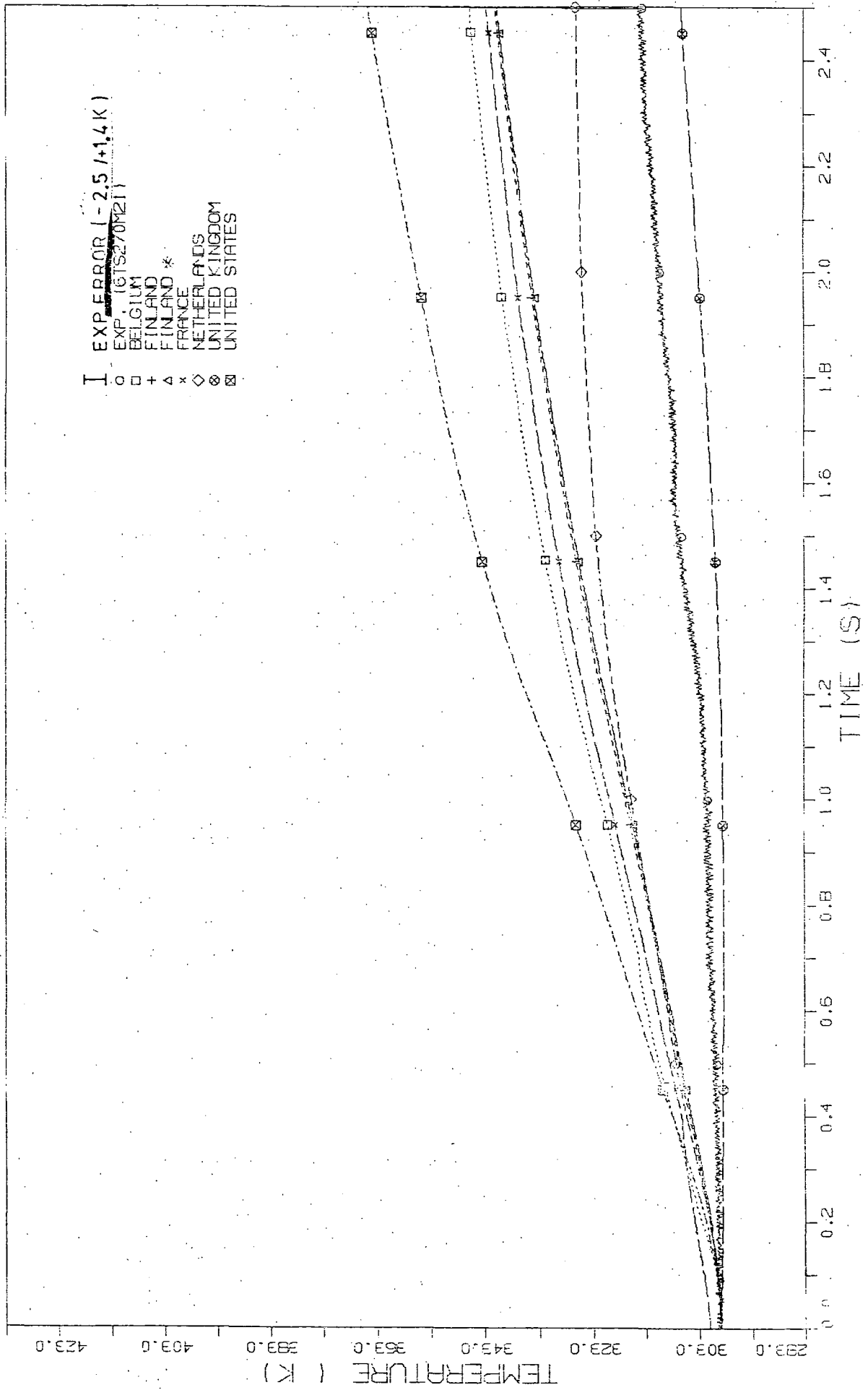


FIG. 36 TEMPERATURE HISTORY IN COMPARTMENT R6

Figs. 37-40 show for the time interval 0-50 s a comparison between measured pressure-time histories within compartments R4, R5, R7 and R9 and the results of the calculations of the participants. Note that the ordinate of all plots start at 2.0 bar (suppressing the initial part of the pressurisation)! This method has been chosen to facilitate the comparison of achievable overall accuracy of calculations for the 2nd Containment-SP with the result of the 1st Containment-SP.

The corresponding comparisons of measured with calculated temperature curves for the time interval 0-50 s are shown in the Figs. 41-46.

2ND CONTAINMENT STANDARD PROBLEM (CASP2)

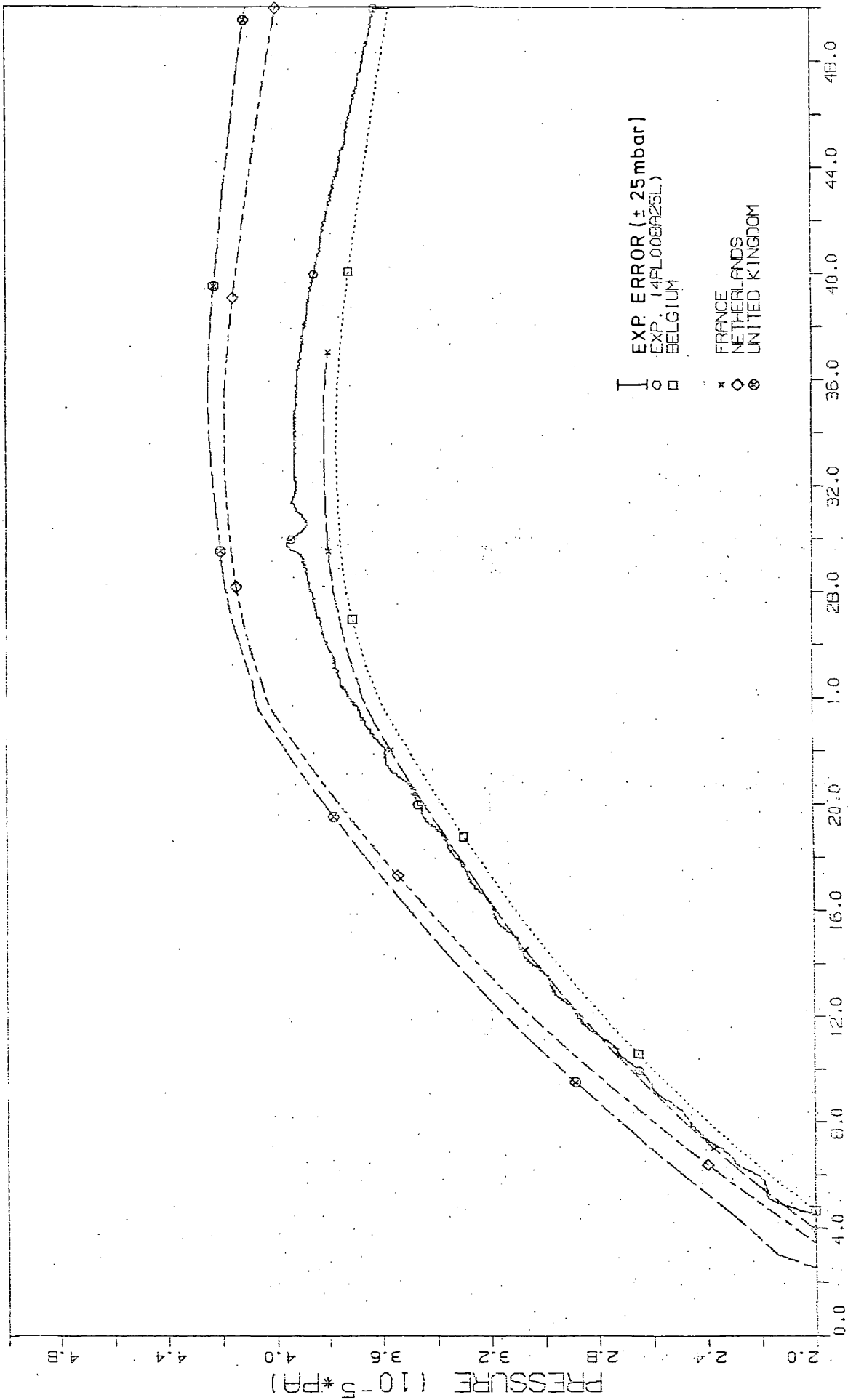


FIG. 37 PRESSURE HISTORY IN COMPARTMENT R4

2ND CONTAINMENT STANDARD PROBLEM (CASP2)

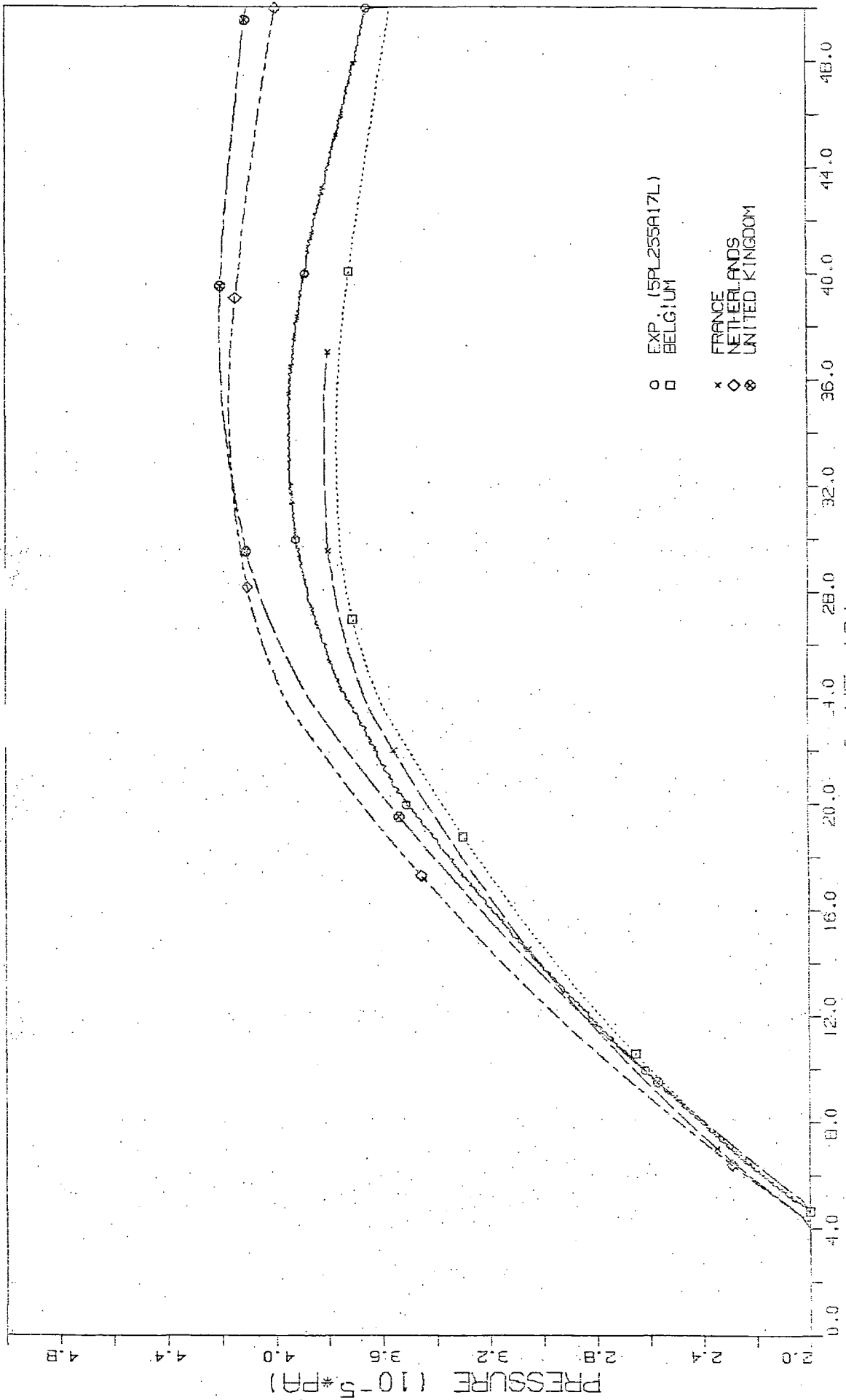


FIG. 38 PRESSURE HISTORY IN COMPARTMENT R5

2<sup>ND</sup> CONTAINMENT STANDARD PROBLEM (CASP2)

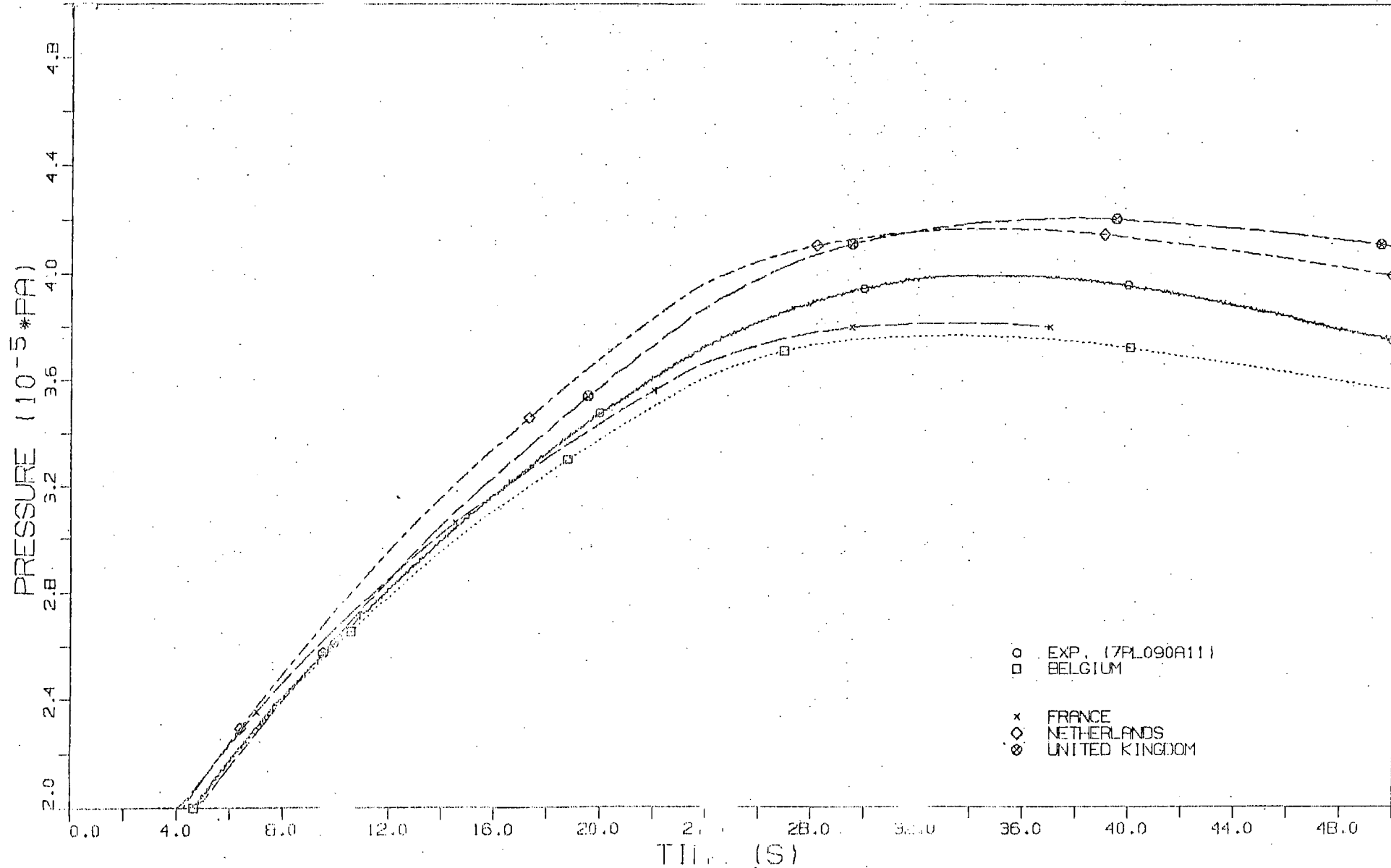
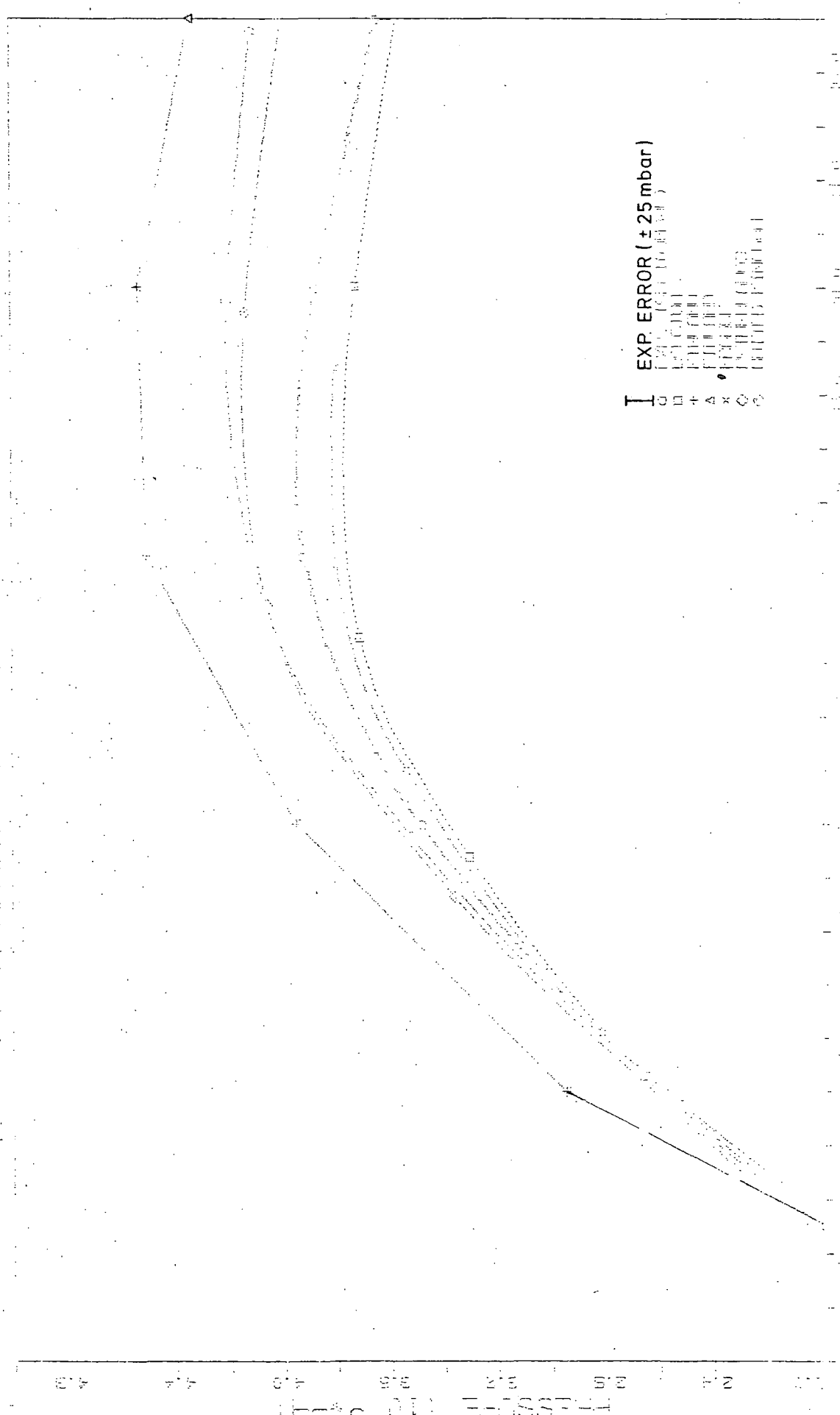


FIG. 39

PRESSURE HISTORY IN COMPARTMENT R7

# 2100 COMPOSITE STANDARD FUNCTION (CFSP2)



# 2ND CONTAINMENT STANDARD PROBLEM (CASP2)

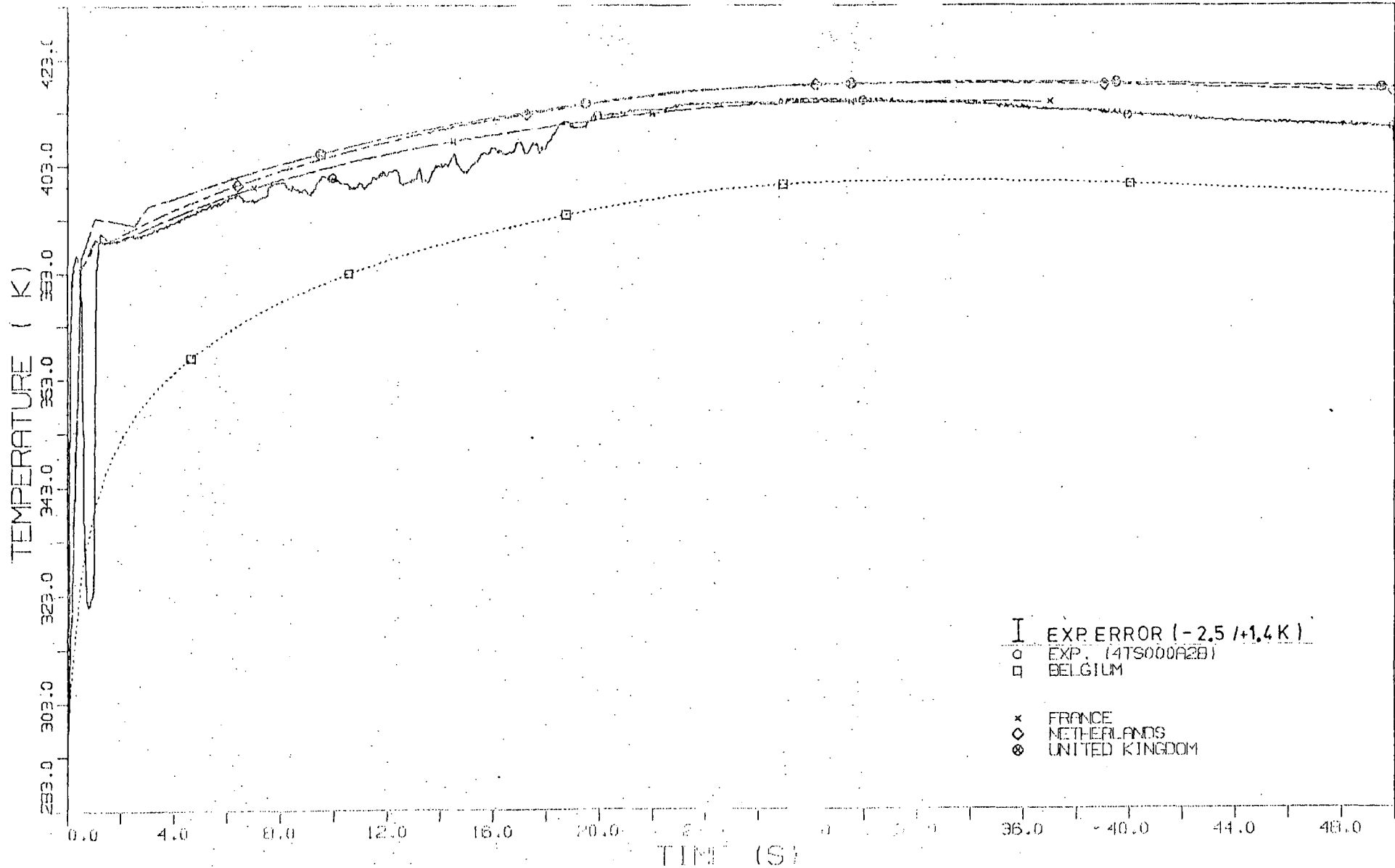


FIG. 41

TEMPERATURE HISTORY IN COMPARTMENT R4

# 2<sup>ND</sup> CONTAINMENT STANDARD PROBLEM (CASP2)

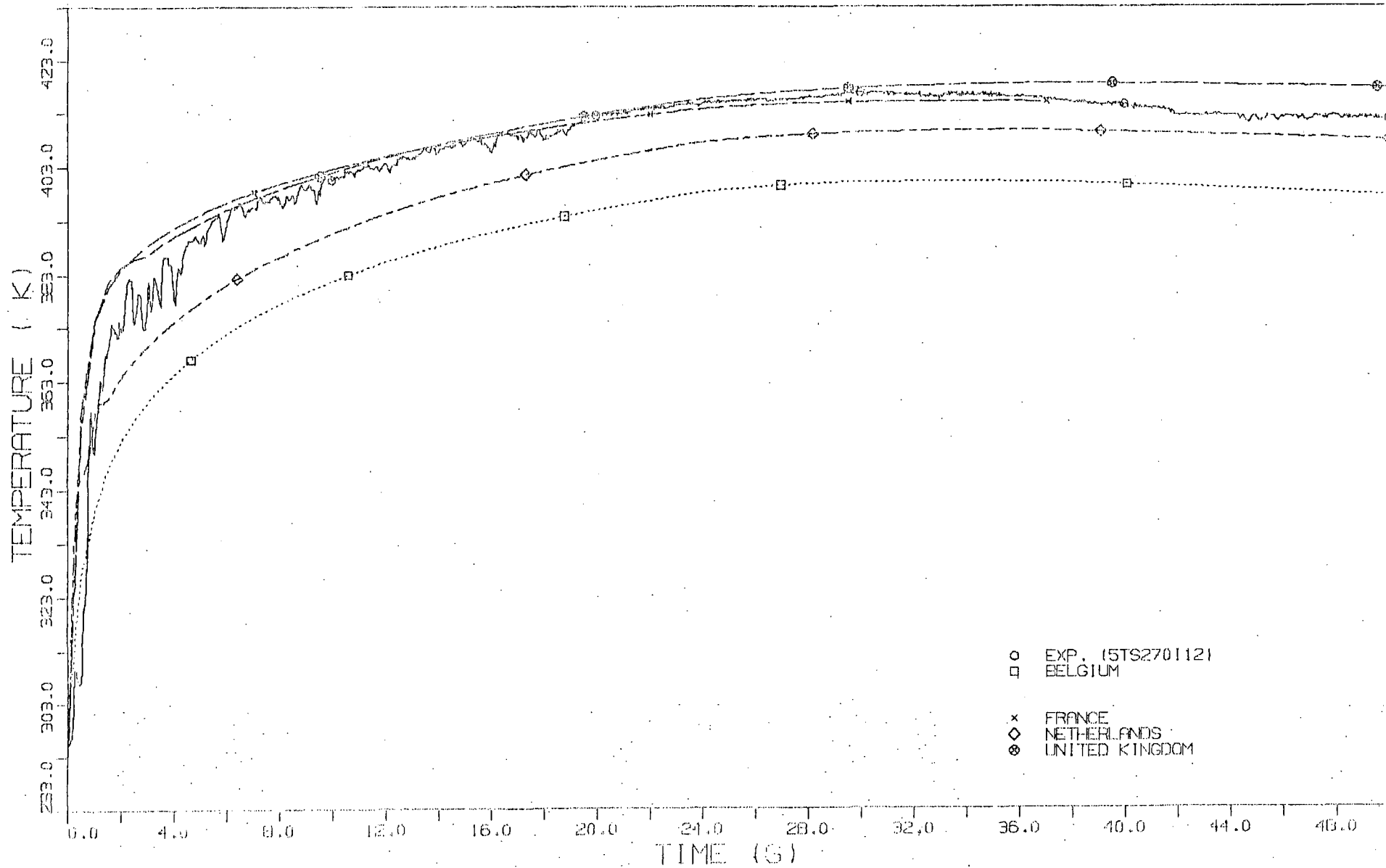


FIG. 42 TEMPERATURE HISTORY IN COMPARTMENT R5



2ND CONTAINMENT STANDARD PROBLEM (CASP2)

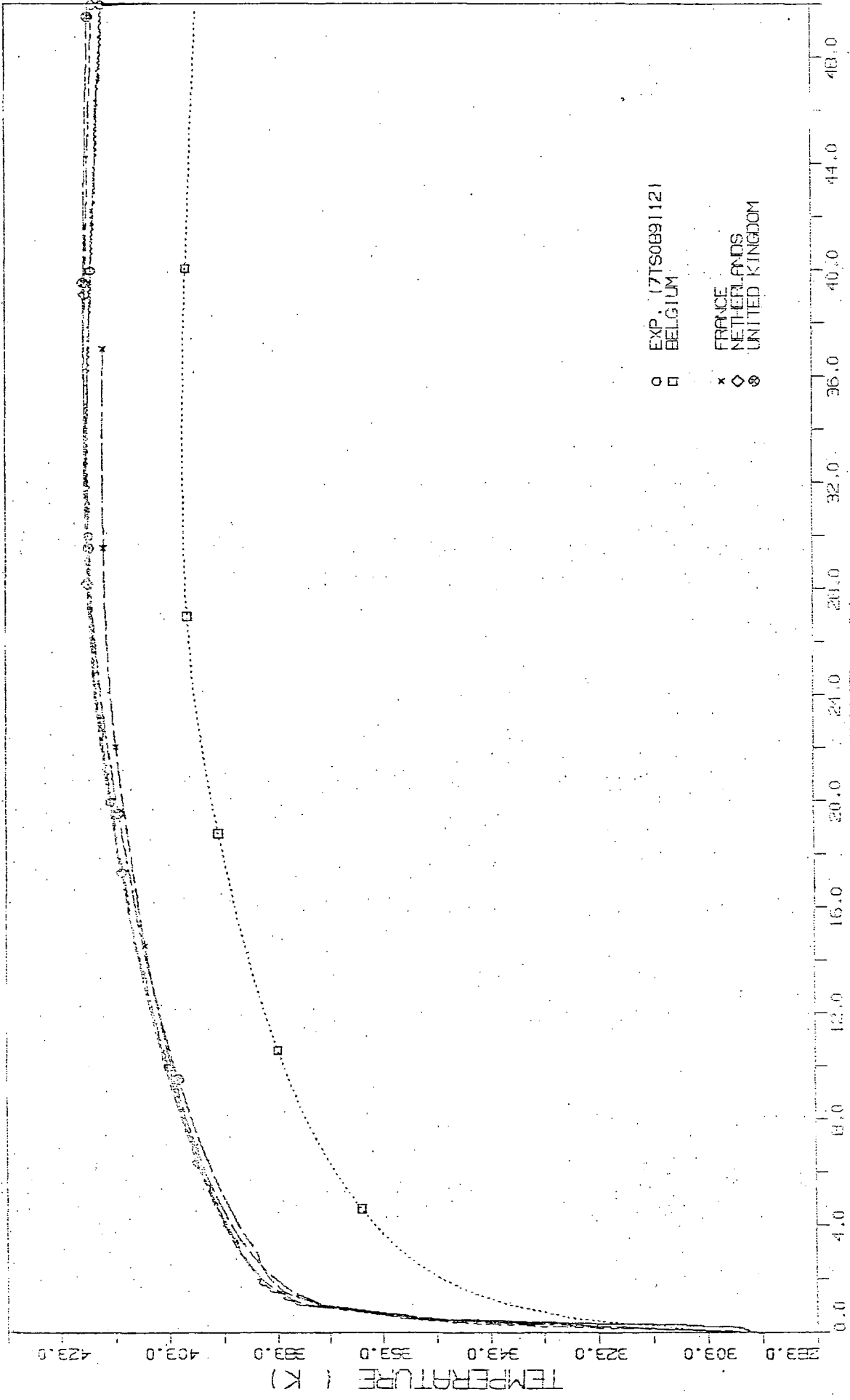


FIG. 43 TEMPERATURE HISTORY IN COMPARTMENT R7

2ND CONTAINMENT STANDARD PROBLEM (CASP2)

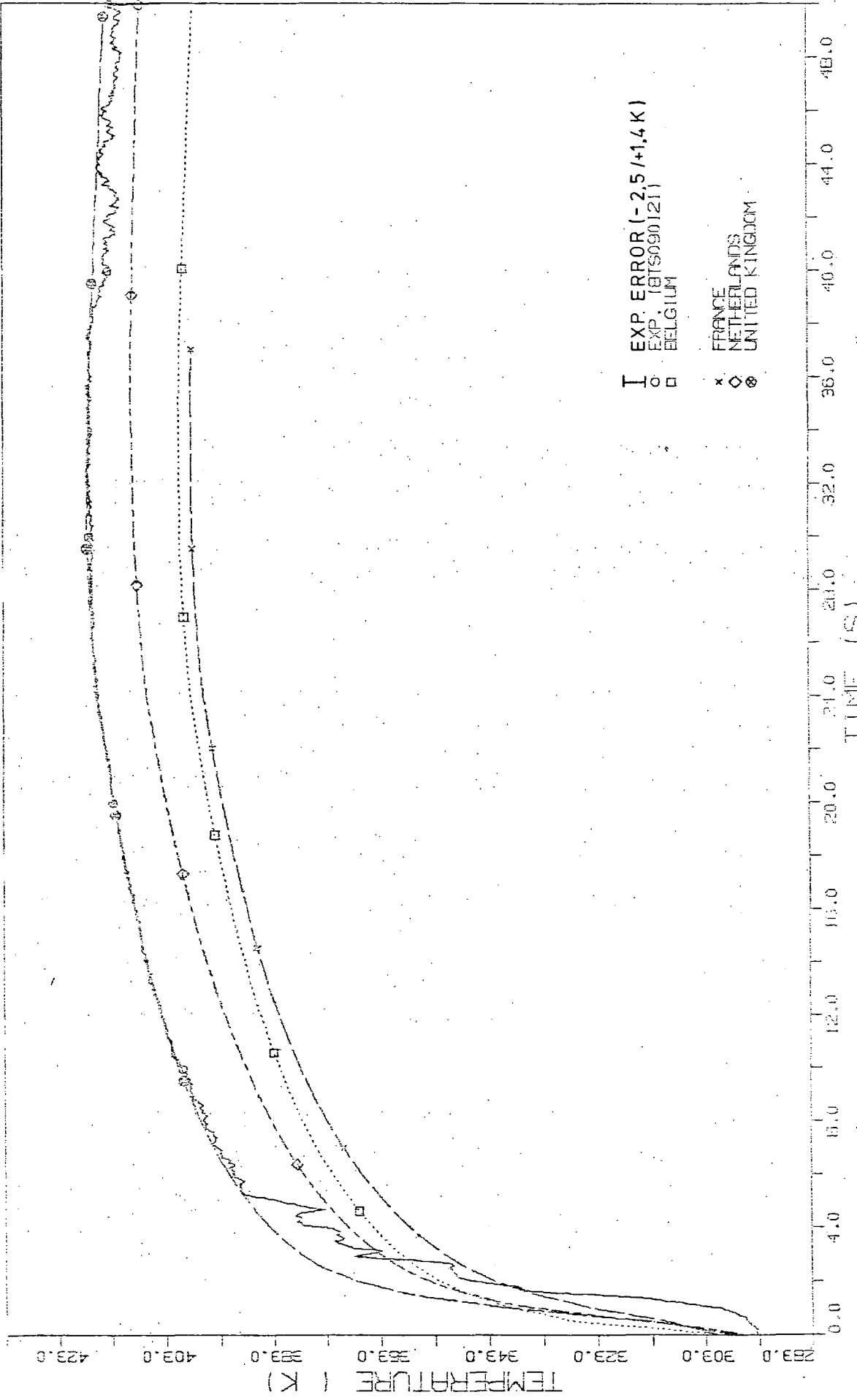


FIG. 44 TEMPERATURE HISTORY IN COMPARTMENT FRB

2ND CONTAINMENT STANDARD PROBLEM (CASP2)

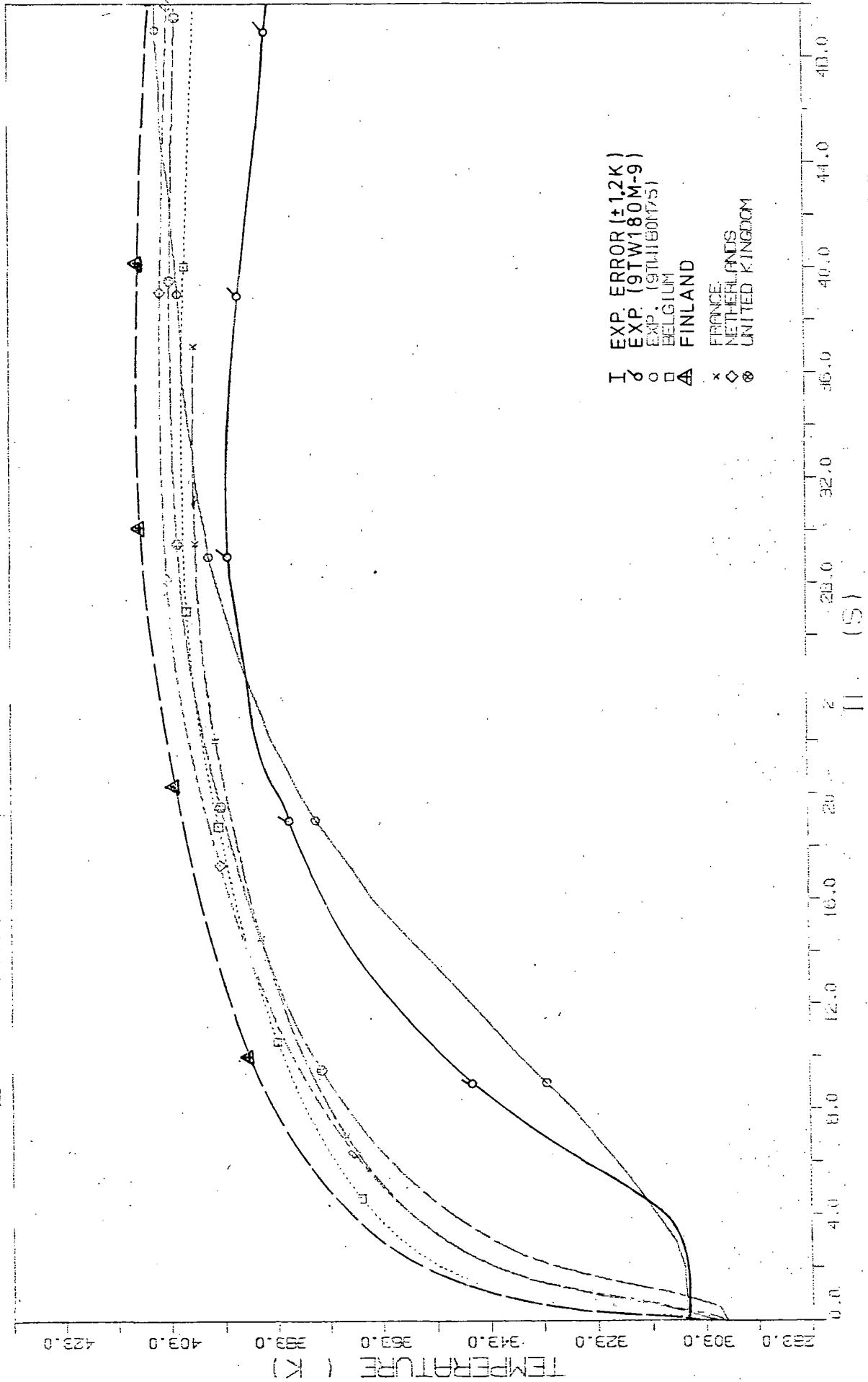


FIG. 45 TEMPERATURE HISTORY IN COI (PAINTMENT R9)

# 2<sup>ND</sup> CONTAINMENT STANDARD PROBLEM (CASP2)

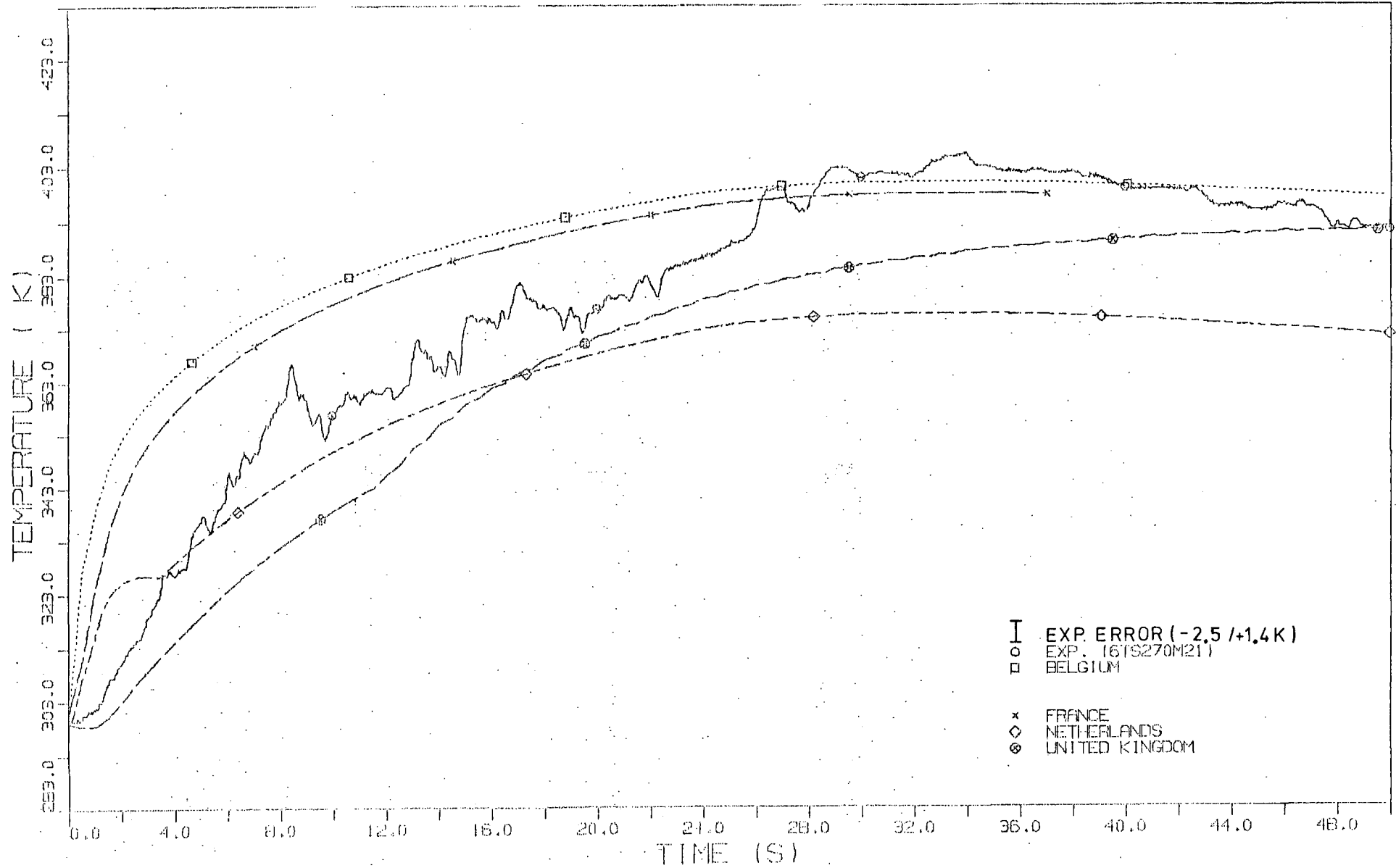


FIG. 46 TEMPERATURE HISTORY IN COMPARTMENT R6

Long term pressure- and temperature-time histories of this experiment are of interest with respect to fluid-structure heat exchange processes in particular. The results of calculations compared to the measured pressure are shown in Fig. 47. For the time interval 0-1000 s one should keep in mind that the leak tightness of the model containment at elevated pressures is not good, probably amplifying the pressure decay in the first 300-400 s. Fig. 48 shows two temperature measurements in comparison with calculated temperature curves. Note the considerable differences in both measured curves! Finally predictions of water masses versus time were requested from the analysts to be compared with rough measurements taken at 5 distinct times during the experiment. The results are compared in Fig. 49, where a large experimental error band associated with this type of measurements is indicated.

# 2ND CONTAINMENT STANDARD PROBLEM (CASP2)

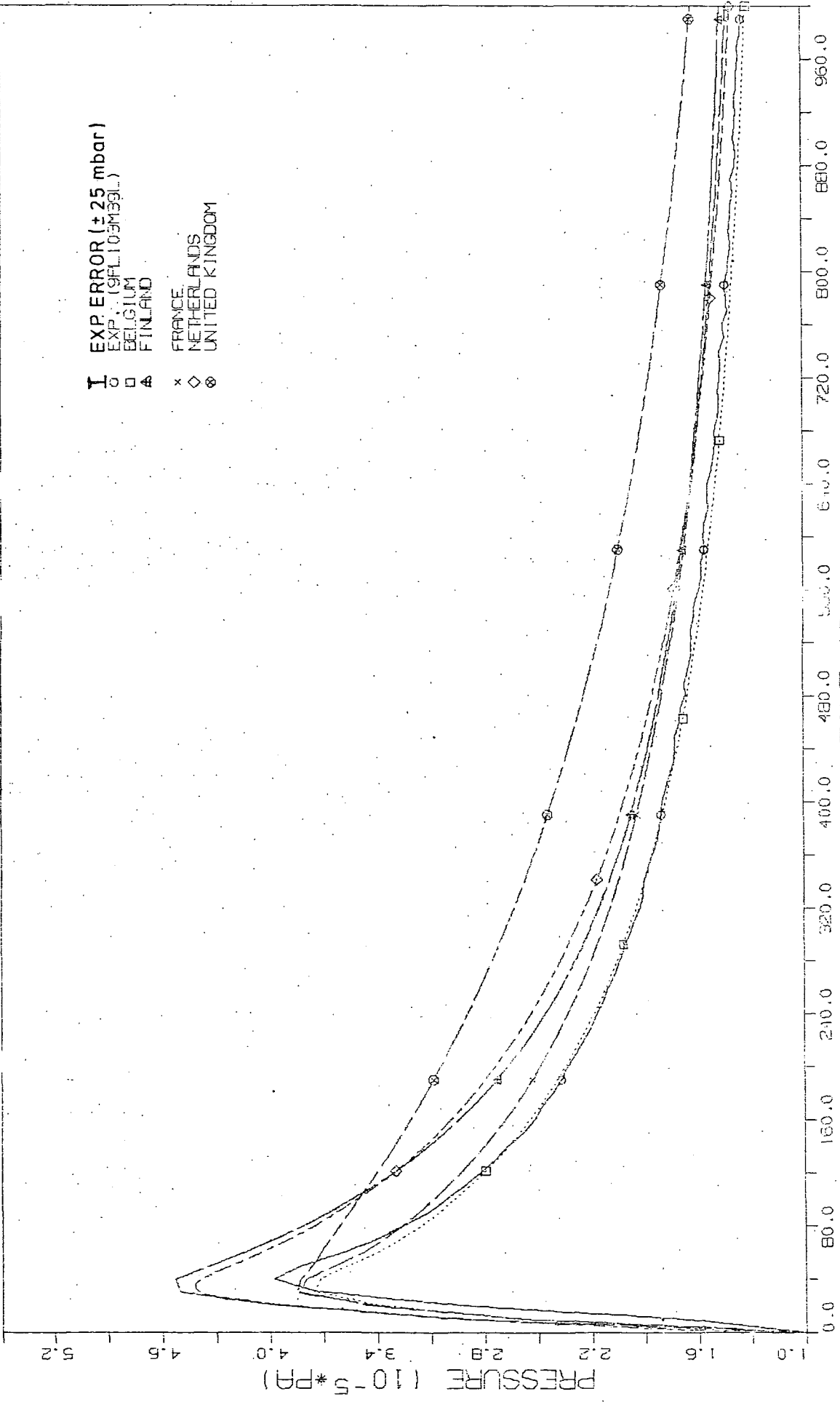


FIG. 47 PRESSURE HISTORY IN CONTAINMENT

2ND CONTAINMENT STANDARD PROBLEM (CASP2)

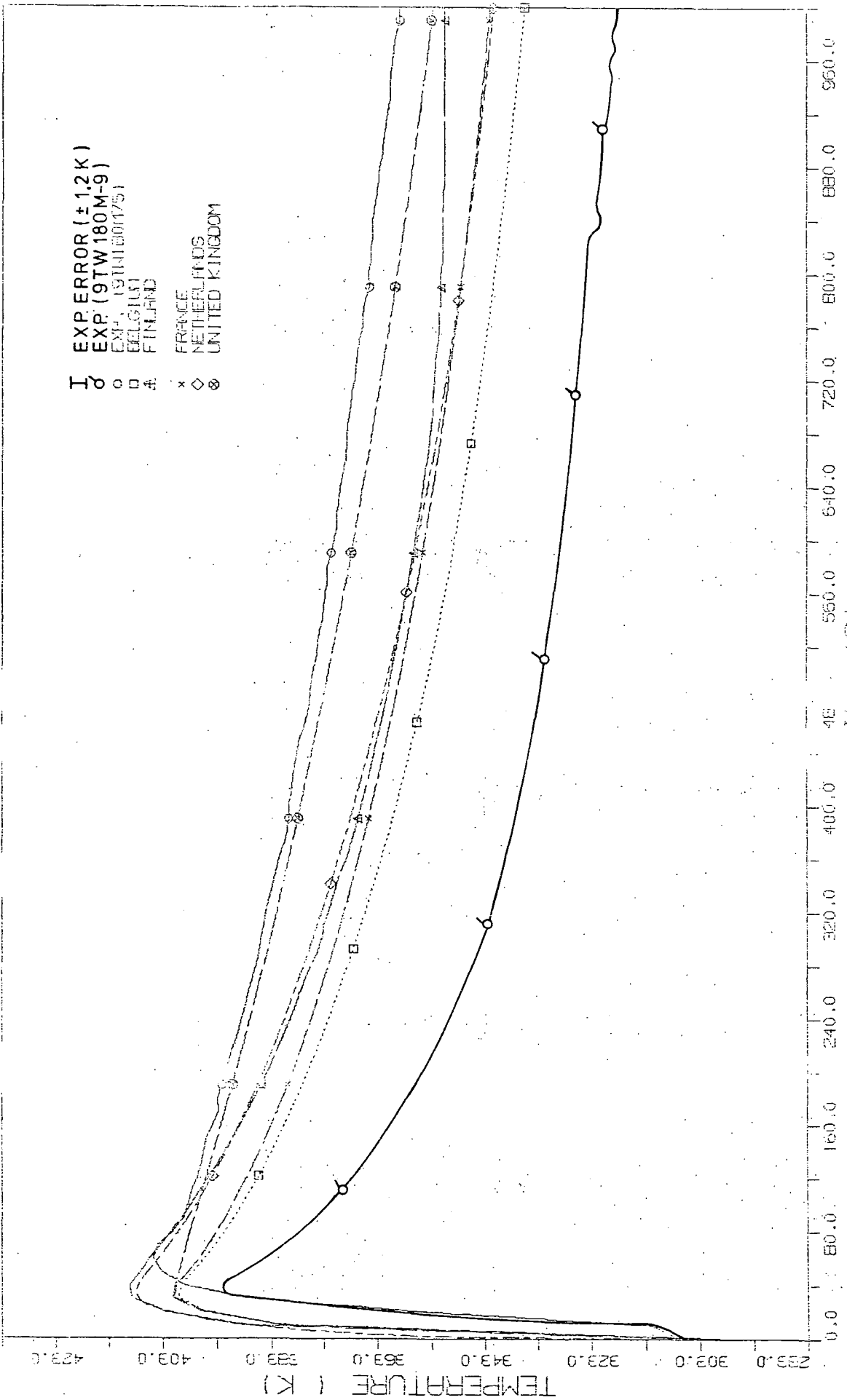


FIG. 48 TEMPERATURE HISTORY IN CONTAINMENT

# 2ND CONTAINMENT STANDARD PROBLEM (CASP2)

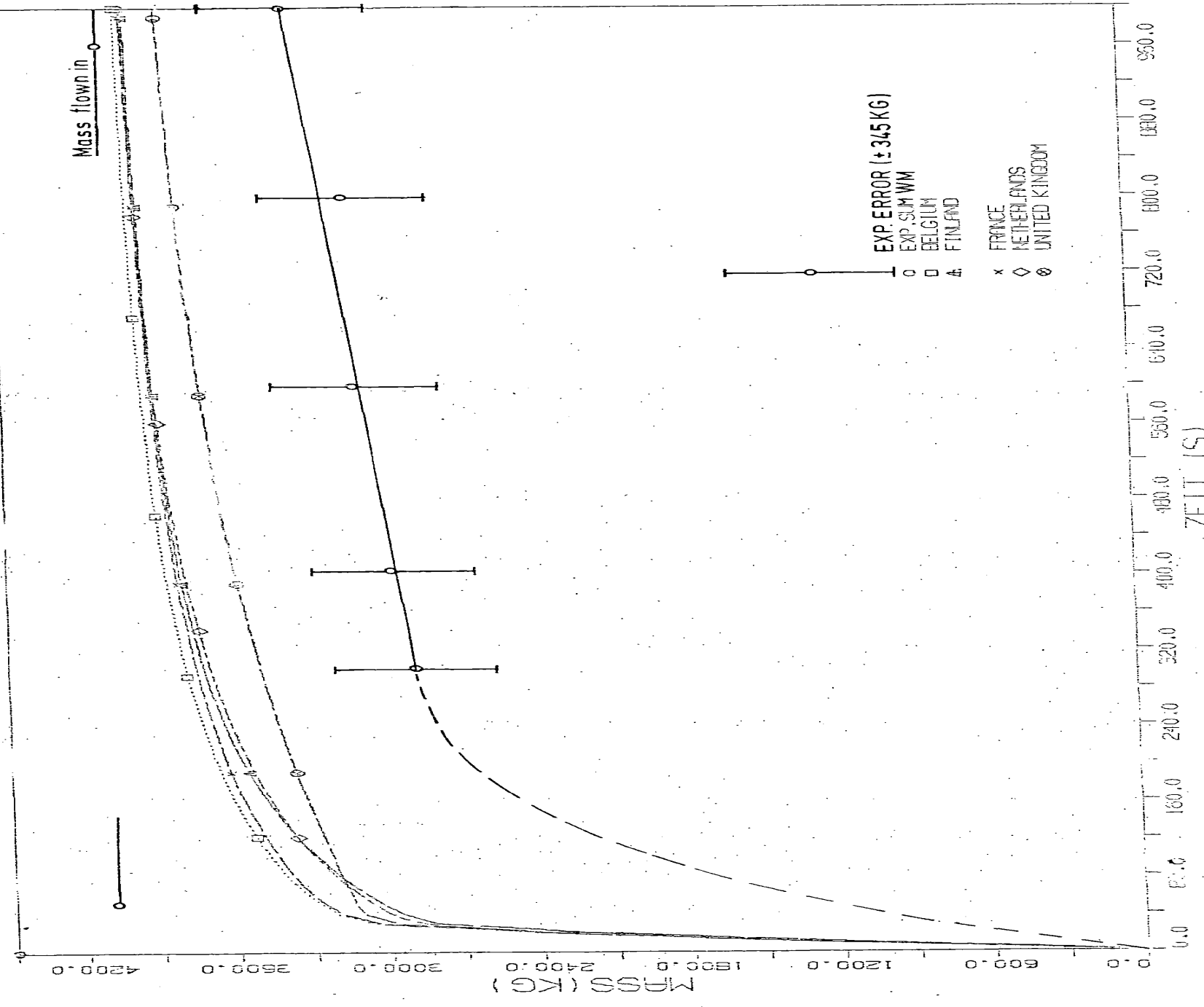


FIG. 49 HISTORY OF WATER MASS IN CONTAINMENT



Additional Information of Participants

Following a suggestion on the workshop the participants Belgium, France, Italy (CNEN/Pisa) and Sweden sent supplementary information on their submitted results (subdivision of walls, heat transfer coefficients, heat flux to walls) and partly results of parametric studies (condensate draining, heat transfer coefficient phenomena). They are in above-mentioned order content of the appendix.

The following figures illustrate the results of the transient between 0 and 1000 seconds using the TRAPCON code by using the same input data and code options as the open calculations documented in the comparison report except for variations on the condensate draining.

The TRAPCON code simulates all containment subcompartments as 1 region and the sump as a second region which is not in thermodynamic equilibrium with the atmosphere region.

The sump collects hot water from different sources :

- breakflow flashing injects part of the breakfluid directly in the sump,
- condensate draining from the cold walls,
- spray flow

The figures illustrate the pressure and temperature transient for a condensate thickness set at 0.25 mm, assuming that this is the maximum uniform repartition of all liquid in the containment which is allowed on the cold walls, and any excess liquid drains in the sump.

The containment pressure and temperature maxima are not noticeably different from the reference calculation (where thickness was set at 1 mm) except for the liquid inventory in the sump (fig. 5).

Table 1 specifies the spatial mesh sizes for the containment heat sinks.

Fig. 1 illustrates the pressure evolution of the containment atmosphere.

Fig. 2 illustrates the temperature evolution of the containment atmosphere (average temperature) and the sump water.

The calculated time-lead for the containment temperature is caused by the 1 volume representation of the containment, while in reality, the dome compartment is located at the end of the chain of compartments. While pressure propagates with the speed of sound, the temperature however has a much slower propagation velocity.

The temperature stratification recorded at later time cannot of course, be reproduced by a 1 mode simulation of the containment atmosphere.

The sump temperature immediately rises to about 100°C, being the temperature of the isenthalpic expansion of the breakfluid down to atmospheric pressure. (The initial sump liquid volume was set at 0.001 m<sup>3</sup>). The sump temperature stays high, as no heat sinks were simulated for the sump.

Fig. 3 illustrates the evolution of the heat transfer coefficient using the TAGAMI-USHIDA correlations (E = 10 GJ).

Fig. 4 illustrates the coldwall heat flux and the heat removal from the containment atmosphere to the sump by condensate draining.

Fig. 5 illustrates the repartition of the fluid in the containment compared to experimental data. This figure shows also the liquid inventory in the sump for 3 different condensate film thicknesses.

---

#### Conclusions concerning this particular exercise :

1. Although the use of the semi-empirical TAGAMI-UCHIDA correlation to describe the complex heat transfer mechanisms during the complete transient is questionable, it nonetheless reproduces the pressure profile quite well over a range of 1000 S (fig 1). The pressure peak depends also strongly on such parameters as pipe characteristics, breakflow flashing, etc...
2. Finer modalisation is required to reproduce the temperature stratification in the containment atmosphere, and sump water heat sinks should be modelled to reproduce the sump water temperature (fig 2). This parameter however is not so relevant for structural integrity evaluation.
3. Parametric studies on condensate draining did not affect the peak pressure very much for this test, but affect the depressurisation rate after 100 S. A best fit with the water inventory in the sump was obtained for an overall homogeneous condensate film thickness of 0.75 mm (Fig 5).

TABLE 1 : SPATIAL MESH SIZES FOR CONTAINMENT HEAVY SINKS

STRUCTURE Description	Surface Area (m <sup>2</sup> )	First layer			Second layer			Third layer		
		material	total thick- ness (mm)	number of sublayers	material	total thick- ness (mm)	number of sublayers	material	total thick- ness (mm)	number of sublayers
Painted concrete	1018.9	paint	0.2	2	con- crete	15	10	con- crete	135	15
steel covered concrete	16.9	steel	11	10	con- crete	15	10	con- crete	135	15
steel compo- nents $0 < \delta < 4$	17.	steel	3.27	10						
steel compo- nents $4 < \delta < 6$	47.9	steel	5	10						
steel compo- nents $7 < \delta < 12$	21.1	steel	9.48	15						
steel compo- nents $\delta > 15$	0.3	steel	20	15						
aluminium components	11.4	alumi- nium	15	15						

FIG. 1. CHSP-2: CONTINUOUS PRESSURE

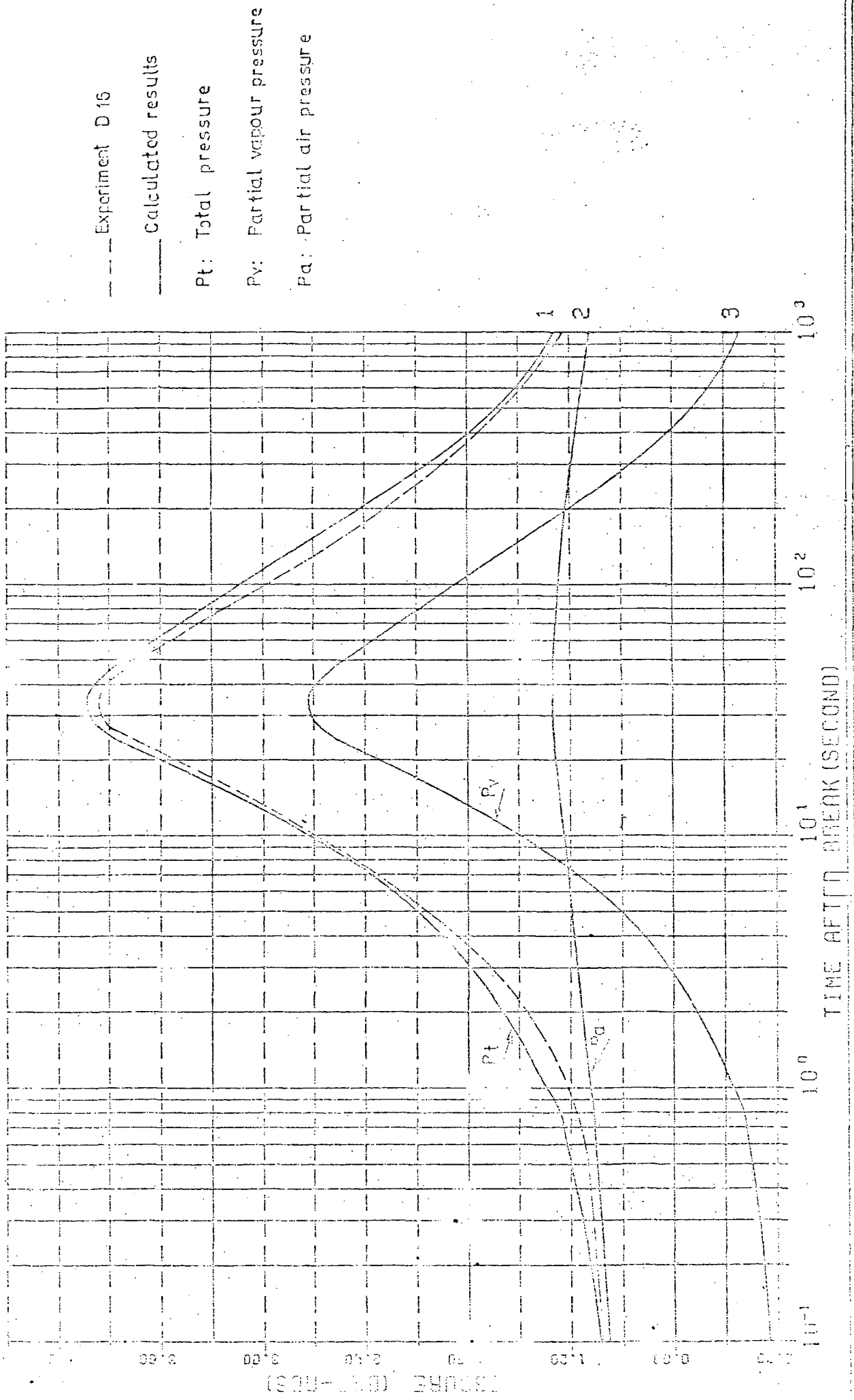


FIG 2 CASFE: CONTAINMENT TEMPERATURE

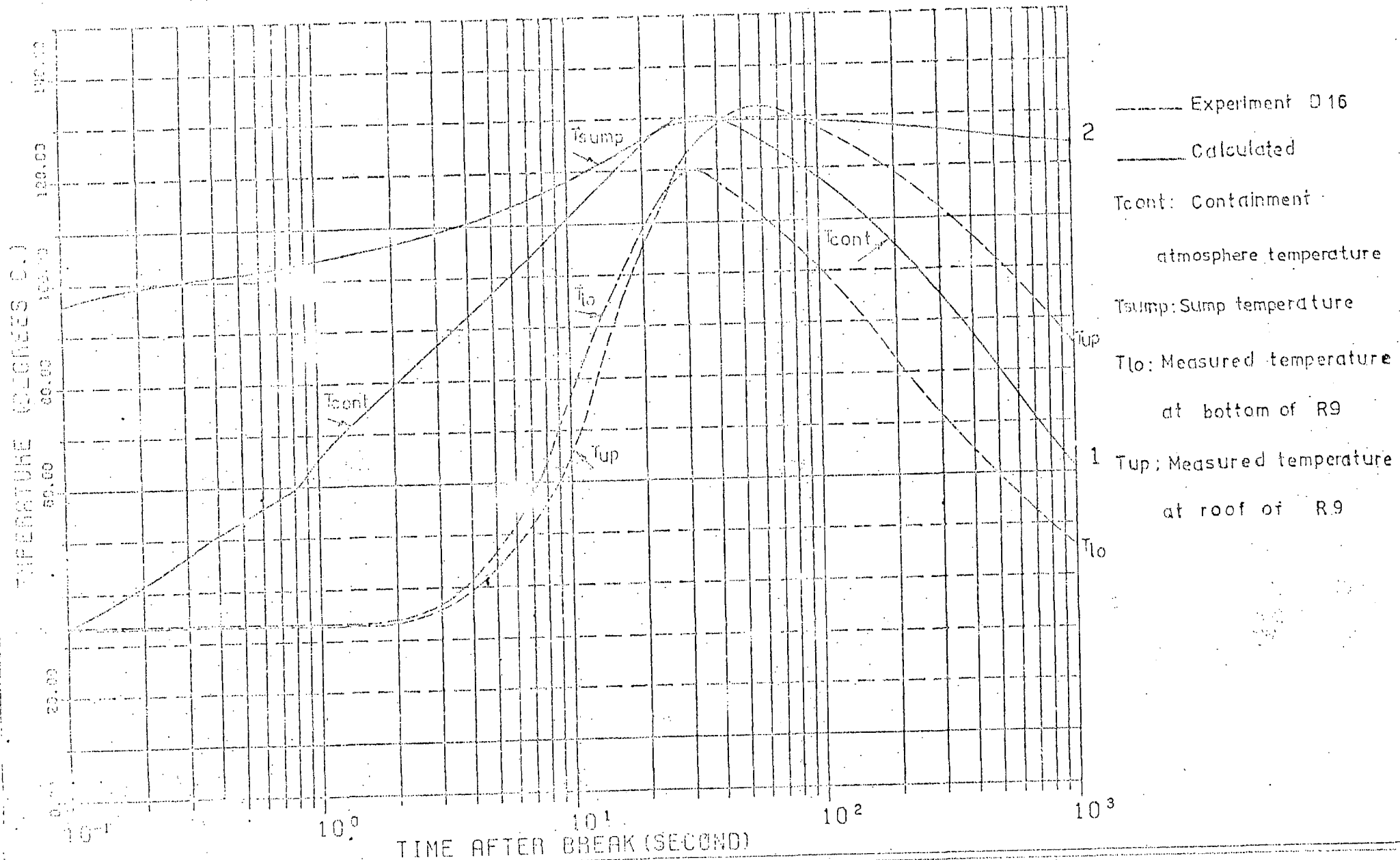
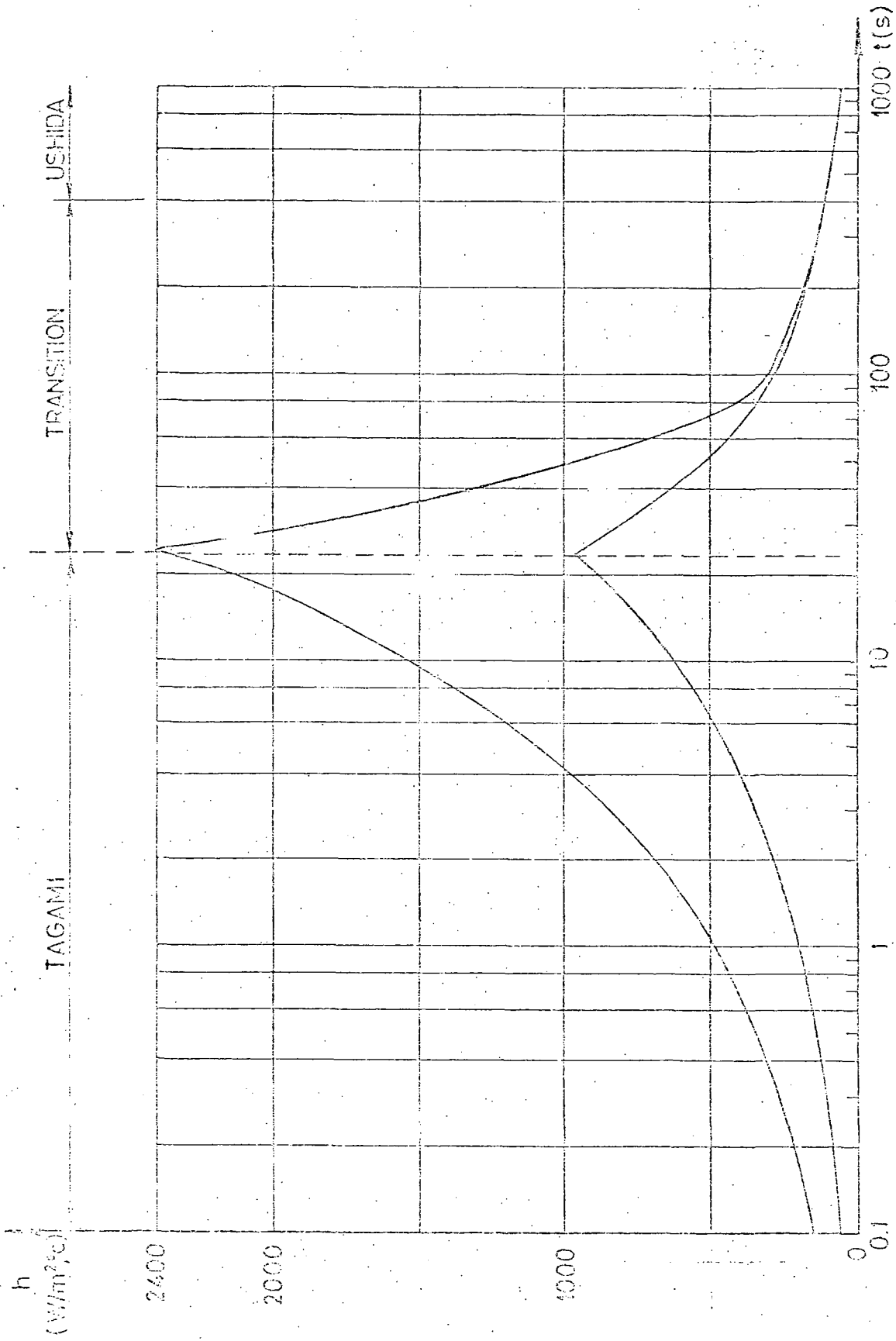


FIG. 3 : EVOLUTION OF THE HEAT TRANSFER COEFFICIENT FOR STEEL AND CONCRETE USING THE TAGAMI TAGAMI HIDA CORRELATION.



Mass  
(in g)

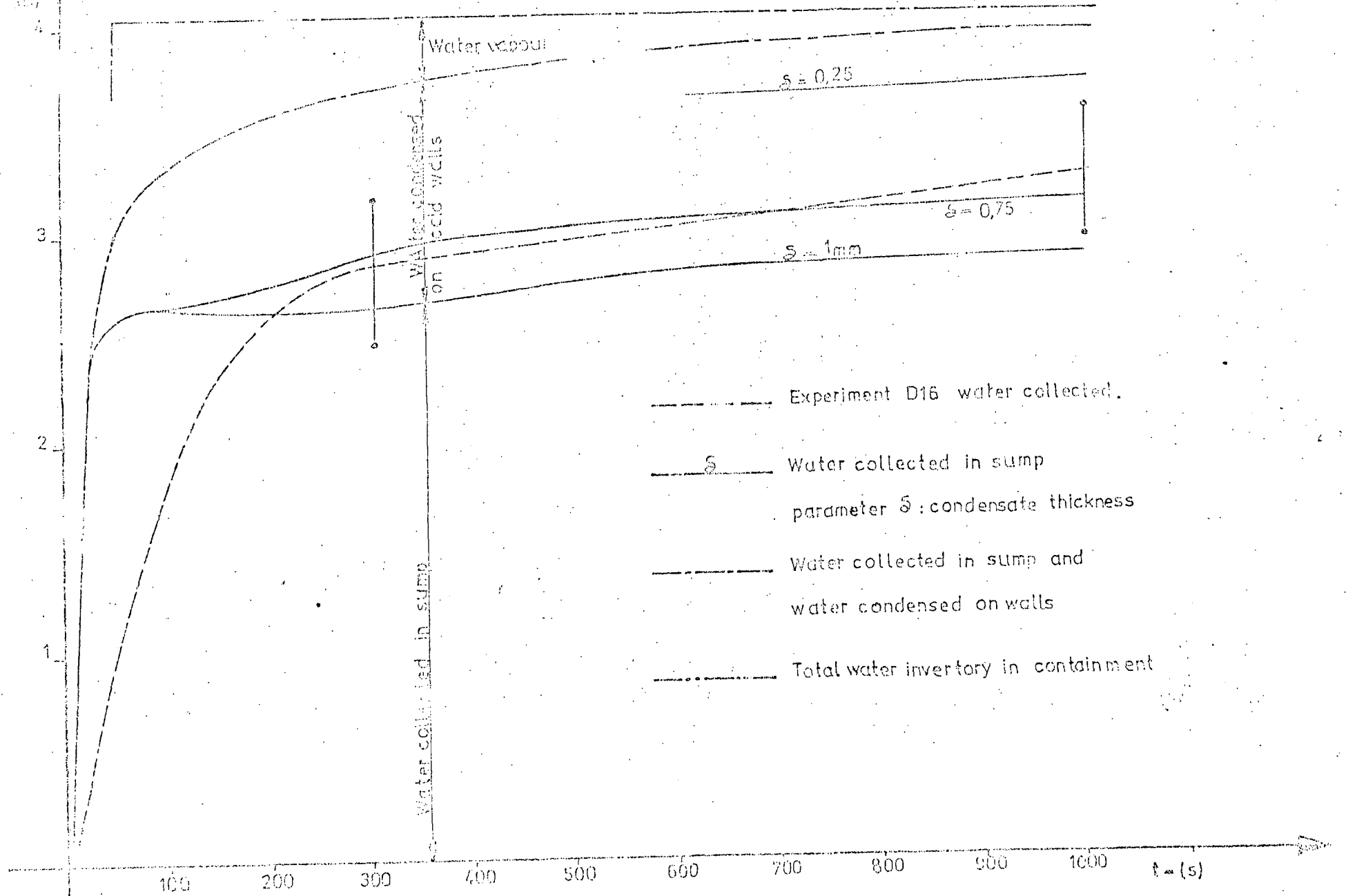
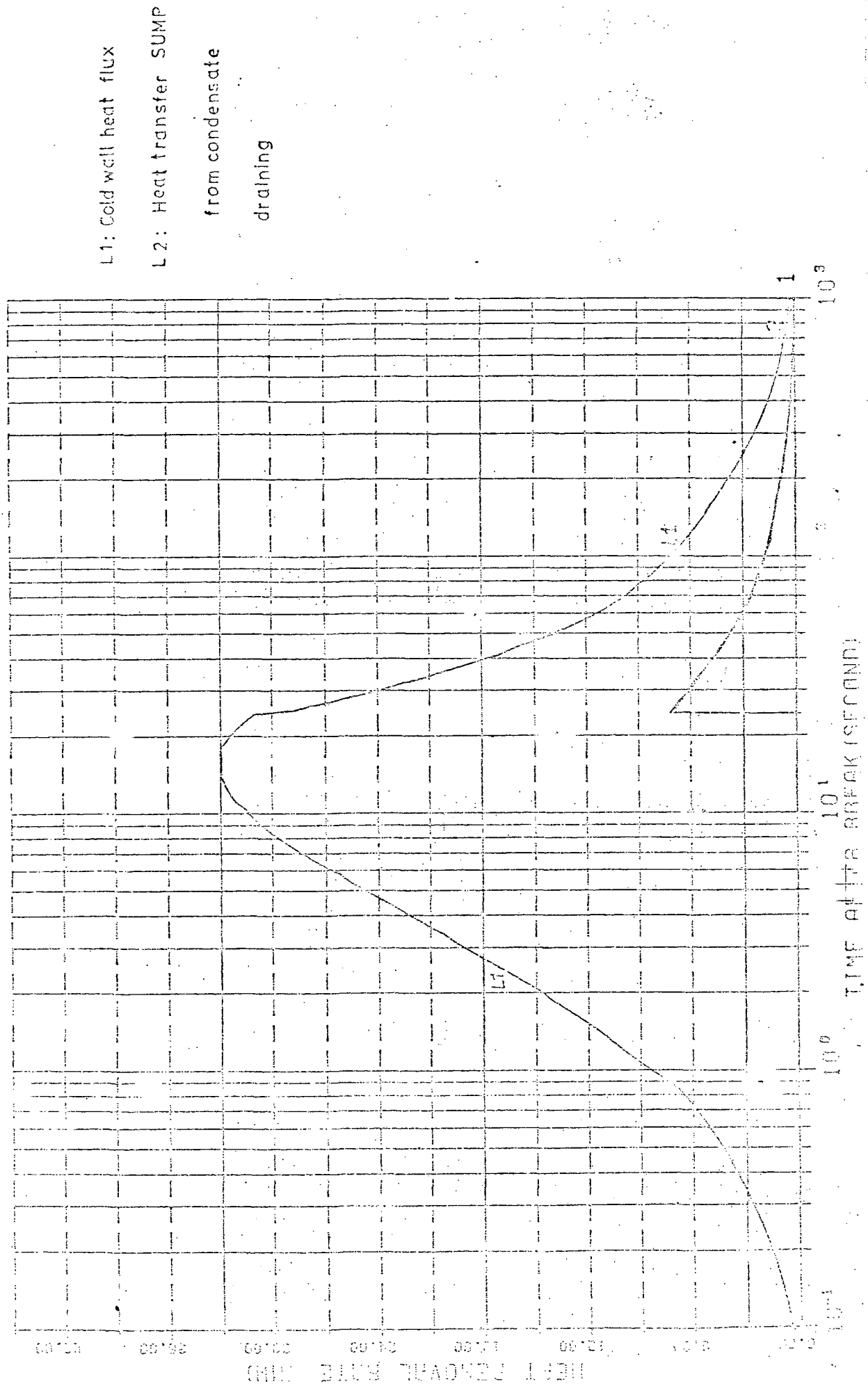


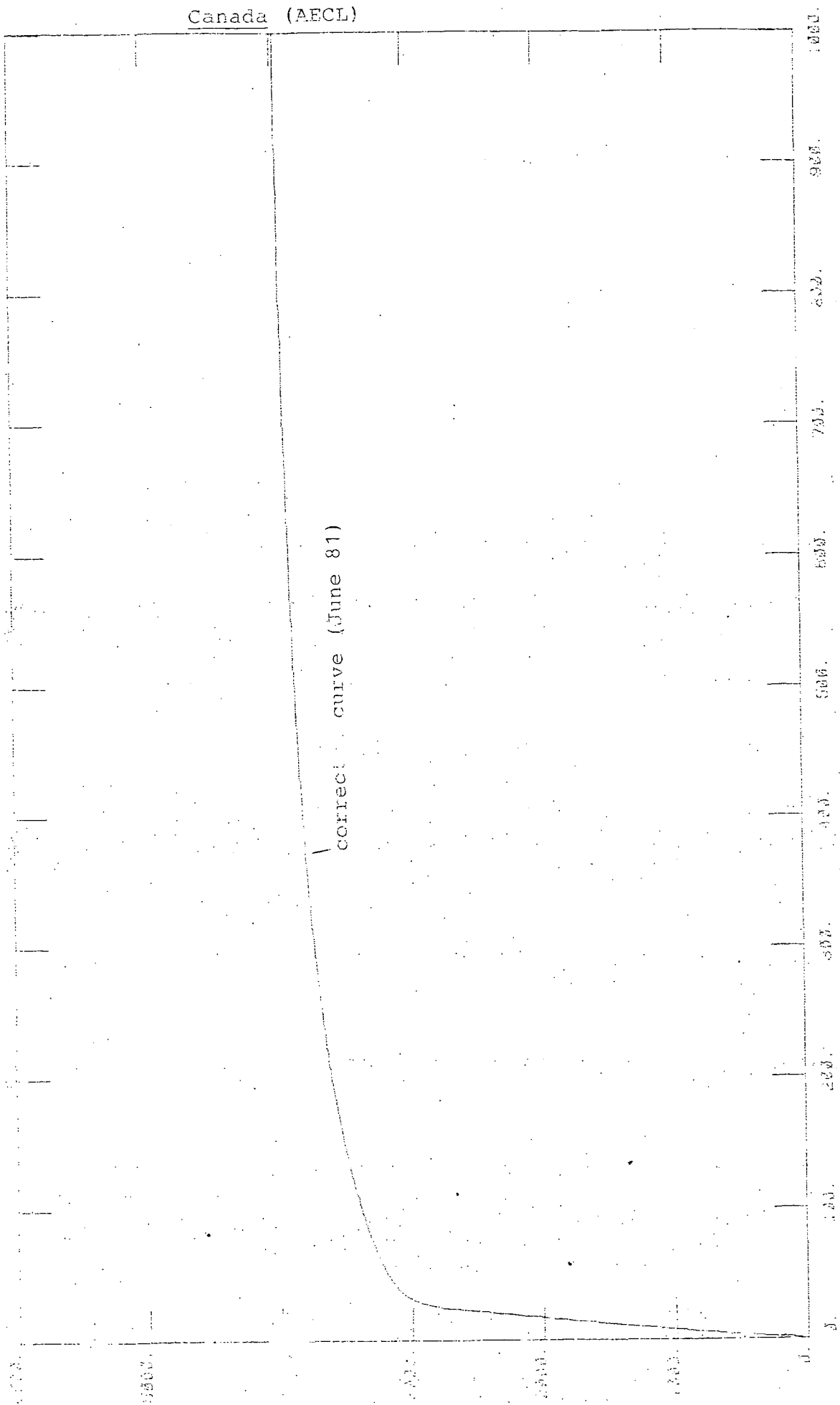


FIG 4 CASP2: COLD WALLS HEAT FLUX.



CONTINENT WATER PLUS

Canada (AECL)



EX 81 11 11 11

TIME SECONDS

## HEAT TRANSFER

The heat transfer correlation (H) used in short term and medium term calculations (when steam condenses on walls) proceeds from ECOTRA tests. It was established for steel coated or not. We assume that it is also valid for coated concrete.

Curves 1, 2, 3, 4, show the correlation values for concrete and steel in each subcompartment.

In the correlation, the temperature difference ( $\Delta T$ ) between gas and surface is at a negative power (less than 1). As the surface temperature of concrete increases more quickly than the one of uncoated steel, H increases more quickly too. It reaches a maximum value of about 20000 w/m<sup>2</sup>°k whereas the peak value for tagami correlation would have been about 1200 w/m<sup>2</sup>°k.

The heat flux is nevertheless smaller for concrete than for steel (curves 5,6, because, in the flux formula,  $\Delta T$  arises at a positive power.

## MESH SIZING

The description of the wall mesh sizing used in GRUYER computer code is available in the appendix I of (1). A copy of this appendix is attached to this letter.

## KINETIC ENERGY

In each subcompartment the mixture is considered to be in equilibrium and in static condition. So the last column of table 7 in (2) should be modified ( $E_k = 0$ ).

---

1) Containment Standard Problem n°2 - Pressure Distribution within the containment following a pipe break - French short report A. MATTEI, D. ROY, A. SONNET (DRE/STRE/LMTA/80/029).

2) Comparison report on OECD-CSNI Containment Standard Report n°2.  
by D.L. NGUYEN, may 1981.

H  
v/m<sup>2</sup>h

GRUYER-FRANCE

20000

10000

0

TR1

TR2

TR3

TR4

TR5

0

1

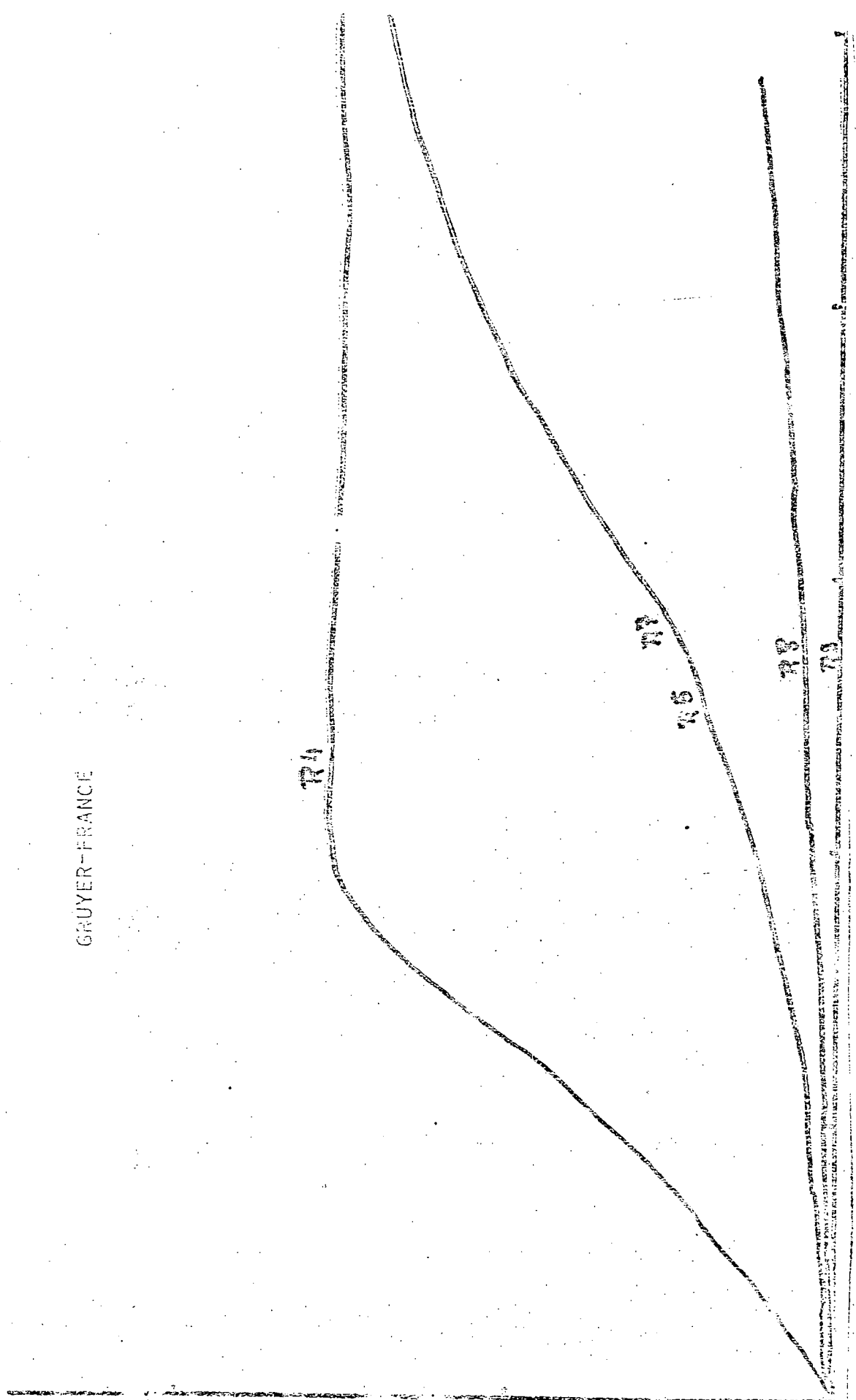
2

TIME (s)

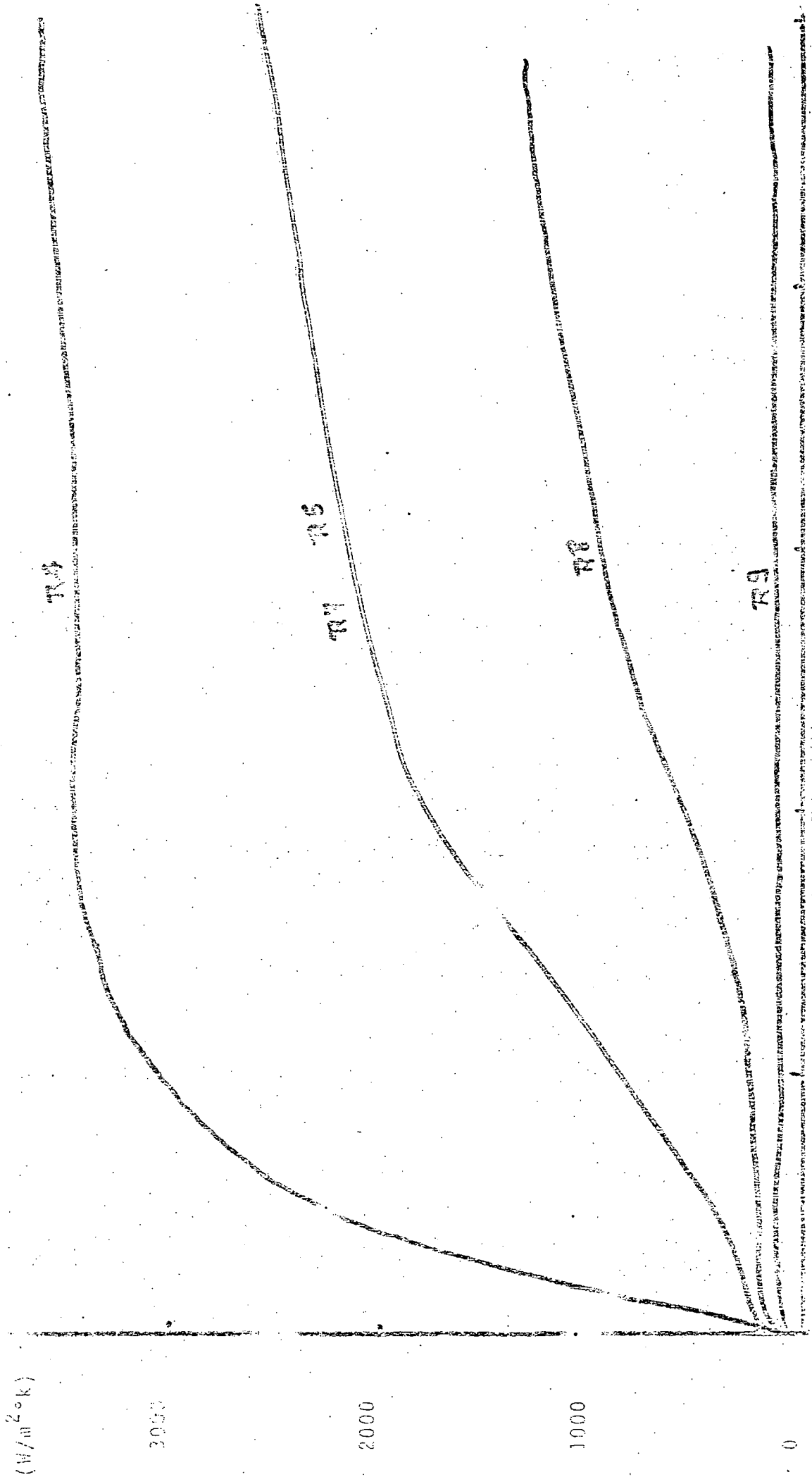
CASP 2

CONCRETE

ECOTRA



GRUYER - FRANCE



STEEL ECOTRA

TIME (s)

Fig. 2

$W/m^2 \cdot s \cdot K$

GRUYER - FRANCE

R5 R7

R4

R8 R9

20000

10000

0

10

20

30

40

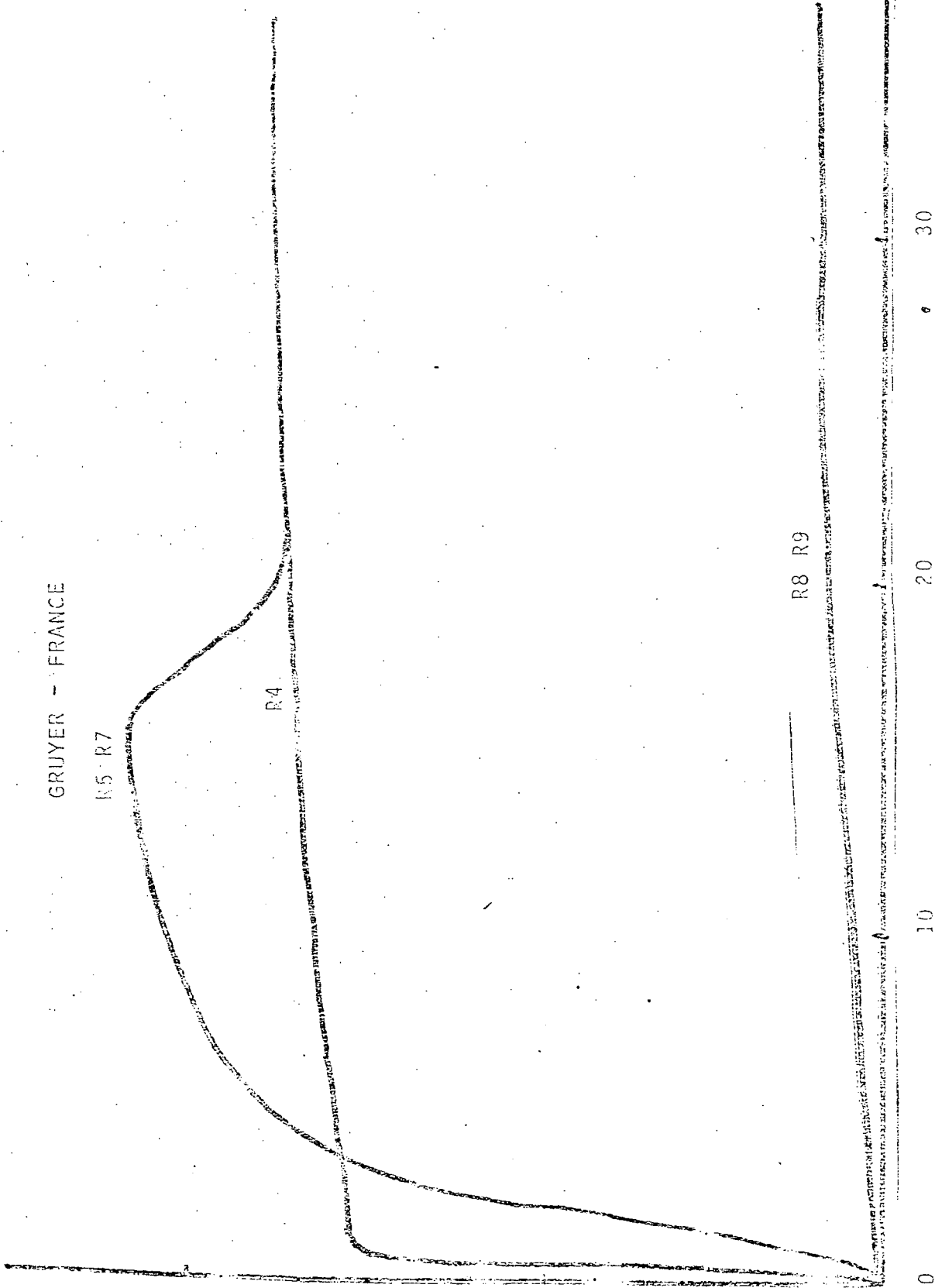
CASP 2

CONCRETE

ECOTRA

TIME (s)

Fig. 3



H.

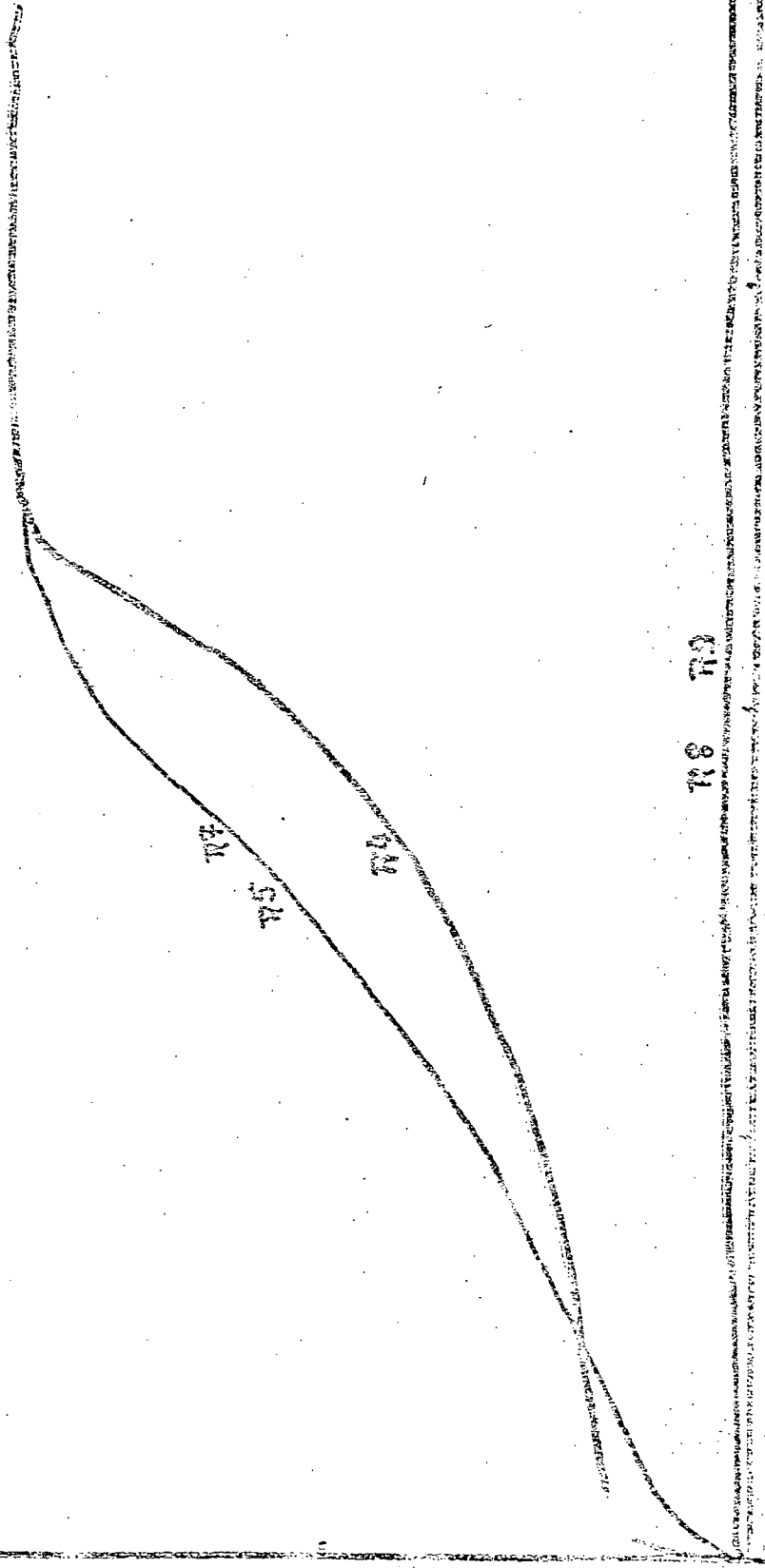
(10<sup>4</sup> m<sup>2</sup>/s)

GRUYER ICE

20000

10000

0



0

10

20

30

40

CASP 2

STEEL

ECOTRA

74 75

TIME (s)

Fig. 4.

GRUYER FRANCE

(kJ/m<sup>2</sup>)

184

200

100

0

R5  
R4

R3

10

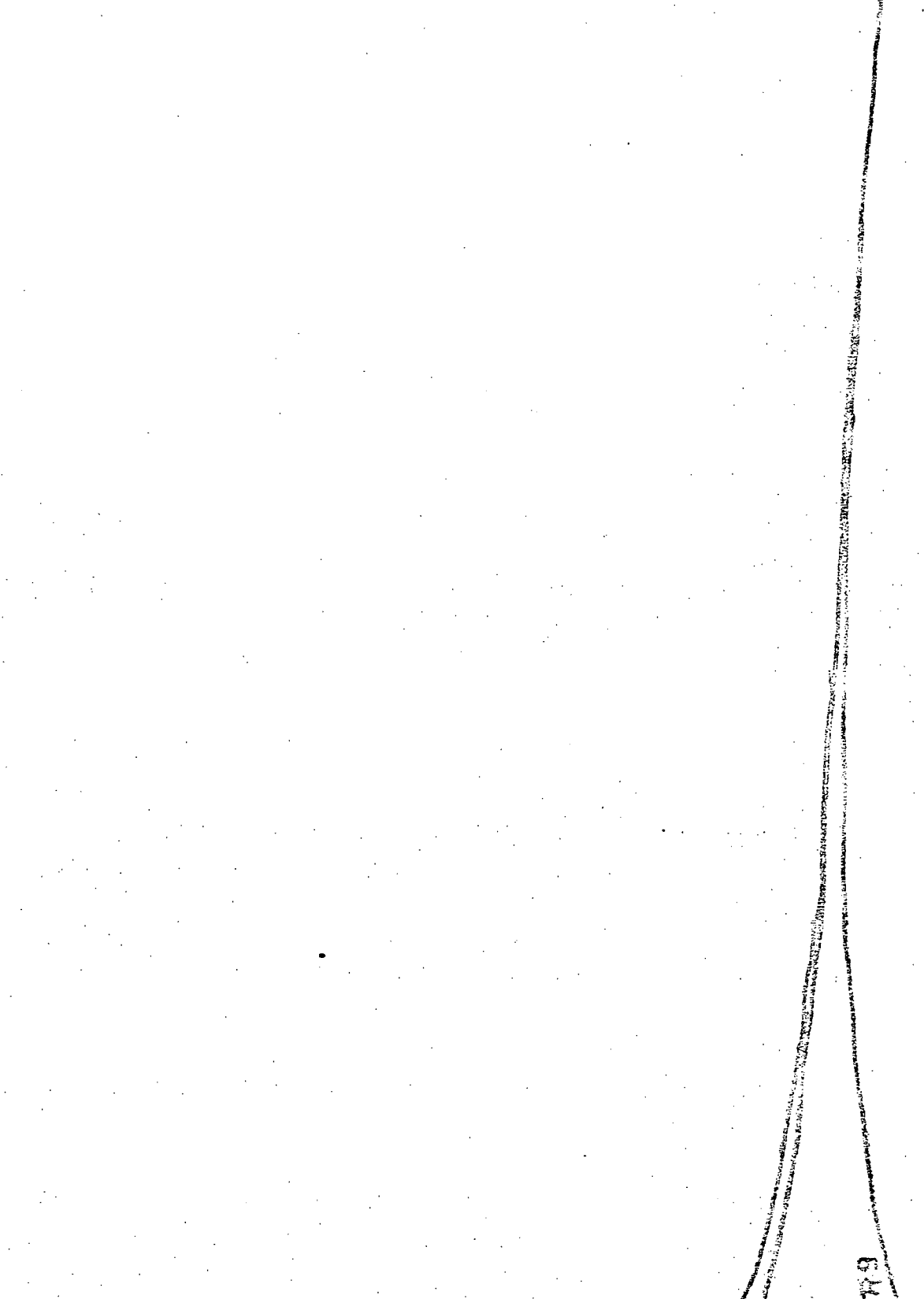
20

30

TIME (s)

GASP 2 CONCRETE ECOTRA

Fig. 5.





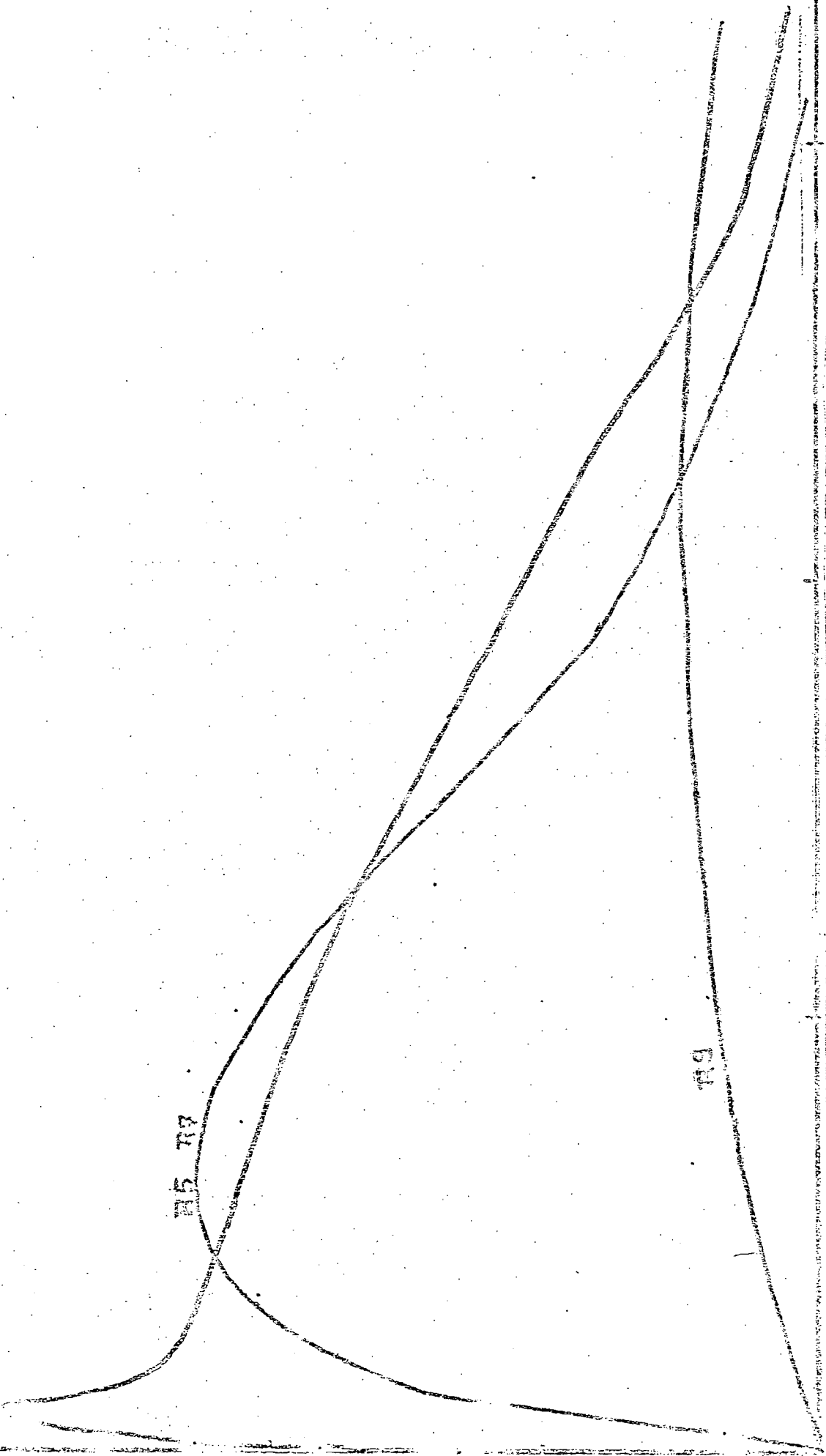
Heat Flux

$\text{kW/m}^2$

GRUYER - FRANCE

100

0



15 75

25 100

0

10

20

30

TIME (s)

CAS 2 STEEL ECOTRA

## 5 - HEAT CONDUCTING SYSTEMS DESCRIPTION

5.1 - 0. to 2.5 s - 0. to 50. s

Heat conducting system	nb	1
Name		concrete within compartment R5
Area		76.08 m <sup>2</sup>
Internal contact		air - water mixture of compartment R5
Internal heat transfer coefficient		ECOTRA CORRELATION
External contact		10°C
External heat transfer coefficient		10 <sup>-3</sup> W/m <sup>2</sup> .°C
Description of successive layers		

0. to 2.5 s

layer nb	nature	thickness (m)	number of nodes
1	coating	0.7 10 <sup>-3</sup>	2
2	concrete	6 × 10 <sup>-3</sup>	34
3	concrete	0.119	11

0. to 50. s

layer nb	nature	thickness (m)	number of nodes
1	coating	0.7 10 <sup>-3</sup>	2
2	concrete	0.024	34
3	concrete	0.101	11

Heat conducting system nb 2

Name steel within compartment R5

Area 8.94 m<sup>2</sup>

Internal contact air - water mixture of compartment R5

Internal heat transfer coefficient ECOTRA CORRELATION

External contact air - water mixture of compartment R5

External heat transfer coefficient ECOTRA CORRELATION

Description of successive layers

0. to 2.5 s

layer nb	nature	thickness (m)	number of nodes
1	steel	0.0190	30

0. to 50. s

layer nb	nature	thickness (m)	number of nodes
1	steel	0.01908	10

Heat conducting system nb 3  
 Name concrete within compartment R4  
 Area 38.63 m<sup>2</sup>  
 Internal contact air - water mixture of compartment R4  
 Internal heat transfer coefficient ECOTRA CORRELATION  
 External contact 10°C  
 External heat transfer coefficient 10<sup>-3</sup> W/m<sup>2</sup>.°C  
 Description of successive layers

0. to 2.5 s

layer nb	nature	thickness (m)	number of nodes
1	coating	0.7 10 <sup>-3</sup>	2
2	concrete	6 × 10 <sup>-3</sup>	34
3	concrete	0.119	11

0. to 50. s

layer nb	nature	thickness (m)	number of nodes
1	coating	0.7 × 10 <sup>-3</sup>	2
2	concrete	0.024	34
3	concrete	0.101	11



Heat conducting system      nb      5

Name      concrete within compartment R7

Area      76.63 m<sup>2</sup>

Internal contact      air - water mixture of compartment R7

Internal heat transfer coefficient      ECOTRA CORRELATION

External contact      10 °C

External heat transfer coefficient      10<sup>-3</sup> W/m<sup>2</sup>.°C

Description of successive layers

0. to 2.5 s

layer nb	nature	thickness (m)	number of nodes
1	coating	0.7 × 10 <sup>-3</sup>	2
2	concrete	6 × 10 <sup>-3</sup>	34
3	concrete	0.119	11

0. to 10. s

layer nb	nature	thickness (m)	number of nodes
1	coating	0.7 × 10 <sup>-3</sup>	2
2	concrete	0.024	34
3	concrete	0.101	11

Heat conducting system      nb      6

Name      steel within compartment R7

Area      8.64 m<sup>2</sup>

Internal contact      air - water mixture of compartment R7

Internal heat transfer coefficient      ECOTRA CORRELATION

External contact      air - water mixture of compartment R7

External heat transfer coefficient      ECOTRA CORRELATION

Description of successive layers

0. to 2.5 s

layer nb	nature	thickness (m)	number of nodes
1	steel	0.01436	30

0. to 50. s

layer nb	nature	thickness (m)	number of nodes
1	steel	0.01436	10

Heat conducting system nb 7

Name concrete within compartment R8

Area 91.67 m<sup>2</sup>

Internal contact air - water mixture of compartment R8 (0 - 2.5) R9 (0 - 50.) ECOTRA CORRELATION

Internal heat transfer coefficient

External contact 10°C

External heat transfer coefficient 10<sup>-3</sup> W/m<sup>2</sup>.°C

Description of successive layers

0. to 2.5 s

layer nb	nature	thickness (m)	number of nodes
1	coating	0.7 10 <sup>-3</sup>	2
2	concrete	6 × 10 <sup>-3</sup>	34
3	concrete	0.119	11

0. to 50. s

layer nb	nature	thickness (m)	number of nodes
1	coating	0.7 10 <sup>-3</sup>	2
2	concrete	0.024	34
3	concrete	0.101	11



Heat conducting system nb 8  
 Name steel within compartment R8  
 Area 2.69 m<sup>2</sup>  
 Internal contact air - water mixture of compartment  
 Internal heat transfer coefficient R8 (0. to 2.5)  
 External contact R9 (0. to 50.)  
 External heat transfer coefficient ECOTRA CORRELATION  
 Description of successive layers air - water mixture of compartment  
 R8 (0. to 2.5) R9 (0. to 50.)  
 ECOTRA CORRELATION

0. to 2.5 s

layer nb	nature	thickness (m)	number of nodes
1	steel	0.01618	30

0. to 50. s

layer nb	nature	thickness (m)	number of nodes
1	steel	0.01618	10

Heat conducting system nb 9  
 Name concrete within compartment R9  
 Area 645.82 m<sup>2</sup>  
 Internal contact air - water mixture of compartment R9  
 Internal heat transfer coefficient ECOTRA CORRELATION  
 External contact 10°C  
 External heat transfer coefficient 10<sup>-3</sup> W/m<sup>2</sup>.°C  
 Description of successive layers

0. to 2.5 s

layer nb	nature	thickness (m)	number of nodes
1	coating	0.7 · 10 <sup>-3</sup>	2
2	concrete	6 × 10 <sup>-3</sup>	34
3	concrete	0.119	11

0. to 50. s

layer nb	nature	thickness (m)	number of nodes
1	coating	0.7 · 10 <sup>-3</sup>	2
2	concrete	0.024	34
3	concrete	0.101	11

Heat conducting system nb 10  
 Name steel within compartment R9  
 Area 30.54 m<sup>2</sup>  
 Internal contact air - water mixture of compartment R9  
 Internal heat transfer coefficient ECOTRA CORRELATION  
 External contact air - water mixture of compartment R9  
 External heat transfer coefficient ECOTRA CORRELATION  
 Description of successive layers

0. to 2.5 s

layer nb	nature	thickness (m)	number of nodes
1	steel	0.01353	30

0. to 50. s

layer nb	nature	thickness (m)	number of nodes
1	steel	0.01353	10

Heat conducting system nb 11  
 Name concrete within compartment R5  
 Area  $90.12 \text{ m}^2$   
 Internal contact air - water mixture of compartment R9  
 Internal heat transfer coefficient ECOTRA CORRELATION  
 External contact  $10^\circ\text{C}$   
 External heat transfer coefficient  $10^{-3} \text{ W/m}^2 \cdot ^\circ\text{C}$   
 Description of successive layers

0. to 2.5 s

layer nb	nature	thickness (m)	number of nodes
1	coating	$0.7 \cdot 10^{-3}$	2
2	concrete	$6 \times 10^{-3}$	34
3	concrete	0.119	11

0. to 50. s

layer nb	nature	thickness (m)	number of nodes
1	coating	$0.7 \cdot 10^{-3}$	2
2	concrete	0.024	34
3	concrete	0.101	11

Heat conducting system nb 12  
 Name steel within compartment R6  
 Area 2.97 m<sup>2</sup>  
 Internal contact air - water mixture of compartment R9  
 Internal heat transfer coefficient ECOTRA CORRELATION  
 External contact air - water mixture of compartment R9  
 External heat transfer coefficient ECOTRA CORRELATION  
 Description of successive layers

0. to 2.5 s

layer nb	nature	thickness (m)	number of nodes
1	steel	0.017	30

0. to 50. s

layer nb	nature	thickness (m)	number of nodes
1	steel	0.017	10

5.2 - 0. to 1000. s

Heat conducting system	nb	1
Name		internal concrete
Area		297 m <sup>2</sup>
Internal contact		air - water mixture within containment
Internal heat transfer coefficient		1300 W/m <sup>2</sup> .°C (0. to 50. s) Uchida (after 50. s)
External contact		air - water mixture within containment
External heat transfer coefficient		1300 W/m <sup>2</sup> .°C (0. to 50. s) Uchida (after 50. s)
Description of successive layers		

layer nb	nature	thickness (m)	number of nodes
1	coating	$0.7 \times 10^{-3}$	2
2	concrete	0.075	15
3	concrete	0.17	11
4	concrete	0.075	15
5	concrete	$0.7 \times 10^{-3}$	2

Heat conducting system nb 2

Name walls, dome, floor

Area 418.74 m<sup>2</sup>

Internal contact air - water mixture within containment

Internal heat transfer coefficient 1300 W/m<sup>2</sup>.°C (0. to 50. s)  
Uchida (after 50. s)

External contact

External heat transfer coefficient 9°C

Description of successive layers 10<sup>-3</sup> W/m<sup>2</sup>.°C

layer nb	nature	thickness (m)	number of nodes
1	coating	0.7 × 10 <sup>-3</sup>	2
2	concrete	0.16	40
3	concrete	0.29	5

Heat conducting system nb 3

Name internal steel

Area 56.38 m<sup>2</sup>

Internal contact air - water mixture within containment

Internal heat transfer coefficient 1300 W/m<sup>2</sup>.°C (0. to 50. s)  
1.5 (ΔT)<sup>1/3</sup> (after 50. s)

External contact air - water mixture within containment

External heat transfer coefficient 1300 W/m<sup>2</sup>.°C (0. to 50. s)  
1.5 (ΔT)<sup>1/3</sup> (after 50. s)

Description of successive layers

layer nb	nature	thickness (m)	number of nodes
1	steel	0.00763	5

Italy (CNEN/Pisa)

Amendments to our Report on CASP2 /25/:

- a new version of pages 5 and 9 of the Report with modifications to the considerations about the choice of heat transfer coefficients in short and medium term calculations;
- the final version of table A1.2 (page 51 of the Report) with the indication of mesh used for the different heat slabs;
- a new Addendum, which presents the work we made on the light of Edward's benchmark problem.



### 3. MODELLING

#### 3.1 - Short and medium term calculations

The experimental facility (Fig.I) has been subdivided into 4 control volumes (Fig.II).

The volumes R9,R6 and R8 have been joined together. In fact, R6 can be considered as an appendix of R9 compartment (R6 is connected only with R9 ; besides, the flow area between R9 and R8 is about four times greater than that between R7 and R8.

33 heat structures with slab geometry have been modelled as specified below (Fig. II).

- 16 steel structures;
- 13 concrete structures with coating;
- 4 aluminum structures.

The gap between R4 and R9 has been taken into account as a time dependent junction area.

The values of the most important parameters are summarized in Appendix 1.

The loss coefficients at the junctions were obtained from Idel'chik formulas<sup>/7/</sup>.

An energy dependent correlation has been used, following an approach similar to that of J. Marshall<sup>/8/</sup>, for heat transfer coefficient for R4,R5 and R7 volumes (which are directly interested by the blow down).

The correlation is based on the proportionality between heat transfer coefficient and blow down energy rate (Fig.III); that is:

$$H = \frac{H_o}{\dot{E}_o} \dot{E} \quad (1)$$

As reference value of the heat transfer coefficient the value  $H_o = 900 \text{ W/m}^2 \cdot \text{K}$  at the knee of the blow down flow-rate (24 sec) has been

chosen, because the initial turbulent phase is finishing and conditions are settling. Obviously  $\dot{E}_0$  is the blow-down power inlet at the same time.

Regarding the heat transfer coefficient in compartment R9, the value about blow-down end (30 sec) has been evaluated on the basis of air/steam ratio. A linear trend has been assumed in the previous time interval, according to the increasing of the steam ratio (Fig. III) and a behaviour similar to that in the up-stream compartments after 30 seconds.

### 3.2 - Long term calculation

The containment is modelled with two nodes containing all the heat structures (Fig. IV).

The first node consists of R4, R5 and R7 volumes (the R4-R7 and R4-R5 flow areas are twice greater than the R5-R9 and R7-R9 ones).

The flow area between the two nodes is a "penetration" leakage (ideal gas flow through orifice).

Up to the end of blow down (40 sec) the same heat transfer coefficients as in the short and medium term calculations have been used. After this period, turbulence diminishes and free convection prevails, with a lower heat transfer; so, for both volumes, a value of  $20 \text{ W/m}^2 \cdot \text{K}$  at 1000 sec has been adopted. A linear behaviour has been assumed in the time interval 40-1000 sec (Fig. V).

MATERIAL	COARSE MESH (m)	IMPROVED MESH (m)
Coating	$2.5 \cdot 10^{-4}$	$2.5 \cdot 10^{-5}$
Concrete	$35.0 \cdot 10^{-3}$	$5+6 \cdot 10^{-3}$
Steel	$1.5 \cdot 10^{-3}$	$0.8 \cdot 10^{-3}$
Alluminium	$1.5 \cdot 10^{-3}$	$0.8 \cdot 10^{-3}$

Table A1.2 Interval lengths used in the finite difference calculations for the heat conduction structures.

ADDENDUM 3



PARAMETRIC ANALYSIS OF HEAT TRANSFER PHENOMENA

### A3.1 Introduction

On the basis of the experience achieved taking part to the "CSNI NUCLEAR BENCHMARK PROBLEM ON CONTAINMENT CODES", a new set of calculations has been executed for CASP2 with an improved mesh for the heat slabs (Table A1.2)

Both medium and long term transient have been analyzed.

The results show that we should acquire more knowledge about the influence of heat transfer coefficient and coating thermal characteristics on the thermohydraulic transient inside the containment system.

### A3.2 Calculations by ARIANNA Code

In calculations with improved mesh, the heat transferred from a compartment to the related structures is reduced if compared with the results obtained in coarse mesh calculations. So temperatures and pressures in the containment are overestimated in comparison with the experimental data and this difference increases with the time; an example is shown in Fig. AD3.1 case b) for the pressure behaviour in R4 compartment, calculated by ARIANNA Code.

To have again a good matching of the experimental data (Fig. AD3.1 case c), the heat transfer coefficients were increased by about 25% in comparison with the cases a) and b) (see Fig. AD3.2)

### A3.3 Calculations by CONTEMPT LT-26 Code

The long term transient was calculated by CONTEMPT Code, using as input data the same heat transfer coefficient (Fig. AD3.2, case c) and also the same mesh of the last ARIANNA calculation.

The results show first an overestimation of the pressure peak (Fig. AD3.3 case c), but after 400 sec they agree to the experimental data very satisfactorily.

The difference between the peak values calculated by ARIANNA and CONTEMPT Codes is due to the different thermohydraulic models: in ARIANNA Code an homogeneous volume is assumed, while CONTEMPT Code adopts a two phase model. More precisely, in this last case each node includes a vapor region and a liquid region; evaporation, condensation and pool boiling process are modelled.

As a result, more energy remains in the vapor region than in the homogeneous mixture case.

The homogeneous model simulates well the physical phenomena in the compartments in the short and medium term transient, due to the strong turbulent flow of blow-down. After the blow-down phase the initial turbulence decreases and the separation between the liquid and the vapor region (CONTEMPT model) approximates better the real situation.

On the basis of the above said experience, some attempts have been made to improve the agreement with the experimental data and also to understand better the influence of the various parameters on the phenomena with the aim of establishing a strategy for the choice of values of these parameters.

The most significant results can be seen in Fig. AD3.3 cases d) and e).

In case d) the heat transfer coefficient  $h$  in the first node is proportional to the blow-down energy till 24 sec (at that time the blow-down energy decreases abruptly) while after 50 sec  $h$  is given by Uchida correlation; also the values of the heat transfer coefficient at 24 and 50 sec are calculated by Uchida correlations ( $h_0 = 1600 \text{ W/m}^2 \cdot \text{K}$  at 24 sec and  $h_1 = 600 \text{ W/m}^2 \cdot \text{K}$  at 50 sec) and a linear behaviour has been assumed between 24 and 50 sec (Fig. AD3.2 case d).

In the external compartment,  $h$  has been calculated by the Uchida correlation, after the blow-down phase ( $t > 50 \text{ sec}$ ), while a linear increase has been assumed during the blow-down phase, starting from the value of  $20 \text{ W/m}^2 \cdot \text{K}$  at 0 sec (see Fig. AD3.4 case d).

All the other parameters (thickness and thermal conductivity of the coating, mesh, ecc) are the same as in the previous case.

In case e), we use heat transfer coefficients similar to case d) <sup>(\*)</sup>, but the coating thickness has been triplicated; all the other input data are the same as in the previous case.

As shown in Fig. AD3.3, in case d) the pressure peak is estimated well, owing to the increasing of heat transfer in the external compartment, which compensates the effect of CONTEMPT phase separation model; later the pressure drops down the experimental curve.

In case e), the pressure peak is little overestimated, due to the effect of coating thickness, but from 100 secs on the agreement with the experimental data is quite satisfactorily.

---

(\*) In the external compartment the Uchida correlation has been used also in the interval 0-50 secs (see Fig. AD3.4 case e)

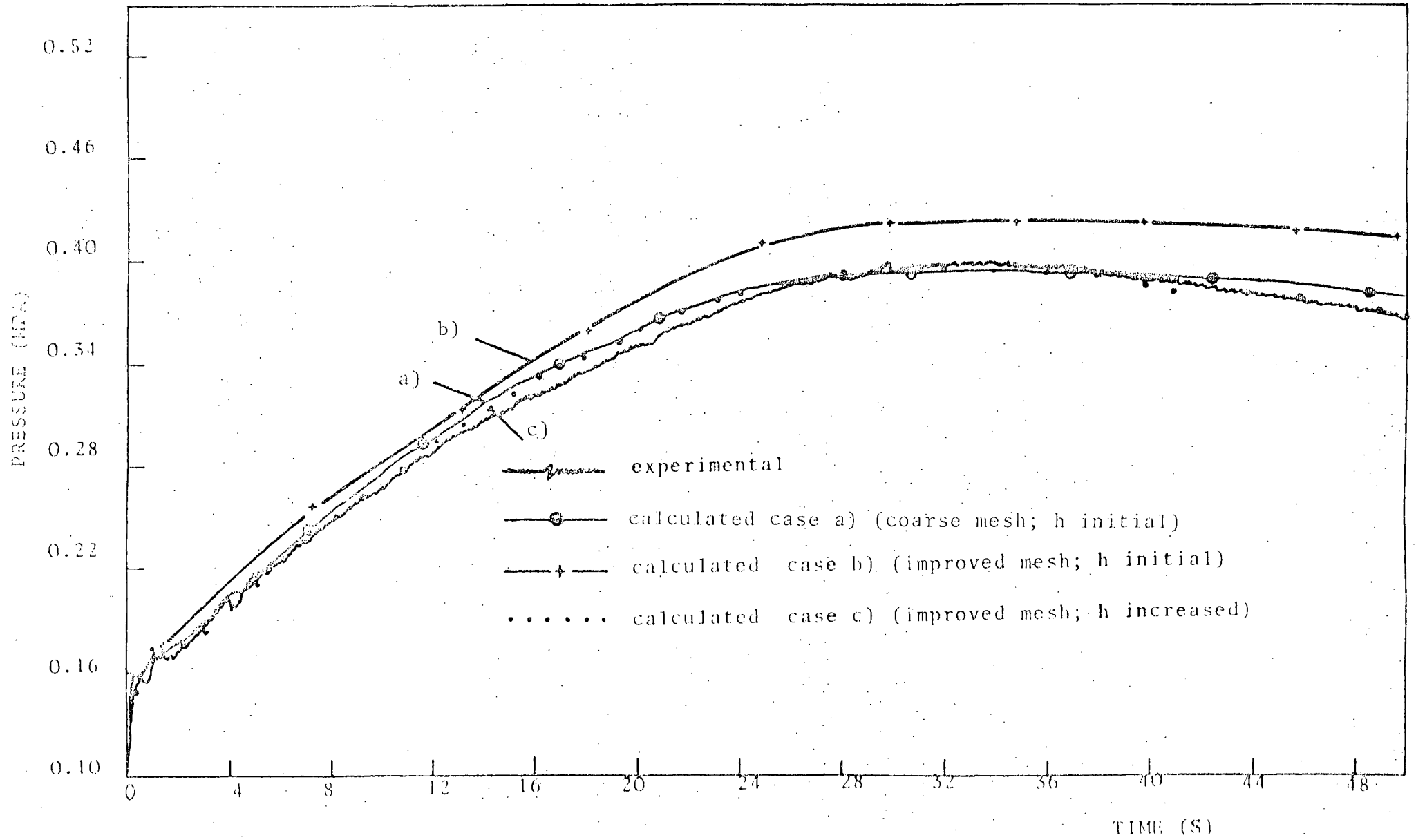


FIG. AD3.1 Pressure in R4 compartment (ARIANNA 1 calculations)



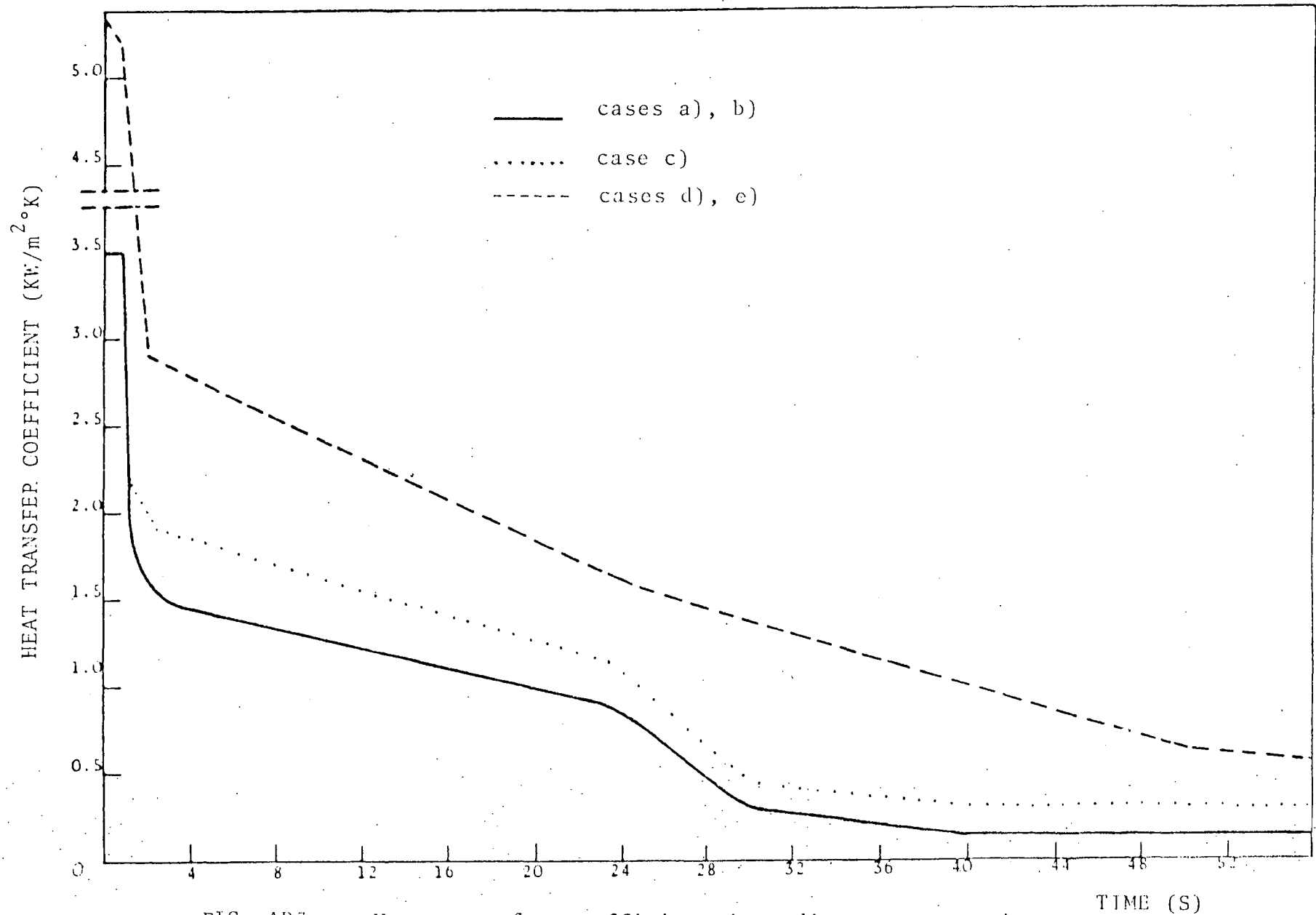


FIG. AD3. Heat transfer coefficient in medium term transient

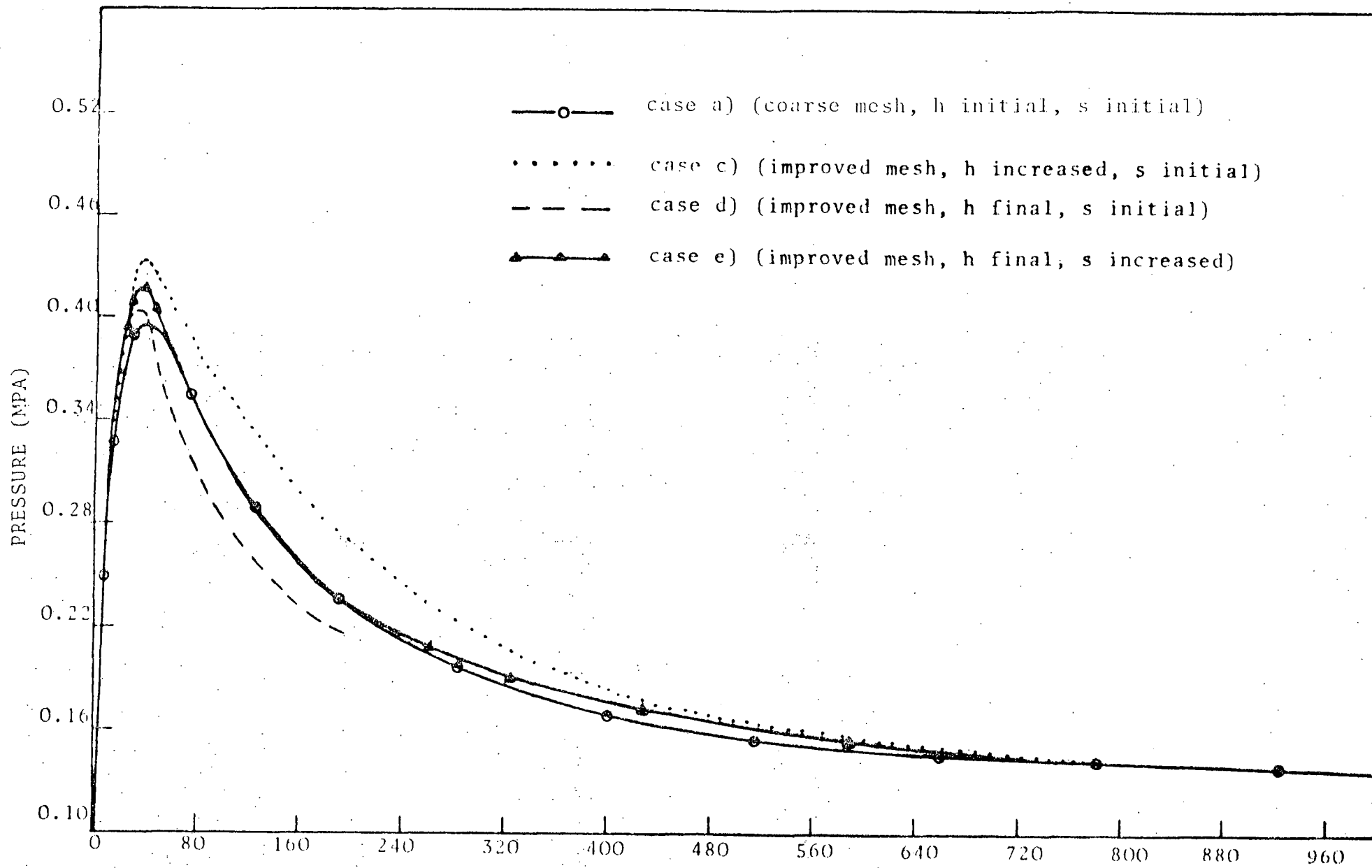


FIG. AD3.3 Pressure in R9 compartment (CONTEMPT LT26 calculations) TIME (S)

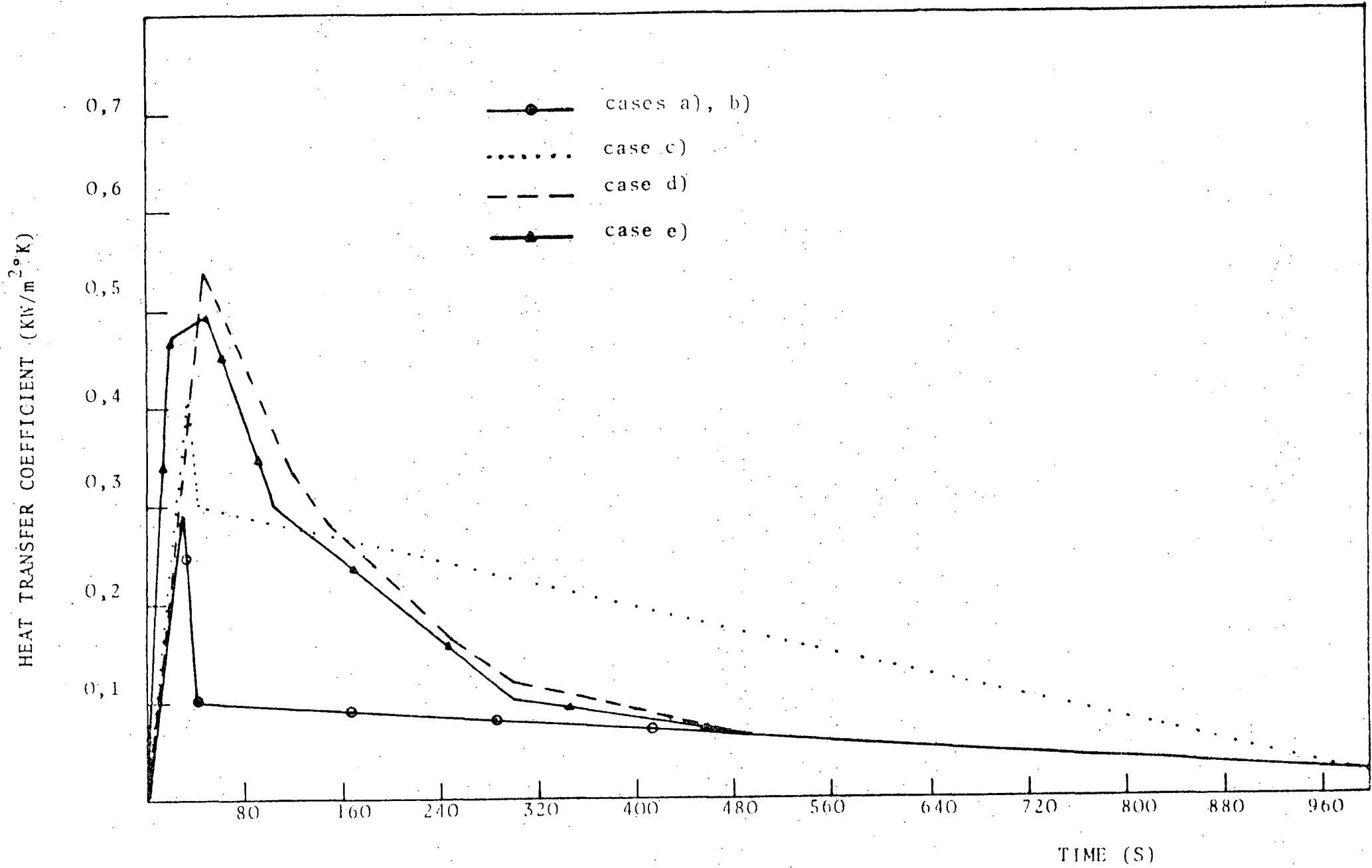


FIG. AD3.4 Heat transfer coefficient in R9 compartment

Sweden (Studsvik)

OECD-CSNI Containment Standard Problem No. 2

Supplementary information for the comparison report for the runs made in Sweden with COPTA-6. The program does not print all those data; so some have been estimated manually.

1. Meshsizes (mm)

Coating:  $0.95/3=0.32$  (3 nodes for 0.95 mm)

Concrete: 0.076, 0.114, 0.171, 0.257, 0.386 etc.

(17 nodes for 150 mm, increasing with factor 1.5)

Steel, typically: 0.29, 0.43, 0.65, 0.97, 1.46, 2.19

(6 nodes for 6 mm, increasing with factor 1.5)

For the concrete the nodesizes

2. Total heat flux into solids, MW

Time(s)	50s case	1000s case
1	34.1	28.6
2	35.7	29.8
5	32.0	27.7
10	28.3	25.4
20	24.2	22.1
50	14.0	13.4
100		8.1
200		4.8
500		1.9
1000		0.74

The difference between the 50s case and the 1000s case is due to two factors

- 4-room model in 50s case, 1-room model in 1000s case
- higher heat transfer to dome compartment in 50s case

3. Specific heat flux, kW/m<sup>2</sup>, for 1000s case

Time(s)	coated concrete	metal	steel, 6mm
1	28.9	140-300	250
2	24.1	66-300	250
5	20.5	21-295	170
10	19.8	11-286	85
20	18.7	5-295	32
50	13.1		
100	7.0		
200	4.4		
500	1.8		
1000	0.7		

Comment: The heat soakage into steel depends on several factors:

- a) Thickness
- b) Temperature and heat transfer at back side
- c) Modelling (e.g. meshsizes)

This makes listing of heat flux to metal less meaningful after some 10 seconds.

4. Specific heat flux, kW/m<sup>2</sup> for 50s case

Time(s)	Concrete		Steel	
	R4	R9	R4	R9
1	48.9	2.6	560	130
2	30.7	8.1	440	210
5	24.6	13.2	345	170
10	22.6	16.4	317	95